MOLECULAR AND GENETIC DETERMINANTS OF THE INHIBITORY ACTION OF EMODEPSIDE ON *C. ELEGANS* MUSCLE

By

Kiran Amliwala

A thesis presented for the degree of

DOCTOR OF PHILOSOPHY

of the

UNIVERSITY OF SOUTHAMPTON

in the

FACULTY OF MEDICINE, HEALTH AND LIFE SCIENCES

SCHOOL OF BIOLOGICAL SCIENCES

January 2005

UNIVERSITY OF SOUTHAMPTON

ABSTRACT

FACULTY OF MEDICINE, HEALTH AND LIFE SCIENCES
DIVISION OF CELL SCIENCES

Doctor of Philosophy

Molecular and genetic determinants of the inhibitory action of emodepside on *C. elegans* muscle.

Kiran Amliwala

The increasing resistance of parasitic nematodes to existing anthelmintics has encouraged the search for novel compounds. Emodepside, a 24 membered cyclic depsipeptide, has been shown to act as a potent broad-spectrum anthelmintic. Emodepside causes a fast onset of paralysis of nematodes, favouring the view that it acts on nerve and muscle systems. The basis of this study was to further investigate the mode of action of emodepside, using the parasitic nematode *A. suum* and the free-living non-parasitic model genetic organism *C. elegans*.

The effects of emodepside and GABA were investigated on the rate of relaxation of *A. suum* muscle pre-contracted with acetylcholine (ACh) using an organ bath preparation. The relaxing effect of GABA was more rapid than that of emodepside. Since the GABA effect on *A. suum* somatic muscle is mediated through an increase in chloride permeability (Martin, 1980), the GABA and emodepside effects on pre-contracted muscle were investigated using chloride-free saline. While the effect of emodepside was unaffected in chloride-free saline, the effect of GABA was converted to a very slow relaxation, or in some cases, a slight contraction. These data suggest that the effect of emodepside is not mediated through a direct GABAergic pathway.

To provide an insight into the molecular mechanisms and signalling pathway involved in emodepside action, the model organism *C. elegans* was used. Emodepside inhibits locomotory behaviour (IC_{50} 4.1nM), and this assay was used as a screen to delineate the mechanism of action of the drug. HC110R, a latrophilin-like receptor, was identified in *H.contortus*, as a possible target site for emodepside (Saeger *et al.*, 2001). In *C. elegans* two latrophilin-like genes exist; *lat-1* and *lat-2*. Individual RNAi to *lat-1* and *lat-2* resulted in a significant reduction in sensitivity to emodepside. The *lat-2 (ok301)* deletion strain also exhibited low level emodepside resistance.

Evidence for stimulation of vesicle release by emodepside was provided by imaging of synapses using the fluorescent dye FM4-64 (Willson *et al.*, 2004). Intracellular uptake of FM4-64 results in fluorescence of synaptic boutons. A rapid and selective loss of fluorescence was observed following application of emodepside, indicating vesicle exocytosis in the presence of emodepside.

The signalling pathway through which emodepside stimulates vesicle release was also investigated. *Egl-30* ($G\alpha_q$) and *egl-8* (phospholipase-Cβ) loss-of-function mutations both resulted in decreased sensitivity to emodepside, whereas *egl-30* gain-of-function mutations resulted in hypersensitivity to emodepside.

Investigation into the potential neurotransmitters that are released following emodepside stimulation, suggests that a cocktail of neurotransmitters may be released at the NMJ, including ACh and inhibitory neuropeptides. A reduced sensitivity to emodepside was observed following RNAi for the *flp-1* and *flp-13* genes. Following growth on emodepside-containing agar plates, *egl-21 C. elegans* (carboxypeptidase E) were less sensitive to emodepside (IC_{50} 15nM) providing further evidence for inhibitory peptides in emodepside action. Taken together these data suggest a model whereby emodepside exerts its potent anthelmintic action through a latrophilin-like receptor in nematodes stimulating vesicle release through a Gαq PLC-β pathway.

To determine if emodepside acts solely through the latrophilin-dependent signalling pathway proposed above, forward genetics was conducted using EMS chemical mutagenesis. Screening of mutagenised worms on 1μM emodepside plates yielded seven resistant lines. SNIP-SNP mapping techniques were used to determine the identity of the mutated gene in two of these resistant strains. This mapping technique, and subsequent sequencing, indicated that resistance to emodepside was conveyed in both these strains due to large deletions in the Ca^{2+} activated K^+ channel gene, *slo-1*.

Emodepside appears to have a complex mode of anthelmintic action, involving a presynaptic latrophilin-dependent pathway and the necessity for the SLO-1 channel.

Acknowledgements.

Throughout the last three years I have been guided and supported by many people, and it is with great pleasure that I have this opportunity to express my gratitude to all of them.

I would firstly like to thank Dr. Lindy Holden-Dye and Professor Robert Walker for their time, help and excellent supervision over the course of this project. I would also like to thank Dr. Neil Hopper and Dr. Neline Kriek and for their technical help, wisdom and consumables! A special thank you to Achim Harder for his hospitality in Germany.

I would especially like to thank Dr. James Willson for being a good mentor and friend. My colleagues in Wormland also helped me in my work, and I wish to thank them all.

I am grateful to the BBSRC and Bayer AG, Germany for their financial support.

Finally, I wish to thank my Mum, Dad, Fareena and Rosalyn. Without their constant encouragement, support and love none of this would have been possible.

Publications

Kiran Amliwala, Katherine Bull, James Willson, Achim Harder, Lindy Holden-Dye and Robert J. Walker. (2004). Emodepside, a cyclo-octadepsipeptide anthelmintic with a novel mode of action. *Drugs of the Future* 29(10): 1015-1024.

Willson J, **Amliwala K**, Davis A, Cook A, Cuttle MF, Kriek N, Hopper NA, O'Connor V, Harder A, Walker RJ, Holden-Dye L. (2004). Latrotoxin receptor signalling engages the UNC-13-dependent vesicle-priming pathway in *C. elegans*. *Current Biol*ogy 10; 14 (15):1374-9.

Willson, J., **Amliwala, K.**, Harder, A., Holden-Dye, L., & Walker, R. J. (2003). The effect of the anthelmintic emodepside at the neuromuscular junction of the parasitic nematode *Ascaris suum*. *Parasitology* 126, 79-86.

Amliwala, K., Willson, J., Harder, A., Holden-Dye, L., & Walker, R. J. (2002). Effect of the anthelmintic emodepside on locomotion in *C. elegans*, and on the somatic muscle of *A. suum*. *Proceedings of the Physiology Society*, 543P

Amliwala, K., Willson, J., Harder, A., Holden-Dye, L., & Walker, R. J. (2002) A comparison of the action of ivermectin and emodepside on *C.elegans European Worm Meeting Abstract* 167

K.K.Amliwala, A.Harder, L.Holden-Dye, R.J.Walker. (2003). Inhibitory effect of emodepside on the locomotor behaviour of *C. elegans* involves a latrophilin-like receptor. *Washington, DC Society for Neuroscience Abstract* 122.6. Oral Communication.

Willson, J., **Amliwala, K.**, Harder, A., Holden-Dye, L., & Walker, R. J. (2002). An investigation into the mechanism of action of the novel anthelmintic emodepside using *A.suum*. *European Worm Meeting Abstract* 121.

Harder, A., Schmitt-Wrede, H. P., Krucken, J., Marinovski, P., Wunderlich, F., Willson, J., **Amliwala, K.**, Holden-Dye, L., & Walker, R. (2003). Cyclooctadepsipeptides-an anthelmintically active class of compounds exhibiting a novel mode of action. *Int.J Antimicrob.Agents* 22, 318-331.

Contents

Chapter 1 - Introduction
Page 1

Figures

Tables

Abbreviations

Alanine	Ala	A
Arginine	Arg	R
Asparagine	Asn	N
Aspartic Acid	Asp	D
Cysteine	Cys	C
Glutamic Acid	Glu	E
Glutamine	Glu	Q
Glycine	Gly	G
Histidine	His	H
Leucine	Leu	L
Lysine	Lys	K
Methionine	Met	M
Phenylalanine	Phe	F
Proline	Pro	P
Serine	Ser	S
Threonine	Thr	T
Tryptophan	Trp	W
Tyrosine	Tyr	Y
Valine	Val	V

4-AP	4-aminopyridine
5-HT	5-Hydroxy-tryptamine
A. suum	*Ascaris suum*
ACh	Acetylcholine
AF1	*Ascaris* FMRFamide-like peptide one
AF2	*Ascaris* FMRFamide-like peptide two
APF	Artificial Perienteric Fluid
α-LTX	α-latrotoxin
CAPS	Calcium Activated Protein for Secretion
C. elegans	*Caenorhabditis elegans*
cDNA	Complementary Deoxyribonucleic acid
DAG	Diacylglycerol
DMS	Dorsal muscle strip
DNA	Deoxyribonucleic acid
dsRNA	Double stranded Ribonucleic Acid
EDTA	Ethylenediamine tetra-acetic acid
EPG	Electropharyngeogram
FLP	FMRFamide-like peptide
gDNA	Genomic Deoxyribonucleic acid
Glu-Cl	Glutamate gated chloride channel
nAChR	Nicotinic acetylcholine receptor
PF1022A	cyclo(D-lactyl-L-N-methylleucyl-D-3-phenyllactyl-L-N-methylleucyl-D-lactyl-L-N-methylleucyl-D-3-phenyllactyl-L-N-methylleucyl)
GABA	γ-amino butyric acid
PCR	Polymerase Chain Reaction
PF1	*Panagrellus* FMRFamide-like peptide one
PF2	*Panagrellus* FMRFamide-like peptide two
PLCβ	Phospholipase-Cβ
RNA	Ribonucleic Acid
RNAi	Ribonucleic Acid interference
TAE	Tris acetate EDTA
TBE	Tris borate EDTA
TEA	Tetraethylammonium

Chapter One

Introduction

1.1 Nematodes and the parasitic problem

The word "Nematode" comes from a Greek word *nema* meaning "thread". This highly adaptive phylum exists in a diverse range of habitats, such as the deep sea, fresh water and soil. Nematodes have evolved to exist as either free living or parasitic, with 12,000 and 15,000 different species identified, respectively. Free-living nematodes have a significant effect on the nutrient cycle in soil, as decomposers they consume fungi, bacteria and other microflora and microfauna aiding to the health of the soil. One such free-living nematode is the model organism *Caenorhabditis elegans.*

Parasitic nematodes occur in all natural communities, sometimes as benign infections, but they may also have massive economic and social impact by seriously damaging populations of domestic animals, fish and crop plants; as well as infecting man, especially throughout the developed and developing world. Parasitic nematodes can be divided into three main types: the Platyhelminths (e.g. *Schistosoma mansoni*), the tissue roundworms or filarial worms (e.g. *Onchocerca volvulus* and *Brugia malayi*) and thirdly, the intestinal roundworms (e.g. *Ascaris suum* and *Ascaris lumbricoides*).

Approximately 2 billion people are affected worldwide, indicating that 1/3 of the world's population are infected with a parasitic worm (Fig 1.1). It is estimated that 300 million are ill as a result of these infections, and of those at least 50% are school aged children (World Health Report 2000). In 1999 it was estimated that schistosomiasis and soil-transmitted intestinal helminths account for over 40% of the disease burden due to all tropical diseases, excluding malaria .

Several helminth infections cause significant mortality, in Africa alone, the death toll due to schistosomiasis is up to 200,000/yr. Each year, approximately 65,000 deaths are directly attributable to hookworm infections and another 60,000 to *Ascaris lumbricoides.*

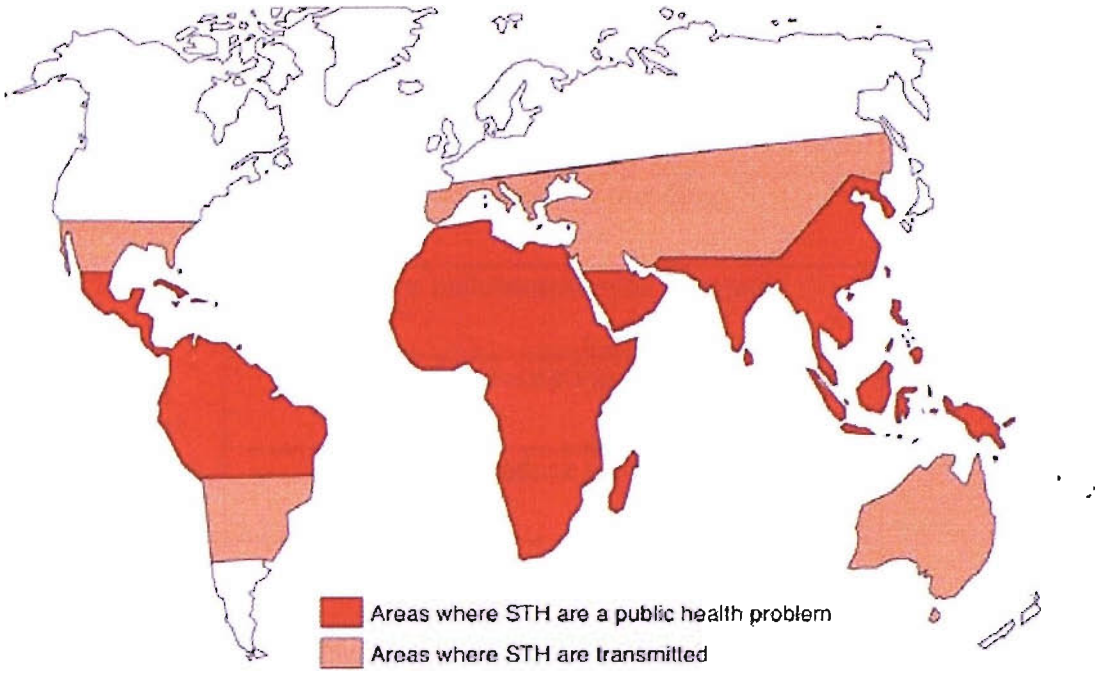

Figure 1.1 Global distribution of soil-transmitted helminth (STH) infections. (Adapted from World Health Organisation).

However, with such a substantial proportion of the world's population infected with one or more species of helminths, it is evident that death is a rare outcome. Nematode infections were recognized as a major cause of human morbidity and losses of disability adjusted life years (DALY's) in the tropics as well as temperate climates (Bundy & de Silva, 1998). Soil-transmitted nematodes (*Trichuris trichiura*) cause morbidity in humans in different ways (Table 1.1).

Multiple infections with several different parasites (e.g., roundworms, hookworms and amoebae) are common, and their harmful effects are usually amplified by co-existent malnutrition or micronutrient deficiencies. Nematode infection of domestic livestock can be devastating for the local economy through lost productivity, death of livestock and increased use of foodstuffs. Plant parasitic nematodes have been estimated to cause 80 billion dollars in crop damage annually.

Affect nutritional equilibrium
Induce intestinal bleeding
Induce malabsorption of nutrients
Compete for absorption of micronutrients
Reduce growth
Reduce food intake
Cause surgical complications such as obstruction

Table 1.1 Causes of human morbidity as a result of intestinal helminth infection.

Fortunately, these parasitic infections are also considered as a disease that can be efficiently controlled by cost-effective intervention (1993 *World Development Report*). At the 54th World Health Assembly in 2001 a resolution was put forward which urged endemic countries to start seriously tackling worms, in particular schistosomiasis and soil transmitted helminths. The Partners for Parasite Control (PPC) was initiated after the World Health Assembly in 2001. It is composed of agencies of the United Nations, WHO Members States, research institutes and a whole host of non-government organisations. The Global Target, against which each country's progress will be measured, is that at least 75% of all school aged children who are at risk of morbidity from schistosomiasis and STH should be targeted and treated by the year 2010.

Progress has been made in the understanding of ecology, epidemiology and related morbidity and in developing new tools for control. The intestinal helminths do not multiply in their human hosts, and the rate at which they are acquired is relatively low. Symptoms, as a rule, are proportional to the number of infecting parasites. In the past, control efforts have concentrated on eradication of the vectors, most commonly various species of snails. However, without adequate sanitary facilities for disposal of faeces and urine and without population-wide education in hygienic

practices, vector control is not very effective. Currently, there are no vaccines against human helminth infections, such that anti-helminth drugs (anthelmintics) continue to carry the burden of efforts to control helminth disease.

The over use of anthelmintics has slowly led to resistance in many strains of parasitic nematodes. The requirement therefore for new anthelmintics acting on novel target sites within nematodes has become of both social and economic importance.

1.2 *Ascaris suum*

A. suum is a large parasitic nematode found in pigs. Due to its size and relative abundance, it has frequently been used with success to examine the physiology and pharmacology of nematodes and the mechanism of a variety of anthelmintic drugs (Holden-Dye *et al.*, 1989;Martin *et al.*, 1991). In addition to this species in swine, a morphologically indistinguishable species *Ascaris lumbricoides* is found in humans, with estimates of the annual incidence of infection being greater than 1.5 billion cases. Female worms range from 25 to 40 cm in length and 5 mm in diameter, with males being smaller, ranging from 15 to 25cm long and 3mm in diameter. The predilection site for *A. suum* is the small intestine of swine. Female worms are capable of producing as many as 2 million eggs daily. These thick-shelled eggs are extremely resilient and can survive for as long as five years under most farm environments. However, they are susceptible to sunlight and prolonged exposure to drying will destroy them. Generally, these factors ensure that the normal swine environment will be well contaminated with *Ascaris* eggs, ensuring that all young pigs, particularly those raised on soil, will become infected.

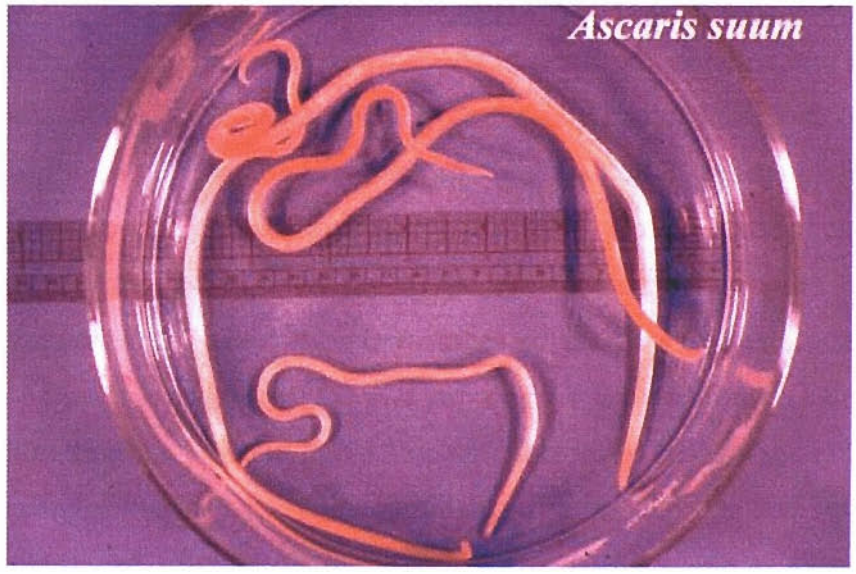

Figure 1.2 Four adult *A. suum.* (Image obtained from www.health-pictures.com)

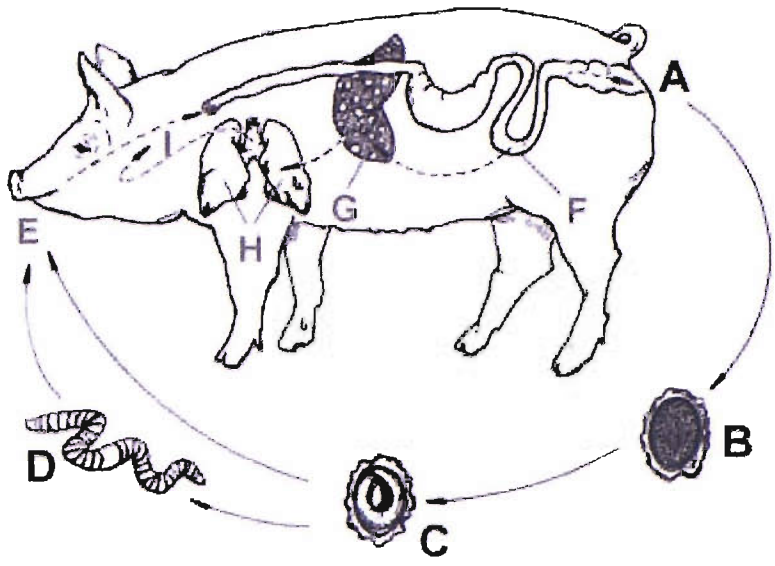

Figure 1.3 The life cycle of *A. suum*. (See 1.2.1 for description).

1.2.1 *A. suum* life cycle

Eggs laid by female worms pass via the host feces to the external environment (Fig 1.3) (**A**). Development to the infective stage occurs inside the egg via a single moult, about two weeks after expulsion from the host (**B-C**). Therefore the infective stage for *A. suum* is an egg containing a second stage (L2) larvae (**C**). Earthworms (**D**) and dung beetles may ingest eggs while feeding on soil and faeces. Pigs are infected when they ingest such infective eggs (**E**). The eggs hatch in the small intestine (**F**); the juvenile (L2) penetrates the small intestine and enters the circulatory system, via the hepatic portal system, migrating to the liver (**G**) within 24 hours of infection. Here the first parasitic moult (L2 to L3) takes place and 4-6 days after infection the juvenile worm enters the lungs, via the venous system, heart and pulmonary arteries (**H**). In the lungs the juvenile worm (L3) leaves the circulatory system and enters the air passages of the lungs. The L3 worm then migrates up the air passages into the pharynx where it is swallowed (**I**), and once in the small intestine the juvenile grows into an adult worm (L3-L4-adult) (**F**). Why *Ascaris* undergoes such a migration through the body, only to end up where it started, is unknown. Such a migration is not unique to *Ascaris*, as close relatives undergo a similar migration in the bodies of their hosts.

1.3 *Caenorhabditis elegans*

C. elegans is a small (1mm) free-living nematode found in soil in temperate climates (Fig 1.4). Although it is a primitive organism, *C. elegans* shares many of the essential biological characteristics that are central problems of human biology. *C. elegans* is diploid, possessing five pairs of autosomal chromosomes: I, II, III, IV, V, as well as a pair of sex chromosomes. The chromosomes are all of an equal size, being holokinetic (no centromere). There are two genders, a self-fertilizing hermaphrodite (XX) and a male (XO). Hermaphrodites produce both oocytes and sperm, and can reproduce by self-fertilization. Males, which are spontaneously produced at low frequencies, can fertilise hermaphrodites.

Figure 1.4 Adult hermaphrodite *C. elegans*. (Image source: Ralph Sommer Max-Planck Institute for Developmental Biology)

1.3.1 *C. elegans* life cycle

One of the advantages of working with *C. elegans* is that it has a short life cycle (Fig 1.5). The life cycle is temperature-dependent. *C. elegans* goes through a reproductive life cycle (egg to egg-laying parent) in 5.5 days at 15°C, 3.5 days at 20°C, and 2.5 days at 25°C. Juvenile worms hatch from these eggs and develop through four larval stages (L-1 to L4), which are punctuated by a series of moults.

During these moults new cuticle is synthesised. The mature adult arises after the fourth moult, is fertile for 4 days, and then lives for an additional 10-15 days producing about 300 progeny. If food is limited early in development *C. elegans* will take an alternative development pathway, at the L2/L3 molt, to produce the dauer larva stage (cryptobiosis). This dauer L3 stage does not feed and can survive for up to 3 months, without further development. If food later becomes available then the dauer stage will develop to L4 larval stage and continue development as normal.

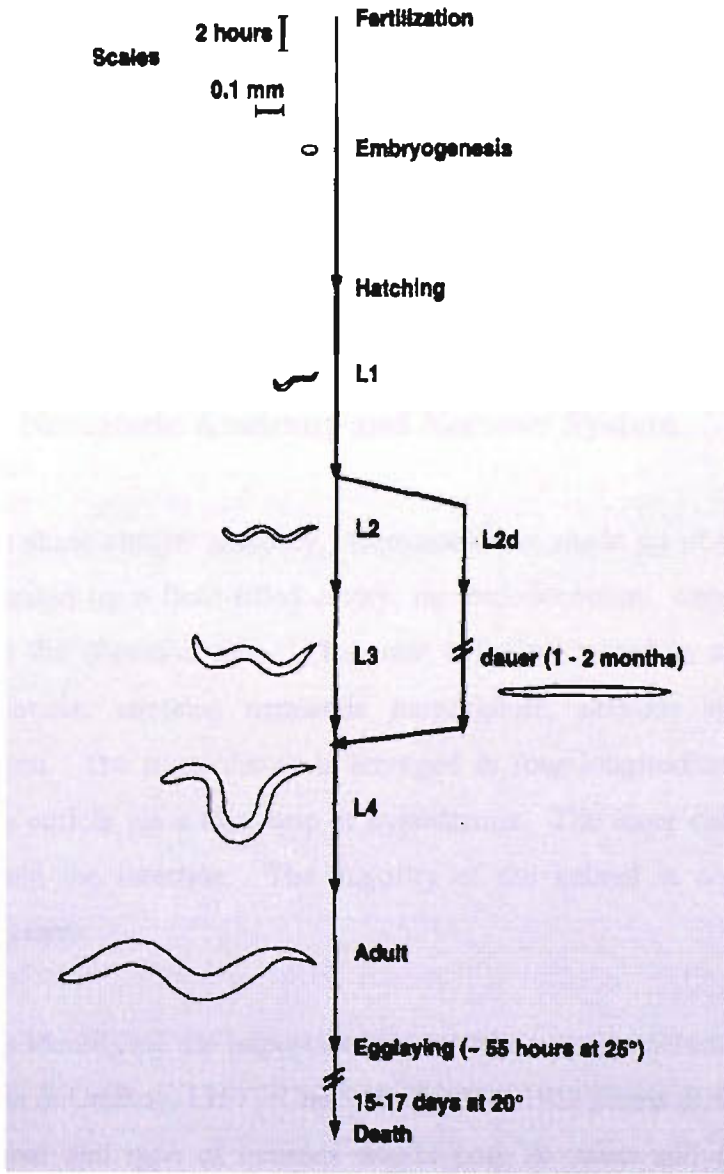

Figure 1.5 Life cycle of *C. elegans*. The time line is to scale, except where indicated by breaks. Schematic diagrams of the larval stages indicate the sizes of the animals at various time points. (Burglin *et al.*, 1998).

1.3.2 *C. elegans* use as a biological model for study.

C. elegans is a useful biological organism for study, due to its simplicity, transparency, and ease of cultivation in the laboratory. With its short life cycle, hermaphrodite mode of reproduction and small genome size, *C. elegans* is well suited for genetic analysis. In 1998 the complete genome sequence for *C. elegans* was published (The *C.elegans* Sequencing Consortium, 1998). The *C. elegans* genome size is relatively small (9.7×10^7 base pairs or 97 Megabases), when compared to the human genome which is estimated to consist of 3 billion base pairs (3×10^9 bp or 3000 Megabases). Numerous molecular biological techniques exist for *C. elegans* experimentation, that are not possible when examining higher eukaryotes. There are about 20,000 protein-coding genes. Identification of genes and the ability to make mutant *C. elegans* strains, which lack particular genes of interest, has also become increasingly useful in the analysis of biological pathways.

1.4 General Nematode Anatomy and Nervous System

All nematodes share similar anatomy. Nematodes are made up of two concentric cylinders separated by a fluid-filled cavity, the pseudocoelum, between the outer body wall and the digestive tube. The outer cylinder, coated in an extracellular collagenous cuticle, contains nematode musculature, nervous system and an excretory system. The musculature is arranged in four longitudinal strips and is attached to the cuticle via a thin strip of hypodermis. The inner cylinder contains the pharynx and the intestine. The majority of the animal is occupied by the reproductive system.

Initial work on identifying the important features of nematode nervous system used *A. suum* (Harris & Crofton, 1957) (Cappe de Baillon, 1911;Davis & Stretton, 1989). The arrangement and type of neurons within both *A. suum* and *C. elegans* are largely homologous. The *C. elegans* nervous system consists primarily of a cranial pharyngeal nerve ring, a ventral nerve cord, a dorsal nerve cord, and an intricate head sensory system (Fig 1.6). These two major nerve cords run along the length of

the body. The nerve ring is located in the head and contains most of the interneurons together with axons from most sensory neurons; essentially this is the brain of the worm. Unlike other animals, where the nerves branch out to the muscle cells, nematode muscle cells branch toward the nerves. *C. elegans* have 959 somatic cells within the hermaphrodite, some 302 of which are neurons. Approximately 5000 chemical synapses and 600 gap junctions connect these neurons. Despite the small size and simplicity, this nervous system regulates a wide range of behaviours such as: mechanosensory and chemosensory responses, thermotaxis, complex responses to food, locomotion, feeding, egg laying, defecation, and male mating.

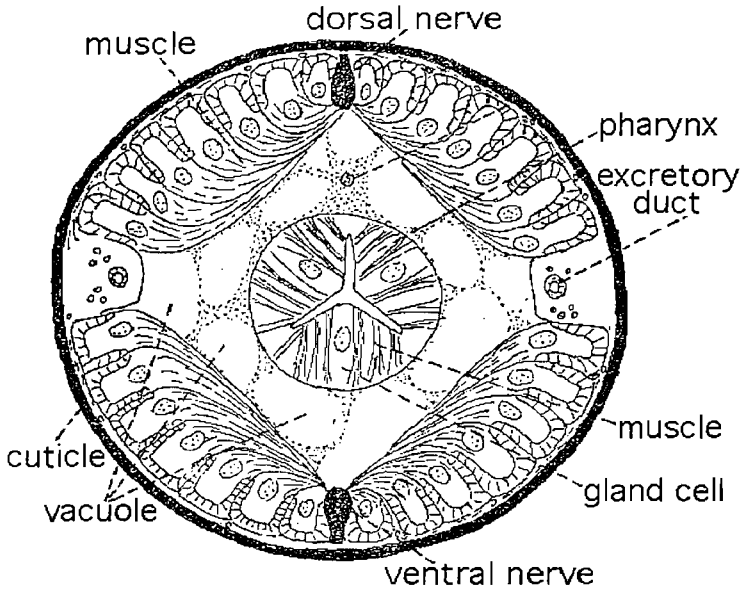

Figure 1.6 Cross section through *C. elegans*. (Image available through www.biodidac.bio.uottawa.ca).

1.5 *C. elegans* Pharynx

Food is pumped into the animal and processed by the pharynx. This is a virtually self-contained organ with its own musculature, epithelium and nervous system. The pharynx functions as a largely autonomous unit, although there are two interneurons that originate in the central nervous system and enter it. These interneurons (RIP) are entirely postsynaptic outside the pharynx and so may mediate the overall control of pharyngeal pumping from the central nervous system. The pharynx is used for ingesting food (usually bacteria), concentrating it via filtration and then grinding it. It may also be responsible for secreting digestive enzymes from its gland cells (Albertson & Thomson, 1976)

1.6 Motor anatomy and neuronal control of movement.

The anatomy and physiology of nematode motor neurons was first described in *A. suum* (Stretton *et al.*, 1978), with the equivalent motor neuron classes identified later in *C. elegans*, using electron microscopy techniques (White *et al.*, 1983). There are 30 classes of motor neurons in *C. elegans* that innervate pharyngeal, egg laying, defecation and body-wall muscles. The pharyngeal and egg laying neuromuscular junctions (NMJs) are located at the terminus of motor axons or branches that extend to the muscles. Conversely, body-wall and defecation muscles have short neuron-like processes onto nearby nerve cords, forming NMJ with their motor neurons. The innervation of body-wall muscle is more complicated in nematodes than for vertebrate systems, in that, muscle cells obtain synaptic input from both excitatory and inhibitory neurons. The framework and synaptic innervation of the body wall muscles allows locomotion to occur as dorsal and ventral flexions of the body. This locomotion is described as a sinusoidal pattern of alternating ventral and dorsal turns, which relies upon out of phase contraction of the dorsal and ventral muscles. Dorsal and ventral body muscles are controlled by distinct classes of motor neurons, A, B, D, AS, and VC, which are defined by similarities in axonal morphologies and patterns of synaptic connectivities (White *et al.*, 1986). The alternating pattern of contraction between dorsal and ventral body wall muscle is achieved through excitatory and inhibitory motor neuron interaction, via excitatory (acetylcholine) and inhibitory (GABA) neurotransmitters.

NMJ on Ventral body muscle	**Neurotransmitter & direction of movement**		**NMJ on Dorsal body muscle**	**Neurotransmitter & direction of movement**	
VA	ACh	Backward	**AS**	ACh	
VB	ACh	Forward	**DA**	ACh	Backward
VC	ACh		**DB**	ACh	Forward
VD	GABA	Inhibit Forward & Backward	**DD**	GABA	Inhibit Forward & Backward

Table 1.2 Summary of motor neuron circuitry. (Created by K.Amliwala)

Each motor neuron class is composed of multiple members, which are arranged along the length of the ventral cord in repeating units (e.g., VA1-VA6).

The A- and B-type neuromuscular junctions are arranged as complexes in which an A or B synaptic terminus acts on two postsynaptic elements, a body wall muscle and a D neuron dendrite (White *et al.*, 1986). The VD neurons receive input at the dorsal A and B type neuromuscular junctions – being activated during dorsal muscle contractions - and they form neuromuscular junctions ventrally that appear to relax the ventral muscles. The opposite set of connections exists for the DD neurons. This circuit suggests that the D neurons act as cross-inhibitors that prevent the simultaneous contraction of the dorsal and ventral muscles (White *et al.*, 1986). Regulation of these motor neurons occurs through command interneurons which in turn receive input from sensory circuits. Therefore, these command interneurons serve to integrate and translate sensory information into the appropriate locomotory response. AVB and PVC command interneurons activate forward movement, whereas AVA, AVD and AVE activate backward movement (Fig 1.7) (Riddle, 1997).

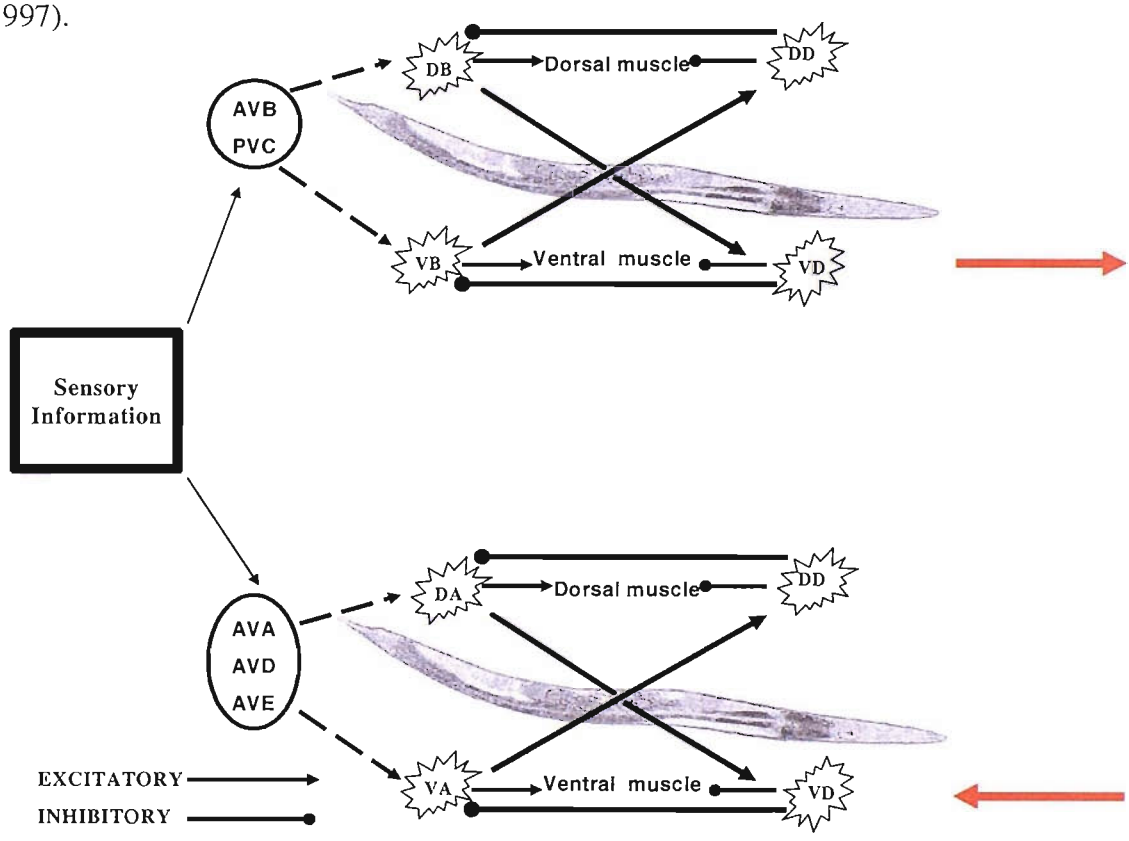

Figure 1.7 Illustration to show circuitry of *C. elegans* motor nervous system. Red arrows indicate direction of movement. (Created by K.Amliwala)

1.7 Neuropeptides in *C. elegans*

Neuropeptides play critical roles in synaptic signalling in all nervous systems, including that of the nematode. FaRPs (FMRFamide-Related Peptides), and FLPs (FMRFamide-Like Peptides) are the most widely studied family of invertebrate regulatory peptides. These structurally-related peptide molecules probably occur ubiquitously in the invertebrate nervous system. (Walker *et al.*, 2000). The first presumptive peptidergic neurons were identified in *Acanthocheilonema viteae*, *A.suum*, *Brugia pahangi*, *Haemonchus contortus* and *Phocanema decipiens* (Davey, 1966) (Rogers, 1968). Since then, extensive peptide immunoreactivites have been demonstrated in nervous tissues of *A. suum*, (Stretton *et al.*, 1991;Brownlee *et al.*, 1993) and *C. elegans* (Li & Chalfie, 1986), as well as other nematode species (Maule *et al.*, 1996;Brownlee *et al.*, 2000).

The completion of the sequenced genome of *C. elegans* enabled the identification of genes that encode for FMRFamide and FaRPs. 23 genes were identified and named *flp* (FMRFamide like peptides) genes 1 through to *flp* 23 (Li *et al.*, 1999b) (Kim & Li, 2004). The putative prohormone or precursor protein encoded by these *flp* genes consistently contains multiple distinct FMRFamide-like peptides, some of which may be present in multiple copies and all of which are flanked by potential proteolytic cleavage sites. In the case of *flp-1*, through alternative splicing, two distinct transcripts are generated. One of these transcripts codes for a precursor protein that contains seven different peptides; the second transcript codes for a precursor protein that contains eight distinct peptides. Thus, the *flp-1* gene generates neuropeptide diversity in two ways: by encoding multiple neuropeptides and by alternative splicing (Rosoff *et al.*, 1992). Each of the *flp* genes are predicted to encode a unique set of FaRPs, which potentially encode around 60 different FaRPs.

Distinct and overlapping expression patterns of the *flp* genes examined suggest that *flp* genes function in both unique and overlapping pathways (Kim & Li, 2004). Onset of *flp* gene expression generally occurs during embryogenesis, suggesting that some of the *flp* genes may have a role in development, perhaps in axonal outgrowth. In addition, sex-specific expression patterns of several *flp* genes suggest that some FLP peptides have roles in reproduction. Cellular expression patterns and

genetic analysis of *flp* genes suggest that neuropeptides in nematodes also have widespread and varied roles in nervous system function (Li *et al.*, 1999b). Further characterization of the *flp* neuropeptide gene family in *C. elegans*, including isolating animals in which each *flp* gene is inactivated, can elucidate the functions and mechanisms whereby these peptides exert their actions.

Gene	Peptide Sequence
flp-1 Gene appears to be expressed only in interneurons in the head region of the animal. *flp-1*-expressing neurons are important intermediates in sensory and motor pathways(Li *et al.*, 1999a).	SADPNFLRFa (same as PF2) SQPNFLRFa ASGDPNFLRFa SDPNFLRFa AAADPNFLRFa PNFLRFa AGSDPNFLRFa
flp-2	SPREPIRFa LRGEPIRFa
flp-3	SPLGTMRFa TPLGTMRFa EAEEPLGTMRFa NPLGTMRFa ASEDALFGTMRFa EDGNAPFGTMRFa SAEPFGTMRFa SADDSAPFGTMRFa NPENDTPFGTMRFa
flp-4	PTFIRFa ASPSFIRFa
flp-5	GAKFIRFa AGAKFIRFa APKPKFIRFa
flp-6	KSAYMRFa (x6)
flp-7	SPMQRSSMVRFa (x3) TPMQRSSMVRFa (x2) SPMERSAMVRFa SPMDRSKMVRFa
flp-8	KNEFIRFa (x3)
flp-9	KPSFVRFa (x2)
flp-10	QPKARSGYIRFa
flp-11	AMRNALVRFa ASGGMRNALVRFa NGAPQPFVRFa

flp-12	RNKFEFIRFa
flp-13 FLP-13 has been shown to inhibit nematode locomotory behaviour (Reinitz *et al.*, 2000a)	SDRPTRAMDSPLIRFa AADGAPLIRFa APEASPFIRFa ASPSAPLIRFa SPSAVPLIRFa ASSAPLIRFa
flp-14	KHEYLRFa (x4)
flp-15	GGPQGPLRFa RGPSGPLRFa
flp-16	AQTFVRFa (x2) GQTFVRFa
flp-17	KSAFVRFa KSQIRFa
flp-18	EMPGVLRFa EIPGVLRFa SEVPGVLRFa DVPGVLRFa SVPGVLRFa KSVPGVLRFa DFDGAMPGVLRFa
flp-19	WANQVRFa ASWASSVRFa
flp-20	AMMVRFGa (x 2)
flp-21	GLGPRPLRFa
flp-22	SPSAKWMRFa
flp-23	TKFQDFLRFa

Table 1.3 The *flp* genes in *C. elegans* and the potential FaRPs they encode.

1.8 Anthelmintics and mechanisms of action

In the past forty years the availability of several classes of oral, single-dose, non-toxic, broad spectrum anthelmintics has made periodic treatment of high-risk populations an attractive strategy for reducing worm burdens to relatively harmless proportions. Anthelmintics achieve selective toxicity by targeting ion channels and receptors together with biochemical processes which are specific to the parasitic nematode (Martin, 1997).

1.8.1 Benzamidazoles

These broad-spectrum anthelmintic compounds have been implemented clinically since 1963. Members of this family, such as, thiabendazole, mebendazole, albendazole, as well as prebenzimidazoles and benzimidazole carbamates, have been shown to be highly effective in numerous domestic and agricultural animals and are widely used in human medicine. They exert their effect by selectively binding free β-tubulin with 400 times greater specificity in helminth tissue compared to mammalian, and by blocking fumerate reductase. This results in greatly reduced microtubule-dependent glucose uptake in the parasite through direct inhibition of β-tubulin polymerisation.

1.8.2 Nicotinic ACh receptor agonists

This anthelmintic class, whose members include levamisole (imidazothiazole) and pyrantel - both of which are used in human medicine, specifically targets the infectious helminth by exploiting the pharmacological differences between host and parasite nicotinic acetylcholine receptors. Investigation into the mechanism of action using *A. suum* showed that these anthelmintics have a depolarizing block effect on the helminth NMJ, via an increased input conductance of the muscle membrane to sodium and potassium ions (Harrow & Gration, 1985), as well as a degree of anticholinesterase activity. This results in spastic paralysis of the

nematode. Patch clamp studies have shown that these anthelmintics open non-selective cation channels. Duration of channel opening depends on the anthelmintic used (Harrow & Gration, 1985).

1.8.3 GABA agonists

Piperazine is an anthelmintic which acts as an agonist at nematode GABA receptors. Both piperazine and GABA increase chloride ion conductance in the muscle membrane leading to an increase in the membrane potential and a reduction in cell excitability (Martin, 1997;Holden-Dye *et al.*, 1989). This results in flaccid paralysis of the nematode.

1.8.4 Macrocyclic lactones

The macrocyclic lactones are natural fermentation products of *Streptomycetes* bacteria. They consist of two sub groups, the avermectins and the milbemycins. Currently there are six commercially available macrocyclic lactones: Ivermectin, Eprinomectin, Moxidectin, Selamectin, Doramectin and Milbemycin. A primary mode of action of macrocyclic lactones is to modulate chloride ion channel activity in the nervous system of nematodes, e.g. Ivermectin (IVM, 22,23-dihydroavermectin B_1) acts through invertebrate specific glutamate gated chloride channels causing an increase membrane permeability to Cl^-. This inhibits the electrical activity of nerve cells in nematodes, resulting in paralysis and death of the parasites.

1.8.5 Other anthelmintics

Apart from the major groups of anthelmintics mentioned above, a number of other compounds have been used and these will be briefly reviewed.

Praziquantel increases membrane permeability to mono and divalent cations, especially Ca^{2+}, within the parasite (Cioli & Pica-Mattoccia, 2003). However, it acts differently to Ca^{2+} and K^+ ionophores. Praziquantel leads to increased muscular activity followed by contraction and spastic paralysis which causes the

parasite to lose its attachment to the intestinal mucosa. Vacuolization and vesiculation of the tegument occurs, which if sufficiently pronounced, activates host defence ultimately leading to the destruction of the parasite. This mechanism correlates well with the effects in *Schistosoma mansoni.*

Certain organophosphates have been used as anthelmintics, e.g., dichlorvos, and act by raising the levels of acetylcholine at the nerve somatic muscle junction, resulting in spastic paralysis due to excessive depolarization of the muscles (Rew *et al.*, 1986). The problem with these compounds is that they also inhibit the host's acetylcholinesterases and so can be toxic to the host.

Other strategies have been proposed for the development of anthelmintics derived from natural products, e.g., cysteine proteinases (from the latex of figs, papaya and pineapples), which digest nematode cuticles (Stepek *et al.*, 2004).

1.9 Anthelmintics and resistance.

Despite the development and clinical efficacy of these anthelmintics in controlling parasitic helminth infections, by the end of the 1970's the first reports of anthelmintic resistance began to emerge (Geerts and Gryseels, 2001). Both platyhelminth (flatworm) and nematode (roundworm) parasites infecting livestock have exhibited an ability to develop strong resistance to chemotherapeutics, such that anthelmintic drugs fail to control parasitism. Resistance has occurred to all major anthelmintic classes in several species of parasite, with several isolates resistant to all major drug classes (Sangster, 2001). Although the current situation of resistance in human helminths is significantly less severe than that in livestock, it has been suggested as an important warning for the medical world as to the possible outcomes of widespread over use of anthelmintics. The ability of parasitic targets to develop resistance means there is a continual requirement for novel anthelmintics capable of breaking the resistance problem. The neuromusculature (nervous system and muscle) of parasitic helminths is a pivotal target for current anthelmintics and, in view of its significance to parasite survival, it is expected to remain so.

1.9.1 Molecular basis of imidazothiazole resistance

Levamisole mimics the action of the excitatory neurotransmitter ACh causing a spastic paralysis of the worm. There is some evidence from studies on levamisole resistant strains of *H. contortus* to suggest that mutations in the somatic muscle ACh receptors may lead to resistance Resistant worms required a 4 to 13-fold increase in levamisole dose to elicit a comparable response in ACh-induced muscle contraction, compared to susceptible strains. Other well established ACh agonists, e.g, morantel and pyrantel, had negligible effect on the resistant worms thus suggesting that levamisole resistant animals have modified ACh receptors (Sangster *et al.*, 1991).

Work on *C. elegans* has also helped elucidate the basis of levamisole resistance. The *lev-1* resistant isolate, has a mutation within the sequence encoding a transmembrane region of the structural receptor molecule. MAL is a radioactive analogue of levamisole, and for this reason it was used in ACh receptor ligand binding studies (Lewis *et al.*, 1980a). In *C. elegans*, binding is specific, saturable and displaced by cholinergic agents. In susceptible worms MAL binds to two sites, a high affinity site, and a non-saturable site which is less profuse. In resistant worms a loss of both high and low affinity sites is observed. In contrast, binding studies using parasitic nematodes showed the amount of high-affinity ligand binding was comparable between a susceptible and a resistant strain of *H. contortus*, but differences between these isolates were found at the low-affinity site (Sangster *et al.*, 1998). At this site, resistant worms have lower drug affinity and more binding sites, possibly reflecting an increased susceptibility for desensitization of the receptor (Sangster & Gill, 1999).

1.9.2 Molecular basis of avermectin & milbemycin resistance

Parasites resistant to avermectins, including ivermectin, are also resistant to chemically related milbemycins (Shoop *et al.*, 1993;Conder *et al.*, 1993), suggesting a similar mechanism of action for these macrocyclic lactones.

C. elegans has proved a useful model system in which to study the mechanism of action of ivermectin, and hence hypothesize a basis for resistance. Ivermectin acts by binding to a glutamate-gated chloride channel which is comprised of two subunits, GluCl-α and GluCl-β (Cully *et al.*, 1994). IVM binds to the α-subunit whereas glutamate binds to the β-subunit. The α-subunit in the GluCl receptor in *C. elegans* is encoded by a family of genes including *glc-1, avr-14* and *avr-15* (Cully *et al.*, 1994). Interestingly, severe loss-of-function mutations in either *glc-1* or *avr-15* do not confer total resistance to ivermectin (Vassilatis *et al.*, 1997). Possible explanations for these observations are that GluCls are not physiologically important targets of ivermectin or, multiple GluCl genes act independently to convey ivermectin sensitivity.

Further investigations using *C. elegans* clarified this, by demonstrating that these GluCl genes are indeed key mediators in the anthelmintic action of IVM (Dent *et al.*, 2000). It is the interaction of all three, *avr-14, avr15* and *glc-1,* via parallel pathways that confers sensitivity to ivermectin. Therefore, strong resistance to IVM will only be conveyed when loss of function mutations occur in all three of these genes.

1.10 The search for novel anthelmintics and the use of *C. elegans*

The resistance of parasitic nematodes to existing anthelmintics in agriculture, and also clinically, has encouraged a search for novel anthelmintics which target sites specific to the nematode. Essentially all commercially available anthelmintics have detectable effects on *C. elegans* which has prompted its development as a model for parasitic nematodes for the purposes of drug screening (Hodgkin, 2001).

The use of the complete nucleotide sequence of the worm can be utilized to determine the effects of inactivating a suspected drug target, through analysis of mutations in the gene that encodes it. Through these pharmacological mode of action studies, the resulting phenotype of the mutation will indicate whether or not the potential target is required for the anthelmintic mechanism.

1.10.1 Reverse genetics in anthelmintic screening

Sequence driven reverse genetics has become a very powerful molecular tool. The original technique for this relied on mutations induced by transposon insertions. Transposons are short sequences of DNA that "jump" or translocate randomly into the genome, typically inactivating genes into which they have been inserted. The technique uses natural mutator strains to mobilise transposons in *C. elegans*, e.g. Tc1. PCR is then used to isolate a fortuitous insertion in a sequence of interest. Once an insertion is isolated a deletion derivative (due to imprecise excision of the transposon) can also be identified by PCR. Mutants isolated this way are generally homozygous, though this must be verified before phenotypic characterization (Geary *et al.*, 1992). This method requires subsequent rescue by complementation, whereby a wild-type copy of the gene of interest is introduced into its genetic mutant background. The mutant phenotype is then rescued and pharmacologically assayed to deduce the function of the targeted gene with respect to anthelmintic action.

More recently an additional reverse genetics method has been developed, RNA interference (RNAi), which results in a "knock-down" of the specifically targeted

gene of interest. RNAi is believed to be an anti-viral and anti-transposon mechanism (Fire, 1999). It is ubiquitous, which suggests that it was evolved very early on in cellular life (Grant, 1999). The phenomenon known as RNA inhibition was revealed in plants, in an experiment first proposed to show the effects of a gene insertion, a number of the resultant transgenic plants showed no expression of the inserted gene. Additional investigation showed that, in these instances, more than one copy of the gene had inserted into the genome, one inverted copy and one inserted normally. It was hypothesized that in these cases the transcript was forming a double stranded RNA (dsRNA), which was then somehow acting as an inhibitor of the gene function (Napoli *et al.*, 1999). The effect was also observed in *C. elegans* through the injection into the germline of either sense or anti-sense transcript from the gene *par-1*, with the resulting progeny showing *par-1* phenotypes. Fire and Mello illustrated that this epigenetic gene inactivation worked with other genes, with the phenomenon being strongest with dsRNA (Fire, 1999).

It was proposed that the key to the interference process is the recognition of the target mRNA by the dsRNA, and because the incoming dsRNA need not be present in stoichiometric levels there must exist a highly efficient catalytic machine, or amplification step (Ketting *et al.*, 2001;Sijen *et al.*, 2001).

Upon entering the cell, long dsRNAs are first processed by the RNAse III enzyme Dicer (Fig 1.8) (Knight & Bass, 2001). This functional dimer contains helicase, dsRNA binding, and PAZ protein domains. The former two domains are important for dsRNA unwinding and mediation of protein-RNA interactions, however, the function of the PAZ domain species is not completely elucidated (Cerutti, 2003). Dicer produces 21–23 nucleotide dsRNA fragments with two nucleotide 3' end overhangs, i.e. siRNAs. It has been suggested that Dicer has a role other than dsRNA cleavage that is required for siRNA-mediated RNAi in mammals (Doi *et al.*, 2003).

RNAi is also mediated by the RNA-induced silencing complex (RISC) which, guided by siRNA, recognizes mRNA containing a sequence homologous to the siRNA and cleaves the mRNA in the middle of the homologous region (Bernstein *et*

al., 2001). Thus, gene expression is specifically inactivated at a post-transcriptional level. In *C. elegans*, Dicer has been shown to interact with RDE proteins. The RDE proteins bind to long dsRNA and are believed to present the long dsRNA to Dicer for processing (Tabara *et al.*, 2002). Mutants displaying a high degree of resistance to RNAi have been reported to possess mutations at *rde-1* and *rde-4* loci (Tabara *et al.*, 1999).

Strains that are more susceptible for RNAi, which are deficient in a RNA dependent RNA polymerase, RRF-3, have made it easier to identify gene function in neurones (Simmer *et al.*, 2002). A recent whole genome screen using RNAi on *rrf-3 C. elegans* identified that 23% of the predicted *C. elegans* genes showed a phenotype (Simmer *et al* 2003) compared with 10% for wild type (Kamath *et al.*, 2003).

Besides gene silencing, RNAi might be involved in other phenomena of gene regulation. DNA/RNA interactions are known to influence DNA methylation. It appears that RNAi can also function on this level by methylating cytosines as well as sequences more classically associated with methylation. If the target sequence shares homology with a promoter, transcriptional silencing may occur via methylation. Moreover, RNA appears to interact with chromatin domains, which may ultimately direct DNA methylation. Studies of *C. elegans* have shown that RNAi can spread among cells through mechanisms that may not hinge upon siRNA (Winston *et al.*, 2002). The systemic RNA interference-deficient locus, *sid-1*, encodes a conserved protein with a signal peptide sequence and 11 putative transmembrane domains, suggesting that the SID-1 protein may act as a channel for long dsRNA, siRNA, or a currently undiscovered RNAi-related signal. *Sid-1* mutants retain cell-autonomous RNAi but fail to show spreading of RNAi. It remains unclear whether this systemic RNAi occurs in mammals, although a strong similarity is reported between *sid-1* and predicted human and mouse proteins.

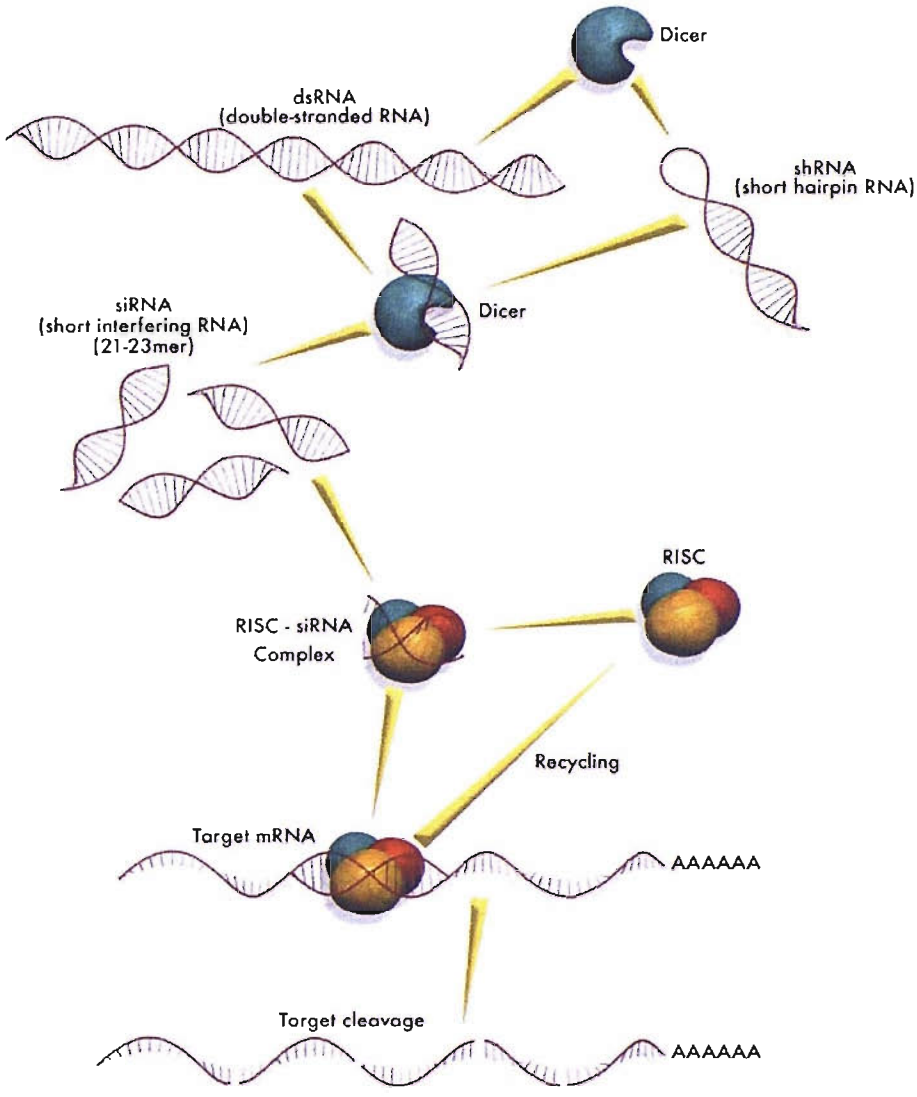

Figure 1.8 Mechanism of RNA interference (RNAi). During RNAi, the cellular enzyme Dicer binds to the dsRNA and cleaves it into short pieces of ~ 20 nucleotide pairs in length known as small interfering RNA (siRNA). These RNA pairs bind to the cellular enzyme called RNA-induced silencing complex (RISC) that uses one strand of the siRNA to bind to single stranded RNA molecules (i.e. mRNA) of complementary sequence. The nuclease activity of RISC then degrades the mRNA, thus silencing expression of the gene. Adapted from www.upstate.com.

1.10.2 Forward genetics in anthelmintic screening

Although reverse genetics ensures focus on a biochemically defined type of gene, it may lead to very diverse phenotypes, ranging from lethality to no obvious phenotype at all. Therefore, forward genetic strategies are also employed. Forward genetics starts with a phenotype of interest, for example, anthelmintic resistance, and seeks mutants of that phenotype for analysis. Unlike reverse strategies, forward genetic screening methods require no prior knowledge of the sequence function.

Random mutations are made in the nematode genome, by mutagens such as trimethylpsoralen, ethylmethanesulfonate (EMS), or U.V light, and large populations of mutagenised animals are screened for a specific phenotype. EMS has an average mutation frequency of $5x10^{-4}$ mutations per gene, or a chance of one in 10 000 genes becoming mutated. 13% of these EMS mutations are deletions (Riddle, 1997). If the mutant phenotype is due to a change in a single gene, it is possible to genetically map the defective gene with respect to other genes of known function. This process is often rate limiting in molecular genetics and several technologies have been developed to facilitate gene mapping.

The transposon insertion display takes advantage of the fact that mutations made by the insertion of a transposon are tagged with the sequence of the inserting element. This PCR-based technique makes it possible to identify genomic DNA adjacent to a mutagenic transposon insertion in a relatively short amount of time (Bessereau *et al.*, 2001).

Another alternative to the use of transposon insertion mutagenesis is mapping using single nucleotide polymorphisms (SNPs). Some wild isolates of *C. elegans* are polymorphic with respect to the canonical laboratory strain (Bristol N2) at a rate of about 1 in 1500 base pairs, yet are robust healthy, and behaviourally similar to N2 (Koch *et al.*, 2000). One such strain is CB4856 (Hawaiian strain), useful for interbreeding as the genome has been shotgun sequenced. There are many single nucleotide polymorphisms (SNPs) between the N2 and CB4856 sequences. Some of these SNPs create or destroy restriction sites, the so-called snip-SNPs. These differences in restriction digest profile are the basis for SNP mapping. By crossing

a strain containing a mutation derived from N2 with this CB4856 polymorphic isolate, it is possible to track the co-segregation or exclusion of a large number of polymorphisms with the mutant phenotype in the progeny from a single cross.

CB4865 males are crossed into the N2 strain, containing the mutation. The resultant F1 is heterozygous, so that for each chromosome pair one copy is N2 and one is CB4856. These F1 cross progeny are individually picked to separate plates and allowed to self-fertilise to yield F2. During which time, at prophase I of meiosis recombination events will occur, with an average of one crossover per chromosome per meiosis. This occurs in the gametes, both the sperm and oocytes.

The genotypes of these F2 animals will be one of three (Fig 1.9). F1 Parental genotypes are either Mc or mC. mC does not survive so will not be present in the progeny. Recombinant genotypes are combinations of the loci other than those of the parents.

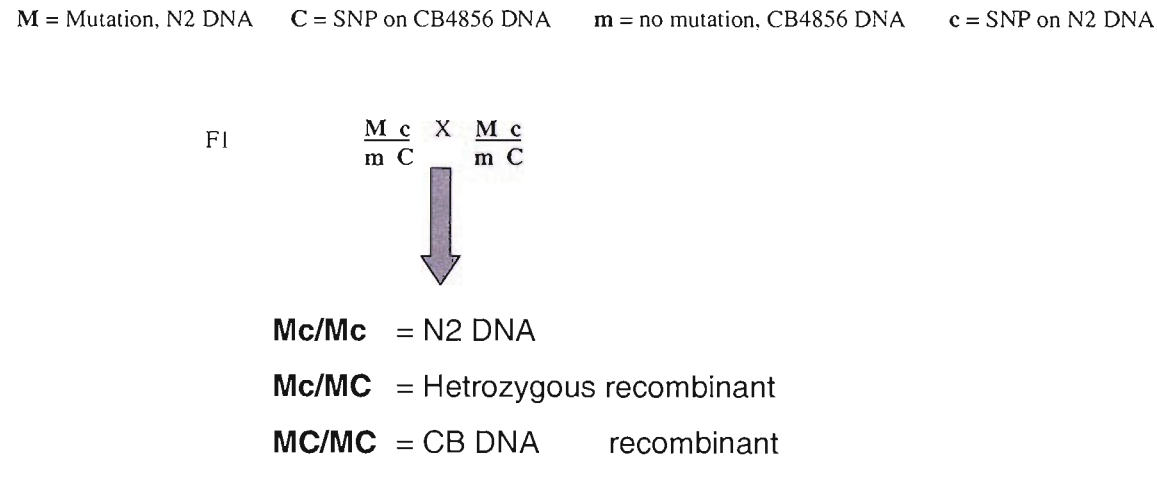

Figure 1.9 F2 Genotypes generated from cross of N2 derived mutation with CB4856 Hawaiian strain.

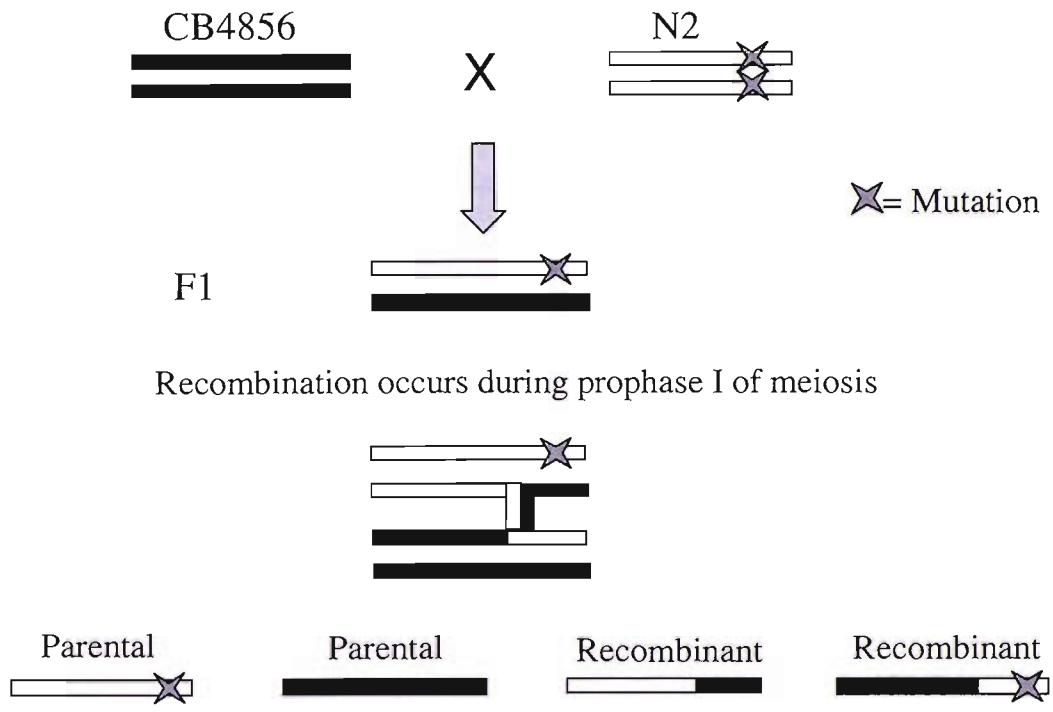

Figure 1.10 Overview of cross between N2 derived mutation strain with CB4856 Hawaiian strain. Recombination events will create or destroy SNP sites required for linkage analysis

The F2 progeny are screened for the phenotype of interest, e.g., anthelmintic resistance, and picked to separate plates where a clonal population is allowed to propagate. Each plate of worms represents an individual recombination event and is treated as a separate sample. These individual worm populations are then lysed to create a crude DNA preparation.

Oligonucleotides are designed around the SNPs and used to amplify the DNA in that locus. Initially a SNP located near the centre of each of the 6 chromosomes is used to assign linkage of the mutation to a particular chromosome. Recombinant frequency is used to determine if loci are linked or not. A recombinant frequency of 50% generally means that the genes or loci being investigated are unlinked (on separate chromosomes). This is the law of independent assortment. A recombinant frequency of significantly less than 50% indicates that the genes or loci are linked i.e. lie on the same chromosome. This is because when two genes are close together on the same chromosome they do not assort independently. The closer together 2 loci are on a chromosome the less recombinant progeny, as the probability of recombination between two points close together is less than for two

further apart. In relation to SNP mapping, this means that if all the samples are N2 DNA at a SNP then this locus must lie very close to the mutation.

Once chromosomal linkage has been determined the PCR process is repeated to determine which arm of the chromosome the mutation is on, and so on, until a precise locus is found.

1.11 Cyclodepsipeptides

It has been stated that the cyclodepsipeptides have emerged as the most promising anthelmintic drug class discovered in the last decade (Nicolay *et al.*, 2000;Saeger *et al.*, 2001;Zahner *et al.*, 2001). This is because they possess the necessary characteristics required by any novel anthelmintic; no mechanistic or structural relation to existing anthelmintics, combined with a broad spectrum of activity at targeting various nematode species in different animals (Nicolay *et al.*, 2000;Zahner *et al.*, 2001).

1.11.1 PF1022A

As a member of this new anthelmintic class, PF1022A was shown to have an intrinsic activity higher than that of all commercially available broad-spectrum anthelmintics, including ivermectin. PF1022A was originally discovered by Meiji Seika Kaisha, LTD (Japan) and is a cyclodepsipeptide (Fig 1.11) isolated from *Mycelia sterilia*, a fungus belonging to the order *Agonomycetales*. This fungus is found in the microflora on the leaf of the native Asian plant *Camellia japonica* (Fig 1.12) (Terada, 1992), originally collected in the Ibaraki Prefecture, Japan.

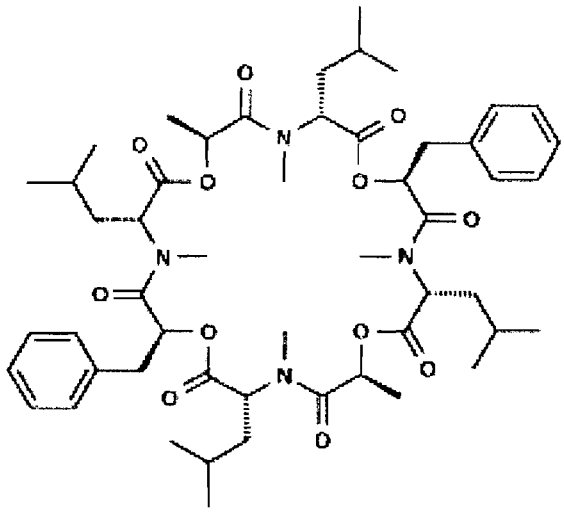

Figure 1.11 Chemical structure of PF1022A (cyclo (D-lactyl-L-*N*- methylleucyl-D-3-phenyllactyl-L-*N*-methylleucyl-D-lactyl-L-*N*- methylleucyl-D-3-phenyllactyl-L-*N*- methylleucyl)). Emodepside is a semi-synthetic derivative of PF1022A; containing two morpholine residues covalently linked to the phenyl rings of the two D-phenyllacetyl residues of PF1022A. (Kachi *et al.*, 1998)

Numerous *in vitro* and *in vivo* studies were carried out between 1998 and 2000 to further investigate PF1022A anti-parasitic action towards diverse parasitic species such as *Strongyloides ratti* and *Nippostrongylus brasiliensis* in rats, *Ancylostoma caninum* in dogs, Cyathostomes in horses, *Haemonchus contortus* and *Trichostrongylus colubriformis* in sheep, *Dictyocaulus viviparus* in cattle, *Ascaridia galli* in chickens and *Ascaris suum* in pigs. High levels of efficacy were observed with doses between 1 – 10mg/kg body weight for oral, intravenous or subcutaneous administration against all these gastrointestinal nematodes, with no clinical signs of intolerability within the host animal (Samson-Himmelstjerna *et al.*, 2000). PF 1022A has little effect on parasites that reside in the CNS of the host due to minimal penetration through the blood brain barrier, a characteristic that ensures few adverse side effects within the host animal (Kachi & Terada, 1994;Kachi *et al.*, 1998).

1.11.2 Emodepside

The novel anthelmintic compound emodepside is a semi-synthetic derivative of PF1022A, containing two morpholine residues covalently linked to the phenyl rings of the two D-phenyllactyl residues of PF1022A, which apart from endowing emodepside to a differing pharmacological profile, allows for greater solubility. Since 1990 there has been a close association between Meiji Seika Kaisha, LTD (Japan) and Bayer AG (Germany) regarding the investigation into the anthelmintic properties of PF1022A and emodepside. Over this time the bis-paramorphonyl derivative of PF1022A was identified under 2 different names; Bay 44-4400 and PF1022-221, with synthesis and use being patented under the latter in 1997 by Fujisawa Pharmaceuticals (Fig1.13). More recently this compound was renamed emodepside.

Figure 1.12 *Camellia japonica* (Theaceae, Tea Family) Native to India, China and Japan. *Mycelia sterilia* fungus within microflora of these leaves led to the isolation of the cyclic depsipeptide PF1022A, and subsequently the semi-synthetic derivative emodepside.

As previously mentioned emodepside has an altered pharmacological profile to PF1022A, in that it not only shows a high degree of efficacy against a variety of gastrointestinal nematodes, but also effectively targets filarial parasites (*Acanthocheilonema viteae, Brugia malayi* and *Litomosoides sigmodontis*). (Zahner *et al.*, 2001;Zahner *et al.*, 2001)

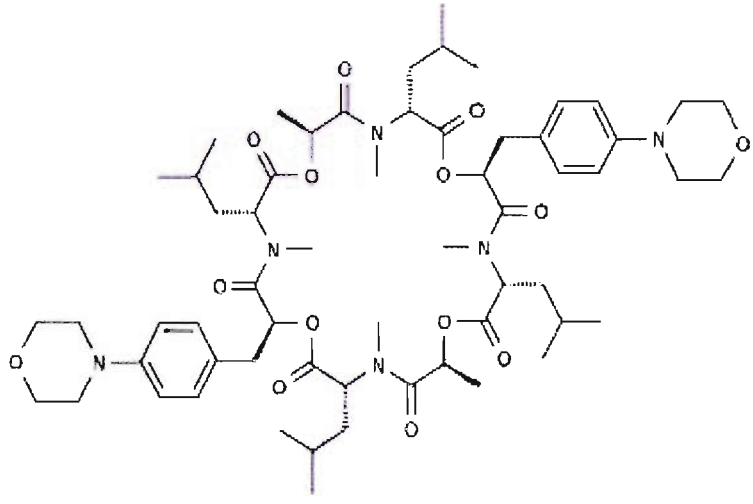

Figure 1.13 Chemical structure of Emodepside (Harder & Samson-Himmelstjerna, 2002a)

Emodepside is highly efficacious against the adult stages of the rat G.I nematodes *Nippostrongylus brasiliensis*, *Strongyloides ratti* as well as against the mouse nematode *Heligmosomoides polygyrus* in the oral dosage range of 1.0 -10 mg/kg.

However, its action against the larval stages of these nematodes varies according to the species (Nicolay *et al.*, 2000), i.e. it is less effectual against those which exist deeply in the intestinal mucosa such as *H.polygyrus* larvae. Emodepside has high efficacy against 3rd and 4th stage larvae as well as pre-adult and adult filariae tissue nematodes, with species related differences of effectiveness apparent, following single doses between 25-100mg/kg in infected *Mastomys coucha.* Emodepside is a particularly effective antifilarial agent as it is extremely potent against microfilariae of the aforementioned species, resulting in long lasting reductions in microfilaraemia levels following single oral, subcutaneous or spot-on application between 3.25 and 25 mg/kg. The anthelmintic profile of emodepside is shown in Table 1.4.

Nematode	Efficacy
Mice, Rats, Mastomys, Chicken	
H.polygyrus	1-10 mg/kg
H.spumosa	1-10 mg/kg
T.spiralis	Yes
N.muris	1-10 mg/kg
S.ratti	1-10 mg/kg
B.malayi	25-100 mg/kg
L.sigmodontis	25-100 mg/kg
A.viteae	25-100 mg/kg
A.galli	Yes
Sheep, Cattle	
H.contortus	Yes
T.circumcincta	Yes
O.ostertagi	Yes
T.colubriformis	Yes
T.axei	Yes
C.spp	Yes
N.spp	Yes
T.ovis	Yes
T.bovis	Yes
D.viviparus	Yes
Horse	
L.strongyles	Yes
S.strongyles	Yes
P.equorum	Yes
Cat, Dog	
T.cati	Yes
T.canis	Yes
T.leonina	Yes
A.tubaeforme	Yes
A.caninum	Yes
U.stenocephala	Yes
T.vulpis	Yes

Table 1.4 Anthelmintic profile of emodepside. "YES" indicates that emodepside does exert an anthelmintic effect, yet the precise dose required is undetermined. (Harder & Samson-Himmelstjerna, 2002a).

1.12 Investigating the Mechanism of Action of PF1022A and Emodepside.

Despite the continuous research into these novel anthelmintics very little is known about the exact mechanism of action. However both PF1022A and emodepside have exhibited resistance breaking properties against drugs such as ivermectin and levamisole, used against *H.contortus* in sheep and *C.oncophora* in cattle, which provides strong evidence that the cyclodepsipeptides have a unique mechanism compared to the other widely used broad spectrum anthelmintics.

Cyclodepsipeptides can form ionophores in lipid-bilayer membranes. PF1022A ionophore activity was therefore proposed as a possible mechanism of action for PF1022A (Gebner *et al.*, 1996). However, it was determined that this ionophore property does not explain the anthelmintic activity. The optical antipode of PF1022A, PF1022-001, also has ionophore activity in a lipid-bilayer but no anthelmintic activity. This finding suggested that there is a specific binding site for PF1022A in nematodes, which upon ligation results in the observed paralytic effect.

In 1992 Terada used an *in vitro* model of *A. cantonensis* to show that PF1022A inhibits the motility of worms. This paralysis was partially antagonised by the GABAergic antagonists picrotoxin and bicuculline, and completely reversed by the addition of N-methylcytisine, which stimulates ACh release from nematode nerve endings. Using a two-microelectrode current-clamp technique, on the pig intestinal parasite *A. suum,* it was shown that PF1022A elicits a gradual increase in chloride ion conductance in *A. suum* muscle cells. This response is not induced by the anthelmintically inactive optical antipode, indicating PF1022A effects may be mediated by Cl^- ions (Martin *et al.*, 1996).

Radioligand binding studies attempted to show that PF1022A binds to GABA receptors in nematodes. The inhibitory effects of PF1022A, 0.1nM - 10μM, were investigated on the binding of (2, 3-^{3}H (N))-GABA, (methyl-^{3}H)-bicuculline and (butyl-4-^{3}H)-baclofen to isolated muscle membranes of *A. suum* (Chen *et al.*, 1996). PF1022A produced a concentration-dependent inhibition of both GABA and bicuculline binding with a Ki (i.e., the ability to displace the binding of radioligand)

of 74.1± 8.5nM and 720 ± 52nM, respectively. These Ki values were very similar to those obtained for the GABA agonist muscimol, i.e., 78.1 ± 5.8nM and 790 ± 67nM, respectively, against GABA and bicuculline binding. The ability of piperazine to displace GABA and bicuculline binding was lower than that of PF1022A by about a factor of ten. PF1022A only weakly displaced baclofen binding, and its Ki value was over 100 times greater than that for baclofen itself, while piperazine did not displace baclofen binding. These data show that PF1022A can displace labelled ligands, which are selective for the mammalian GABA receptors, from *A. suum* somatic muscle membranes.

However, it is still unclear whether PF1022A acts through a GABAergic mechanism. It is not clear what the baclofen was binding to in this latter preparation since 5-aminovaleric acid was unable to displace baclofen, and baclofen had no effect on *A. suum* muscle membrane potentials. In addition bicuculline does not block nematode GABA receptors but it does block *A. suum* somatic muscle acetylcholine receptors with an IC_{50} value of 182μM (Walker *et al.*, 1992). Also, unlike most GABA agonists, PF1022A does not induce any hyperpolarization, which suggests that either it is not a direct GABA agonist, or alternatively that PF1022A binds to an identified GABA receptor isotype that is not accessed by other classical GABA agonists such as piperazine (Nicolay *et al.*, 2000).

Research has also been conducted to elucidate the mechanism of action of emodepside. It was shown that a synergistic activity exists between emodepside and the GABA agonist piperazine in anthelmintic targeting of *T.spiralis* larvae, *H.polygyrus,* and *H.spumosa.* A combination of piperazine and emodepside exerted an expulsion rate of *Heterakis spumosa* from the intestine of mice of more than five orders of magnitude greater than the sum of the effects of the two compounds alone. The combination of these two anthelmintics also resulted in a significantly greater degree of degeneration of the intestine and nerve cords of *H. spumosa* compared with the compounds administered on their own (Nicolay *et al.*, 2000). However, the basis of this synergism is still not fully understood with regards to the interaction of these two compounds, and does not provide sufficient evidence to state that emodepside has a GABAergic mechanism of action. To clarify, the potent effect may merely be due to the additive effect of two mechanistically dissimilar anthelmintic compounds, rather than a dual activity via a single pathway.

In the late 1990s a new study using electrophysiological and pharmacological techniques was undertaken using the body wall muscle of *A. suum* to explore further the mechanism of action of PF1022A and emodepside (Willson *et al.*, 2003). For these pharmacological studies 1cm strips of dorsal body wall muscle were suspended in an organ bath and recordings made using an isometric transducer. Emodepside, up to 10μM, produced a small relaxation of basal tension of the muscle strip. Emodepside, 10μM, also reduced the amplitude of a twitch contraction of the muscle due to application of 30μM acetylcholine, the body wall muscle excitatory transmitter (Johnson & Stretton, 1985). This effect was maximum following incubation of the muscle with emodepside for 10 minutes prior to the application of acetylcholine. The threshold for the inhibition of the acetylcholine contraction was around 5μM.

Electrophysiological experiments have furthered the understanding of emodepside mechanism by providing evidence for the necessity of specific ions, namely Calcium (Ca^{2+}) and Potassium (K^{+}) (Willson *et al.*, 2003). Perfusion of emodepside (2 min duration) over *A. suum* muscle cells resulted in a slow significant hyperpolarization (5.5 ± 0.96mV) with an abolition of this change in membrane potential if Ca^{2+} was removed from the bathing medium. This is interesting with regards to the parent compound PF1022A, as it suggests a distinctly different mode of action for emodepside, as early electrophysiological studies indicated that PF1022A-induced paralysis is antagonized by addition of Ca^{2+} (Martin *et al.*, 1996). The hyperpolarizing effects of emodepside have also been shown to be K^{+}-dependent, through the use of selective potassium channel blockers such as 4-aminopyridine (250μM) and tetraethylammonium (5mM). Addition of these compounds resulted in a slight depolarization of the muscle cell (2.8± .05mV), which failed to be hyperpolarized upon addition of 10μM emodepside, until the potassium channel blockers were washed out. Amalgamation of this ion dependency data has led to the hypothesis that emodepside-induced relaxation may be governed by a Ca^{2+}-activated potassium channel (Harder & Samson-Himmelstjerna, 2002b).

1.13 Emodepside Acts through a Latrophilin-like Receptor.

Molecular techniques have been successful in identifying a possible protein target in *H.contortus* for PF1022A and emodepside (Saeger *et al.*, 2001). Using PF1022A ligand immunoscreening of an *H.contortus* cDNA library, a novel orphan heptahelical transmembrane receptor (110kDa) was identified and named HC110-R. HC110-R has about 31% identity with the latrophilin receptor from human, bovine, and rat (Saeger *et al.*, 2001). Latrotoxin, a vertebrate specific neurotoxic protein of the black widow spider venom, is a ligand for the mammalian orphan latrophilin receptor. Latrophilin-1 isolated from mammalian brain is a G-protein coupled receptor of 210 kDa, with two close homologs latrophilin-2 and latrophilin-3 recently identified (Matsushita *et al.*, 1999). The mammalian latrophilins, HC110-R, CEB0457.1 and CEB0286.2 form a highly significant monophyletic subfamily within the secretin receptor family.

α-Latrotoxin (α-LTX) bound the extracellular N-terminal region of HC110-R transfected in HEK-293 cells and induced an influx of calcium through channels which were blocked by both cadmium and nifedipine. Emodepside antagonised α-LTX binding to HEK-293 cells transfected with HC110-R. However, emodepside on its own did not induce calcium signalling in HEK-293 cells transfected with HC110-R. It was concluded that both PF1022A and α-LTX bound to the N-terminal portion of HC110-R (Saeger *et al.*, 2001) and that identification of the natural ligand for HC110-R would reveal which nematode physiological signalling pathways were affected by both PF1022A and emodepside.

1.14 α-Latrotoxin and its mechanisms of action

α-LTX is the active component of black widow spider venom, being synthesised in the venom glands of the spider (Frontali *et al.*, 1976). α-LTX functions as a powerful neurotoxin by triggering massive synaptic vesicle exocytosis from presynaptic nerve terminals, which results in disastrous effects of the spider bite on

the neurosecretory, neuromuscular and cardiovascular system (Grishin, 1998;Saibil, 2000). α-LTX is a large protein toxin (120 kDa) that contains 22 ankyrin repeats, which are thought to mediate intra and inter-molecular interactions (Sedgwick & Smerdon, 1999).

The first three-dimensional structure of α-LTX has shown that it is not a monomer but exists either as a dimer or tetramer (Orlova *et al.*, 2000). The dimers form in the presence of EDTA (divalent ion chelator). However, the tetramers will only form in the presence of either Ca^{2+} or Mg^{2+} ions. The tetrameric 3D structure, molecular weight ~520KDa, is believed to be propeller-shaped consisting of an open upper side and a compact base (Fig 1.14). There are three distinct domains present within the tetrameric structure: the wings, the body and the head. The dimer corresponds to one half of the tetramer and therefore also consists of the same three domains, albeit with a different orientation. The L-shaped body forms the backbone of the complex, with the wings attached to the vertical parts of the body. A key characteristic of the tetrameric α-LTX molecule is the presence of a 10-25 Å central channel, formed as the gap between the four heads.

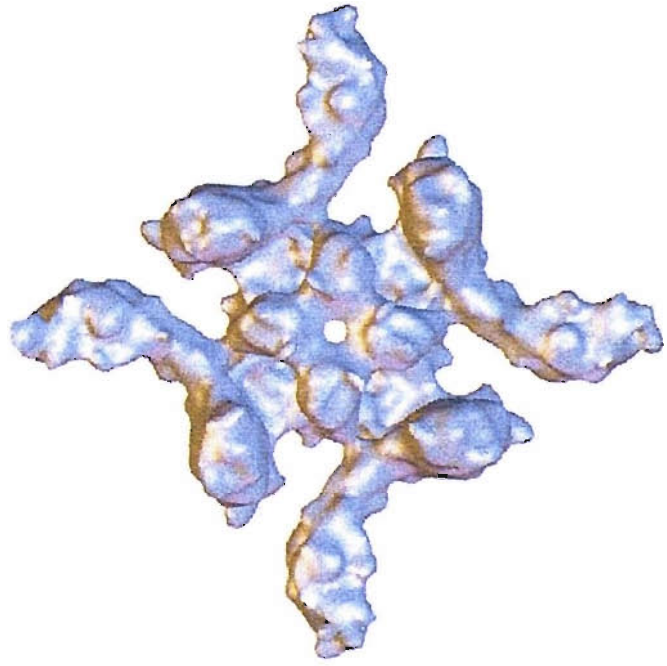

Figure 1.14 The tetrameric form of α-LTX. Taken from (Orlova *et al.*, 2000)

Application of LTX to nerve terminals is known to cause massive neurotransmitter release via synaptic vesicle exocytosis. This process has duality, in that, the toxin first binds to highly specific receptors on the terminals and then triggers synaptic vesicle exocytosis (Sudhof, 2001). The mechanism by which this occurs has come under much scrutiny. Latrotoxin is able to form stable pores in lipid bi-layers, but can also bind to two different presynaptic membrane receptors, acting in both a calcium dependent and independent manner (Saibil, 2000), depending on the receptor class. Both these receptors were first identified in brain tissue, existing with similar abundance and nanomolar affinity for α-LTX. However, the first class, the neurexins, require binding of α-LTX in the presence of calcium and are therefore thought to inable the toxin to exert its detrimental effects via a calcium dependent pathway. Whereas, the second class, the latrophilins or Calcium-Independent Receptor for Latrotoxin (CIRL), are capable of binding α-LTX in a calcium independent manner. α-LTX has also been shown to require the core fusion proteins, the SNARE proteins (synaptobrevin, syntaxin, and SNAP-25) and Munc13-1, to cause vesicular release. Blockade of these proteins with botulinum toxin and tetanus toxin diminishes α-LTX action (Capogna *et al.*, 1997). These proteins therefore must play a role in one of α-LTXs many mechanisms of action to cause vesicle release.

1.14.1 Pore formation

α-LTX causes massive release of neurotransmitter through toxin insertion into the plasma membrane followed by pore formation. These pores act as non-selective cation channels (Wanke *et al.*, 1986;Finklestein *et al.*, 1976). α-LTX induces pores by assembling into cyclical tetramers that possess a central channel and a hydrophobic base, which allows the toxin to incorporate into the membrane. The dimeric form was unable to cause efflux of noradrenaline from isolated rat brain synaptosomes, unlike the tetrameric form (Orlova *et al.*, 2000).

Based on EM images it is believed that, α-LTX in its tetrameric form fully permeates the lipid bilayer with its base. The upper part of the tetramer remains above the membrane with its wings partially embedded within the membrane. The

central channel is then able to permeabilize the membrane. These α-LTX channels conduct both divalent and monovalent cations such as Ca^{2+}, Mg^{2+}, Na^{+} or K^{+} but are blocked by La^{3+} (Hurlbut *et al.*, 1994). Channel formation is believed to occur at toxin concentrations in excess of 100pM as application at this dose to rat adrenal chromaffin cells caused the development of large conductance changes in Ca^{++} permeable ion channels, and a rise in cytosolic Ca^{++} to levels near 1μM (Liu & Misler, 1998). These events preceded the enhancement of spontaneous exocytosis. α-Latrotoxin-induced channels where also shown to be induced *de novo*, where they occur concurrently with a blockade of voltage-dependent Na^{++} and Ca^{2+} currents.

The induction of pore formation does not occur merely by the addition of the toxin to the medium, in that, insertion into biological membranes is firstly dependent on a receptor interaction (Khvotchev & Sudhof, 2000). In *Xenopus* oocytes, which do not express α-LTX receptors, application of α-LTX resulted in no opening of calcium channels. Only when brain proteins were expressed by injection of total brain mRNA into the oocytes (and thus synthesis of α-LTX receptors) were calcium channels observed (Filipov *et al.*, 1990;Umbach *et al.*, 1990). This, therefore, suggested that binding of α-LTX to receptors is necessary for the toxin to insert into biological membranes (Khvotchev & Sudhof, 2000).

1.14.2 The Neurexins

The first work on the nature of α-LTX receptors was produced by affinity chromatography experiments through the purification of binding proteins on immobilized α-LTX (Petrenko *et al.*, 1990). From the numerous proteins purified it was discovered that the neuron-specific cell-surface polymorphic proteins, the neurexins, were candidate α-LTX receptors (Ushkaryov *et al.*, 1992).

Neurexins are synthesised in vertebrates by three separate genes, governed by two different promoters. This results in the formation of three neurexin-α (Iα, IIα, IIIα) and three shorter neurexin β proteins (Iβ, IIβ, IIIβ). These proteins all exhibit numerous alternative splicing patterns leading to the production of many hundreds

of isoforms (Missler & Sudhof, 1998). Neurexin α and β have the following extracellular regions: an O-linked glycosylation site, a transmembrane domain and a short C-terminal region. Only α-, but not β-neurexins are evolutionarily conserved.

Although *in situ* hybridisations indicate that neurexins are expressed in neurons, no precise ultrastructural localization is available. However, there exists indirect evidence for high neurexin density at the synapse, as subcellular fractions revealed a high degree of enrichment of neurexins within active zones (Butz *et al.*, 1998). More recently neurexins have been shown to act as presynaptic cell-adhesion molecules. Neurexins are capable of binding to postsynaptic cell-adhesion molecules such as dystroglycan and neuroligins, which are thought to perform important functions in shaping synapses. Intracellularly, neurexins interact with the PDZ domain protein CASK, and the synaptic vesicle protein synaptotagmin, which may lead to the modulation of Ca^{2+} channels. This polymorphic nature and binding activity demonstrated by the neurexins indicates that they act as cell-recognition and cell-adhesion molecules at the synapse (Missler & Sudhof, 1998). Using knockout mice, it has been demonstrated that α-neurexins are necessary for the functional organization of synapses where they are required for the activity of presynaptic Ca^{2+} channels (Missler *et al.*, 2003).

Neurexin Iα was shown to bind α-LTX in the nanomolar range, only in the presence of calcium, therefore presenting itself as a good candidate for an α-LTX receptor (Petrenko *et al.*, 1990;Ushkaryov *et al.*, 1992;Davletov *et al.*, 1995). However, the fact that α-LTX could produce vesicle exocytosis in the absence of calcium initially negated the evidence for neurexins as true α-latrotoxin receptors.

To further investigate this, neurexin I-α deficient mice were utilised to clarify the role of neurexin I -α in α-LTX-induced vesicular exocytosis (Geppert *et al.*, 1998). It was found that neurexin I-α deficient mice did not exhibit any behavioural or developmental defects, however a 50% reduction in α-LTX binding to brain membranes was noted. These effects only occurred in the presence of calcium. It was also noted that α-LTX-induced glutamate release from neurexin I-α deficient mice synaptosomes was not affected in the absence of calcium but greatly reduced in the presence of calcium. These results showed that *in vivo*, neurexin 1α is

responsible for approximately half of the α-LTX binding sites in the presence of calcium, and is required for α-LTX to elicit transmitter release.

Expression of neurexin 1α in PC12 cells resulted in a 10-100-fold increase in sensitivity to α-LTX (Sugita *et al.*, 1999), an equal efficacy to that obtained with expression using latrophilin (see 1.14.3). This implies that both these classes of α-LTX receptor can mediate α-LTX action in transfected PC12 cells, a typical example of dense-core vesicle exocytosis.

Neurexin I-α contributes only to the calcium-dependent affects of α-LTX, suggesting an alternative pathway for α-LTX toxic action independent of neurexin I-α, and thus calcium.

1.14.3 The Latrophilins

The fact that α-LTX causes vesicular release in the absence of calcium ions, and when the pore-forming properties of α-LTX are blocked (Pashkov *et al.*, 1993), suggested that α-LTX must be acting through a further receptor type, in order to stimulate vesicular exocytosis.

The purification and cloning of a calcium–independent receptor for α-LTX was concurrently described by two groups, hence the two separate names for the same receptor, CIRL (Calcium-Independent Receptor for Latrotoxin) and latrophilin (Davletov *et al.*, 1996;Krasnoperov *et al.*, 1997;Krasnoperov *et al.*, 1996). Further cloning revealed three closely related forms of latrophilin in vertebrates, namely latrophilin 1, 2 and 3 (Sugita *et al.*, 1998;Ichtchenko *et al.*, 1999).

The structure of latrophilin is that of a glycosylated, seven transmembrane, G-protein coupled receptor, belonging to the ubiquitous secretin family of receptors (Lelianova *et al.*, 1997). Latrophilin has a large extracellular domain, like that of cell adhesion molecules, and a large intracellular domain (Krasnoperov *et al.*, 2002).

At the N terminus, after the signal peptide, there is a succession of individual domains spanning approximately 500 amino acids. Latrophilin may therefore be involved in cell-to-cell interaction as well as signal transduction. Within these is a lectin-like sequence; a region homologous to olfactomedins and myocilin and a short, cysteine-rich sequence (Fig 1.15). The latter is located outside of the first transmembrane region in latrophilin and is highly homologous to sequences found in several G-protein-linked receptors (Sugita et al 1998), where it may direct cleavage of the receptors after the last cysteine residue just N-terminal to the first transmembrane region (Gray et al 1996; Krasnoperov et al 1997). This sequence may represent a proteolytic cleavage signal during the maturation of G-protein linked receptors, and has been termed GPS domain for G-protein-coupled receptor proteolytic site domain (Gray et al 1996; Krasnoperov et al 1997; Ichtchenko et al 1999). Following the seven transmembrane regions, latrophilins have an unusually long cytoplasmic tail of approximately 500 residues that is subject to extensive alternative splicing (Sugita et al 1998; Matsushita et al 1999). Various extracellular domains of the three latrophilins may also indicate multiple ligand binding sites.

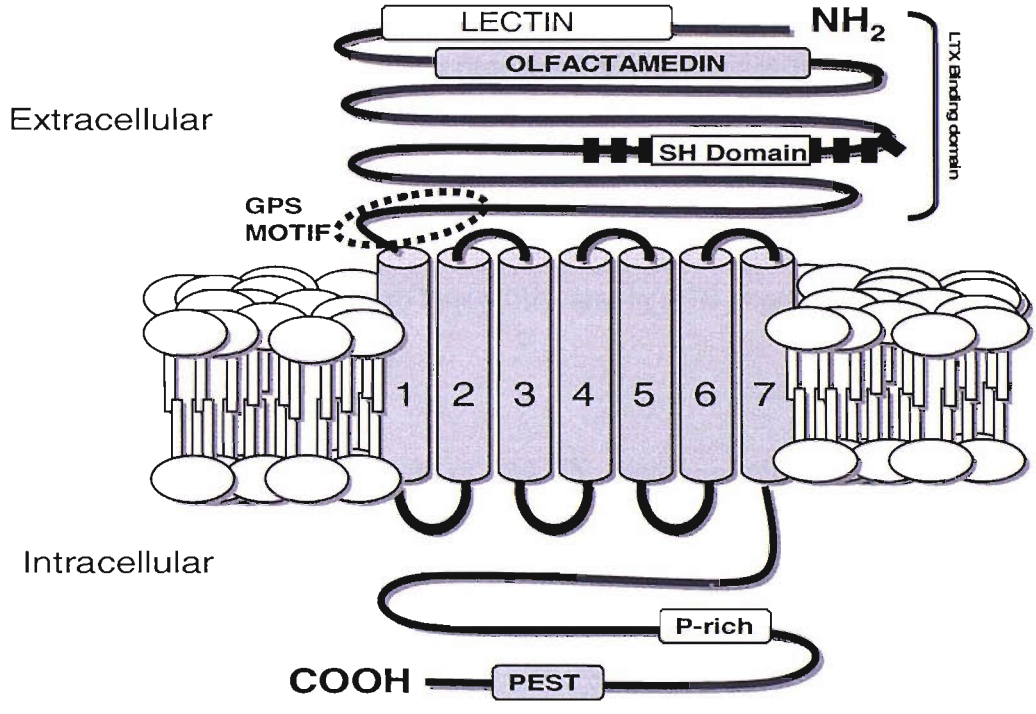

Figure 1.15 Diagram showing the conserved domains within the *C. elegans* LAT-1 receptor. 1-7 represent the transmembrane domains. The GPS motif indicates a proteolytic cleavage site, implicated in receptor trafficking (Krasnoperov *et al.*, 2002). The cysteine rich extracellular region is indicated as SH Domain. The PEST sequence is found in many short-lived eukaryotic proteins and plays a role in their degradation (Chen & Clarke, 2002). (Created by K.Amliwala).

There exists differential expression of the three vertebrate latrophilins in a pattern that suggests an extensive function not related wholly to neurons. Latrophilin-1 was initially thought to be predominant in brain regions (Krasnoperov *et al.*, 1997), however, recent studies have shown low levels of expression in all tissues (Sugita *et al.*, 1998). Northern blotting experiments indicate latrophilin-2 is found ubiquitously with highest concentrations found in placenta, kidney, spleen, ovary, heart, and lung (Ichtchenko *et al.*, 1999). Both latrophilin-1 and -2 bind α-LTX with nanomolar affinity, albeit with latrophilin-2 doing so with less affinity than latrophilin-1 (Ichtchenko *et al.*, 1999).

That fact that many parts of the latrophilin isomers resemble that of other G-protein receptors indicates that calcium-independent α-LTX-stimulated neurotransmitter release may be controlled by a receptor-mediated activation of these heterotrimeric G-proteins. G-protein superfamily receptors have been shown before to bind peptide hormones and stimulate exocytosis via a second messenger mechanism (Krasnoperov *et al.*, 1997). G-protein receptors have also been shown to be highly enriched in synapses (Aronin & DiFiglia, 1992). How this latrophilin G-protein interacts with the docking / fusion processes of the vesicles is unclear. It has been demonstrated that α-LTX causes an elevation in cAMP and IP_3 levels (Lelianova *et al.*, 1997). This group also found that latrophilin co-purifies with a 42kDa protein, which reacts with antibodies raised to $G\alpha_o$, but not against $G\alpha_I$ subunits. It has also been shown that $G_{\alpha q}$ is linked to latrophilin, and in cells expressing latrophilin there is an increase in IP_3 production.

The calcium-independent action of α-LTX therefore requires interaction with latrophilin to cause vesicular release. Whether it is the direct activation of the G-protein, which interacts with the docking and fusion mechanism, or, the stimulation of a second messenger system to increase vesicular fusion, is at this moment unclear.

It is important to note that two latrophilin homologues have been identified in *C. elegans* namely B0457.1 (Lat-1) and B0286.2 (Lat-2). C-terminal GFP constructs have attempted to characterise expression patterns for these receptors in *C. elegans* (Mastwal,) Findings indicate that *lat-1* expression starts after gastrulation and

continues into the adult. It is expressed in the hypodermal, pharyngeal and some neuronal cells in the embryo. During larval development it is expressed in mechanosensory neurons and interneurons in the head and tail, gland cell in pharynx, gonadal sheath cells, spermatheca, uterine epithelial cells and intestinal cells. *Lat-2* appears to be expressed in the g1 gland cell and arcade cells in the head in which it localizes to the syncytial end of the process, and the expression cycles with the moults.

More recently a mutant form of α-LTX, LTX^{N4C}, has helped elucidate the mechanisms of action of the toxin, and shed new light on the relative importance of the latrophilin and neurexin receptors. The mutant toxin (Ichtchenko *et al.*, 1998) differs form LTX^{WT} by a four amino acid insert between the N-terminal and the ankyrin repeats, which results in an inability of the mutant toxin to form a tetrameric structure. Unlike LTX^{WT}, this mutant form is therefore unable to act through pore formation due to an inability to insert into the membrane, and so acts only through receptor stimulation. To further investigate receptor mediated α-LTX action, using this mutant form, it was necessary to exclude the toxin's action at either the neurexin or the latrophilin receptors. Neurexins were chosen for two reasons, namely; they are apparent candidates to mediate the receptor-transduced LTX action, which critically requires calcium, and secondly toxin binding to all members of this family can be totally abolished by a simple replacement of Ca^{2+} with Sr^{2+}. Importantly, the use of Sr^{2+} did not alter the interaction of the mutant toxin with the latrophilin receptor.

It was found that Sr^{2+} could fully replace calcium in LTX^{N4C}-evoked exocytosis of glutamate-containing synaptic vesicles in rat synaptosomes and hippocampal cultures, acetylcholine-containing synaptic vesicles at mouse NMJs, and catecholamine-containing large dense core vesicles in bovine chromaffin cells. In all the models, the mutant toxin was inactive when only magnesium ions were present, confirming the previous observation that receptor-mediated LTX-evoked secretion requires extracellular calcium. These results cannot be attributed to an ionophore action of the mutant toxin.

These findings indicate latrophilin as the main LTX receptor that transduces an exocytotic signal. This signalling is masked by massive calcium influx leading to exocytosis when LTX^{WT} was used and can only be observed with the mutant toxin. The role of extracellular calcium remains unclear, it may be necessary to serve as an extracellular co-factor for latrophilin and its signalling partners, or participate in the activation of intracellular calcium stores required for LTX^{N4C}-induced release, or may even directly induce secretion after entering the cell via latrophilin-linked cation channels.

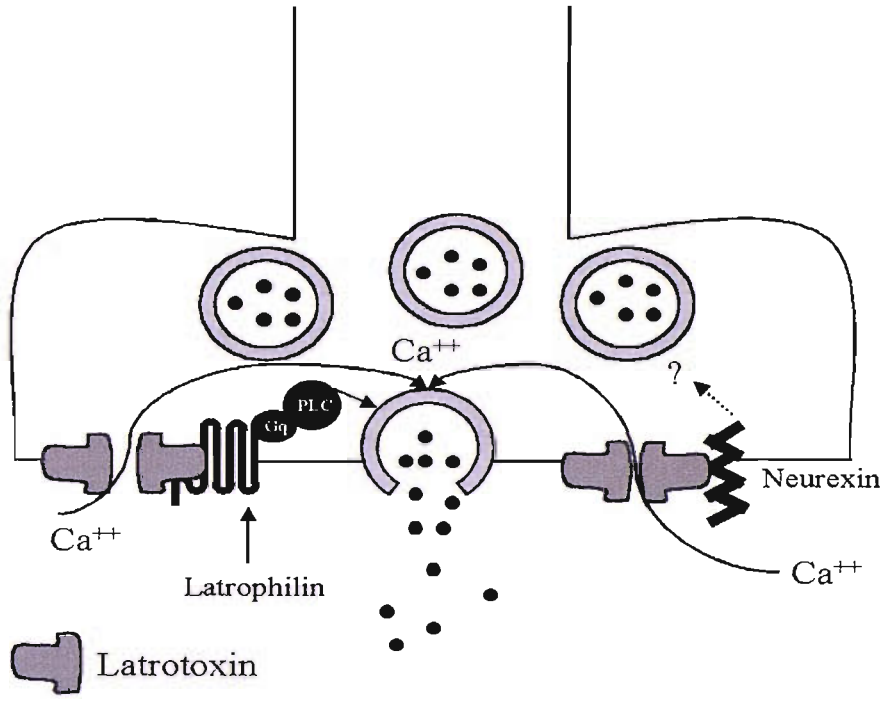

Figure 1.16 Diagram to summarise the multiple mechanisms of αLTX action taken from (Saibil, 2000). αLTX is represented in a dimer form . αLTX has three distinct mechanisms. In a tetrameric form, it forms pores in the membrane allowing influx of cations. Secondly, it binds neurexins in a calcium dependent manner. Thirdly, it binds latrophilin independently from calcium ions.

Project Aims

The increased resistance to existing anthelmintics requires the need to develop novel compounds. Emodepside is a novel drug which has a broad-spectrum and resistance breaking anthelmintic properties. The precise mechanism of action of this drug is unclear. In this study two nematode species, *A. suum* and *C. elegans*, were used to investigate the mechanism of action of emodepside.

A. suum muscle has previously been used to provide insights into the mechanisms underlying the action of PF1022A and emodepside (Martin *et al.*, 1996) (Willson *et al.*, 2003). Using an *in vitro* muscle preparation, this study aimed to provide further insight into the mechanisms underlying emodepside induced relaxation of nematode muscle.

The model genetic organism *C. elegans* has been previously used to determine the target site of the existing anthelmintic ivermectin (Dent *et al.*, 2000). *C. elegans* were therefore used as a model organism to determine the molecular and genetic determinants underlying emodepside action. This investigation has been greatly aided by the availability of numerous mutants and the use of forward and reverse genetic techniques that interfere with gene expression.

Chapter 2

Materials & Methods

2.1 *A.suum*

2.1.1 *A. suum* maintenance

A.suum were obtained from a local abattoir and maintained for up to 5 days in artificial perienteric fluid (APF) with the following composition in mM NaCl 67, CH_3COONa 67, $CaCl_2$ 3, $MgCl_2$ 15.7, KCl 3, glucose 3,Trizma® base 5, pH 7.6 with glacial acetic acid, at 37°C. For reduced Cl^- experiments, chloride salts were replaced with impermeant anions, either isethionate or acetate.

2.1.2 Muscle strip tension recordings

A.suum dorsal muscle strips (DMS) were prepared by dissecting a 1cm strip of the body wall muscle immediately anterior to the genital pore. This was obtained by cutting length-wise along both lateral cords and discarding the ventral portion. Any remaining intestine still attached to the somatic muscle was carefully removed. Dorsal muscle was used as it is devoid of motorneurone somata, which are only present in the ventral nerve cord. Dorsal muscle however does contain the dorsal inhibitory and dorsal excitatory motorneurone terminals, which have reciprocal synapses with each other. Muscle preparations remained viable for up to two hours. Preparations that did not respond to ACh were rejected.

Effects of resting tension and activity of the DMS in response to exogenous ACh were investigated by securing the muscle strips in a 15ml organ bath and connecting them by thread to a 2g isometric transducer. The preparation was subject to a 1g load and maintained at 37°C with a heated water jacket. Drugs were added in volumes of no greater than 1% of the bath volume. Drugs were rapidly mixed within the organ bath by gassing the bath with room air. Drugs were then washed out by at least 3 times the bath volume of APF. A hard copy of the data was obtained on a flat bed chart recorder (BBC, Goerz, Metrawatt, Austria).

2.1.3 Drugs

ACh, GABA and emodepside were prepared fresh on the day of the experiment. ACh and GABA were prepared in APF (normal or reduced Cl^-). Emodepside was initially dissolved in 100% ethanol at 10^{-1} M and then diluted in APF (normal or reduced Cl^-) so that the final concentration of ethanol in the organ bath was no greater than 0.1%.

50μM ACh was used to pre-tone the *Ascaris* dorsal muscle strips. Once consistent contractions were observed to ACh, following a 30 sec application, 50μM ACh was administered and left bathing the tissue for 10min, to observe the natural relaxation back to basal muscle tone levels. ACh was again administered (50μM) and a supra-maximal concentration of GABA (100μM) applied at the point of maximal contraction. This protocol was subsequently repeated with 10μM emodepside, again added at the point of maximal ACh induced contraction. A 10 min resting interval was employed between drug applications.

2.1.4 Data analysis

In order to standardise data from muscle strip tension recordings, and thereby eliminate differences in individual DMS preparations, the relaxation rate per minute was calculated as follows:

$$\textbf{\% Relaxation rate min}^{-1} = \textbf{P-R/10 x 1/100}$$

Where "P" is the muscle tension (g) during the peak contraction and "R" is the muscle tension immediately prior to the wash.

2.2 *C. elegans*

2.2.1 Strains

C. elegans were grown on nematode growth medium (NGM) plates as described by Brenner (1974). Nematode Growth Medium for *C. elegans* (500ml) was made, pre-autoclave, with the following composition; NaCl 1.5g, Agar 10g, Peptone 1.25g, Distilled Water 487.5ml. Post-autoclave the medium was supplemented with the following sterile 1M solutions; $CaCl_2$ 0.5ml, $MgSO_4$ 0.5ml, KH_2PO_4 12.5ml, and cholesterol 0.5ml of 5mg/ml stock (in 100% EtOH).

Hermaphrodite animals were fed and grown on a bacterial lawn (*E. coli* OP50) and picked for experiments from 3-5 day–old plates. *C. elegans* strains used and details of mutations are listed in Appendix 1.

Locomotion assays

2.2.2 Ivermectin and emodepside agar plate assay

Plates were prepared fresh for each set of assays. NGM for *C. elegans* was prepared as above (Brenner, 1974). Ivermectin, emodepside, or vehicle control (ethanol 1%) was added after autoclaving, once the media had cooled to 60°C. Drug additions were made from a 10^{-3} M or 10^{-4} M stock (ivermectin or emodepside), prepared fresh in 100% ethanol, to generate drug concentration ranges on plates (5cm or 9cm) from 600 fg/ml^{-1} to 1000 ng/ml^{-1} (emodepside) and 0.125ng/ml – 40ng/ml (ivermectin), whilst ensuring final ethanol content of $\leq$1%.

Once set, the plates were inverted and left overnight to dry. Twenty-four hours after the plates had been poured, 50 µl of OP-50 bacterial culture was spread on each plate. Plates were incubated for 2 more days at room temperature for the

culture of a robust bacterial lawn. To allow comparison between different sets of assays, plates were always prepared as described above, duplicate assays were performed, and an N2 wild type control was included with each experiment.

Eggs were isolated from gravid adult hermaphrodite worms by the alkaline hypochlorite method as outlined below (Riddle, 1997).

Worms were harvested after 3-5 days growth at 20°C on 9cm NGM plates. Adults were floated off the plate in 5ml of sterile M9 buffer (composition in g/litre Na_2HPO_4 6, KH_2PO_4 3, NaCl 5, $MgSO_4.7H_2O$ 0.25), and transferred by pipette to a sterile disposable 15ml screw cap centrifuge tube. Care was taken to ensure that eggs already present on the plate were not removed in the washing process. The solution was then centrifuged for 2mins at 1000 rpm using a Sorvall® Legend RT desktop centrifuge. The resultant pellet was washed 2x in 5ml M9 buffer to remove contaminants and OP-50. 7ml of alkaline hypochlorite solution (2ml fresh clorox bleach, 5ml 1M NaOH) was then added to the pellet, to dissolve adult bodies. The solution was left for ≤5mins, inverting every 1min to mix, until the adult worms were no longer visible. The tube was then centrifuged at 1500 rpm using a Sorvall® Legend RT desktop centrifuge for 2min to collect a white egg pellet, the supernatant removed, and the pellet quickly resuspended in 10ml M9 buffer. The tube was inverted several times and centrifuged at 1500 rpm using a Sorvall® Legend RT desktop centrifuge for 1min to re-collect the white egg pellet. This wash procedure was carried out 3x until the smell of the alkaline hypochlorite solution had dissipated. The egg pellet should be white or very pale yellow; if it appears dark yellow, eggs have been over exposed to the bleaching process and are probably unviable. The pellet was suspended in a final volume of 0.5ml M9 buffer. 10µl of this solution was placed on a glass slide and viewed under a dissecting microscope (40x objectives) to determine egg yield (approx 100 eggs/20µl).

Approximately 100 eggs were placed on the different concentration drug plates (ivermectin or emodepside) or vehicle control (1% ethanol). The plates were incubated for up to 5 days at 20°C and the developmental progress of the worms was monitored through larval stages (L1-L4), to fertile adulthood. Locomotion rate was quantified by counting body bends/min, over 1min, of mature adult animals on

the plates. A body bend was counted each time the tip of the tail passed through half maximum or minimum amplitude

2.2.3 Aldicarb and Levamisole agar plate assay

Plates were prepared fresh for each set of assays. NGM for *C. elegans* was prepared as above (see 2.2.1) (Brenner, 1974). Aldicarb, levamisole or vehicle control (ethanol 1%) was added after autoclaving, once the media had cooled to 60°C. Drug additions were made from a 10^{-3} M or 10^{-4} M stock, prepared fresh in 100% ethanol, to generate drug concentration ranges in plates (5cm or 9cm) of 0.5mM, 1mM and 2mM (aldicarb) and 150μM and 300μM (levamisole), whilst ensuring final ethanol content of ≤1%. Plates were seeded with an OP-50 bacterial lawn (see above).

To assay the effect of these drugs on *C. elegans* locomotion, 20 adult worms were transferred from seeded NGM plates or F2 generation RNAi plates in the case of RNAi experiments (see 2.10 below for RNAi protocol) to aldicarb or levamisole plates, and left to equilibrate for 5mins (time 0). Following 10 mins exposure, the number of worms totally paralysed was recorded. Total paralysis was observed as a lack of locomotion, even in response to gentle nose tap, and a rod-like appearance. For aldicarb, paralysis was assayed at 10 min intervals until such time that 100% of worms were totally paralysed. For levamisole, paralysis was assayed at 2 min intervals for the first 20 min, and then every 5 mins thereafter, until all worms were paralysed.

These assays were kindly performed by Nemisha Patel.

2.2.4 Emodepside thrashing assay

Adult *C. elegans* were placed into a 3 cm Petri dish containing Dent's saline (mM: 144 NaCl, 10 $MgCl_2$, 1 $CaCl_2$ 6 KCl, and 5 Hepes, pH 7.4) supplemented with a few flakes of Bovine Serum Albumin (0.1%). *C. elegans* body bends were counted for 30 seconds. Emodepside (10μM final concentration) or vehicle control (0.1% ethanol) was applied to the Petri dish and body bends were measured at 1, 5, 10, 15, 20, 30 and 60 minute intervals. A body bend was counted each time the tip of the tail deflected and returned to the same maximal position.

2.2.5 Electropharyngeogram [EPG] recordings.

Individual worms were placed in a Petri dish containing modified Dent's saline (mM: 144 NaCl, 10 $MgCl_2$, 1 $CaCl_2$ 6 KCl, and 5 Hepes, pH 7.4). A razor blade was used to cut the worm just posterior to the pharynx, which caused the cuticle to retract, exposing the isthmus and terminal bulb. This semi-intact worm preparation consisted of the pharynx, the nerve ring, and the enteric nervous system.

Dissected *C. elegans* heads were transferred to a custom built chamber (volume 500μl) on a glass clover slip. Suction pipettes were pulled from borosilicate glass (Harvard instruments, diameter 1mm). Tip diameter ranged from 20 to 40μm, depending on the size of the worm. The suction pipette was filled with Dent's saline and mounted in a holder with a tubing port through which suction can be applied. The pipette was lowered into the chamber and placed close to the nose of the worm. Suction was applied to capture the worm. The suction pipette was connected to a silver electrode, which was connected to a HS2 head stage (Axon Instruments), which in turn was connected to an Axoclamp 2B-recording amplifier. Data were acquired using axoscope 8.0 (Axon Instruments), and a hard copy was displayed on a Gould RS 3200 chart recorder. Dissected pharynxes where recorded in normal Dent's for 2mins. Normal Dent's was then the replaced with Dent's containing 500nM, or 1μM 5-HT for 2mins, where stated. Dent's containing no 5-HT and various concentrations of emodepside was then applied for 10 minutes. Dent's containing 5-HT was then re-applied. These assays were kindly performed by Dr. J. Willson.

2.2.6 Chemicals, reagents, kits and oligonucleotides

Enzymes for DNA and RNA work were purchased from Promega (UK), New England Biolabs (NEB), or Roche Applies Science (UK) and were used as recommended by the manufacturers. All other chemicals or reagents were analytical grade or better and purchased from Sigma (UK). TOPO® cloning kits, as well as custom designed oligonucleotide primers were purchased from Invitrogen life technologies (UK) and used as directed by the manufacturer. Mini-prep, PCR product purification and gel extraction kits for use with DNA samples were purchased from Qiagen (UK) and used as recommended by manufacturer.

2.2.7 Genomic DNA extraction

Adult worms were floated from 5cm plates, using 2ml M9 buffer, and transferred in solution to a sterile micro-centrifuge tube. The worms were left at room temperature to sink naturally to the bottom of the tube, after which the bacterial supernatant was discarded. 100µl lysis buffer (50 mM KCl, 10 mM Tris pH 8.3, 2.5 mM $MgCl_2$, 0.45% NP-40 (IGEPAL), 0.45% Tween-20, 0.01% Gelatin) supplemented with proteinase K (10 mg/ml) was then added to the micro-centrifuge tube and the samples subjected to the following conditions: -80 °C 15 mins, 60°C 1hr (vortexed every 15 mins), 95°C for 15 mins. This end product was diluted with 500µl T.E. buffer (10 mM Tris adjusted to pH 8.0 with HCl, 1 mM EDTA).

2.2.8 Trizol RNA extraction

The following protocol was carried out in a well ventilated fume cupboard. Adult worms were washed from 5cm plates using 1ml of sterile M9 buffer, per plate, and transferred by pipette to 1.9ml microcentrifuge tubes. 1ml of Trizol was added to each tube and the tubes vortexed to lyse worms. The samples were allowed to incubate at room temperature for 1hr, vortexing every 20mins. The tubes were then centrifuged at 13,000 rpm for 10mins (4°C) to remove any insoluble material. The resultant supernatants were transferred into fresh tubes, supplemented with 200µl chloroform, vortexed for 15secs and allowed to incubate at RT for an additional

5mins. In order to separate the phases samples were then centrifuged for 15mins at 13,000 rpm (4°C), and the upper aqueous phase transferred to a fresh microcentrifuge tube supplemented with 500µl isopropanol. To precipitate, RNA samples were subsequently incubated for 10mins at RT, and the RNA recovered by centrifugation at 13,000 rpm for 10min (4°C). After discarding the supernatant, the pellet was washed with 100µl of 75% ethanol (in DEPC H_2O) and re-centrifuged to collect the pellet. The supernatant was removed and the pellet allowed to air dry. Finally, the pellet was re-suspended in 50µl DEPC H_2O.

2.2.9 Construction of *C. elegans* complementary DNA library

Complementary DNA (cDNA) was synthesised from *C. elegans* mRNA using Superscript™ Choice system for cDNA synthesis (GibcoBRL, USA).

2.3 Polymerase chain reaction (PCR)

New primer pairs were designed for all PCR reactions. $MgCl_2$ concentration influences PCR conditions, however, the $MgCl_2$ concentration within the supplied enzyme buffer for Taq DNA polymerase was found to be optimal for this work (10x : 500mM KCl, 100mM Tris-HCl (pH 8.3), 15 mM $MgCl_2$). Details of all primer sequences used in this study can be found in Appendix 2.

2.3.1 Annealing temperature (Ta)

This is the temperature at which the primers anneal to their complimentary sequences on the target DNA. This depends on, and varies with, the melting temperature (Tm) and the base sequence of the primers used:

$$Ta = Tm - 5°C = 2(A\&T) \ \& \ 4\ (G\&C) - 5°C$$

Initially all amplifications were performed using an annealing temperature of 55°C. However, if the resultant amplification was unsuccessful, or yielded non-specific products, the effect of changing annealing temperature on the specificity and efficiency of the PCR amplification was determined; with annealing temperatures ranging from 55°C to 65°C utilised for each primer pair.

2.3.2 PCR cycle parameters

The number of PCR cycles plays a critical role and is dependent on the efficient optimisation of the other parameters. One PCR cycle consists of the initial heat denaturation of the double stranded DNA template into 2 single strands. This is followed by cooling the reaction mixture to a temperature, which will allow the primer to anneal to its target sequence. Finally, the temperature is increased to allow the optimal extension of the primer by the DNA polymerase. These 3 steps are repeated leading to an exponential increase in the number of copies of DNA generated.

2.3.3 Primer concentration

The efficiency of amplification can be compromised if the concentration of primer is too low. Therefore, PCR was optimised with primer concentrations around 1-10pM final.

2.3.4 PCR controls

The following controls were used:

-PCR amplification in the absence of Cdna or gDNA.

-PCR amplification in the absence of Taq polymerase.

2.3.5 Reaction conditions

Reagent	**Volume µL (50µL total mix)**
Water (dd H_2O)	36.5
Primer forward (10pM/µl)	2
Primer reverse (10pM/µl)	2
dNTPs (10mM)	2
Buffer (10x)	5
Template DNA (100ng/µl)	2
Taq DNA Polymerase (native enzyme)	0.5

Cycling conditions were optimised to denaturation of template at 94°C for 30 secs, annealing of primer pair at 55°C for 1min and elongation at 72°C for 1min. PCR was performed on a MJ Research PTC-200 Thermal Cycler.

2.4 Agarose gel electrophoresis

The size of amplified DNA was verified by agarose gel electrophoresis with ethidium bromide staining.

Agarose was dissolved by heating in 100ml 1xTBE buffer (89mM Tris, 89mM Boric Acid, 1.8mM EDTA), to achieve a 1% agarose solution. Upon cooling, 2µl of 1x working solution of ethidium bromide was added to the gel solution. The gel

solution was poured in a H2 Horizontal Electrophoresis unit (Anachem) and allowed to polymerize at room temperature for 30 min.

5µl of DNA obtained from the PCR reaction was added to 1µl of 6x loading dye. Agarose gels were run at between 80-110 volts for ~ 45min in 1xTBE running buffer. The integrity and size of DNA samples was verified by co-migration of 1Kb DNA ladder (Promega or MBI GeneRuler). Gels were imaged by transillumination of the gel using a UV light box and subsequently photographed with a digital camera system.

2.5 Purification of DNA.

The total amount of PCR amplified DNA was loaded onto 0.8% TAE (40mM Tris, 40mM acetic acid, 1mM EDTA, pH 8.0) agarose gel following appropriate addition of 6x loading dye. Agarose gels were run at 50 volts for ~ 1hr in 1xTAE buffer. Gels were then illuminated using UV light box and sections of gel containing DNA were excised with a sterile scalpel blade and then purified using QIAQuick Gel extraction kit (Qiagen).

Alternatively, PCR products were purified using Qiagen PCR Purification kit which uses a silica-gel membrane assembly for binding of DNA in high-salt buffer and elution with low-salt buffer or water. The purification procedure removes primers, nucleotides, enzymes, mineral oil, salts, agarose, ethidium bromide, and other impurities from DNA samples.

2.6 DNA sequencing using ABI Big Dye Terminator Cycle Sequencing Kit

2.6.1 Sequencing reaction

For each reaction (template/primer combination), the following reagents were added to a separate 0.2 ml tube:

Reagent	Volume µl (10µl total)
Terminator Big Dye	4
Template (50ng/µl)	4
Single primer (3.2 pM)	1
ddH_2O	1

Cycling conditions were set at 95°C for 10 secs, annealing of primer at 50°C for 15secs and elongation at 72°C for 4mins, 30 cycles. PCR was performed on a MJ Research PTC-200 Thermal Cycler.

2.6.2 Purifying sequencing extension products by precipitation.

Following PCR, tubes were briefly spun and the entire contents transferred into 1.5 ml microcentrifuge tubes. The following were then added: 10µl ddH_2O, 2 µl 3M sodium acetate (pH 5.2) and 50 µl 100% ethanol. The tubes were then vortexed and left on ice for 30mins. After this time samples were centrifuged at 13,000 rpm for 20mins, and the resultant supernatant discarded. The remaining pellet was rinsed within the microcentrifuge tube with 250 µl 75% ethanol (ice cold). Samples were re-centrifuged at 13,000rpm (10mins) and the resultant supernatant removed. The remaining pellet was finally dried by placing the tubes in a heating block for 1 min 95°C, and stored at -20°C until ready for electrophoresis. This latter electrophoresis step was carried out by Dr. M.Dixon, (University of Southampton, U.K) on an Applied Bio- Systems B73XL sequencer.

2.7 Cloning of PCR products

Purified inserts were ligated with pCR® 2.1-TOPO® vector under the following conditions:

Reagent	Volume µL (6 µL total)
PCR insert	3µl
Salt Solution	1µl
Water	1µl
Vector (pCR® 2.1-TOPO®)	1µl

The reaction was left for 5 minutes at room temperature (22-23°C) and immediately transferred to ice.

2.8 Transformation of competent cells.

2µl of the TOPO-ligation reaction was added to One Shot® chemically competent *Escherichia coli* and incubated at 4°C for 30mins. Cells were heat shocked for 30 seconds at 42°C, followed by incubation on ice for 2min. 250µl of SOC (a bacterial growth medium, composition g/l Bacto-tryptone 20, Bacto-yeast extract 5, NaCl 0.5, glucose 20mM final) was added to the competent cells and mixed for 1hr at 37°C. 25µl, 50µl and 125µl aliquots of the competent cell mix were spread onto LB Ampicillin Agar Plates. These plates were prepared by the addition of 15g bacto-agar per litre of standard LB (Luria-Bertani) medium (g/l 10 Bacto-tryptone, 10 Bacto-yeast extract: 10 sodium chloride, pH7.0 with 5M NaOH), and sterilized. Following cooling to below 50°C to prevent loss of antibiotic function, ampicillin was added at a concentration of 50µg/ml, to allow only bacterial cells expressing the pCR® 2.1-TOPO®vector to culture. 40µl of 50ng/ml X-gal was added to the plates to allow selection of blue/white colonies. The pCR® 2.1-TOPO®vector contains the gene LacZα which is disrupted if an insert is correctly ligated into the vector. X-gal is then unable to be broken down by *E. coli* containing the vector

with the correct insert and so grow as white colonies. Any *E. coli* with the vector containing an intact LacZα gene (i.e. no insert) will appear as blue colonies.
Plates were then cultured overnight at 37°C and individual white colonies then picked and transferred to 10ml LB medium containing ampicillin. These colonies were then incubated overnight at 37°C whilst shaking to optimise colony growth.

2.9 Isolation of plasmid DNA from bacterial cells.

DNA was isolated from bacterial cells using the QIAPrep Miniprep Kit (Qiagen), according to the manufacturer's instructions.

5ml of bacterial culture was centrifuged at 13K rpm to isolate the bacterial cells. The supernatant was then decanted off and the bacterial cells resuspended. Cells were then lysed using NaOH/SDS buffer and this buffer was then neutralised in high salt buffer to precipitate any denatured proteins, chromosomal DNA, cellular debris and SDS. Resulting lysate was centrifuged at 13K rpm for 10min, leaving plasmid DNA in the supernatant which was pipetted onto a 1ml spin column. Supernatant was spun through the column silica gel membrane for 1min at 13K rpm into a collecting tube, leaving the DNA bound to the column membrane. This membrane was then treated with alkali buffer to wash through any salts and ensure that only DNA was bound to the membrane and DNA was eluted from the column using RNAse-free H_2O and centrifugation at 13Krpm for 1min. This method produced the expected 1-2μg of DNA.

The presence of isolated DNA was verified by 1% agarose gel electrophoresis with ethidium bromide staining. 5μl of the DNA obtained from the plasmid mini-prep was added to 1μl of 6x tracking dye and loaded into the wells. Agarose gels were run at 80 volts for ~30min in 1xTBE running buffer. Size of DNA samples was verified by co-migration of 1Kb DNA ladder. Gels were imaged by transillumination of the gel using a UV light box and subsequently photographed with a digital camera system.

2.10 Feeding RNAi.

Exon rich fragments of the *lat-1*, *lat-2* and FLP-13 genes were amplified by PCR (see below) from *C. elegans* genomic DNA (obtained by genomic extraction from N2 wild type, or cosmid) using oligonucleotides produced by Invitrogen Ltd. The primers designed for *lat-1*, *lat-2* and FLP-13 are summarised in the table below. For the *flp-1* gene the L4440 ($Ppd_{129.36}$) feeding vector containing the *flp-1* gene fragment was obtained from Chris Keating, University of Sussex, Brighton.

Oligonucleotide Primer Description	**Sequence 5'---3'**
B0457.1 (*lat-1*) Forward	CGTTCCATCCAACATCAACTG
B0457.1 (*lat-1*) Reverse	CCATTCCATAAAGCGGCTGAC
B0286.2 (*lat-2*) Forward	ATTCCAGGCATGGACAGAAC
B0286.2 (*lat-2*) Reverse	CTCGATTTCGTTGTTGCTCA
FLP-13 Forward	CTCTGCTCTACCAAGTAGGGT
FLP-13 Reverse	AAATGAAGTACAGATATCACG

The amplified 1 kb products of *lat-1, lat-2* and *flp-13* designated for RNAi were prepared for ligation by restriction enzyme digest, and subsequently cloned into the L4440 feeding vector ($Ppd_{129.36}$), also cut with restriction enzyme. Ligation was performed under the following conditions:

Reagent	**Volume µL (10 µL total)**
PCR insert	3µl
Buffer	1µl
Water	1µl
Feeding Vector L4440 ($Ppd_{129.36}$)	5µl

The reaction was left at 15°C for at least 12 hours. The resulting plasmids were transformed into the competent HT115 (DE3) Rnase III-deficient *E. coli* strain, preferential for RNAi feeding (Timmons & Fire, 1998), by addition of 1µl of the

ligation reaction to 100µl of *E. coli* cells. Incubation occurred for 30min at 4°C. Cells were heat shocked for 1 minute at 37°C, followed by incubation on ice for 2min. 1ml of SOC medium was added to the competent cells and mixed for 1hr at 37°C. 10µl, 100µl and 250µl aliquots of the competent cell mix were spread onto LB tetracycline and Ampicillin agar plates. These plates were prepared by the addition of 15g bacto-agar per litre of standard LB (Luria-Bertani) medium (g/l 10 Bactotryptone, 10 Bacto-yeast extract, 10 sodium chloride: pH7.0 with 5M NaOH), and sterilized. Following cooling to below 50°C to prevent loss of antibiotic function, 100µg/ml ampicillin and 12.5µg/ml tetracycline were added, to allow only bacterial cells expressing the L4440 feeding vector (which contains an ampicillin and tetracycline resistant gene) to culture.

Plates were then cultured overnight at 37°C and individual colonies picked and transferred to 10ml LB medium containing tetracycline (12.5µg/ml) and ampicillin (100µg/ml). These colonies were then incubated between 8 and 18 hours at 37°C whilst shaking to optimise colony growth.

This bacterium was then seeded directly onto NGM plates containing 1mM IPTG (isopropyl-beta-D-thiogalactopyranoside) and 50µg/ml Amp, or 50µg/ml Amp only (un-induced control). Seeded plates were allowed to dry at room temperature and induction was continued at room temperature overnight.

Single L4-stage hermaphrodite worms (either wild-type N2 Bristol strain, or RNAi sensitive *rrf-3 (NL2099)* as specified in results section) were placed onto NGM plates (either Amp only or Amp + IPTG) containing seeded bacteria expressing dsRNA for each gene and were incubated for 40-60 hrs at 15°C. Then, three F2 worms were independently replica-plated onto plates seeded with the same bacteria and were allowed to populate the plate. The adult progeny from these F2 worms were assayed for emodepside sensitivity.

2.11 Detection of *lat-1* gene deletion

lat-1 (ok379) RB629 was obtained from the *C. elegans* gene knockout consortium. Worms were subjected to genomic extraction protocol (see 2.2.7 above). Nested PCR was then performed on target exon 5 (*C. elegans* gene report, Oklahoma city) to confirm the presence of a deletion.

First and second round nested PCR reaction conditions:

Reagent	**Volume µL (25µL total)**
Template DNA	5
Outside forward primer (100pM stock)	2.5
Outside reverse primer (100pM stock)	2.5
dNTPs (100mM stock)	0.5
10x Buffer	2.5
dd H_2O	11.5
Taq DNA polymerase	0.5

Cycling conditions were optimised to denaturation of template at 92°C for 30 secs, annealing of primer pair at 55°C for 20 secs and elongation at 72°C for 2mins, for 35 cycles. PCR was performed on a MJ Research PTC-200 Thermal Cycler. The template DNA for the second round reaction was created by diluting the entire reaction mixture product from the first round reaction 10 fold.

The presence of a deletion, and approximate size, were confirmed from the amplified second round DNA by agarose gel electrophoresis with ethidium bromide staining. *NB.* Amplification of product by this method indicates the presence of a deletion in the target exon, as the product would be too large to successfully amplify with these PCR conditions and primers in N2 wild type intact sequence.

The precise nature of this deletion was sequenced using an ABI Big Dye Terminator® cycle sequencing kit (see above).

2.11.1 Backcross protocol

lat-1 K.O (*ok379*) males, created by heat shock of approx 30x L4 hermaphrodites at 30°C for 6hrs, were crossed into *rol-6* (*e187*) :: *unc-4* (*e120*) hermaphrodites (*rol-6* [II:0.87±0.003cM] and *unc-4*[II:1.75±0.017cM] lie either side of *lat-1* [II:0.92±0.000cM] on chromosome II). F2 non-rolling, non-uncoordinated progeny were picked and those not segregating *rol* or *unc* were picked. At the end of backcrossing the presence of *lat-1* (*ok379*) was confirmed by PCR. As the *lat-1 (ok379)* deletion was detected in these backcrossed animals, it was assumed that *lat-1(ok379)* RB629 strain was homozygous for the deletion. Indeed *lat-1(ok379)* would have to be homozygous from this procedure if it mapped between *rol-6* and *unc-4*.

This backcross strategy can be employed with heterozygous mutant strains. However, following backcross the presence of the deletion must be confirmed in a specific line, and subsequent assays performed on this line.

This backcross strategy utilising *rol-6* (*e187)* :: *unc-4* (*e120*) was also employed for the *lat-2* (*ok301*) VC158 strain (II:-4.75 +/- 0.000 cM).

2.12 Chemical mutagenesis

N2 worm populations were floated off 10x 5cm NGM plates with 2ml fresh M9 buffer. The resultant worm solutions were batched into 2x 50ml sterile screw cap centrifuge tubes, and washed 2x in 10ml sterile M9, using a Sorvall® Legend RT desktop centrifuge at 1000 rpm., then resuspended in 10ml M9.

10ml of ethylmethanesulphonate (EMS, Sigma) working solution (20µl/2ml M9 buffer), was added to each screw cap centrifuge tube, and the tubes inverted several times to mix. This mutagenesis reaction was allowed to occur over 4hrs at room temperature in a well ventilated fume cupboard, with gentle mixing every hour.

After this time the supernatant was carefully discarded into a container of 1M NaOH. The worms were washed 3x in M9 buffer, with the worms being allowed to settle naturally between each wash, each time discarding the supernatant into 1M NaOH. The worms were resuspended in 5ml M9 buffer and 250µl of this solution pipetted onto each of 20 NGM plates, at the opposite side of the plate to a small OP-50 lawn. After 20mins any L4 larvae that had migrated to the food source were deemed viable. 100 of these larvae were individually picked onto labeled (F1 1-100) standard NGM plates, containing a healthy OP-50 bacterial lawn. It was predicted that each of these worms would produce at least 50 eggs, equivalent to 100 diploid genomes. A total of 100 plates would equate to 10,000 screened genomes.

The progeny of these picked L4 worms were allowed to develop to adulthood, at which time they were floated off the plate in 1ml M9 buffer. The resultant worm solutions from each of the 100 plates were not batched, but individually transferred to the appropriately labelled (1-100) 2ml sterile microcentrifuge tube. These solutions were washed 2x in 1ml M9, as outlined previously, using a desktop centrifuge. The worms were subjected to alkaline hypochlorite treatment (0.75ml) (Riddle, 1997), followed by 3x 2ml washes of M9, for each tube.

The egg solutions was transferred to an appropriately labelled emodepside agar plate (1000ng/ml F2 1-100), and the growth of the worms monitored in order to screen for emodepside resistant mutants.

It should be noted that EMS is a highly potent chemical mutagen, and therefore all work was carried out in a designated fume cupboard. Double gloves, lab coats and eye protection were worn at all times. Two 10L containers of 1M NaOH were used, one for the decontamination of disposable items, a second for the washing of outer gloves when it was necessary. All disposable equipment was left to soak in 1M NaOH overnight, and then incinerated.

2.13 SNIP-SNP mapping

2.13.1 Mating mutant *C. elegans* with Hawaiian strain (CB4856)

Visible Marker:

Resistant strain = y/y

If no clear intrinsic phenotype is present within the emodepside resistant strain it is first necessary to cross this strain with another that exhibits a highly defined visible phenotype, in order to distinguish between self and cross propagation in the subsequent crosses with the Hawaiian Strain (CB4856). For this study *dpy-20 C. elegans* were used. As the name suggests these worms have a dumpy appearance characterised by a bulbous tail region and compacted lower gut.

dpy-20 males ♂ **X** y/y

Results in:

dpy-20/+ ; y/+

Dpy-20s from this cross were then picked onto emodepside agar plates (1000 ng/ml) to screen for dpy-20-emodepside resistant worms.

dpy-20/dpy-20; y/+ ⟶ *dpy-20*/y

Crossing the visible marker resistant strain into Hawaiian strain (CB4856):

CB4856 ♂ **X** *dpy-20*;y

This produced non-dumpy cross progeny F1 and results in:

dpy-20/CB ; y/CB (non-dumpy, non-resistant). N.B. This entire method relies on "y" being a non-dominant suppressor.

OR

dpy-20/dpy-20 ; y/y (*dpy-20*, NON-X, self propagation)

Non-dumpy F1 were picked, one per standard NGM plate (x5 plates).

The F2 adults of these plates were then screened for emodepside resistance, by firstly chunking onto 10x 5cm emodepside plates (1000 ng/ml, primary screen) for 2 hrs. After this time any resistant animals were then individually picked onto a set of 100 5cm NGM emodepside plates (1000 ng/ml), one worm/plate (secondary screen), and the worms allowed to propagate the plates. These worms represent y/y in CB/+ background, where each parent worm represents an individual recombination event between the resistant DNA and CB4856. Once these plates were near starved (1 week), the worms were subjected to the genomic extraction protocol (see 2.2.7 above) for use in the subsequent PCR steps (see 2.13.2).

2.13.2 SNP PCR

Oligonucleotides were designed around the SNPs (see Appendix 2) and PCR used to amplify the DNA in that locus, under the following reaction conditions:

Reagent	**Volume µL (25µl total per tube of 96x plate)**
Water (dd H_2O)	18.5
Primer forward (10pM/µl)	0.7
Primer reverse (10pM/µl)	0.7
dNTPs (10mM)	0.3
Buffer (10x)	2.5
Template DNA (from genomic extraction see 2.2.7)	2
Taq DNA Polymerase	0.125

50 µl of mineral oil was added to each of the 96 tubes of the plate immediately prior to thermo cycling, to prevent evaporation of products. Cycling conditions: denaturation of template at 94°C for 40 secs, annealing of primer pair at 55°C for 40 secs and elongation at 72°C for 1min, for 35 cycles. PCR was performed on a MJ Research PTC-200 Thermal Cycler.

As a control, PCR amplification of candidate SNP site, using both N2 genomic and CB4856 genomic DNA as a template, was included with every 96 tube plate.

2.13.3 SNIP-SNP restriction digests

The amplified SNP products were subjected to an overnight restriction digest with a restriction endonuclease intended to generate a different digest profile between N2 and CB4856 DNA at that locus.

Reagent	**Volume µL (10 µl total added to each tube)**
Enzyme	0.5
Buffer (enzyme specific)	3.5
dd H_2O	6

The above enzyme mix was typically made up as a 100x master mix and 10µl pipetted directly into each of the 96 wells containing the SNP PCR product (see 2.13.2) following completion of PCR cycling. Incubate overnight at 37°C. See Appendix 3 for a list of SNIP-SNP restriction enzymes used in this work.

2.13.4 SNIP-SNP agarose gel electrophoresis

The size of amplified and digested DNA fragments was verified by agarose gel electrophoresis with ethidium bromide staining.

Agarose was dissolved by heating in 200ml 1xTBE buffer (89mM Tris, 89mM Boric Acid, 1.8mM EDTA), to achieve a 2% agarose solution. Upon cooling, 2µl of 1x working solution of ethidium bromide was added to the gel solution. The gel solution was poured in a Horizontal Electrophoresis unit (OWL Separation Systems) and allowed to polymerize at room temperature for 30 min.

20µl of DNA obtained from the PCR and subsequent digest reactions was added to 5µl of 5x SNIP-SNP loading dye (40% glycerol, 0,032% cresol red). Agarose gels were run at 150 volts for ~ 45min in 1xTBE running buffer. The integrity and size of DNA samples was verified by co-migration of 1Kb DNA ladder (Promega or

MBI GeneRuler). Gels were imaged by transillumination of the gel using a UV light box and subsequently photographed with a digital camera system. See Appendix 3 for an example gel of SNIP-SNP restriction digest products.

2.14 Reverse Transcriptase (RT) PCR for amplification of *slo-1*

RT PCR was carried out using the SuperScript. III One-Step RT-PCR System with Platinum® *Taq* DNA Polymerase. This kit enables cDNA synthesis and PCR amplification in a single tube using gene-specific primers and target RNAs from either total RNA or mRNA. SuperScript. III Reverse Transcriptase is a version of M-MLV RT that has been engineered to reduce RNase H activity and provide increased thermal stability. The enzyme can synthesize cDNA at a temperature range of 45-60°C, providing increased specificity, higher yields of cDNA, and more full-length product than other reverse transcriptases. Because SuperScript III RT is not significantly inhibited by ribosomal and transfer RNA, it can be used to synthesize cDNA from total RNA. Platinum® *Taq* DNA polymerase is recombinant *Taq* DNA polymerase complexed with a proprietary antibody that blocks polymerase activity at ambient temperatures. Activity is restored after the denaturation step in PCR cycling at 94°C, providing an automatic hot start in PCR for increased sensitivity, specificity and yield.

Reaction conditions:

0.2-ml, nuclease-free, thin-walled PCR tube on ice.

Reagent	**Volume µl (total 50µl)**
2x Reaction mix*	25
Template RNA (0.01pg-1µg)	x
Forward primer (10µM)	1
Reverse primer (10µM)	1
SuperScript. III RT/ Platinum® *Taq* mix	2
dd H_2O	Up to 50µl

* A buffer containing 0.4mM of each dNTP, 3.2mM $MgSO_4$)

Cycling conditions:

cDNA synthesis

1 cycle: 55°C for 30 min

Denaturation

1 cycle: 94°C for 2 min

PCR amplification

40 cycles: 94°C for 15 s (denature)

55-65°C for 30 s (anneal)

68°C for 1 min/kb (extend)

Final extension (optional)

1 cycle: 68°C for 5 min

2.15 Statistical analysis

Data are presented as the mean ± S.E.Mean of "n" independent determinations. Statistical significance was determined using unpaired two tailed Student's t-test with a significance level of $P<0.05$, calculated by comparing individual data points. IC_{50} values were determined from inhibition curves for pooled data sets fitted to the modified logistic equation using Graph pad prism (version 3.0 San Diego California).

Chapter 3

Effect of emodepside on *A. suum* & *C. elegans*

3.1 Introduction

3.1.1 *Ascaris suum*

Cyclooctadepsipeptides, of which PF1022A and emodepside are members, are a new class of anthelmintic (Harder & Samson-Himmelstjerna, 2002a) which inhibit nematode motility (Samson-Himmelstjerna *et al.*, 2000;Terada, 1992). The precise mechanism of PF1022A and emodepside action is unknown, although its fast onset of paralysis favours the view that it is neuropharmacologically active. Many of the commercially available anthelmintics act by inhibiting nematode motility. A number of classical transmitters, such as ACh and GABA, and neuropeptides have been shown to regulate muscle function. Many anthelmintics mimic the action of the classical neurotransmitters which control nematode movement. Such examples of these anthelmintics include levamisole that acts on the ACh receptor (Harrow & Gration, 1985) and piperazine which acts on the GABA receptor (Martin, 1982). To date no anthelmintic has been shown to mimic the action of neuropeptides.

Previous investigations into the mechanism of emodepside action have focused on the inhibitory GABAergic system (see 1.12). However, application of PF1022A to *A. suum* muscle cells resulted in no marked hyperpolarisation, and no large change in input conductance (Martin *et al.*, 1996) which is not consistent with a GABA response (Holden-Dye *et al.*, 1989;Walker *et al.*, 1992;Parri *et al.*, 1991).

The pharmacological profiles of ACh and GABA towards *Ascaris* muscle have been investigated. ACh is excitatory causing muscle contraction through activation of a nicotinic receptor, which resembles the mammalian ganglionic receptor (Colquhoun *et al.*, 1991). GABA is inhibitory, causing an increase in Cl^- conductance, a decrease spike activity and hyperpolarization resulting in muscle relaxation. This occurs through activation of a chloride-linked receptor, which in terms of agonist profile, resembles the mammalian GABA-A receptor (Holden-Dye *et al.*, 1989;Martin *et al.*, 1991;Walker *et al.*, 1992)

Emodepside has previously been shown to relax the isolated dorsal muscle strip of *A. suum*, reflecting the ability of this anthelmintic to paralyse parasitic nematodes (Willson *et al.*, 2003). As the effect of emodepside on basal muscle tension is very slight, the inhibitory action of the compound on the contraction elicited by ACh was measured. Emodepside causes a concentration and time-dependent reduction in the amplitude of the ACh contraction. This effect is significant at 10μM emodepside and maximal at 10 min incubation, with 10μM emodepside being the greatest concentration tested due to limitations in solubility of the compound. This effect is irreversible and reflects the highly lipophilic nature of emodepside. This range of concentrations although relatively high is consistent with those observed with PF1022A, in that, at concentrations of 10μM paralysis of *A. suum* occurred over a 24 hour period (Geßner *et al.*, 1996). The inhibitory action of emodepside is not specific for ACh-mediated contraction as it also inhibits the action of the excitatory neuropeptide, AF2 (Willson *et al.*, 2003).

To provide further investigate the possibility that emodepside acts via a GABAergic mechanism, an *in vitro* preparation of the dorsal muscle strip of the pig intestinal parasite *A. suum* was used. The muscle preparation consisted of the dorsal muscle and the dorsal nerve cord, which contains projections of the excitatory and inhibitory motorneurones. Changes in *A. suum* muscle tension were measured using an isometric transducer. This muscle preparation, pre-contracted with ACh, was used to compare the effect of emodepside and GABA on muscle relaxation, to determine if emodepside acts through a GABAergic mechanism.

3.1.2 *Caenorhabditis elegans*

For anthelmintic investigations, *C. elegans* is a highly useful as it is both easier and cheaper to acquire, maintain, and derive genetic information from, than a parasitic nematode such as *A. suum.* All commercially available anthelmintics have detectable effects on *C. elegans* at reasonably low concentrations, which has prompted its development as a model for parasitic nematodes for the purposes of drug screening (Hodgkin, 2001).

A drug screen previously designed for identifying the sensitivity of *C. elegans* to the anthelmintic ivermectin (IVM) (Dent *et al.*, 1997;Dent *et al.*, 2000) was adapted to determine the effects of emodepside on this free-living species.

Ivermectin, a member of the macrocyclic lactone family, is a widely used anthelmintic drug. M3 neurons induce fast inhibitory glutamatergic signalling through neuromuscular synapses in the *C. elegans* pharynx. *Avr-15* is a gene that confers ivermectin sensitivity on worms and is necessary post-synaptically for a functional M3 synapse resulting in the hyperpolarizing effect of glutamate on pharyngeal muscle. *Avr-15* encodes two alternatively spliced channel subunits that share ligand binding and transmembrane domains and are members of the family of glutamate-gated chloride channel subunits. An *avr-15*-encoded subunit forms a homomeric channel that is ivermectin-sensitive and glutamate-gated. Therefore, an ivermectin-sensitive chloride channel mediates fast inhibitory glutamatergic neuromuscular transmission. The nematocidal property of ivermectin derives from its activity as an agonist of glutamate-gated chloride channels in excitable cells such as those of the pharynx (Dent *et al.*, 1997). Ivermectin activates glutamate-gated chloride channels (GluCls) that contain α-type channel subunits. In *C. elegans,* α-type subunits are encoded by a family of genes including *avr-15* (encoding AVR-15/GluClα2). Thus, *avr-15 (ad1051) C. elegans* exhibit a reduced sensitivity to ivermectin.

Synchronized populations of *C. elegans* were grown on a series of NGM plates containing different concentrations of ivermectin plus ethanol vehicle, emodepside

plus ethanol vehicle or ethanol vehicle control alone. The growth and development of the worms through larval stages to fertile adulthood was examined to determine the concentration of anthelmintic necessary to arrest development of the larvae, and thus prevent proliferation of the nematode. Any other developmental or behavioural abnormalities resulting from anthelmintic exposure that could be visualised under a standard dissecting microscope (40x objective) were noted. Previous screens of this nature using ivermectin impregnated agar plates have shown that growth of *C. elegans* is prevented at a concentration of <10 ng/ml (11.4nM) and paralysis induced at ~20 ng/ml (22.8nM) (Arena *et al.*, 1995;Dent *et al.*, 1997).

Locomotion of adult N2 wild-type *C. elegans* was quantified as the number of body bends per minute (B.B/min). Two separate assays were used to analyse the effects of emodepside on this behaviour (see 2.2.2). Firstly, to obtain IC_{50} data, the above emodepside agar plate assay was used and the B.B/min of adult worms foraging on the agar surface recorded. Secondly, to precisely determine a possible time-dependent effect of emodepside action on *C. elegans* motility, worms were transferred to Dent's saline. In this medium wild-type *C. elegans*, in the absence of drug, exhibit a rapid "thrashing motion". Locomotion in Dent's saline was recorded at defined intervals in the presence of 10μM emodepside or ethanol vehicle control.

3.2 Comparison of GABA and emodepside-induced relaxation on pre-contracted *A. suum* dorsal muscle strip

Prolonged application of ACh to the DMS caused an initial contraction followed by a slow relaxation of 4.7 ±1.3 % min^{-1} (n=4) (Fig 3.1). In vehicle control experiments, addition of 0.1% EtOH at the point of maximal ACh contraction resulted in a similar relaxation rate of 5.2 ± 1.1 % min^{-1} n=4 graph not shown). In contrast to the slow, partial relaxation of the muscle observed with emodepside (8.9 ±1.3 % min^{-1}, n=4) the response to GABA was rapid (38.1 ±1.8 % min^{-1}, n=4, $P<0.001$) and relaxation was back to base line tension.

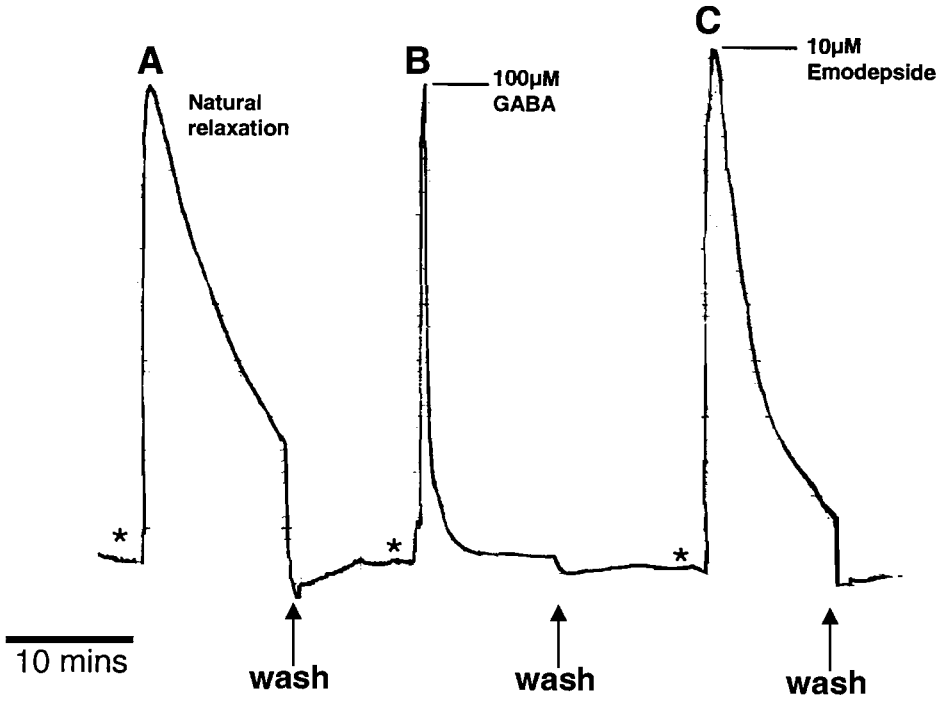

Figure 3.1 Comparison of GABA and emodepside-induced relaxation on pre-contracted *A. suum* dorsal muscle strip. 50µM ACh was used to pre-tone the *Ascaris* dorsal muscle strips (* indicates ACh application). (**A**) Natural relaxation of muscle back to basal tone. (**B**) GABA (100µM) was applied at the point of maximal ACh contraction. (**C**) 10µM emodepside was applied at the point of maximal ACh-induced contraction.

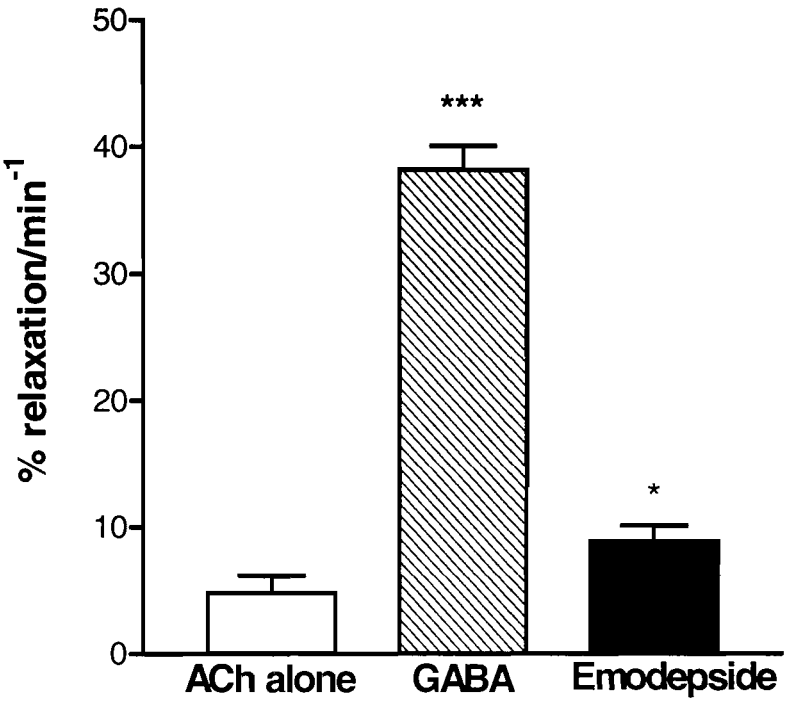

Figure 3.2 Relaxation rates % min-1 of pre-contracted *A. suum* dorsal muscle strips. 50μM ACh was used to pre-tone the *Ascaris* dorsal muscle strips. "ACh alone" indicates natural relaxation rate of muscle back to basal tone. GABA, 100μM, and emodepside, 10μM, were applied independently at the point of maximal ACh contraction. 10μM emodepside was applied at the point of maximal ACh induced contraction. The relaxation was measured as the difference in tension at the peak of the response and prior to the wash, expressed as a percentage of the peak contraction and divided by 10, to yield the % relaxation rate min^{-1}. * $P<0.05$, *** $P<0.001$, compared to ACh alone. n=4.

To further compare the response to GABA and emodepside the effect of reduced chloride APF was determined (Fig 3.3 & 3.4). For these experiments chloride salts were replaced with the impermeant anions, either isethionate or acetate (Martin, 1982).

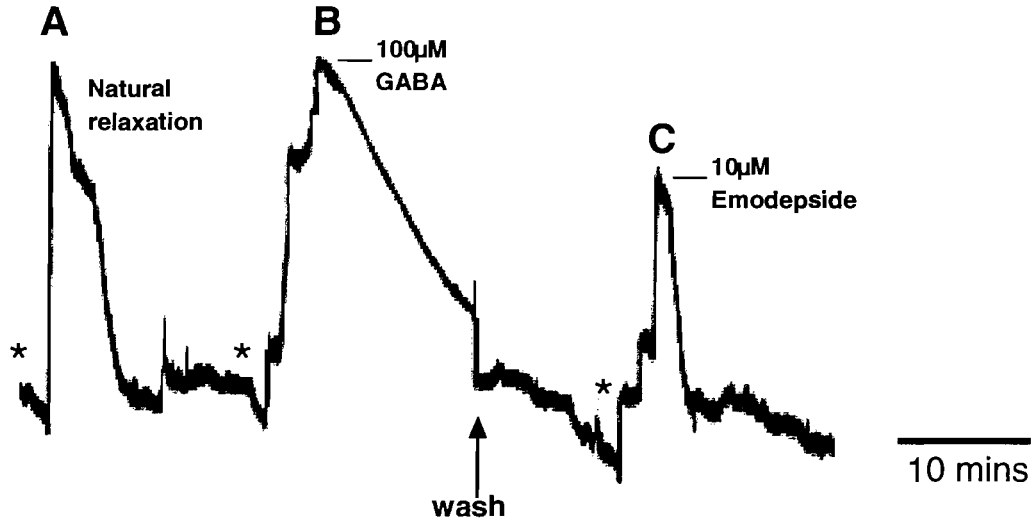

Figure 3.3 Comparison of GABA and emodepside-induced relaxation on pre-contracted *A. suum* dorsal muscle strip in reduced chloride APF. 50μM ACh was used to pre-tone the *Ascaris* dorsal muscle strips (* indicates ACh application). (**A**) Natural relaxation of muscle back to basal tone. (**B**) GABA (100μM) was applied at the point of maximal ACh contraction. (**C**) 10μM emodepside was applied at the point of maximal ACh-induced contraction. n=5.

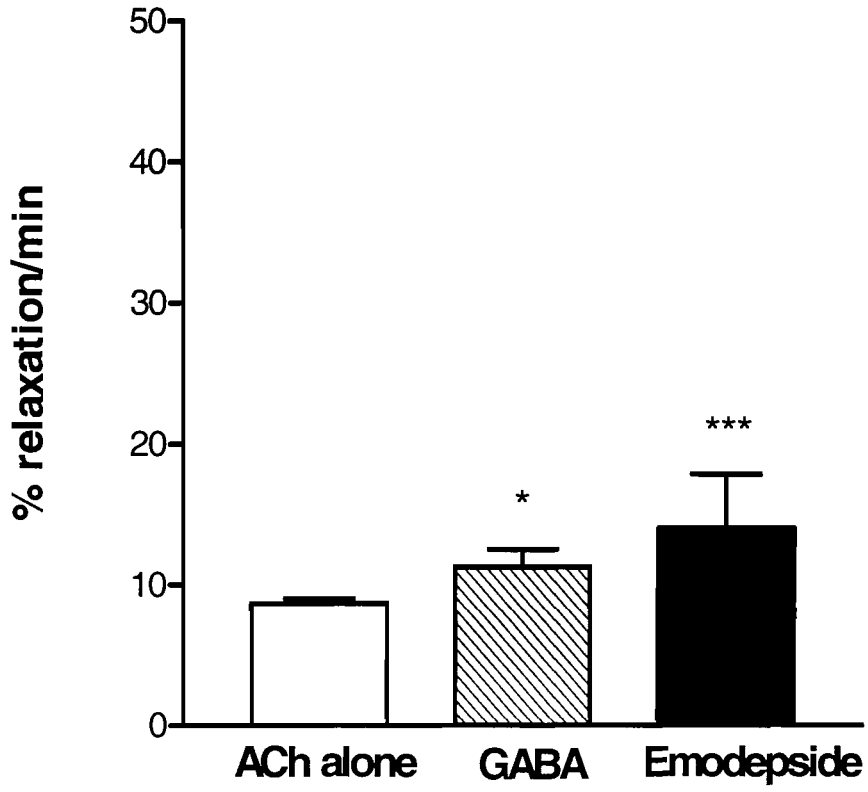

Figure 3.4 Relaxation rates % min-1 of pre-contracted *A. suum* dorsal muscle strips bathed in reduced Cl- APF. 50μM ACh was used to pre-tone the *Ascaris* dorsal muscle strips. "ACh alone" indicates natural relaxation rate of muscle back to basal tone. GABA (100μM) was applied at the point of maximal ACh contraction. 10μM emodepside was applied at the point of maximal ACh induced contraction. The relaxation was measured as the difference in tension at the peak of the response and prior to the wash, expressed as a percentage of the peak contraction and divided by 10, to yield the % relaxation rate min^{-1}. * $P<0.05$, *** $P<0.001$, compared to ACh alone. n=5.

Removal of chloride ions from the extracellular environment produced highly variable results, due to the change and instability of the resting membrane potential of the muscle cells (Fig 3.3). In some cases the response to GABA (100μM) changed from a rapid relaxation to a contraction (n=3). However, the predominant response to GABA (100μM) in reduced Cl^- was a significantly slower relaxation (11.2 ±1.2 % min^{-1}, n=4, $P<0.001$) compared to that observed in normal APF (38.1 ±1.8 % min^{-1}, n=4). In contrast, emodepside (10μM) continued to exhibit the same slow relaxation (13.9 ±3 % min^{-1}, n=4 reduced Cl^-, compared to 8.9 ±1.3 % min^{-1}, n=4 normal APF).

3.3 Effect of ivermectin on growth and development of N2 wild-type and *avr-15 C. elegans*

As mentioned above (3.1.2), *C. elegans* is a highly useful model nematode for anthelmintic screening. Before investigating the effect of emodepside on *C. elegans*, it was necessary to determine the effect of ivermectin on the growth and development of N2 wild type and *avr-15 C.elegans.* This was done as a positive control for subsequent experiments, and to corroborate data from an identical screen (Dent *et al.*, 1997).

Ivermectin inhibited the development of both N2 wild-type and *avr-15* mutant larval stages to fertile adults at concentrations as low as 2.5ng/ml (Fig 3.4A). However, *avr-15* mutants exhibited a reduced sensitivity to IVM in that at 2.5ng/ml there was only a 50% reduction in the number of fertile adults, compared to 5% with N2 wild-type. A concentration-dependent inhibition of wild-type larval development to adulthood was observed, up to 10ng/ml, at which point almost all juvenile worms were arrested at the L1 stage (Fig 3.4B). This concentration-dependent inhibition of larval development was also observed in *avr-15* mutants, however, to a lesser extent as 10 ng/ml IVM allowed 50% and 49% of these worms to develop to L1 and L2-L4 larval stages, respectively.

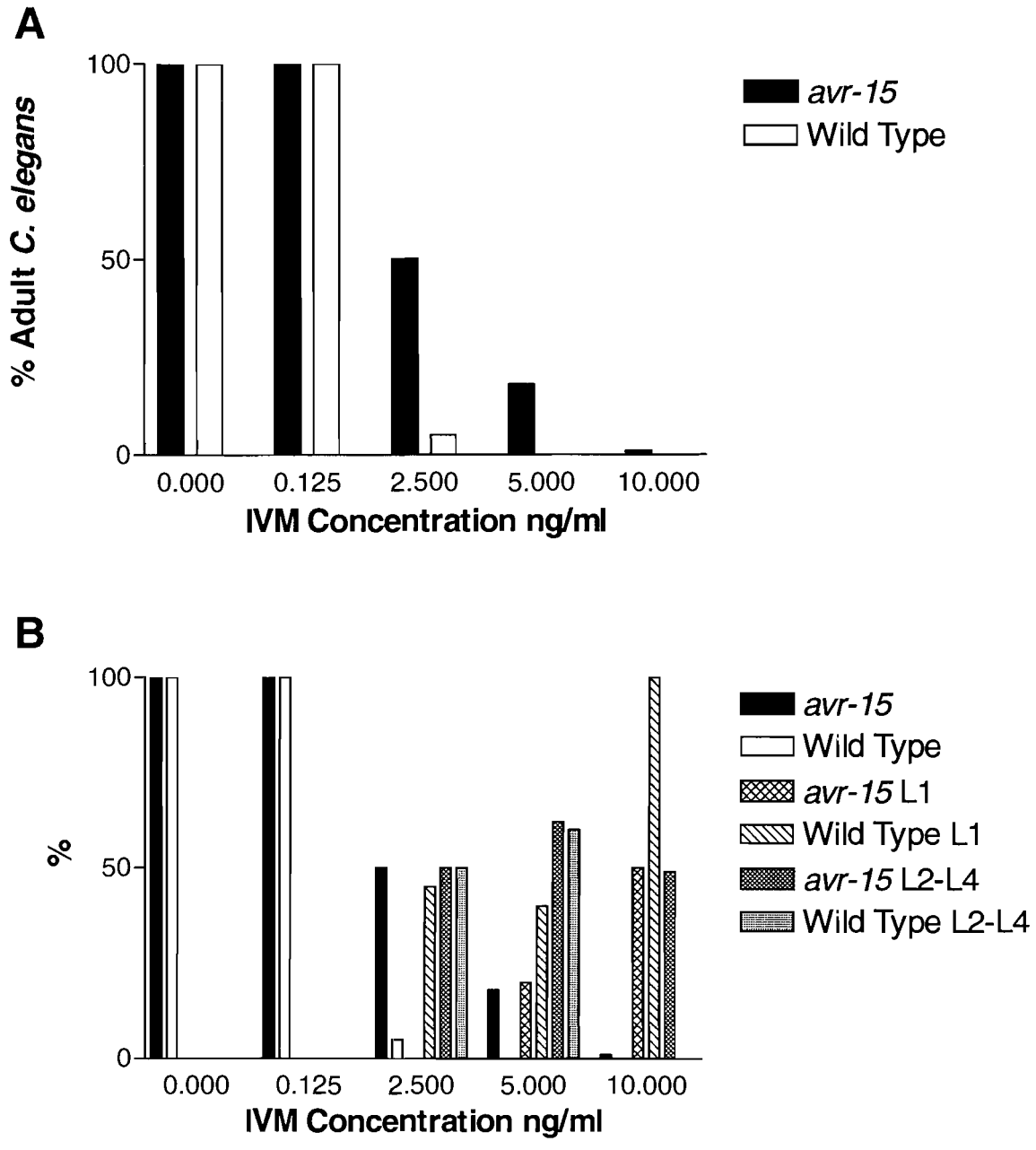

Figure 3.5 Ivermectin inhibited the development of both N2 wild-type and *avr-15* mutant larval stages to fertile adulthood. Eggs were isolated from gravid adult hermaphrodite worms (N2 and *avr-15*, the latter having greatly reduced sensitivity to IVM) by the alkaline hypochlorite method (Riddle, 1997). Approximately 100 eggs were placed on agar plates containing OP50-*E.coli* and either ivermectin (concentration range 0.125ng/ml-10ng/ml) or vehicle control (1% ethanol). The plates were incubated for 3-5 days at 20°C and the developmental progress of the worms, through larval stages (**B**) (L1-L4), to fertile adulthood (**A**), monitored. Animals were scored by counting the number of non-paralysed worms, i.e. the ability to move and a lack of a rod like appearance. Data expressed as %. (n=2)

3.4 Effect of emodepside on growth and development of wild-type *C. elegans*

Following the positive controls using ivermectin agar plates, the screen was adapted for emodepside to determine the concentration window within which this novel anthelmintic could arrest larval development of wild-type N2 *C. elegans* to adulthood. Interestingly, emodepside did not arrest larval stages of *C. elegans* at any of the concentrations tested (600 fg/ml to 1000 ng/ml), exerting a profound anthelmintic effect only when development to young adult stage had occurred (data not shown).

On vehicle control plates developmental progress from egg to fertile adulthood was realised over a period of 3-5 days at 20°C. However, on emodepside plates above 200ng/ml growth to adulthood was retarded, by approximately 24 hours, when compared with worms on lower emodepside concentration and control plates (data not shown).

Below 1000 ng/ml emodepside, adult worms were capable of laying eggs and producing progeny before becoming paralysed and subsequently dying. Alternatively, prior to death the adult worms were often observed to undergo "bagging", whereby the internal hatching of progeny with subsequent emergence of active larvae from the parent occurred. In turn these progeny were also observed to develop through larval stages to adulthood before arresting. However, at 1000ng/ml, hermaphrodite adults were arrested before egg laying could occur, with no apparent bagging phenomenon.

Inhibition of pharyngeal pumping was also observed in fertile adults at a threshold of 5ng/ml, which became more pronounced with increasing concentration up to 100ng/ml. Between 200ng/ml and 1000ng/ml inhibition of pharyngeal pumping was brought about earlier in development, at late L4 stage, again in a concentration-dependent manner.

3.5 Effect of emodepside on locomotory behaviour of wild-type *C. elegans*

Emodepside immobilized mature fertile adults, growing on drug-containing agar plates (600 fg/ml to 1000 ng/ml), in a dose-dependent manner with an IC_{50} 4.2nM (95% confidence limits 1.1 to 15nM) (Fig 3.6). An example of the effect of emodepside on sinusoidal body bends is shown in Fig 3.7B, compared to the control (Fig 3.7A).

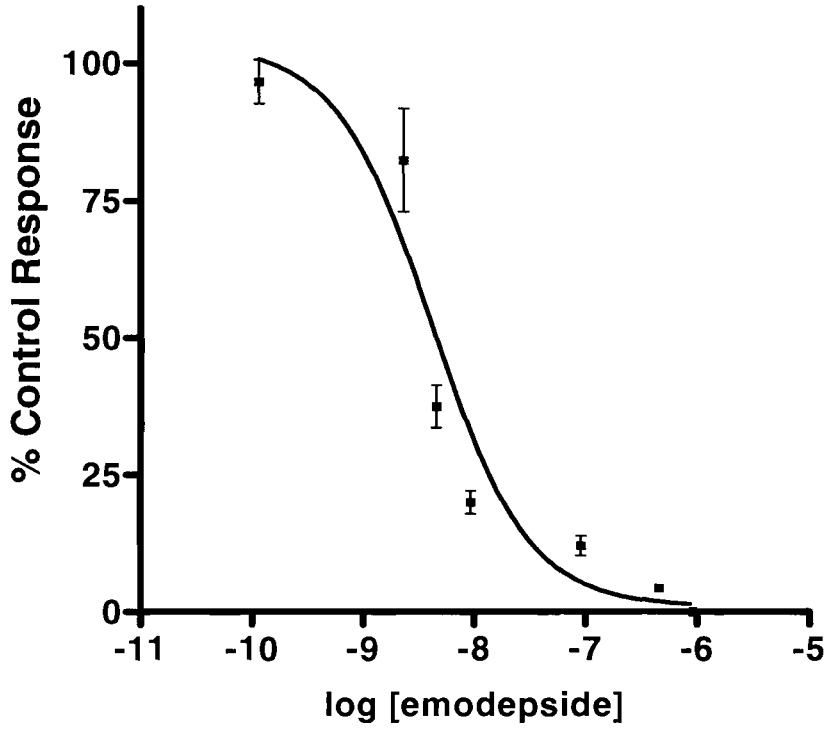

Figure 3.6 Concentration response curve for the effect of emodepside on locomotion in wild type *C. elegans*. '% Control Response' is the number of body bends per minute of adult worms grown on emodepside agar plates as a % of the body bends per minute of wild type worms grown on vehicle control plates (1% ethanol). IC_{50} 4.2nM (95% confidence limits 1.1 to 15nM. (n=10)

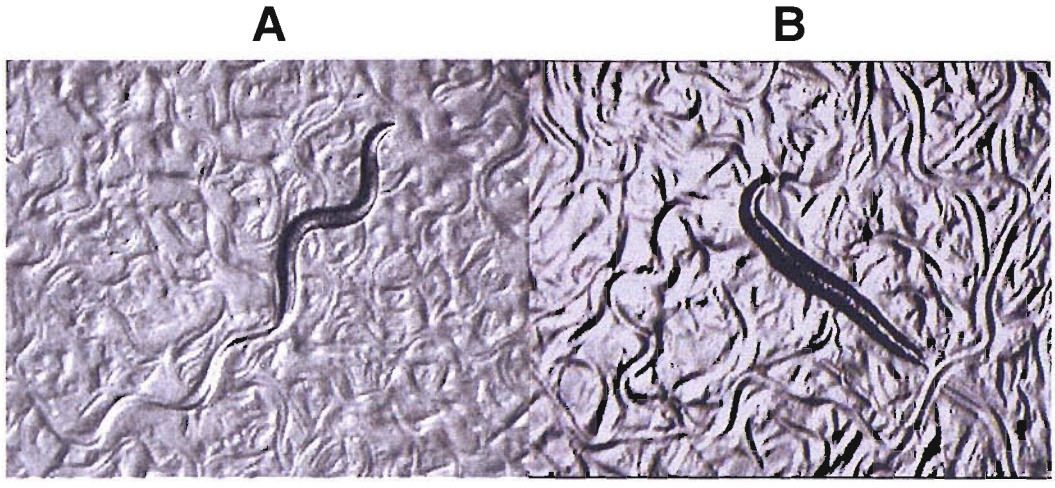

Figure 3.7 An example of the effects of emodepside on sinusoidal body bends. **A**. *C. elegans* grown in the absence of emodepside (control 1% ethanol); compared to **B**. *C. elegans* grown in the presence of emodepside (200ng/ml). Note the flat wave-form of the worm on the emodepside treated plate.

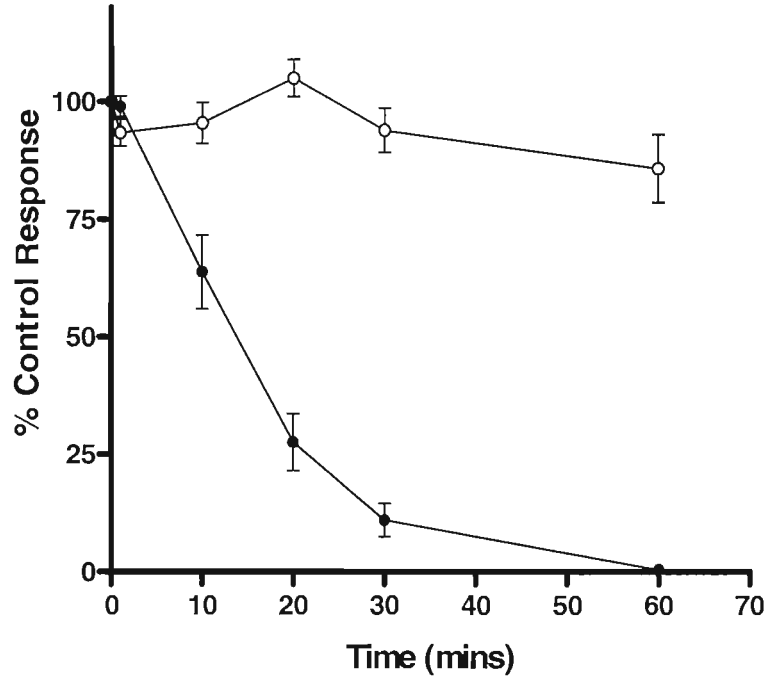

Figure 3.8 Comparison of the time-dependent effect on N2 wild-type *C. elegans* of 10μM emodepside (closed circles) and vehicle control (0.1% ethanol, open circles) on the thrashing locomotory behaviour exhibited in Dent's saline. '% Control Response' is the number of body

bends per minute of adult worms following exposure to 10μM emodepside as a % of the body bends per minute of vehicle control wild type worms (0.1% ethanol). (n=27)

Following 60 mins incubation with either 10μM emodepside or vehicle control (ethanol) there was a 7 fold reduction in the number of B.B/30sec (standardised as % inhibition compared to control response) in the emodepside treated worms compared to the control group (99.5 ±0.2 % inhibition of body bends, S.E.M n=27 10μM emodepside, compared to 14.2 ±7% inhibition of body bends, S.E.M n=10 vehicle control). However, the anthelmintic action of emodepside on *C. elegans* thrashing locomotion can initially be observed following 10 mins incubation with 10μM emodepside as there was a reduction in the number of B.B/30sec (standardised as % inhibition compared to control response) in the emodepside treated worms compared to the vehicle control group (36.3 ±7% inhibition of body bends, S.E.M n=27 10μM emodepside, compared to 4.6 ± 4% inhibition of body bends, S.E.M n=10 vehicle control).

3.6 Discussion

3.6.1 *Ascaris suum*

Emodepside relaxes an isolated dorsal muscle strip of *A. suum*, reflecting the ability of this anthelmintic to paralyse parasitic nematodes (Willson *et al.*, 2003). Previous studies have suggested, as one possiblity, that emodepside may act by mimicking the action of the endogenous inhibitory neuromuscular junction transmitter, GABA (Martin & Valkanov, 1996;Chen *et al.*, 1996;Martin & Harder, 1996). For example, (Martin *et al.*, 1996) observed a chloride-dependent increase in membrane input conductance that would be consistent with activation of a GABA-gated chloride channel (Martin, 1982;Holden-Dye *et al.*, 1989). Therefore the inhibitory actions of GABA and emodepside on muscle tension were compared.

The inhibitory action of emodepside and GABA appear distinctly different in relaxation rate/min^{-1}, on *A. suum* muscle strips pre-contracted with ACh. In control experiments with continued presence of ACh, and no further drug additions, the initial peak contraction is followed by a slow reduction in muscle tension, or 'fade' in the response, prior to the wash. This fade may be due to desensitisation of the muscle. As would be expected of an inhibitory neurotransmitter, addition of GABA (100μM) at the peak of the ACh contraction increased the relaxation rate of the muscle back to basal tension levels. Addition of emodepside at the peak of the ACh contraction also increased the relaxation rate of the muscle, compared to the natural fade observed with ACh alone. However, the emodepside effect was distinctly slower in onset compared to GABA, and muscle tension did not fully relax back to baseline before the wash.

The actions of emodepside on the electrophysiological properties of the muscle are also not like those of GABA. In contrast to an earlier study (Martin & Harder, 1996), it was found that emodepside does not cause an increase in input conductance but rather it elicits a slow, K^+-dependent hyperpolarization with no consistent change in input conductance (Willson *et al.*, 2003). Taken together, these data do not support a role for GABA, or its receptor, in the action of emodepside.

Emodepside may exert its action either pre-synaptically or directly on the muscle. To test the latter possibility emodepside was applied to muscle from which the major nerve cords had been removed (Willson *et al.*, 2003). The muscle was probably compromised by the dissection procedure as the base-line tension was not stable and the response to ACh was reduced compared to an intact preparation. In these preparations, emodepside caused a slight decrease in base-line tension. This could be due to a mechanical artefact of drug addition, an action on nerve endings of the minor nerves of the lateral cords, or a slight post-synaptic action. Most notably, however, emodepside did not inhibit the response to ACh when the nerve cord was removed. As a positive control, intact dorsal muscle strips were taken from the same worms as the denervated muscle, and emodepside inhibited the response to ACh in these preparations. Furthermore, the nerve cord was not required for the inhibitory response to PF2, consistent with the post-synaptic action of this neuropeptide (Holden-Dye *et al.*, 1995).

Further insight into the possible pre-synaptic cellular mechanisms of emodepside action was provided by electrophysiological experiments (Willson *et al.*, 2003). Removal of calcium ions from the perfusate prevented the hyperpolarization in response to emodepside. This could be due to a requirement for calcium for activation of a current on the muscle membrane e.g. a calcium-activated potassium channel. However, it is also consistent with a role for calcium-dependent neurotransmitter release in the mechanism of action of emodepside, and taken together with the experiments of denervated muscle described above, the latter explanation appears more favourable.

Two peptides, PF1 and PF2 are structurally very similar with the sequence SDPNFLRFamide and SADPNFLRFamide respectively, and both peptides have a potent inhibitory action on *Ascaris* somatic muscle (Holden-Dye *et al.*, 1995). To determine whether a PF1/2-like peptide may be involved in the response to emodepside, the action of emodepside was compared with that of PF2 (Willson *et al.*, 2003). As with emodepside, PF2 elicited a slow but incomplete relaxation of *A. suum* dorsal muscle tonically contracted with ACh. Pre-incubation of the muscle with PF2 also reduced the amplitude of subsequent contractions to ACh, in a similar manner to emodepside. The receptors for PF2 are likely to be located post-synaptically on the muscle as the inhibitory effect of PF2 on the ACh contraction was also observed in a denervated muscle strip.

Electrophysiologically the response to PF2 is also like the response to emodepside. PF2 causes a slow hyperpolarization with no consistent change in input conductance (Holden-Dye *et al.*, 1995). The hyperpolarization caused by PF2 is blocked by potassium channel blockers (Walker *et al.*, 2000). Similarly, the hyperpolarization caused by emodepside was blocked by potassium channel blockers, and enhanced in low external potassium (Willson *et al.*, 2003). Furthermore, it has also been shown that the response to PF1/PF2 is dependent on calcium and that this reflects the involvement of a nitric oxide signalling cascade in the peptide response (Maule et al., 1995). Therefore it would seem that the ionic mechanism for the response to PF2 and to emodepside is similar.

Overall, these data suggest that emodepside may mimic the action of inhibitory neuropeptides at the neuromuscular junction, possibly by triggering neuropeptide release from inhibitory nerve terminals. Whether or not this contributes to the anthelmintic action remains to be determined. Further studies on the model genetic animal *C. elegans* were performed to refine this hypothesis.

3.6.2 *Caenorhabditis elegans*

To provide further insight into the mechanism of emodepside action, using the model nematode *C. elegans*, it was necessary to establish the effective concentration for paralysis of this nematode. This was achieved by culturing synchronised populations on anthelmintic-containing agar plates and monitoring the developmental progress, and subsequent concentration-dependent arrest of growth, as well as observing any gross behavioural abnormalities resulting from anthelmintic treatment. Drugs are ingested as the worm feeds on the bacterial lawn of the plate and inevitably eats parts of the agar surface. It has also been shown that ivermectin, being highly lipophilic, is able to undergo drug absorption via the *C. elegans* cuticle to exert an anthelmintic effect (Bernt, 1998). As emodepside is also highly lipophilic, it may also utilise this mode of entry. Alternatively, anthelmintics may accumulate within the bacteria upon which the worms feed, providing a third possible route of administration for these drugs.

To serve as a positive control the screen was firstly performed using ivermectin against N2 wild-type and *avr-15 (ad1051) C. elegans*, the latter exhibiting a reduced sensitivity to ivermectin (Dent *et al.*, 1997;Dent *et al.*, 2000). From the IVM agar plate assay it was found that ivermectin inhibits the development of both N2 wild-type and *avr-15 (ad1051)* larval stages to fertile adults, with the latter exhibiting a reduced sensitivity to IVM. These data are in agreement with (Dent *et al.*, 1997) whereby ivermectin inhibited the growth of *C. elegans* at concentrations <10ng/ml.

In comparison to ivermectin, emodepside did not arrest development of synchronised populations of *C. elegans* to adulthood. Using the anthelmintic agar plate assay, 10ng/ml ivermectin was able to arrest *C. elegans* development at L1 larval stage, whereas emodepside only had a detrimental effect on nematode

viability at young adulthood (threshold 5ng/ml). Differences in anthelmintic sensitivity between larval *C. elegans* and adults is not uncommon and has been previously observed for drugs such as mebendazole (Bernt, 1998). This may be due to structural changes in the cuticle leading to a different penetrance in juveniles and adults. Such stage specific variations in the composition of the cuticle, e.g., the pattern of collagen species, have been well documented (Cox *et al.*, 1981;Cox *et al.*, 1985;Johnstone, 1994). It is also possible that a switch in the pathway of incorporation (from oral to cuticular or vice versa) takes place with increasing age as described for the uptake of pyrantel pamoate in *Toxocara canis* (Mackenstedt *et al.*, 1993). Alternatively, these data may suggest that emodepside interacts with a target that is expressed, or functionally important, primarily in the adult stage only.

To further investigate the effect of emodepside on *C. elegans* two locomotion assays were employed, the emodepside agar plate assay and the Dent's saline thrashing assay. From these it was shown that emodepside immobilised mature fertile adults in a concentration-dependent manner with an IC_{50} 4.2nM (plate assay), and that this inhibition is first observable following 10 mins exposure to 10μM emodepside (thrashing assay). Interestingly, these data differ greatly to those obtained using PF1022, the parent compound of emodepside, in a similar agar plate assay (Bernt, 1998). PF1022 (1, 10, 100μM) produced no significant effects on co-ordination or velocity of movement in *C. elegans.*

The PF1022 agar plate assays did however detect some subtle effects of this anthelmintic on *C. elegans* developmental rates (Bernt, 1998). Namely, at 100μM PF1022, egg laying was retarded by about 1 day and late stage larvae took 1-2 days longer to start egg production. Although emodepside is much more potent than PF1022 at affecting *C. elegans* development in this assay, producing total arrest of young adults and subsequent egg laying at 1000ng/ml (1μM), it also retarded the development of larval stages, above 200nM, by 1 day. Similarly, both PF1022 and emodepside caused an increase in the "bagging" phenomenon. This internal hatching is referred to as *endotokia matricida* in cases where the parent is killed during the process. Given that larvae of *C. elegans* cannot become dauers under complete starvation, a possible benefit of bagging is that the parental body provides nutrition and so allows larvae to become dauers under extremely food-limited

conditions. This internal hatching is also indicative of dysfunctional vulval musculature. Analysis with Nomarski optics of PF1022-treated *C. elegans* at high magnification revealed that gut cells in the posterior part of the animal contained a reduced amount of cytoplasmic granules even under optimal food conditions which suggests insufficient uptake or leakage of nutrient components (Bernt, 1998). This is supported by observation of *C. elegans* pharyngeal pumping on emodepside agar plates, whereby, inhibition of pharyngeal pumping occurred at a threshold of 5ng/ml, and became more pronounced with increasing concentration up to 100ng/ml. Indeed, subsequent electropharyngeogram (EPG) recordings quantified this by demonstrating that emodepside is highly potent at inhibiting basal pharyngeal pumping rate (IC_{50} 2.2 nM) and the response of the pharynx to two stimulatory neurotransmitters, either 5-HT (IC_{50} 4.1 nM) or AF1 (Willson *et al.*, 2004). Therefore, emodepside inhibits both the tonically-active pharynx, and pharyngeal pumping stimulated by pharmacological activation of the enteric neuronal circuit.

These data show that emodepside is highly potent at inhibiting locomotion of *C. elegans* through muscle paralysis. This cessation of motility inevitably results in reduced foraging capability, which when combined with the profound inhibitory effect on pharyngeal pumping, results in an impaired utilisation of available food and subsequent death of the worm.

Chapter 4

Reverse genetic approach to investigate the mechanism of emodepside action

4.1 Introduction

C. elegans is a useful model organism for studying signalling pathways. The relative ease of reverse genetic techniques such as RNA interference, and the availability of numerous mutant strains, has enabled the discovery of drug target sites. It was the use of expression cloning with *C. elegans* that enabled the target site for the anthelmintic ivermectin to be identified (Cully *et al.*, 1994). To further elucidate the mechanism of emodepside, reverse genetic strategies were employed in this study, using the model nematode *C. elegans*.

In the previous chapter, it was shown that emodepside causes a non-GABAergic relaxation of *A. suum* muscle, and the major target site for emodepside appears to be pre-synaptic (Willson *et al.*, 2003). Emodepside has also been shown to mimic the effects of the inhibitory peptide PF2, favouring the view that emodepside may cause vesicle release of an inhibitory peptide, leading to muscle relaxation and nematode paralysis (Willson *et al.*, 2003).

Molecular techniques have been successful in identifying a possible protein target in *H.contortus* for PF1022A and emodepside (Saeger *et al.*, 2001). A cDNA expression library from the parasite *H. contortus* was constructed and screened with an emodepside-KLH conjugate and anti-emodepside-KLH antiserum. Screening of 1.5 x10^6 non-amplified recombinant clones resulted in isolation of a novel orphan heptahelical transmembrane receptor (110kDa) named HC110-R. Database and phylogenetic examination showed that HC110-R has two *C.elegans* homologs, namely the heptahelical transmembrane proteins B0457.1 or *lat-1* (1014 amino acids) and B0286.2 or *lat-2* (1449 amino acids). Both *lat-1* and *lat-2* encode seven transmembrane domain, Family 2, G protein-coupled receptors with characteristics of latrophilins, including large extracellular and intracellular domains, a lectin-like sequence, a G protein proteolysis site domain (GPS), and short cysteine-rich sequence (Lelianova *et al.*, 1997) (see Fig 1.15). LAT-1 has 22, 23, and 21% amino acid identities to rat, bovine, and human latrophilin, respectively. LAT-1 and LAT-2

have 21% amino acid identity with each other.

Latrotoxin (αLTX), a neurotoxic protein of the black widow spider venom that causes massive vesicular release (Grishin, 1998;Saibil, 2000), is a ligand of the mammalian orphan latrophilin receptor (See Chapter 1, section 1.14.3). It is known that this mechanism involves the G_q, G-protein and phospholipase (PLC) pathway (Rahman *et al.*, 1999).

This raised the question as to whether emodepside exerts anthelmintic activity *via* a pre-synaptic mechanism causing vesicle-mediated transmitter release similar to the effect of αLTX. Evidence for stimulation of vesicle release by emodepside was provided by imaging of synapses using the fluorescent dye FM4-64 (Willson *et al.*, 2004). Intracellular uptake of FM4-64 results in fluorescence of synaptic boutons. Neuronal uptake of the dye was confirmed by co-localisation with a pan neuronal GFP strain of *C. elegans* (Altun-Gultekin et al., 2001). When the labelled vesicles fuse with the synaptic membrane, FM4-64 fluorescence decreases. This was utilized to see whether emodepside is stimulating vesicle release. A selective loss of fluorescence was observed following application of emodepside, indicating vesicle exocytosis in the presence of emodepside.

Vesicular release of neurotransmitter from nerve terminals requires the fusion of synaptic vesicles with the pre-synaptic membrane (Scheller, 1995;Sudhof, 1995). Vesicle fusion involves an evolutionary conserved protein cascade utilising vesicle-associated and pre-synaptic membrane-associated proteins. Of importance are the proteins involved in the SNARE complex. The complex consists of vesicle-associated SNARE (v-SNARE), synaptobrevin (VAMP), and two target or plasma membrane SNAREs (tSNARE), SNAP-25 and syntaxin. The SNARE proteins, synaptobrevin on the vesicle, syntaxin with SNAP-25 on the plasma membrane form *trans* complexes that bring vesicle and pre-synaptic membrane into close apposition to drive membrane fusion (Weber *et al.*, 1998). Synaptotagmins act as calcium sensors to regulate the calcium-dependent fusion of the vesicle machinery (Jahn & Sudhof, 1999). Synaptic activity is dependent on the number of vesicles (the readily releasable pool) available for fusion with the pre-synaptic membrane. Second messenger activation plays an important role in modulating the number of vesicles available in this pool. For example, phorbol esters have been shown to

increase the size of the readily releasable pool in neurones and chromaffin cells (Gillis *et al.*, 1996;Stevens & Sullivan, 1998). Pre-synaptic proteins that bind these second messenger signals are therefore potential sites for regulating synaptic efficacy.

UNC-13, a synapse-specific plasma membrane-associated protein is essential for synaptic vesicle release in *Drosophila*, mammals and *C. elegans (*Aravamudan et al., 1999;Augustin *et* al., 1999;Richmond et al., 1999*). C. elegans unc-13* mutants phenotypically exhibit uncoordinated movement and varying degrees of paralysis (Brenner, 1974;Maruyama & Brenner, 1991;Kohn *et al.*, 2000). Decreased synaptic activity suggests *unc-13* mutants are deficient in the release of most neurotransmitters (Miller *et al.*, 1996). Over expression of the mammalian homologue, MUNC-13, in cultured Xenopus neuromuscular systems increases synaptic transmission (Betz et al., 1998). Cloning of the UNC-13 gene in *C. elegans* identifies C1 and C2 binding domains (Maruyama & Brenner, 1991;Kohn *et al.*, 2000). The C1 domains bind diacylglycerol (DAG) and phorbol esters (Burns & Bell, 1991), whereas the C2 domains bind calcium and phospholipids (Kaibuchi et al., 1989). MUNC-13s were also shown to be the main pre-synaptic DAG/β phorbol ester receptors in hippocampal neurones (Rhee et al., 2002). Upstream regulators of UNC-13 have also been identified in *C. elegans*. Activation of Gαq, phospholipase Cβ (PLCβ) and the DAG binding protein UNC-13 led to increased ACh release at neuromuscular junctions (Lackner *et al.*, 1999). PLCβ and DAG are also major determinants of DUNC-13 synaptic levels in *Drosophila* (Aravamudan & Broadie, 2003). Gαo activation inhibits ACh release at the synapse by reducing levels of UNC-13 at release sites (Nurrish *et al.*, 1999).

A possible mechanism of action for emodepside was investigated using a combined approach of RNAi and available *C. elegans* mutants. The question whether emodepside causes vesicle mediated release via interaction with a latrophilin-like receptor and the subsequent activation of a signalling pathway was investigated.

4.2 Comparison of emodepside effect on locomotion of *rrf-3 (pk1426)* and N2 wild type *C. elegans*

Emodepside caused a concentration-dependent inhibition of locomotion on *rrf-3 (pk1426) C. elegans*, similar to N2 wild type *C. elegans* (Fig 4.1).

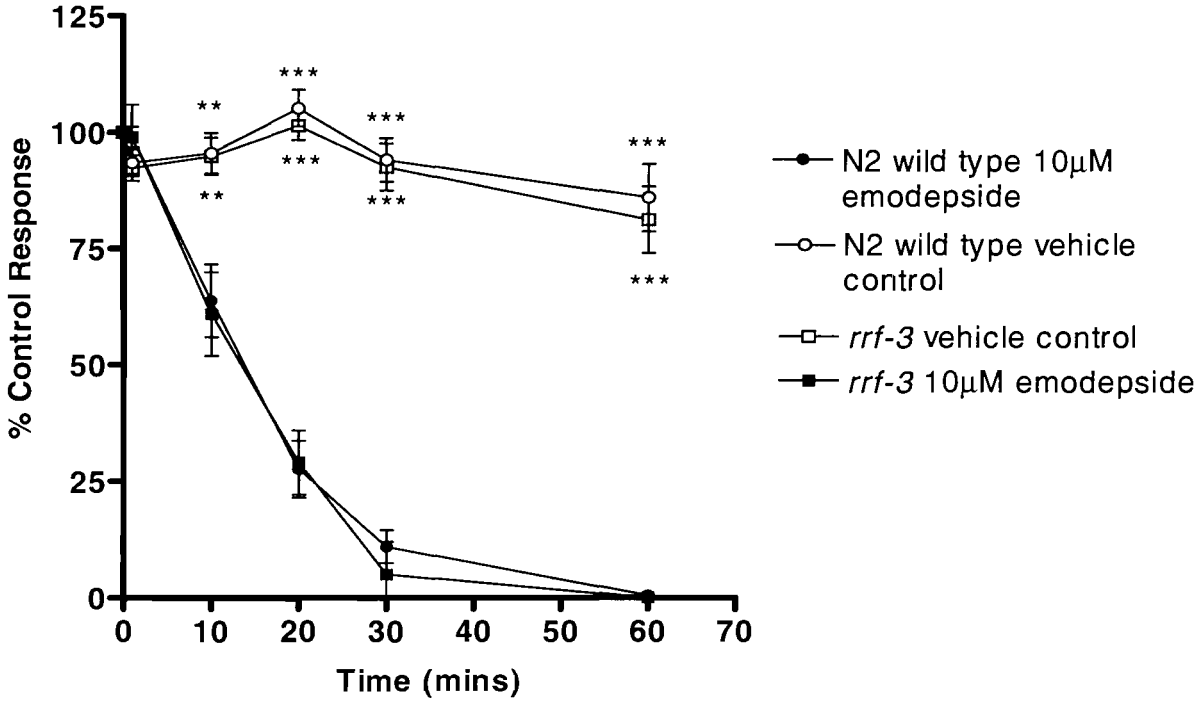

Figure 4.1 Time–dependence comparing the effect of emodepside (10μM) on *rrf-3 (pk1426) C.elegans* and N2 wild-type (thrashing assay). (○) N2 wild-type ethanol vehicle control 0.1%, (●) N2 wild-type with 10μM emodepside, (□) *rrf-3 (pk1426)* ethanol vehicle control 0.1%, (■) *rrf-3 (pk1426)* with 10μM emodepside. % control response is the number of body bends following emodepside application compared to the initial body bends prior to drug addition. Each point is the mean ± S.E.Mean of 27 determinations for N2 wild-type and ± S.E.Mean of 10 determinations for *rrf-3 (pk1426)*. ** indicates $P<0.01$, and *** indicates $P<0.001$ compared to uninduced control.

These experiments were performed as a control, to test the effect of emodepside on RNAi hypersensitive *rrf-3 C. elegans*. This strain was then used for all RNAi experiments. Following 60 mins incubation with either 10μM emodepside or vehicle control (0.1% ethanol) there was a reduction in the number of B.B/30sec (standardised as % inhibition compared to control response) in the emodepside treated *rrf-3 (pk1426)* compared to the control group (99 ± 0.4 % inhibition of body

bends, n=10 10μM emodepside, compared to 15 ± 6% inhibition of body bends, S.E.M n=10 vehicle control).

4.3 Effect of emodepside on locomotion of *rrf*-3 *C. elegans* treated with RNA-interference of the latrophilin-like genes

RNAi *via* bacterial feeding was utilised to knock-down expression levels of *lat-1* and *lat-2* in *rrf-3 (pk1426)* (pk1426) *C. elegans.* In order to express the dsRNA, HT115 (DE3) bacteria require IPTG. *C. elegans (rrf-3 (pk1426))* were therefore grown on plates in the presence (induced) or absence (uninduced, control) of IPTG.

To assess the effect on locomotion the 'thrashing' assay was used. In this assay 10μM emodepside virtually abolished body bends of *rrf-3 (pk1426)* after 1 hour, and caused an 86 ± 4.5% inhibition of body bends in the uninduced control (Fig 4.2). *C.elegans* treated with RNAi for *lat-1* were resistant to 10μM emodepside with only a 25 ±6%, (n=18) inhibition in body bends after 1hr. This equates to a 3.45 fold reduction in sensitivity to emodepside (% inhibition of body bends compared to uninduced control response).

The decreased sensitivity to emodepside following RNAi for *lat*-2 in the locomotion thrashing assay was not as marked as for *lat-1* RNAi. Emodepside (10μM) caused a 93 ± 3% inhibition of body bends in uninduced *rrf-3 (pk1426)* control, but only a 53 ± 9%, (n=12) inhibition in body bends in *lat-2* RNAi induced *rrf-3 (pk1426).*

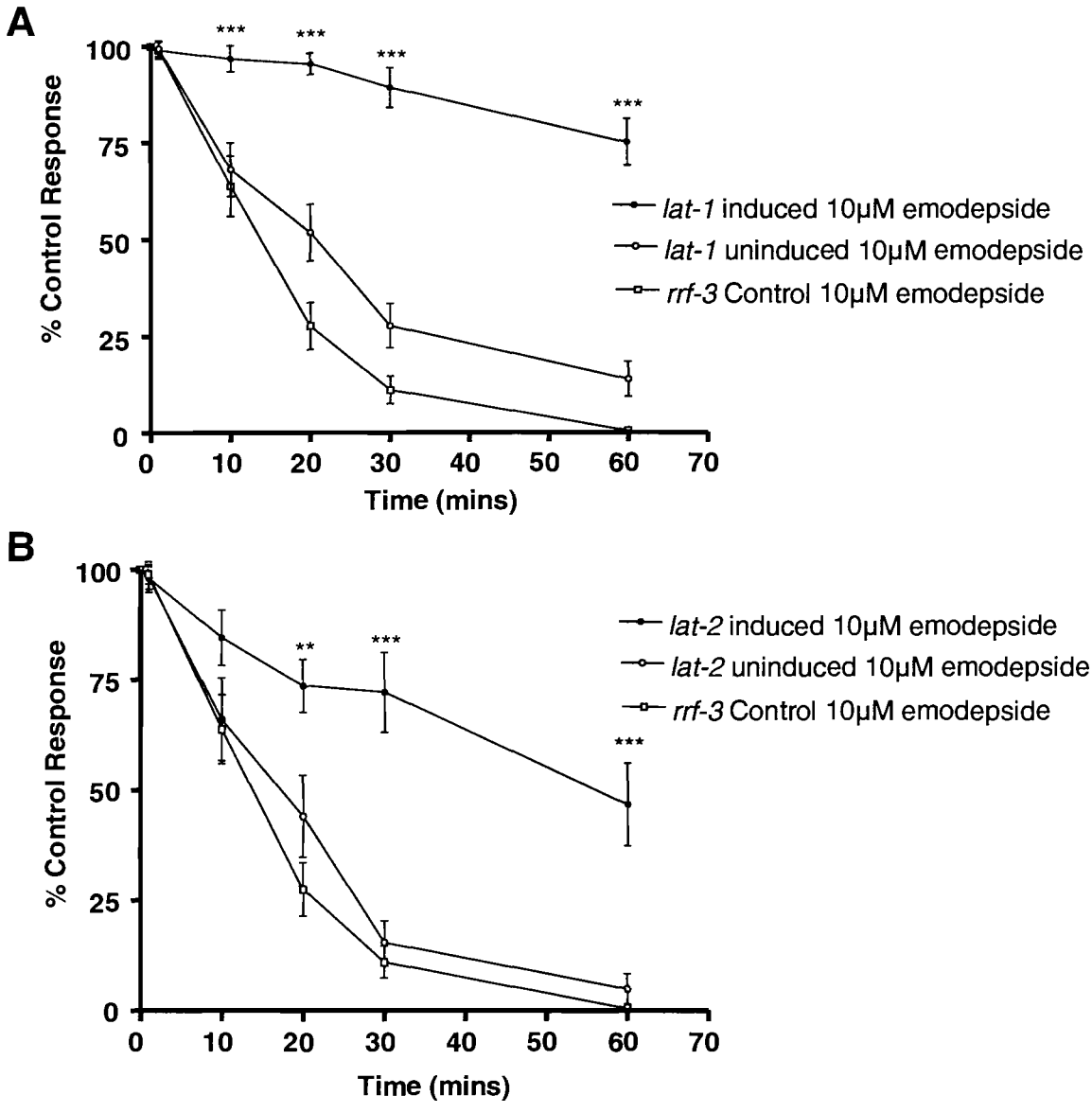

Figure 4.2 Time–dependence of the effect of emodepside (10μM) on (**A**) *lat-1* RNAi treated *rrf-3 (pk1426) C.elegans*, and (**B**) *lat-2* RNAi treated *rrf-3 (pk1426) C.elegans* (thrashing assay). (○) Uninduced control, (●) induced RNAi, (□) *rrf-3 (pk1426)* empty vector control. % control response is the number of body bends following emodepside application compared to the initial body bends prior to drug addition. Each point is the mean ± S.E.Mean of 18 determinations (*lat-1*) and ± S.E.Mean of 12 determinations (*lat-2*). ** indicates $P<0.01$, and *** indicates $P<0.001$ compared to uninduced control.

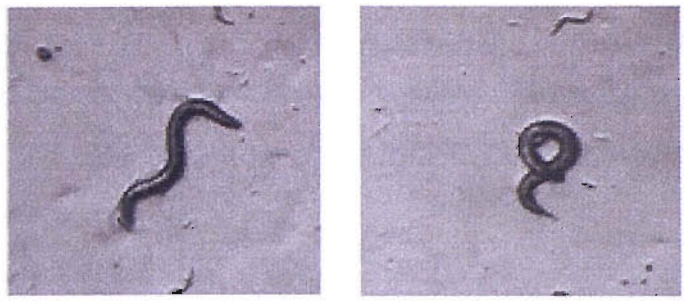

Figure 4.3 Animals treated with RNAi for *lat-1* exhibit loopy body bends (right) compared to control (left)

RNAi for *lat-1* resulted in an uncoordinated (*unc*) phenotype characterized by loopy, exaggerated body bends (Fig 4.3). This phenotype was not observed in *lat-2* RNAi treated worms.

Simultaneous RNAi for both *lat-1* and *lat-2* was attempted; however, the effect was less marked than for *lat-1* RNAi alone (Fig 4.4). In this assay 10μM emodepside caused a 90 ± 3% inhibition of body bends in the uninduced control. *C. elegans* treated with RNAi for both *lat-1* and *lat-2* were only resistant to 10μM emodepside with a 47 ± 5%, inhibition in body bends after 1hr, compared to RNAi for *lat-1* alone where worms were resistant to 10μM emodepside with only a 25 ± 6%, inhibition in body bends after 1hr. This concurs with published observations that RNAi for more than one gene at a time is not effective, probably due to the saturation of the cellular machinery required for RNAi (Timmons *et al.*, 2003).

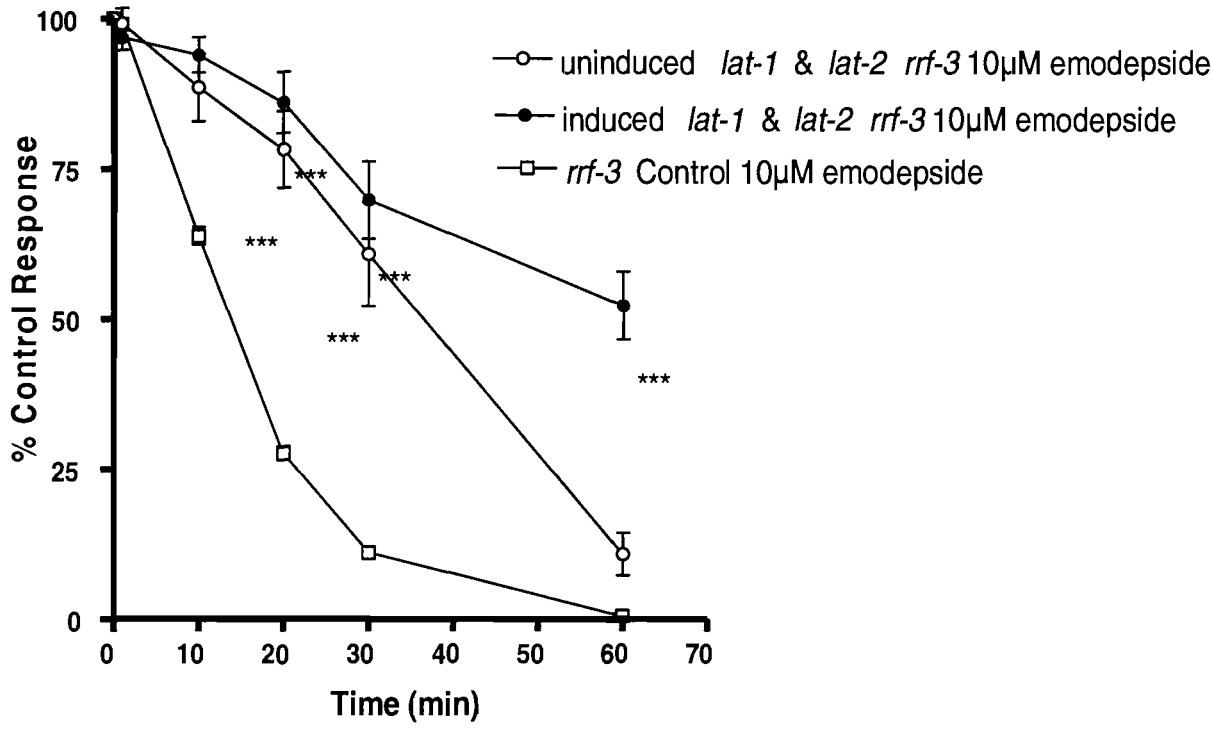

Figure 4.4 Time–dependence of the effect of emodepside (10μM) on simultaneous *lat-1* and *lat-2* RNAi treated *rrf-3 (pk1426) C. elegans* (thrashing assay). (○) Uninduced control, (●) induced RNAi, (□) *rrf-3 (pk1426)* empty vector control. % control response is the number of body bends following emodepside application compared to the initial body bends prior to drug addition. Each point is the mean ± S.E.Mean of 21 determinations. *** indicates $P<0.001$ compared to uninduced control. Where error bars are not visible, they are within symbol.

4.4 *lat-1 ok379* and *lat-2 ok301* deleted regions

Following the RNAi approach to identifying a role for a latrophilin receptor in the mechanism of emodepside action, two latrophilin mutant *C. elegans* strains became available, namely: *lat-1 (ok379)* RB629 and *lat-2 (ok301)* VC158.

For *lat-1 (ok379)* the deleted region was detected and amplified using the suggested nested PCR oligonucleotide sequences supplied with the mutant strain (R. Barstead and the *C. elegans* gene knockout consortium). Following this, these nested oligonucleotides, along with another set designed for sequencing, were used to determine the precise nature of the *lat-1* deletion. It was determined that *lat-1 (ok379)* has a 2054 bp deletion spanning exons 3, 4, and 5 of the gene (Appendix 4). This translates to an in-frame deletion of amino acids 100-583 (Fig 4.5). Although this deletion is in-frame, it has been suggested that the resultant receptor will be totally unviable, as it lacks the first transmembrane region yet retains the signal peptide which would result in incorrect membrane topology. In addition, the GPS domain (548-799 a.a), which is vitally important for the functioning of the protein, is missing (Dr. Yuri Ushkaryov, personal communication).

1 MRRNKTTYSLLQTILVACLLTVTPTFASNKPTTDESGTISHTICDGEAAELSCPAGKVIS
61 IVLGNYGRFSVAVCLPDNDIVPSNINCQNHKTKSILEKKCNGDSMCYFTVDKKTFTEDPC
121 PNTPKYLEVKYNCVVPATTTTTTTTTSTTTTDSSLIVDEEEEAQKDALNSDVIKPVKKKE
181 DVFCSATNRRGVNWQNTKSGTTSSAPCPEGSSGKQLWACTEEGQWLTEFPNSAGCESNWI
241 SSRNSVLSGVISSEDVSGLPEFLRNLGSETRRPMVGGDLPKVLHLLEKTVNVIAEESWAY
301 QHLPLSNKGAVEVMNYMLRNQEIWGSWDVTKRKEFASRFILAAEKAMVASAKGMMTSAES
361 NVIVQPAITVEISHKIKMSSQPTDYILFPSAALWNGQNVDNVNIPRDAILKINKDETQVF
421 FSSFDNLGAQMTPSDVTVAIAGTDQTEVRKRRVVSRIVGASLIENGKERRVENLTQPVRI
481 TFYHKESSVRHLSNPTCVWWNHHELKWKPSGCKLSYHNKTMTSCDCTHLTHFAVLMDVRG
541 HDLNEIDQTLLTLLTYVGCIISIICLLLTFFAYLIFSRNGGDRVFIHENLCLSLAIAEIT
601 FLAGITRTEDSLQCGIIAVALMYMFLSALTWMLLEGYHIHRMLTEVFPSDPRRFTYLLVG
661 YIPPAIITLVAYLYNSDGFGTPDHCWLSTQNNFIWFFAGPACFIFCANSLVLVKTLCTVY
721 QHTSGGYLPCRHDVDSGRSIRNWVKGSLALASLLGVTWIFGLFWVEDSRSIVMAYVFTIS
781 NSLQGLFIFLFHVVFAEKMRKDVGHWMYRRGCGGSSNSSPNHKRHNVQRDLMSPGVNSST
841 GSDFLYNTNDKYLTNSDTTNRLVYNGIMNHPNQMSVYQQHPHHQIYEQQPGTYDYATIAY
901 GDMMPGHRVAAPPAYQRLAVAEGRYGSQHQLYQGWHHRPPPEFSPPPPPLSTGPPNSRHY
961 GTGSSGRRPPSSKMSDDSAYSDGSSSMLTTEVTPQGQTVLRIDLNKPSMYCQDL

Figure 4.5 Amino acid sequence and conserved domains for *C. elegans* B0457.1 (LAT-1). The motifs that are conserved between latrophilin from different phyla are colour coded; galactose binding lectin domain (pink 51-133); hormone receptor domain (blue 181-240); latrophilin/CL-1-like GPS domain (orange 493-541); 7 transmembrane receptor, secretin family (red 548-799). Shaded grey area is region of deletion in *lat-1 (ok379)*.

A backcross protocol was carried out on *lat-1 (ok379)* RB629 (see Chapter 2, section 2.11.1), assuming that the *lat-1* mutation mapped to position 0.92 on chromosome II (*lat-1*(+) in wild-type worms). In the original strain, a deletion corresponding to *ok379* was detected, using nested PCR with the two sets of primers used by the Oklahoma consortium. After backcrossing once, several lines not segregating *rol-6 unc-4* were recovered. In one of these lines the presence of the deletion was confirmed by PCR (though not re-sequenced). As the *ok379* deletion was detected in these backcrossed animals, it was assumed they were homozygous for *ok379*. Indeed *lat-1 (ok379)* would have to be homozygous from this procedure if it mapped between *rol-6* and *unc-4*. However wild-type *lat-1*(+) was identified by PCR in these lines and therefore they cannot be homozygous for *lat-1 (ok379)* at chromosome II 0.92. It is possible that *lat-1 (ok379)* is carried on a chromosomal re-arrangement.

No homozygous *lat-1 (ok379)* line was available for analysis. These backcrossed worms were inhibited by 10μM emodepside in the locomotion thrashing assay, in an identical way to that observed with N2 wild-type (n=15, data not shown), and gave an identical IC_{50} to wild-type with the emodepside agar plate assay (n=20, data not shown).

```
1    MNSATLPLVESAEDQAFFAGYLQAMIPSNPPADMRPPPDGIWTAVRGVNNVTRASWV
58   YYPGSFLVTDTFWAPQEPNIYVNYNDVCVALQSDSFYREWTTALCTILKYTVCKVAP
115  TQIQAKYVAQCSCPNGYGGQTCETQSTTNQQASTQRTCGSDFQFSCPNDQTITVDFA
172  SFGAQGGSIITSPPDALLQQIVQKVNAETKKTVNFWIGTPNNCQLLMVTGSSTSYSQ
229  CPSSPSSTANVICSTVPQSTASVSARPTQSAPVDPVSQTMARREVYTGVQPIASALG
286  GQSKKTNRKLNNICQTKIGAPLSLFLFSRNEVITGFVCISLISASPQIIYYLCAVSL
343  ICHPSVPDSINKPRYCKKEKKDGITYEQTRACMLHEQPCPDPQNVEGTVTRYCNCQT
400  AKWETPDTTNCTHRWVAEMETAIKDNQPVEDISSTVNRQLKSTIERTLFGGDITGTV
457  RLSNDMLSLARNQFSVLNDRNLRENKARNFTENLGGSGDQLLSPVAATVWDQLSSTI
514  RIQHASKLMSVLEQSVLLLGDYMTDQKLNLQYINWAMEVERSEPEVQTFGAAASPNV
571  QDDMGMMRVMAAAPPAPQPETNTTIMFPSLKLSPTITLPSASLLSSLASPTPVAGGG
628  PSILSSFQDDTPVGMASTPNLNRNPVKLGYYAFAGFGQLLNNNNDHTLINSQVIGAS
685  IQNATQSVTLPVDHPVTFTFQHLTTKGVSNPRCVYWDLMESKWSTLGCTLIATSSNS
742  SQCSCTHLTSFAILMDISGQVGRLSGGLASALDVVSTIGCAISIVCLALSVCVFTFF
799  RNLQNVRNSIHRNLCLCLLIAELVFVIGMDRTGNRTGCGVVAILLHYFFLSSFCWML
856  LEGYQLYMMLIQVFEPNRTRIFLYYLFCYGTPAVVVAISAGIKWEDYGTDSYCWIDT
913  STPTIWAFVAPIIVIIAANIIFLLIALKVVLSVQSRDRTKWGRIIGWLKGSATLLCL
970  LGITWIFGFLTAVKGGTGTAFAWIFTILNCTQGIFIFVLHVVLNEKVRASIVRWLRT
1027 GICCLPETSSAAYNSRSFLSSRQRILNMIKVNGHSYPSTASTDDKEKQLTPITKTTD
1084 WLSRLPNQDSVSIPESNFNNLNGTLENSNLNSAEIKEEDEIPELRRRVTVDLNPMIV
1141 SNNEIERMSHASSDPRGSQIIEVTAVEKKAPVKRIKFPLGAKQSERGSQHRTKAKHG
1198 TGTLVSPWHIVTAAHLIGISEDPLPDCDTGNLREAYFVRDYKNFVAFVNVTCAVPEM
1255 CKGLHRKDMFKPLAIKSLYIRKGYVGDGCIDRESFNDIAVFELEEPIEFSKDIFPAC
1312 LPSAPKIPRIRETGYKLFGYGRDPSDSVLESGKLKSLYSFVAECSDDFPYGGVYCTS
1369 AVNRGLSCDGDSGSGVVRTSDTRNVQVLVGVLSAGMPCPELYDTHNRQRQQRRQLTQ
1426 ETDLLVDVSAHVDFFCTCCGMCS
```

Figure 4.6 Amino acid sequence and conserved domains for *C. elegans* B0286.2 (LAT-2). The motifs that are conserved between latrophilin from different phyla are colour coded; galactose binding lectin domain (purple 69-194); hormone receptor domain (blue 479-539); latrophilin/CL-1-like GPS domain (orange 837-885); 7 transmembrane receptor, secretin family (red 894-1140). Shaded grey area is region of deletion in *lat-2 (ok301).*

The *lat-2 (ok301)* allele deletion (created by R. Barstead lab, Oklahoma City) was sequenced by the Vancouver Gene Knockout Lab. This mutant has a 1083 b.p deletion with an insertion (gtcggca). This corresponds to an in frame deletion of the last 253 a.a (1196-1449 missing) (Fig 4.6).

Prior to assaying the effect of emodepside on locomotion of this latrophilin mutant, backcrossing was performed 1x using rol-6 (e187) :: unc-4 (e120) (see Chapter 2).

4.5 Effect of emodepside on locomotion of *lat-2 (ok301) C. elegans*

It was observed that emodepside had a concentration-dependent effect on *lat-2 (ok301)*. As in N2 wild-type, an emodepside effect was observed in *lat-2 (ok301)* at 4.5nM (23.4 ± 0.5 compared to ethanol vehicle control 29.4 ± 1.2, body bends/min, n=10) (Fig 4.7). However, *lat-2 (ok301)* were significantly less affected than wild-type worms through the concentration range. *lat-2 (ok301)* mutants were less sensitive to emodepside than wild type control (IC_{50} = 20nM, 95% confidence limits 17 to 23nM, compared to wild-type IC_{50}=4nM, 95% confidence limits 1.1 to 15nM).

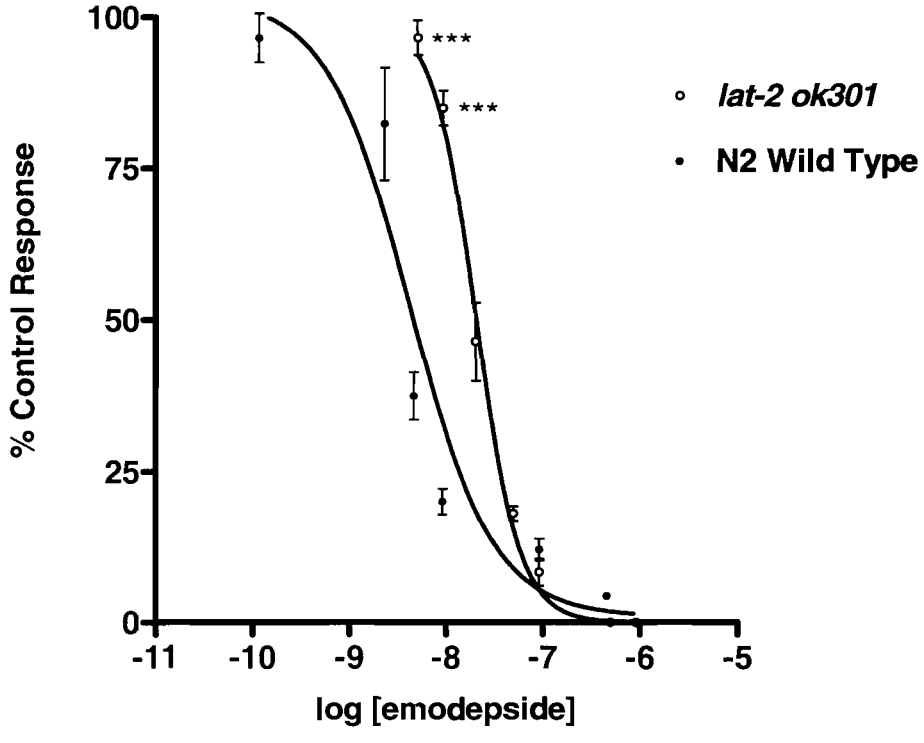

Figure 4.7 Concentration-response curves comparing the effect of emodepside on locomotion of wild type N2 *C. elegans* (●) and *lat-2 (ok301)* (○). '% control response' is the number of body bends per minute following emodepside application as a % of the body bends per minute of wild type worms grown on vehicle control plates (1% ethanol). N2 wild-type IC_{50} 4.2nM (95% confidence limits 1.1 to 15nM), *lat-2 (ok301)* IC_{50} 20nM (95% confidence limits 17 to 23nM). Each point is the mean ± S.E.Mean of >10 determinations. *** indicates $P<0.001$ compared to uninduced control.

4.6 Effect of emodepside on locomotion of *egl-30 C. elegans*

Latrophilin has been shown to couple to $G\alpha_q$ (Rahman *et al.*, 1999). *C. elegans egl-30 n686* and *ad810* are reduction of function alleles which have a mutation in the α-subunit of G protein q (80% identity to mammalian Gqα) (Brundage et al., 1996). *egl-30 (n686)* have a disruption at the acceptor intron 4 site, which disrupts sequences at the intron/exon junctions that specify sites for mRNA splicing. This results a debilitated phenotype in these animals characterised by bloating, extreme sluggishness, egg retention and variable tracks (Brundage *et al.*, 1996). It is for these reasons that *egl-30 (ad810)* DA1096 were also used in this study. *egl-30 (ad810)* mutations produce premature termination of Gq alpha after amino acid 211; homozygotes of this allele arrest as paralyzed L1 larva (Brundage *et al.*, 1996). However, *egl-30 (ad810)* DA1096 is a balanced strain (*egl-30(ad810)/szT1[lon-2(e678)] I; +/szT1 X*), which overcomes the problem of homozygous lethal animals and allows for less-sluggish levels of locomotion. The *egl-30* gene encodes an ortholog of the heterotrimeric G protein alpha subunit Gq (Gq/G11 class) that affects viability, locomotion, egg laying, synaptic transmission, and pharyngeal pumping; it genetically interacts with the *goa-1* pathway, and is probably expressed ubiquitously, with highest expression in excitable cells (Trent et al., 1983; Brundage et al., 1996). Identification of *egl-30* alleles in selections for aldicarb (inhibitor of ACh-esterase) resistant mutants, suggests that *egl-30* positively regulates synaptic transmission (Miller et al., 1999).

It was observed that emodepside had an effect on both *egl-30* alleles at 4.5nM (21.5 ± 4.1 n=5, *ad810*, compared to 1% ethanol vehicle control 29.75 ± 1.8, body bends/min, and 6.2±0.3 n=5, *n686,* compared to 1% ethanol vehicle control 9.6 ±0.5,). However, *egl-30* alleles were significantly less affected than W.T. worms through the concentration range. *egl-30 (ad810)* mutants were less sensitive to emodepside than wild type control (IC_{50} = 24nM, 95% confidence limits 6.5 to 91nM, compared to W.T. IC_{50}=4nM, 95% confidence limits 1.1 to 15nM) (Fig 4.8A). *egl-30 (n686)* mutants were less sensitive to emodepside than wild type control (IC_{50} = 12nM, 95% confidence limits 6.2 to 22nM, compared to W.T. IC_{50} = 4nM, 95% confidence limits 1.1 to 15nM) (Fig 4.8B).

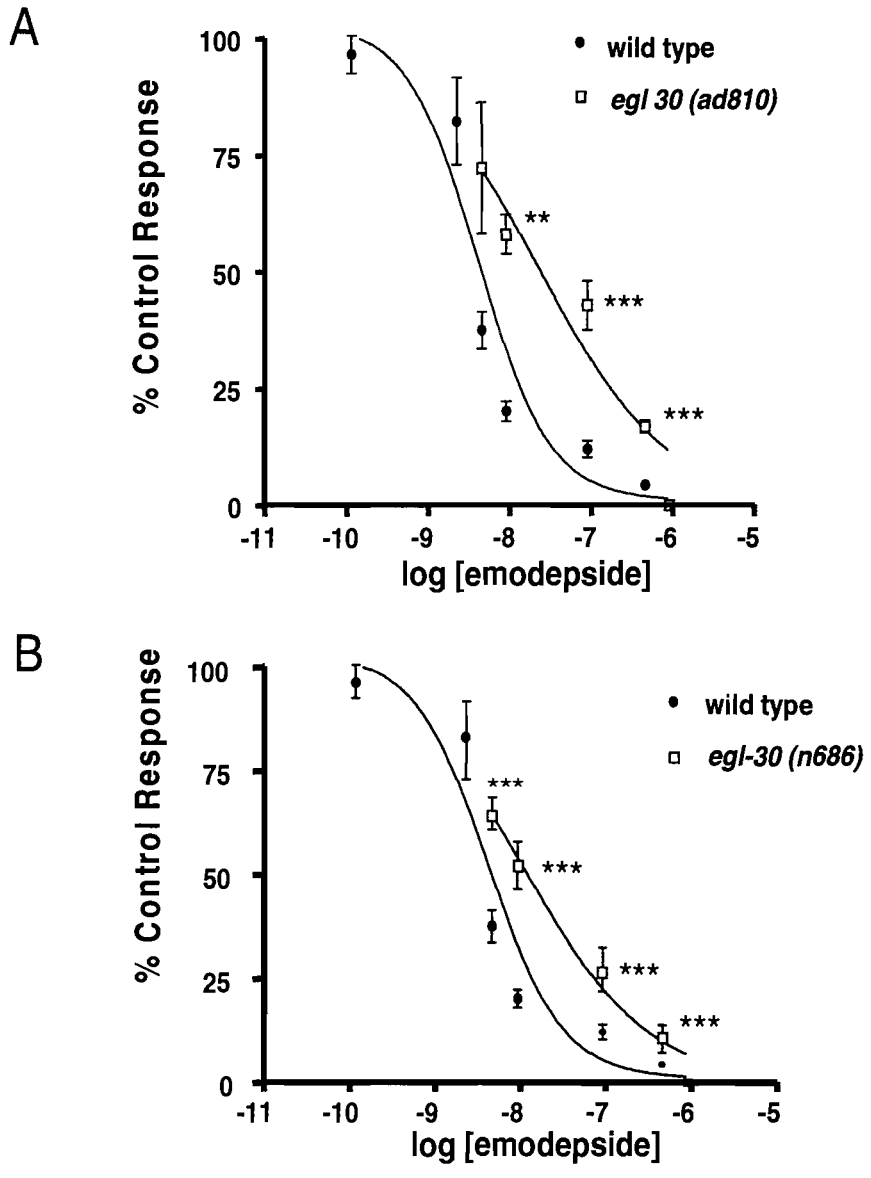

Figure 4.8 Concentration-response curves comparing the effect of emodepside on locomotion of wild type N2 *C. elegans* and (**A**) *egl-30 (ad810)* (**B**) *egl-30 (n686)*. '% control response' is the number of body bends per minute following emodepside application as a % of the body bends per minute of wild type worms grown on vehicle control plates (1% ethanol). IC_{50} 4.2nM (95% confidence limits 1.1 to 15nM wild type), IC_{50} 24nM, (95% confidence limits 6.5 to 91nM *egl-30 (ad810)*), and IC_{50} 12nM, (95% confidence limits 6.2 to 22nM *egl-30 (n686)*). Each point is the mean ± S.E.Mean of >5 determinations. ** indicates $P<0.01$, and *** indicates $P<0.001$ compared to W.T. control.

A gain-of-function (gf) allele exists for *egl-30* in *C. elegans* (Doi & Iwasaki, 2002). Emodepside elicited a hypersensitive inhibition of *egl-30 (tg26)* gain-of-function locomotion compared to wild-type (IC_{50}< 0.1nM compared to 4.1nM in wild-type) (Fig 4.9).

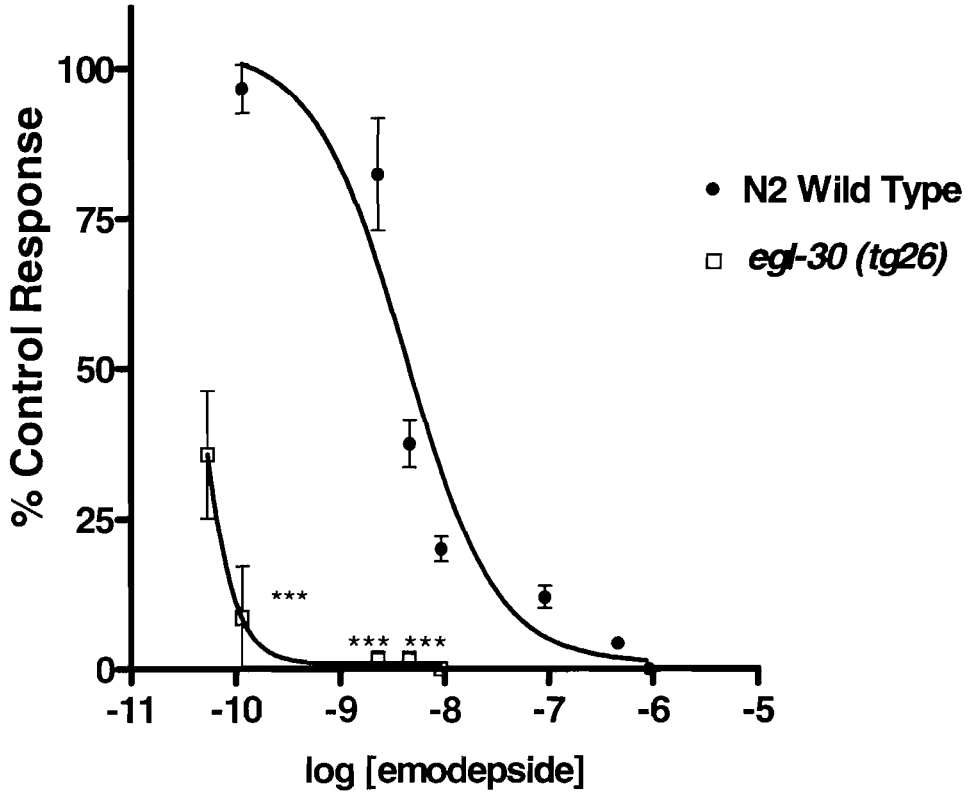

Figure 4.9 Concentration-response curves comparing the effect of emodepside on locomotion of wild type N2 (•) *C. elegans* and *egl-30 (tg26)* gain of function (□). '% control response' is the number of body bends per minute following emodepside application as a % of the body bends per minute of wild type worms grown on vehicle control plates (1% ethanol). IC_{50} 4.2nM (95% confidence limits 1.1 to 15nM) wild type, IC_{50} < 0.1nM *egl-30 (tg26)*. Each point is the mean ± S.E.Mean of >5 determinations. *** indicates P<0.001 compared to W.T. control.

4.7 Effect of emodepside on locomotion of *egl-8 C. elegans*

$G\alpha_q$ has been shown to stimulate phospholipase Cβ activity (Taylor & Exton, 1991;Lee *et al.*, 1992), encoded in *C. elegans* by *egl-8* (Miller *et al.*, 1999;Lackner *et al.*, 1999). Like Gqα (*egl-30*), the downstream effector PLCβ (*egl-8*) is also implicated in the positive regulation of synaptic transmission, as loss-of-function mutations result in strong aldicarb resistance as well as reduced locomotion (Miller et al., 1999). To determine if *egl-8* mutations affect the efficacy of emodepside, alleles that most strongly reduce EGL-8 function were assayed. Such alleles are those which disrupt the highly conserved catalytic Y domain, namely, *egl-8 (n488)* which has a deletion that eliminates exons 10 and 11 and disrupts the reading frame before the Y domain, and *egl-8 (md1971)*, a strong loss-of-function allele that contains an early stop codon believed to prevent formation of part of the catalytic Y domain and the C-terminal region of the protein (Miller et al., 1999). The latter of these two is the more severe loss of function allele.

egl-8 (n488) mutants were less sensitive to emodepside than wild type control (IC_{50}=54nM, 95% confidence limits 52 to 55nM, n=8 compared to IC_{50}=4.2nM, 95% confidence limits 1.2 to 1.5nM, n=6) in the emodepside plate assay (Fig 4.10A). *egl-8* (md1971) mutants were less sensitive to emodepside than wild type control (IC_{50}= 216nM, 95% confidence limits 202 to 233nM, n=8 compared to IC_{50}= 4.1nM, 95% confidence limits 4.6 to 4.8nM, n>6) in the emodepside plate assay (Fig 4.10B).

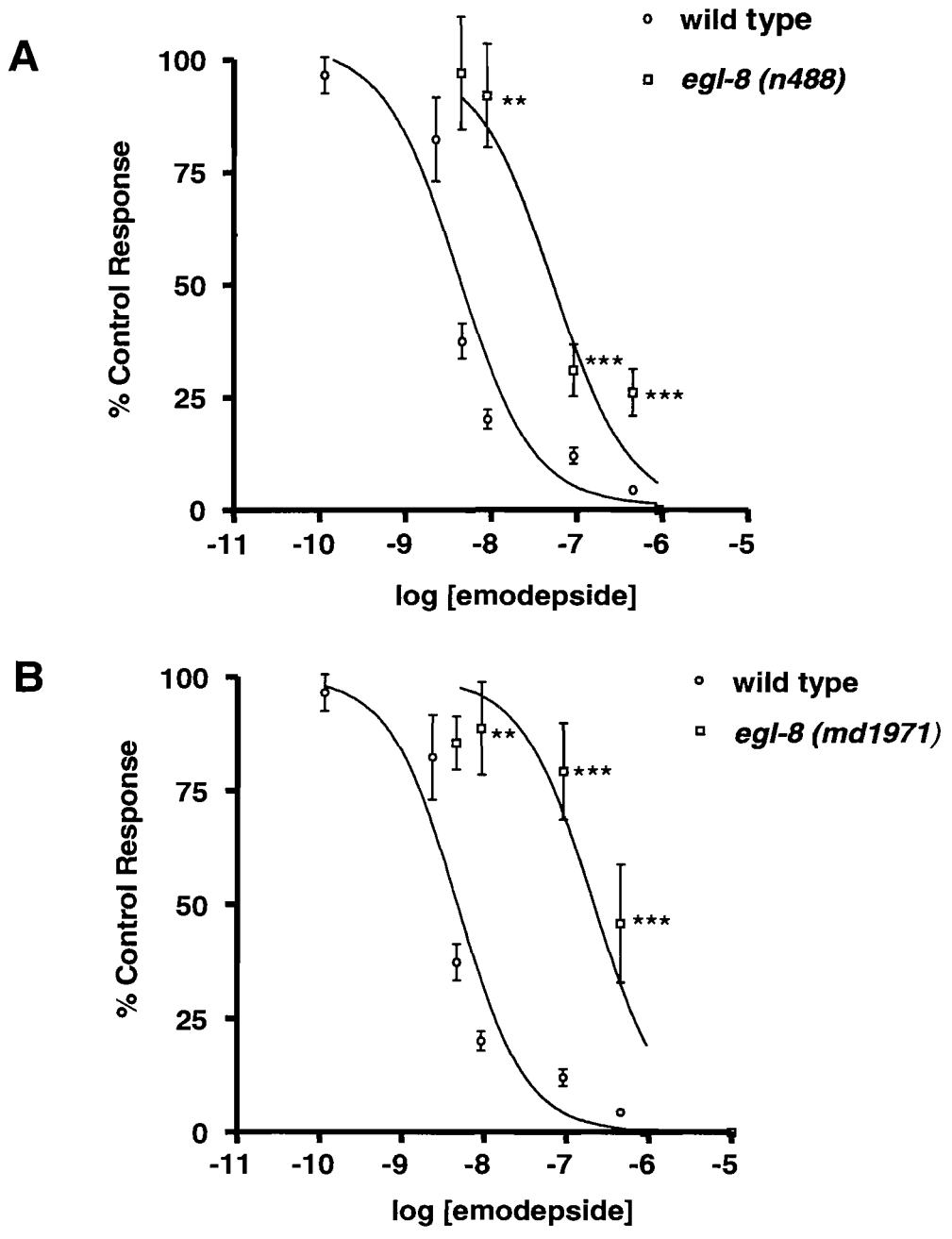

Figure 4.10 Concentration-response curves comparing the effect of emodepside on locomotion of wild type N2 *C. elegans* and (**A**) *egl-8 (n488)* (**B**) *egl-8 (md1971)*. '% control response' is the number of body bends per minute following emodepside application as a % of the body bends per minute of wild type worms grown on vehicle control plates (1% ethanol). IC_{50} 4.2nM (95% confidence limits 1.1 to 15nM) wild type, IC_{50} 54nM, (95% confidence limits 52 to 55nM) *egl-8 (n488)*, and IC_{50} 216nM, (95% confidence limits 202 to 233nM) *egl-8 (md1971)*. Each point is the mean ± S.E.Mean of 10 determinations for N2 wild-type and ± S.E.Mean of 8 determinations for *egl-8* alleles. ** indicates $P<0.01$, and *** indicates $P<0.001$ compared to W.T. control.

4.8 Effect of emodepside on locomotion of *goa-1 C. elegans*

Previous studies on the neuromuscular junction of *C. elegans* have shown that $G\alpha_q$ (EGL-30) and $G\alpha_o$ have reciprocal effects on ACh release, with the former stimulating release through activation of PLC-β and production of DAG (Lee et al., 1992; Taylor and Exton, 1991), and the latter inhibiting release through activation of a DAG kinase (Miller et al., 1999; Nurrish et al., 1999). Therefore the possibility that the Gαo loss-of-function mutant (*goa-1*, *n1134*) would also have altered sensitivity to emodepside was investigated. These mutants were more sensitive to emodepside in the emodepside agar plate assay (IC_{50} 0.02nM compared to 4.1nM in wild-type).

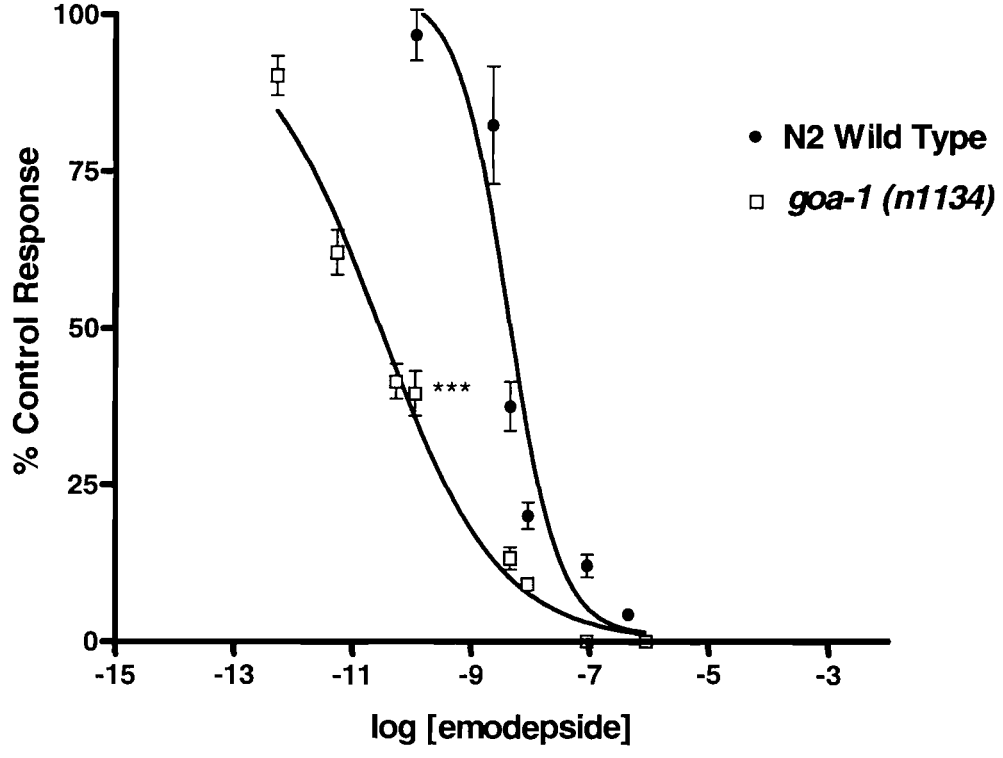

Figure 4.11 Comparison of the concentration-response curves for the effect of emodepside on locomotion in wild type N2 *C. elegans* (•), and *goa-1* (*n1134*) (□). '% control response' is the number of body bends per minute following emodepside application as a % of the body bends per minute of wild type worms grown on vehicle control plates (1% ethanol). IC_{50} 4.2nM (95% confidence limits 1.1 to 15nM wild type, IC_{50} 0.02nM (95% confidence limits 0.01nM to 0.08nM) (*goa-1 n1134*). Each point is the mean ± S.E.Mean of 10 determinations for N2 wild-type and ± S.E.Mean of 16 determinations for *goa-1* (*n1134*). *** indicates $P<0.001$ compared to W.T. control.

4.9 Effect of PF1022-001 on locomotion of *C. elegans*

In order to control for the possibility that the anthelmintic action of emodepside simply derives from a pore forming capability, rather than through a latrophilin-G protein linked pathway, the action of PF1022-001 was determined. This is an optical antipode of PF1022-A which is structurally related to emodepside. PF1022-001 has pore forming capability, yet no anthelmintic activity (Gebner *et al.*, 1996). PF1022-001 had no inhibitory action on *C. elegans* thrashing behaviour (Fig 4.12).

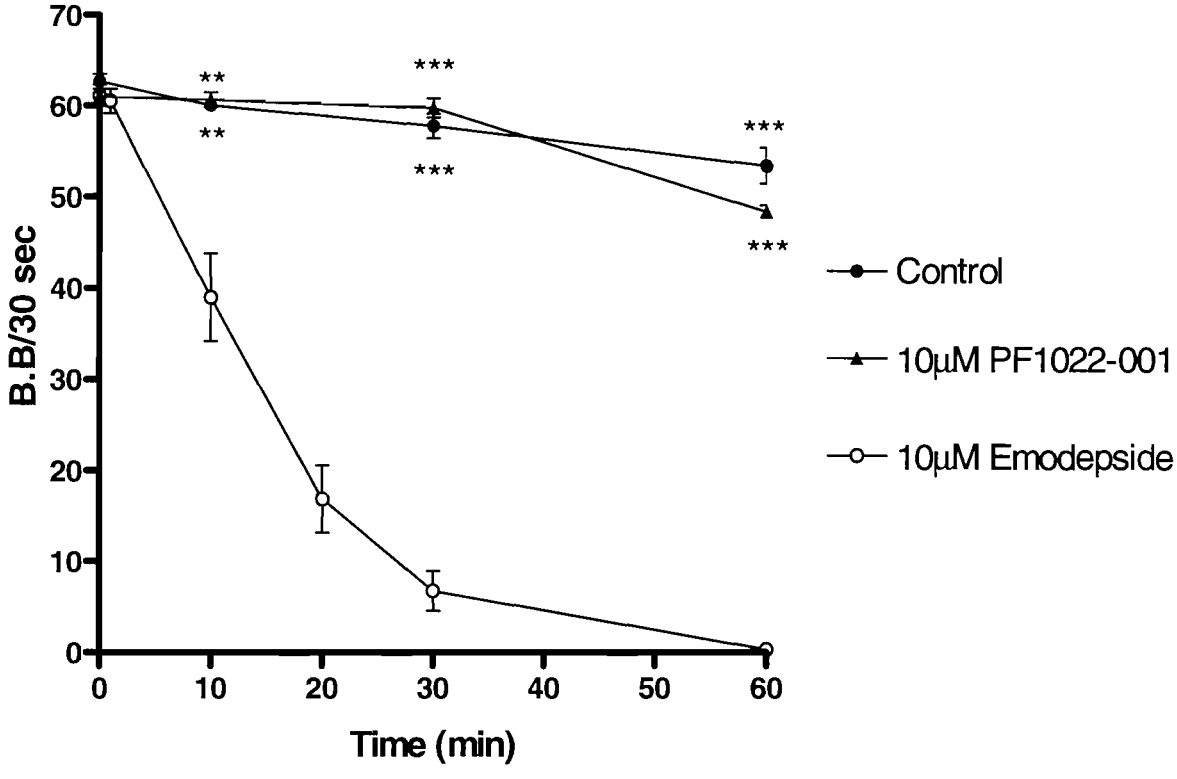

Figure 4.12 Comparison of the time-dependent effect on wild type *C.elegans* of 10µM emodepside (○), ethanol vehicle control 0.1% (●) and PF1022-001 (▲) on the thrashing locomotory behaviour exhibited in Dent's saline. S.E.M of body bends/30 secs (n=27 N2 W.T, n=5 PF1022-001). ** indicates $P<0.01$, and *** indicates $P<0.001$ compared to W.T. control.

4.10 Emodepside and neurotransmitter release.

A number of neurotransmitters and neuromodulators are known to affect nematode body wall muscle (Walker *et al.*, 2000). To elucidate which neurotransmitters or neuromodulators may be released by emodepside, *C. elegans* mutants to these neurotransmitters / neuromodulators were tested for emodepside resistance. In cases where relevant mutants were not available RNAi techniques were used to knock-down gene expression.

ACh, GABA, dopamine, octopamine, 5-HT and glutamate are the major classical neurotransmitters that modulate complex behaviours in *C. elegans*. Dopamine, octopamine and 5-HT have been shown to be important in regulating egg laying, starvation responses and male mating behaviour (Horvitz *et al.*, 1982;Loer & Kenyon, 1993). Glutamate is primarily involved in the response to light mechanical stimulation of the head, the response to strong mechanical stimulation in the anterior body and the effects of the M3 motor neuron on the pharyngeal muscle, mediated through the AVR-15 postsynaptic receptor (Hart *et al.*, 1995;Lee *et al.*, 1999). The classical transmitters involved in regulating nematode locomotion are ACh (excitatory) and GABA (inhibitory) (see Chapter 1). From the previous chapter it was demonstrated that emodepside action does not occur via a GABAergic mechanism. Therefore, an investigation into ACh release at the *C. elegans* NMJ, as a result of emodepside action, was carried out.

As the above data indicate a role for a latrophilin receptor in the mechanism of emodepside action, aldicarb was used to determine if ACh is released presynaptically via a latrophilin receptor (Fig 4.13). Aldicarb is an AChesterase (AChE) inhibitor that prevents the degradation of ACh at synapses, leading to prolonged ACh at the cleft and continual stimulation of post-synaptic receptors, resulting in spastic paralysis (Cox C, 1992). If emodepside action, via LAT-1, results in vesicular exocytosis of ACh at the *C. elegans* NMJ, *lat-1* RNAi treated worms should exhibit a reduced sensitivity to the aldicarb induced paralysis observed in wild-type animals.

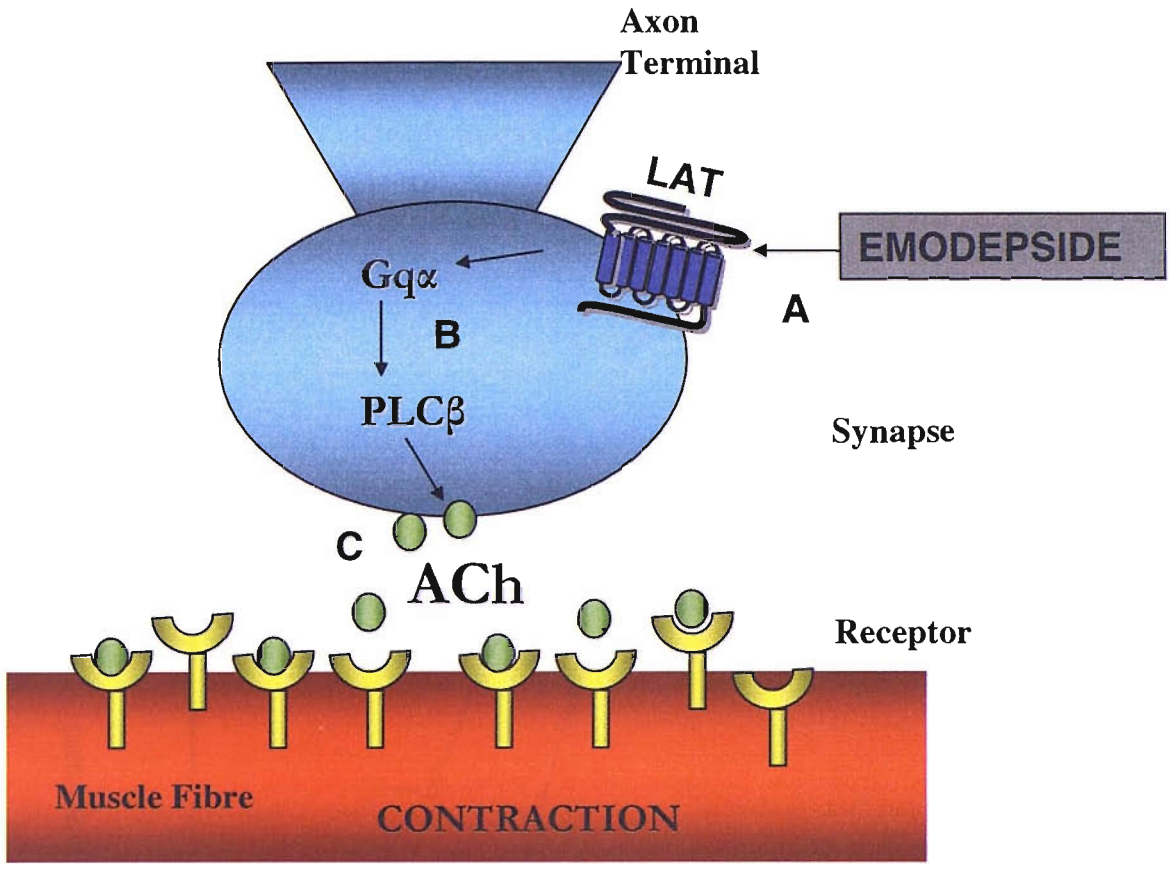

Figure 4.13 A possible mechanism for the action of emodepside. Upon binding of emodepside to the presynaptic latrophilin receptor (**A**), a second messenger signalling cascade involving $G_q\alpha$ and PLCβ (**B**) leads to release of ACh (**C**) and subsequent contraction of the post-synaptic muscle fibre. This hypothesis was investigated in this study using the AChesterase inhibitor Aldicarb and *lat-1* RNAi treated *C. elegans*.

4.11 Comparison of the effect of 1mM aldicarb on *rrf-3 (pk1426)* and N2 wild-type *C. elegans*

100% of both N2 wild-type worms and *rrf-3(pk1426) C. elegans* were totally paralysed at 110 mins following exposure to 1mM aldicarb (Fig 4.14). The onset time for partial paralysis to aldicarb (response to nose tap) was similar for both strains (10min, data not shown). However, the *rrf-3* strain progressed to become totally paralysed (no response to nose tap), between 20 and 100 mins, more rapidly than the wild-type worms, indicating an increased sensitivity to aldicarb for the *rrf-3* strain.

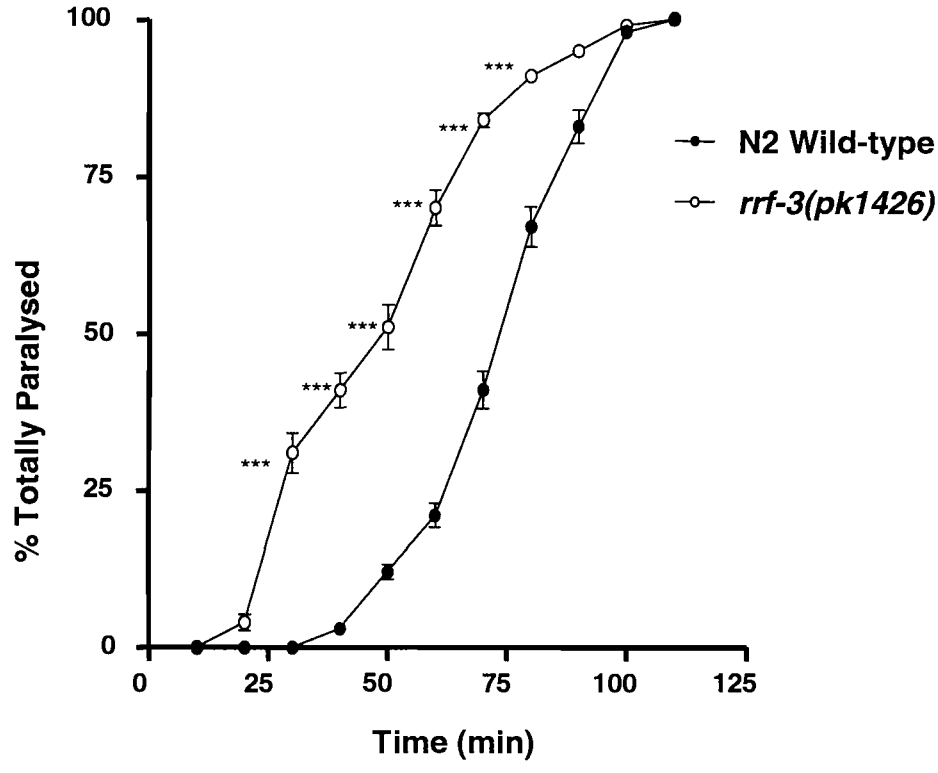

Figure 4.14 Comparison of the time-dependent effect of 1mM aldicarb on *rrf-3 (pk1426)* (○) and N2 wild-type *C. elegans*. The number of worms totally paralysed at each time point was determined (no response to nose tap). All data points are shown as ± S.E.M (n=100). *** indicates $P<0.001$ compared to wild-type.

4.12 Effect of aldicarb on *lat-1* RNAi treated *rrf-3 (pk1426) C. elegans*

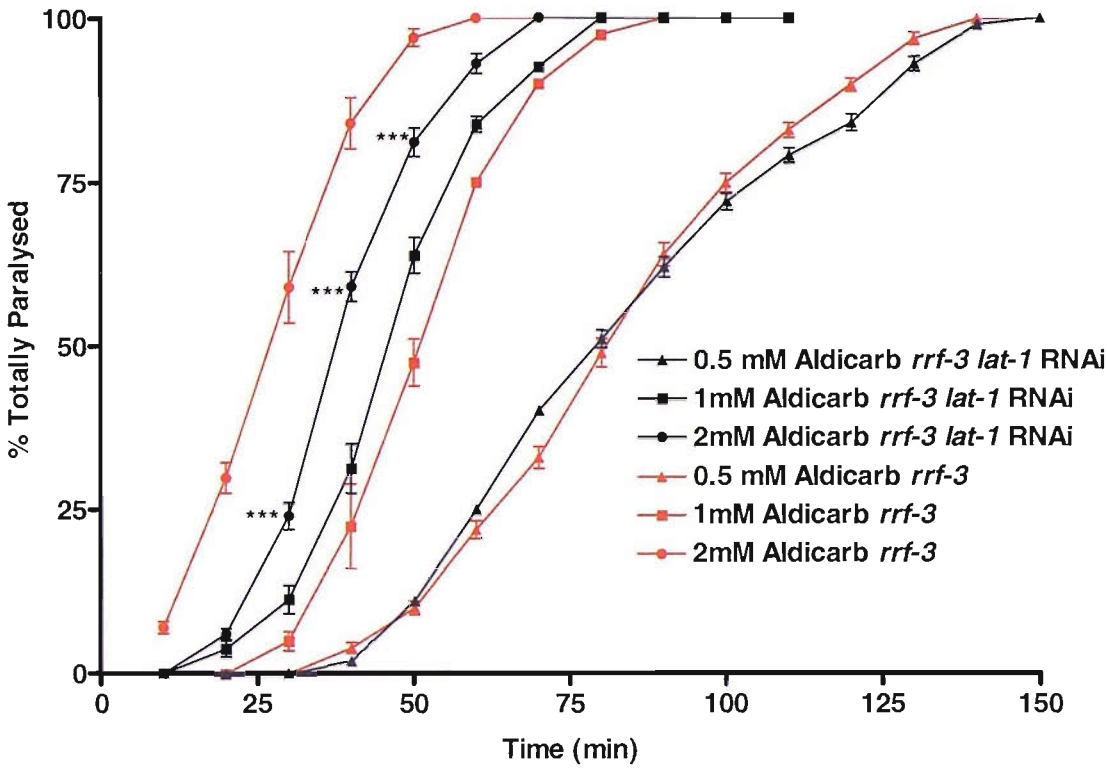

Figure 4.15 Comparison of the time-dependent effect of 0.5mM (triangle), 1mM (square) and 2mM (circle) aldicarb on lat-1 RNAi treated *rrf-3 (pk1426) C. elegans* (black) and control *rrf-3 (pk1426) C. elegans* fed on empty vector (red). The number of worms totally paralysed are shown as ± S.E.M (n=100). *** indicates $P<0.001$ compared to empty vector control.

0.5mM and 1mM aldicarb paralysed both *lat-1* RNAi treated *rrf-3 (pk1426)* and empty vector control worms in a comparable, concentration-dependent manner (Fig 4.15). However, at 2mM aldicarb there was a significant difference between the rates of paralysis of *lat-1* RNAi treated *C. elegans* and the empty vector fed *C. elegans*. At 30 mins only 24% of *lat-1* RNAi treated worms were totally paralysed by 2mM aldicarb, compared to 59% paralysed in the control group (n=100, $P<0.001$).

4.13 Effect of emodepside on locomotion of *unc-38 (x20) C. elegans*

C. elegans unc-38 encodes an alpha subunit of the nicotinic ACh receptor (nAChR) superfamily; UNC-38 is required for normal locomotion and egg-laying, and functions as a subunit of a ligand-gated ion channel that likely mediates fast actions of ACh at neuromuscular junctions and in the nervous system (Schafer, 2002). *unc-38 (x20)* mutants were less sensitive to emodepside than wild type control (IC_{50} = 15nM compared to N2 wild-type IC_{50} = 4.2nM) (Fig 4.16).

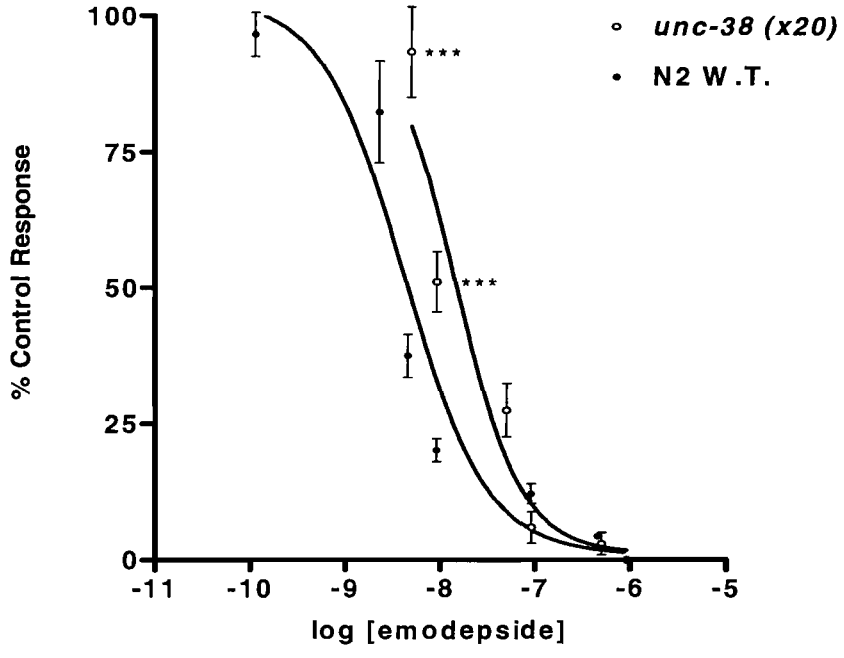

Figure 4.16 Comparison of the concentration-response curves for the effect of varying concentrations of emodepside on locomotion in wild type N2 *C. elegans*, and *unc-38(x20).* '% control response' is the number of body bends per minute following emodepside application as a % of the body bends per minute of wild type worms grown on vehicle control plates (1% ethanol). IC_{50} 4.2nM (95% confidence limits 1.1 to 15nM) wild type, IC_{50} 15nM (95% confidence limits 3.8 to 55nM) *unc-38 (x20).* Each point is the ± S.E.Mean of 10 determinations for N2 wild-type and ± S.E.Mean of 8 determinations for *unc-38(x20).* *** indicates $P<0.001$.

4.14 Effect of levamisole on *lat-1* RNAi treated *rrf-3 (pk1426) C. elegans*

Levamisole is a more potent agonist than ACh at nematode muscle nAChRs (Lewis *et al.*, 1980b). To control for a possible depletion of post-synaptic nAChRs due to *lat-1* RNAi, worms were subjected to 150μM and 300μM levamisole and the time dependence of any drug induced paralysis assayed.

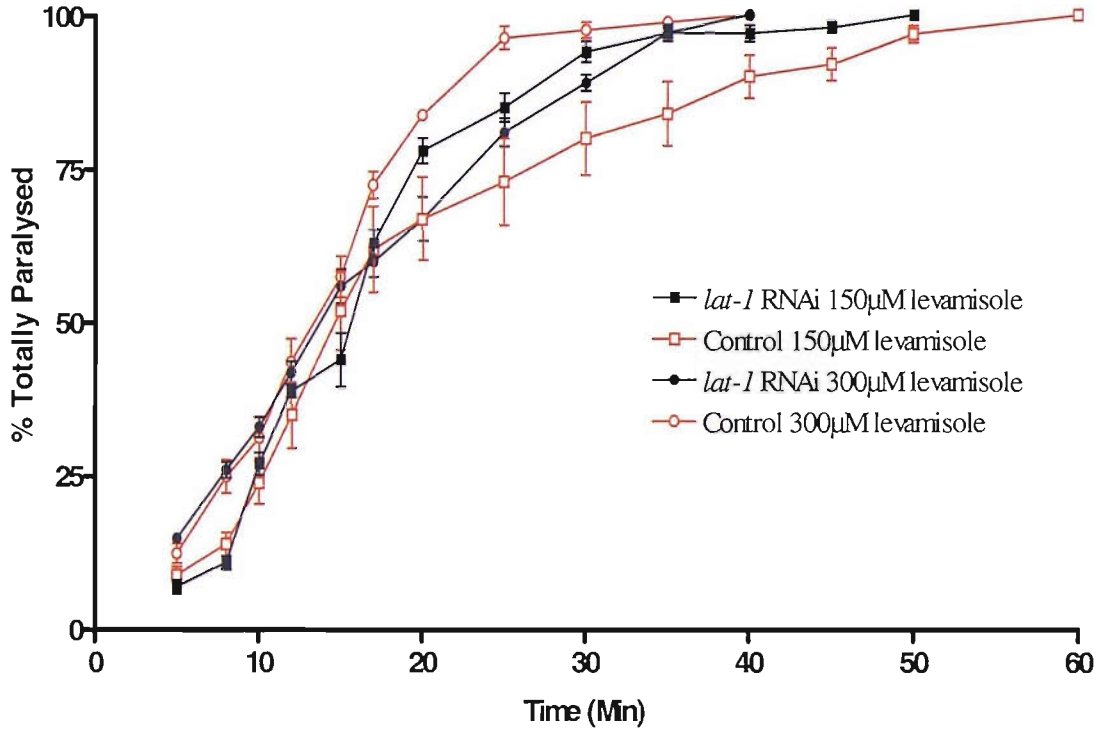

Figure 4.17 Comparison of the time-dependent effect of 150μM (square) and 300μM (circle) levamisole on *lat-1* RNAi treated *rrf-3 (pk1426) C. elegans* (black) and control *rrf-3 (pk1426) C. elegans* fed on empty vector (red). The number of worms totally paralysed are shown as ± S.E.M (n=100).

No significant difference was observed between the *lat-1* RNAi treated *C. elegans* and the empty vector control animals in the time-dependent paralysis induced by levamisole (150μM totally paralysed 100% at 60min, 300μM totally paralysed 100% at 40 min).

4.15 Effect of emodepside on peptide release in *C. elegans.*

Neuropeptides constitute a large, diverse set of neurotransmitters which are proposed to play varied roles in physiology and behaviour. It has been demonstrated that emodepside mimics the action of the FMRFamide peptide PF2 when applied to *A. suum* DMS (Willson *et al.*, 2003). Classical transmitters are packaged in small, clear, synaptic vesicles that are clustered near release sites, whereas large dense-core vesicles filled with neuropeptides are seen throughout the presynaptic compartment (Richmond & Broadie, 2002;Li & Chin, 2003). Neuropeptides are initially synthesized as large preproteins that are packaged into dense-core vesicle precursors in the *trans*-Golgi network (Rosoff *et al.*, 1992). The effect of emodepside on peptide release was therefore investigated in the *C. elegans* system.

4.16 Effect of emodepside on locomotion of *egl-21 (n476) C. elegans.*

The *egl-21* gene encodes a carboxypeptidase E (CPE), which mediates an enzymatic step in peptide processing, removal of C-terminal basic residues. The *egl-21* CPE is expressed in 60% of the nervous system, including interneurons, motor neurons, and sensory neurons. Mutations in *egl-21* were first isolated in a screen for egg laying defective mutants, but also showed defective defecation and uncoordinated locomotion (Trent *et al.*, 1983). *egl-21(n476)* mutants are defective for processing of endogenously expressed FMRFamide (Phe-Met-Arg-Phe-NH2)-related peptides (FaRPs), and exhibit greatly reduced levels of endogenous FaRPs, as visualised by Anti-FaRP immunostaining (Jacob & Kaplan, 2003). Furthermore, *egl-21* is essential for processing endogenous neuropeptides that facilitate ACh release at the *C. elegans* NMJ (Jacob & Kaplan, 2003).

egl-21(n476) mutants were less sensitive to emodepside than wild type control (IC_{50} = 15nM, 95% confidence limits 11 to 16nM, compared to N2 wild-type (IC_{50} = 4.2nM, 95% confidence limits 1.1 to 15nM) (Fig 4.18).

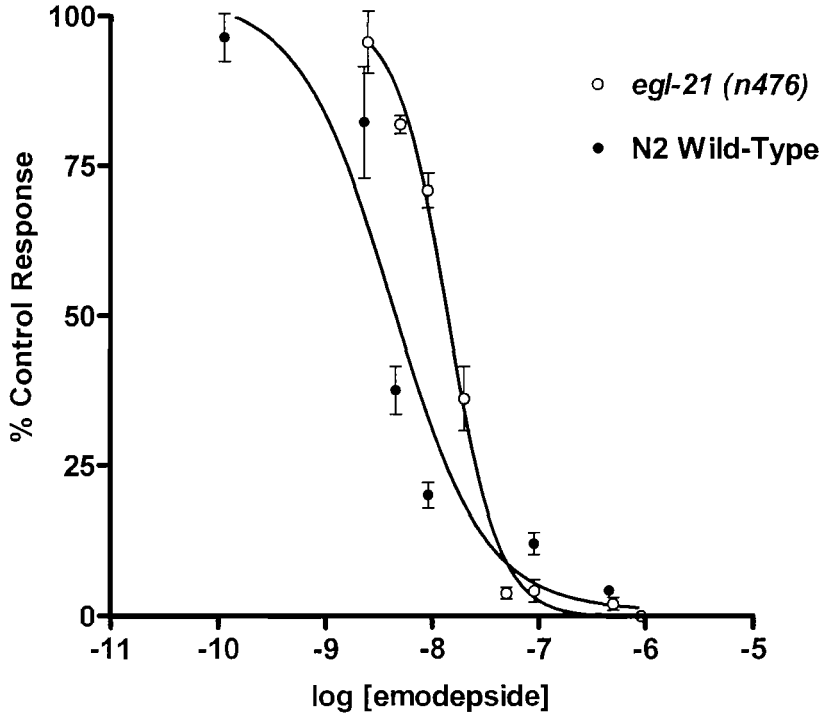

Figure 4.18 Comparison of the concentration-response curves for the effect of varying concentrations of emodepside on locomotion in wild type N2 *C. elegans*, and *egl-21(n476)*. '% control response' is the number of body bends per minute following emodepside application as a % of the body bends per minute of wild type worms grown on vehicle control plates (1% ethanol). IC_{50} 4.2nM (95% confidence limits 1.1 to 15nM) wild type, IC_{50} 14nM (95% confidence limits 11 to 16nM) *egl-21 (n476)*. Each point is the ± S.E.Mean of 10 determinations for N2 wild-type and *egl-21(n476)*. *** indicates $P<0.001$ compared to W.T. control.

4.17 Effect of emodepside on locomotion of *flp-13 RNAi* treated *C. elegans.*

FaRPs (FMRFamide-Related Peptides) and FLPs (FMRFamide-Like Peptides) are the most widely studied family of invertebrate regulatory peptides. FLP-13 has been shown to inhibit nematode locomotory behaviour (Reinitz *et al.*, 2000a). FLP-13 is therefore a possible candidate for release following emodepside-induced stimulation. No mutant was available for *flp-13* therefore RNAi was performed by bacterial feeding. No visible phenotype was observed in these animals.

FLP-13 RNAi resulted in a reduction in the sensitivity to 10μM emodepside after 60 mins, compared to the uninduced control (84% ± 8 inhibition of body bends/30sec induced, compared to 98% ± 2 inhibition of body bends uninduced, n=16) (Fig 4.19).

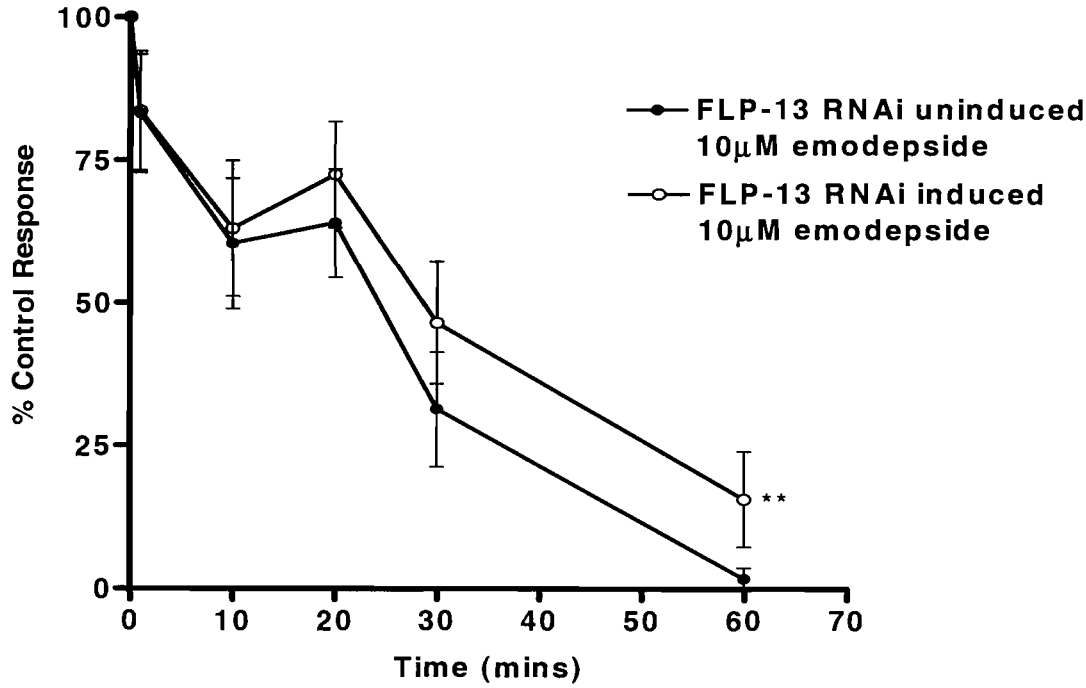

Figure 4.19 Time–dependence of the effect of emodepside (10μM) on *flp-13* RNAi treated *rrf-3 (pk1426) C.elegans.* (●) Uninduced control, (○) induced RNAi. % control response is the number of body bends following emodepside application compared to the initial body bends prior to drug addition. Each point is the mean ± S.E.Mean of 16 determinations. ** indicates $P<0.01$ compared to W.T. control.

4.18 Effect of emodepside on locomotion of *flp-1 RNAi* treated *C. elegans.*

The *C. elegans flp-1* gene codes for 6 peptide sequences, one of which is identical to PF2 (Nelson *et al.*, 1998b). *Flp-1*-deletion in *C. elegans* results in a hyperactivity phenotype (Nelson *et al.*, 1998b;Waggoner *et al.*, 2000), indicating that *flp-1* peptides may be inhibitory and negatively regulate locomotion. The effect of emodepside on *C. elegans rrf-3 (pk1426)* exposed to RNAi for the *flp-1* gene was therefore investigated.

FLP-1 RNAi resulted in a reduction in the sensitivity to 10μM emodepside after 60 mins, compared to the uninduced control (52% ± 8 inhibition of body bends/30sec induced, compared to 90% ± 2 inhibition of body bends uninduced, n=18) (Fig 4.20).

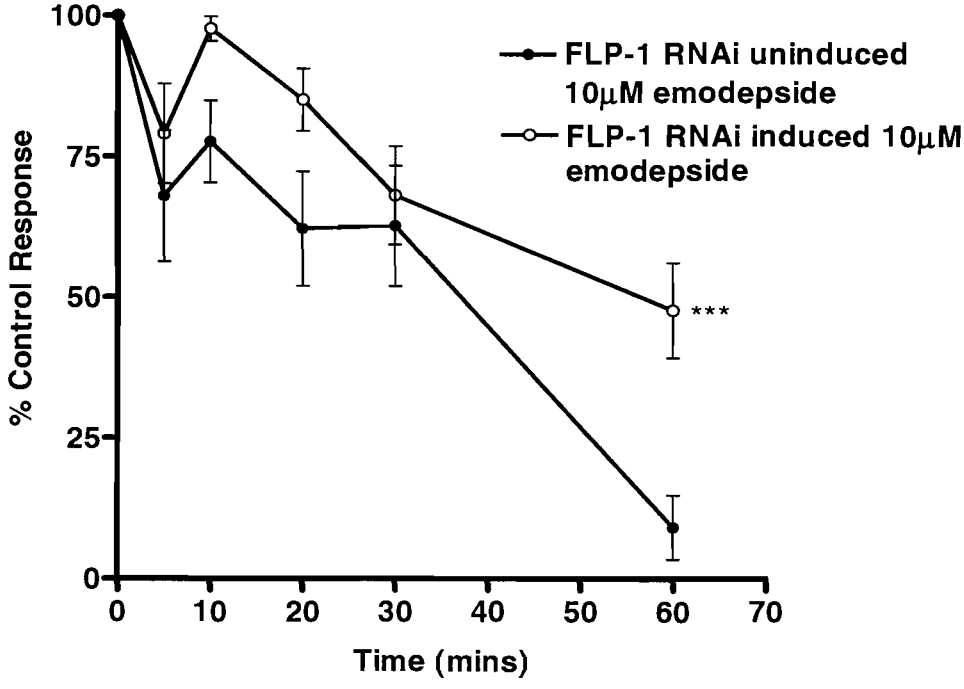

Figure 4.20 Time–dependence of the effect of emodepside (10μM) on *flp-1* RNAi treated *rrf-3 (pk1426) C.elegans.* (●) Uninduced control, (○) induced RNAi. % control response is the number of body bends following emodepside application compared to the initial body bends prior to drug addition. Each point is the mean ± S.E.Mean of 18 determinations. *** indicates $P<0.001$ compared to W.T. control.

4.19 Discussion

Emodepside interacts with a latrophilin-like G-protein-coupled receptor in the parasitic nematode *H.contortus*, HC110-R (Saeger *et al.*, 2001). There are two candidate genes encoding latrophilin-like receptors in *C. elegans*, *lat-1* and *lat-2*. To determine whether emodepside requires either of these for its biological effect, RNAi was utilized to reduce the expression of both of these receptors. RNAi for *lat-1* resulted in uncoordinated movement characterised by looping body bends. It has also been observed that *lat-1* RNAi results in prolonged pharyngeal pump duration (Willson *et al.*, 2004), providing further evidence that *lat-1* can modulate neuronal function. Furthermore, *lat-1* RNAi led to a reduction in sensitivity to emodepside, in the thrashing locomotion assay in this study and in the electropharyngeogram (EPG) assays carried out by Willson *et al* (2004).

RNAi of *lat-2* also led to a significant reduction in sensitivity to emodepside in this study; however, this degree of resistance to the anthelmintic was not as marked as that observed with RNAi for *lat-1,* and no visible phenotype was observed. These data, combined with those by Willson et al (2004) where it was shown that RNAi for *lat-2* resulted in a lower basal pharyngeal pumping rate and only a very slight reduction in sensitivity to emodepside, suggest that *lat-1* and *lat-2* may have different roles within the animal.

Simultaneous RNAi for both *lat-1* and *lat-2* was less marked than for *lat-1* RNAi. This is consistent with the findings of Kameth *et al* (2000) who demonstrated that simultaneous RNAi for two genes greatly reduces the strength of phenotype produced when RNAi is performed for only a single gene.

To provide further insight into the role of a latrophilin receptor in the mechanism of action of emodepside, the gene deletion mutants *lat-1 (ok379)* and *lat-2 (ok301)* were used in this study. Unfortunately, following backcrossing, it was not possible to isolate a homozygous *lat-1 (ok379)* line. The *lat-1* RB629 strain exhibited no resistance to emodepside inhibition of locomotion, with an IC_{50} virtually identical to that seen with N2 wild-type (data not shown). However, *lat-1* RB629 pharynxes were shown to be resistant to emodepside and continued pumping up to

concentrations of 100nM (Willson *et al.*, 2004). It was subsequently found that animals derived from the RB629 strain can lose the *ok379* deletion but remain resistant to the inhibitory effect of emodepside on the pharynx (data not shown, personal communication). The RB629 strain therefore highlights an interesting difference between the mechanism of action of emodepside on pharyngeal pumping and paralysis of body wall muscle.

This study indicates that *lat-2*, may be involved in mediating the inhibitory action of emodepside on locomotion. The *lat-2* gene deletion mutant *lat-2 (ok301)* did exhibit a significant degree of resistance to emodepside.

Taken together, the RNAi experiments for *lat-1* and *lat-2* and the reduced emodepside sensitivity of the *lat-2 (ok301)* gene deletion mutant suggest there is sufficient evidence for a role for a latrophilin-like receptor in the mechanism of emodepside action. Compared to the findings of Willson *et al* (2004), where emodepside action on the *C. elegans* pharynx was found to be predominantly mediated by *lat-1*, this study provides evidence that in terms of mediating the inhibitory action of emodepside on locomotion, *lat-2* is also important.

It was then necessary to try and elucidate the signalling pathway through which latrophilin mediated vesicular release may occur. Latrophilin acts through a $G\alpha_q$, PLCβ mediated pathway (Rahman *et al.*, 1999). The effects of emodepside on locomotion in two *C. elegans* mutant strains *egl-30 (ad810)* and *egl-30 (n686),* which have defects in the α subunit of $G\alpha_q$, were examined. A significant reduction in the sensitivity to emodepside in the emodepside agar plate assay was observed. Further evidence for a $G\alpha_q$-mediated pathway in emodepside action came from analyses of gain-of-function mutants for $G\alpha_q$ which were hypersensitive to emodepside.

$G\alpha_q$ subunit couples to the signalling molecule PLC-β which is a key modulator of pathways that regulate vesicle release in *C. elegans* (Miller *et al.*, 1999;Lackner *et al.*, 1999). To further define the mechanism of action of emodepside the *C. elegans* mutant strains *egl-8 (md1971)* and *egl-8(n488)* were utilised. These two alleles have disruptions to the catalytic Y domain of the gene which encodes PLCβ

(Lackner *et al.*, 1999). A significantly reduced sensitivity to emodepside in terms of the inhibition of locomotion was seen. The stronger loss of function allele, *egl-8 (md1971)* (Miller *et al.*, 1999), exhibited the greater resistance.

PLC-β hydrolyses PIP2 to generate inositol 1,4,5-trisphosphate (IP_3) and DAG, a process which is negatively regulated through the action of $G\alpha_o$ on DAGkinase (Miller *et al.*, 1999;Lackner *et al.*, 1999); Nurrish 1999). *goa-1* mutants with a loss of function of the $G\alpha_o$ subunit are characterized by hyperactivity resulting from increased synaptic activity (Mendel *et al.*, 1995). Application of emodepside to these mutants resulted in an increased sensitivity to emodepside, providing further evidence that the emodepside mechanism involves $G\alpha_q$ and PLCβ stimulation of pre-synaptic vesicular neurotransmitter release.

A number of neurotransmitters and neuromodulators are known to affect nematode body wall muscle (Walker *et al.*, 2000). To elucidate which neurotransmitters or neuromodulators may be released by emodepside, *C. elegans* mutants to these neurotransmitters / neuromodulators were tested for emodepside resistance.

Having established in Chapter 3 that emodepside does not act via a GABAergic mechanism when inducing relaxation in *A. suum* DMS, an investigation was conducted into the release of ACh, the other classical neurotransmitter involved in controlling nematode locomotion. To test this possibility, synaptic release of ACh was assayed by measuring the sensitivity of animals to the AChesterase inhibitor aldicarb. Aldicarb enhances the effects of endogenously released ACh at the neuromuscular junction, causing hypercontraction of the body wall muscles and paralysis in wild-type animals (Nonet *et al.*, 1993;Lackner *et al.*, 1999;Nguyen *et al.*, 1995;Brenner, 1974). Firstly, to establish a positive control it was necessary to examine the time-dependent effect of aldicarb on N2 wild-type and *rrf-3 (pk1426)*, as the latter would be used in subsequent RNAi/aldicarb assays. Interestingly, there was a distinct and highly significant difference between these two strains in the sensitivity to 1mM aldicarb. From these data it appears that *rrf-3 (pk1426)* are hypersensitive to aldicarb-induced paralysis as they became paralysed more rapidly than N2 wild-type. Aldicarb hypersensitivity suggests that presynaptic release of ACh at the NMJ is increased in *rrf-3 (pk2426)*. *rrf-3* encodes an RNA-directed

RNA polymerase (RdRP) homolog that inhibits somatic RNAi, and thus promotes activity of repeated genes; therefore, *rrf-3* mutants are hypersensitive to somatic RNAi (Simmer *et al.*, 2002). However, *rrf-3* mutants do not appear to exhibit any other phenotypes associated with increased synaptic transmission, such as increased rates of locomotion and egg laying; or larval lethality preceded by hyperactive behaviours (Miller *et al.*, 1996). Further investigation into this apparent aldicarb hypersensitivity was not carried out in this study, and therefore any molecular basis for this effect remains unknown. However, as a time dependent effect of 1mM aldicarb on *rrf-3 (pk1426)* had been established, the use of this strain in subsequent RNAi experiments was continued.

0.5mM and 1mM aldicarb paralysed both *lat-1* RNAi treated *rrf-3 (pk1426)* and empty vector control worms in a comparable, concentration-dependent manner. However, at 2mM aldicarb there was a significant difference between the rates of paralysis of *lat-1* RNAi treated *C. elegans* and the empty vector fed *C. elegans*, in that, *lat-1* RNAi worms exhibited a resistance to aldicarb. Although this decrease in sensitivity was not as marked as one would expect if LAT-1 were exclusively linked to ACh release, it does suggest that a portion of the vesicular release resulting from a latrophilin, G-protein signalling pathway, may be ACh release. To provide further evidence for this the time-dependent effect of levamisole paralysis on *lat-1 rrf-3 (pk1426)* was investigated and no significant difference was observed between the *lat-1* RNAi treated *C. elegans* and the control animals. This indicates that the aforementioned decrease in sensitivity to 2mM aldicarb in *lat-1* RNAi treated worms is due to a decrease in the amount of ACh released at the NMJ.

It has been observed that emodepside mimics the effects of the FMRF-amide peptides PF1 and PF2 (Willson *et al.*, 2003). In *C. elegans* there are 23 genes that code for at least 63 FMRF-amide like peptides (Li *et al.*, 1999a;Nelson *et al.*, 1998a). These peptides have been shown to cause a number of effects on nematode muscle (Walker *et al.*, 2000). In *C. elegans* the *egl-21* gene encodes a carboxypeptidase E (CPE), which mediates an enzymatic step in peptide processing, removal of C-terminal basic residues. Mutants lacking *egl-21* CPE are

defective for processing endogenously expressed FMRFamide (Phe-Met-Arg-Phe-NH2)-related peptides (FaRPs) (Jacob & Kaplan, 2003). Following growth on emodepside-containing agar plates, *egl-21 C. elegans* exhibited a reduced sensitivity to locomotion inhibition, suggesting a role for inhibitory peptides in emodepside action. The neuropeptide encoded by *flp*-13 (APEASPFIRFa) has been shown to inhibit locomotory behaviour, dramatically decrease the number of wave crests, and substantially increase body length in *A. suum* (Reinitz *et al.*, 2000b). The *C. elegans flp-1* mutants have numerous behavioural defects including a loopy, exaggerated body movement reminiscent of *lat-1 (ok379)*. Furthermore, epistasis analysis has shown that *flp-1* gene products appear to interact with G protein-coupled second messenger systems (Nelson *et al.*, 1998b). RNAi was therefore performed on both the *flp-1* and *flp-13* genes to investigate a role for these peptides in emodepside action. A resistance to emodepside was observed for both genes, suggesting a role for these peptides in emodepside action.

Using this reverse genetics approach it appears that the mechanism of emodepside action appears pre-synaptic, involving the receptor latrophilin. Stimulation of the latrophilin receptor activates G_q, G-protein. This may then activate PLCβ causing an increase in levels of DAG. Studies using emodepside and recording *C. elegans* EPGs have shown the mechanism of this novel anthelmintic is dependent on UNC-13 (Willson *et al.*, 2004) (The *unc-13 (s69)* mutant was not used in this study due to the high level of uncoordinated locomotion of these animals). Therefore, DAG may then bind UNC-13 which in turn activates syntaxin (Richmond *et al.*, 2001). This allows binding and activation of the SNARE complexes that bring vesicles and pre-synaptic membranes into close apposition to drive membrane fusion (Weber *et al.*, 1998). This may then result in release of a cocktail of neurotransmitters, including ACh and inhibitory neuropeptides.

Chapter 5

Forward genetic approach to investigate the mechanism of emodepside action

5.1 Introduction

In the last chapter a reverse genetics strategy was employed to elucidate the mechanism of emodepside action; using as a starting point the prior knowledge that emodepside has been shown to interact with a latrophilin-like receptor in *H. contortus* (Saeger *et al.*, 2001). Although this reverse genetics approach provided considerable insight into the mode of action of this novel anthelmintic, this type of approach can be limiting. The systematic methodology of using RNAi and mutant strains to assay emodepside sensitivity of animals deficient in genes putative to a latrophilin signalling pathway did indeed yield reductions in sensitivity to the drug. However, it is possible that emodepside may have an alternative mechanism/s than that via a latrophilin dependent pathway. Indeed, it would be of great benefit to Bayer AG and anthelmintic medicine if emodepside had multiple modes of action, as it would allow for greater field use before the eventual development of resistance within parasites. Therefore, to provide further insight into the mechanism of emodepside action a forward genetics strategy was employed.

EMS (ethylmethanesulfonate) is a mutagen that induces point mutations and deletions in DNA. L4 stage worms are usually mutagenised as they have a large number of mostly mitotic germ cells. Thus, several rounds of replication can occur between the mutagenesis and gamete formation fixing the mutations. After the mutagenesis, the worms recover on seeded plates and then individuals are picked for the specific screen desired, in this case to seeded 1μM emodepside plates. This emodepside concentration was chosen for the screen due to the potent inhibitory effect of this dose on *C. elegans* locomotion (see Chapter 3, section 3.4). Animals that are able to survive and propagate on these emodepside plates are deemed to be resistant.

SNPs (single nucleotide polymorphisms) are valuable markers for mapping mutations. Wicks *et al.* (2001) describe a SNP-based strategy for rapid mapping in the *C. elegans* genome. They sequenced the entire genome of the CB4856 Hawaiian worm isolate and compared it with the standard laboratory wild type

strain (Bristol N2). This alignment identified 6,222 potential polymorphisms, more than half of which modify restriction enzyme sites (referred to as 'snip-SNPs').
Such a high-density map of snip-SNPs (about one every 200 kb) allows for rapid mapping of gene mutations using restriction fragment length polymorphism (RFLP) analysis. Successful mapping can be achieved with a relatively small number of PCR reactions and restriction digests, after isolating F2 animals from a single cross between CB4856 and N2 strains.

Through the use of an EMS/snip-SNP forward genetic approach the aim was to either determine an alternative mechanism for emodepside action, or if the mechanism is solely through the pathway outlined in Chapter 4, identify important genes up/downstream of this pathway.

5.2 Identification of emodepside resistant *C. elegans*

Following chemical mutagenesis with EMS, and a 10,000 genome screen of mutagenised worms on emodepside agar plates (1μM), seven resistant lines were identified. These lines represent individual worms that survived the initial first round screening on individual emodepside plates (1-100), and continued to propagate through subsequent generations with continual exposure to 1μM emodepside. Any visible phenotypes/behavioural abnormalities were noted following daily observation of the individual lines over a two week period immediately after the initial screen.

Name (sample number 1-100)	**Phenotype**
Emo 35	Uncoordinated (jerky/loopy body bends), Slightly dumpy (dpy)
Emo 42	Slightly dumpy (dpy)
Emo 76	Slightly dumpy (dpy), Unc (slow moving)
Emo 66	Slightly dumpy (dpy), Unc, (slow moving, kinked)
Emo 48	Slightly dumpy (dpy), Unc
Emo 69	Slightly dumpy (dpy), Unc (slow moving, kinked), slow growth
Emo 13	Slightly dumpy (dpy), Unc (slow moving, kinked), slow growth

Table 5.1 Emodepside resistant lines derived from EMS mutagenesis screen

From these seven, Emo 35, 42 and 48 appear to exhibit the greatest degree of resistance, in that all animals appear healthy, and propagate at a rate comparable to

wild-type. The remaining strains (76, 66, 69 and 13) exhibit varying degrees of lethargy, reminiscent of unhealthy animals; and yet still propagate on 1μM emodepside plates.

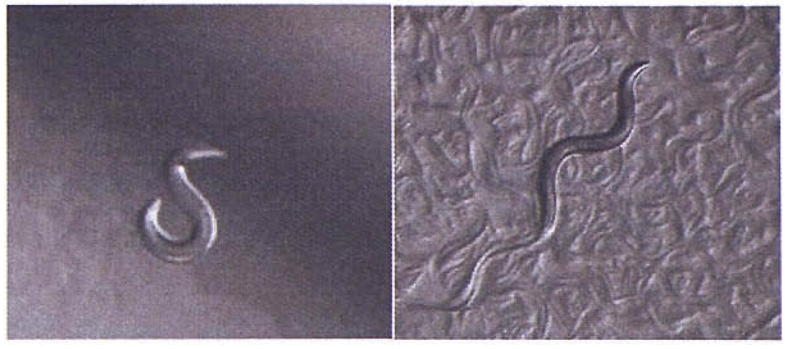

Figure 5.1 Photograph comparing Emo 35 (left) and N2 wild-type (right) adult worms. Note the dumpy uncoordinated phenotype of Emo 35.

5.3 Effect of emodepside on locomotion of emodepside resistant *C. elegans* from chemical mutagenesis screen

Following 60 mins incubation with 10μM emodepside there was a reduction in the number of B.B/30sec (standardised as % inhibition compared to control response) in the emodepside treated N2 wild-type worms compared to the Emo 35 animals (99 ± 0.2 % inhibition of body bends N2 wild-type, S.E.M n=27 10μM emodepside, compared to 0.5 ± 2% inhibition of body bends, S.E.M n=9 Emo 35) (Fig 5.2A). Similarly, Emo 42 and Emo 48 only exhibited a 27.8% ± 7 and 12.7% ± 6 inhibition of body bends after 60mins exposure to 10μM emodepside, respectively (Fig 5.2B & C), indicating highly significant resistance to the drug compared to N2 wild-type (99 ± 0.2 % inhibition of body bends).

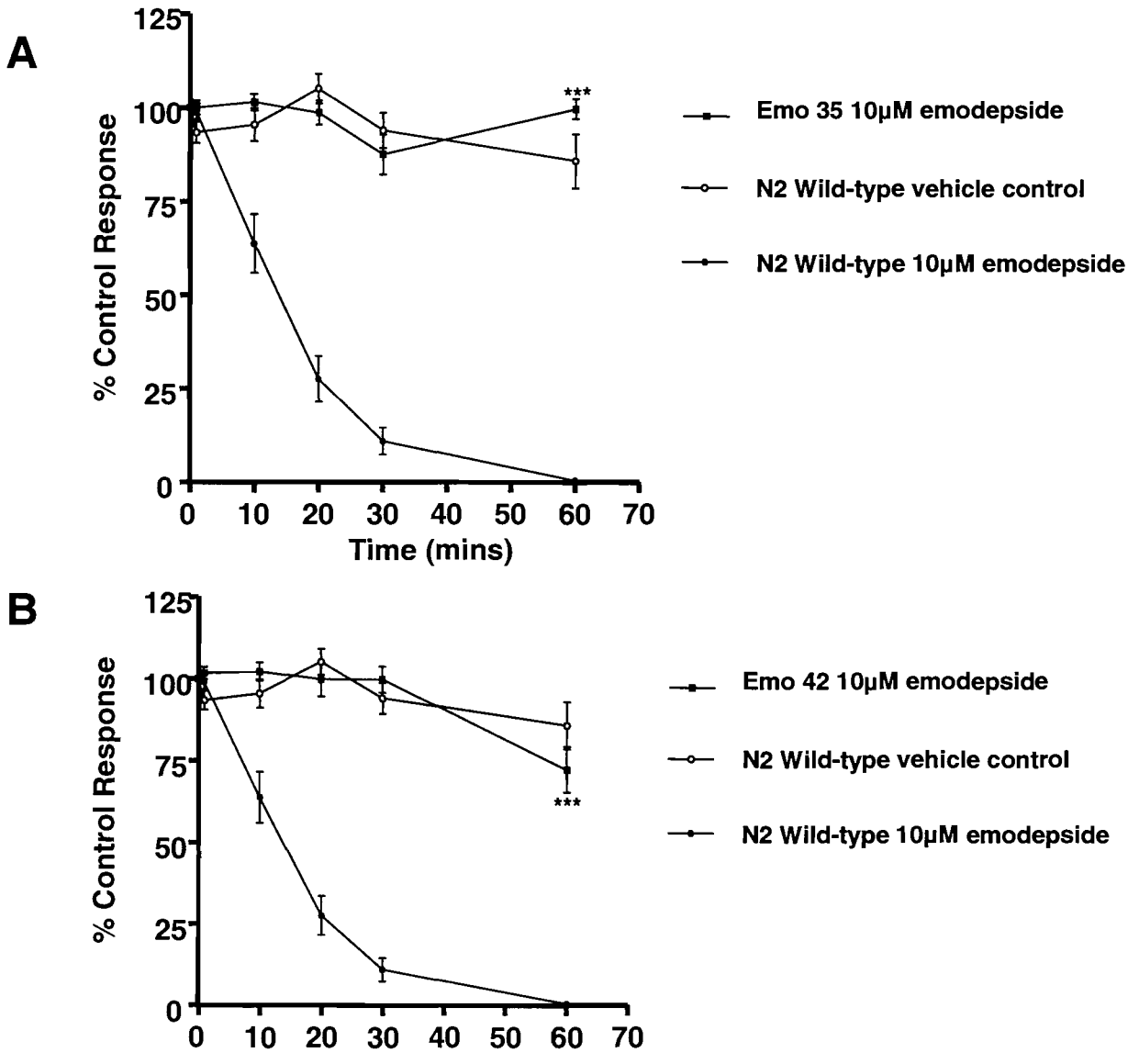

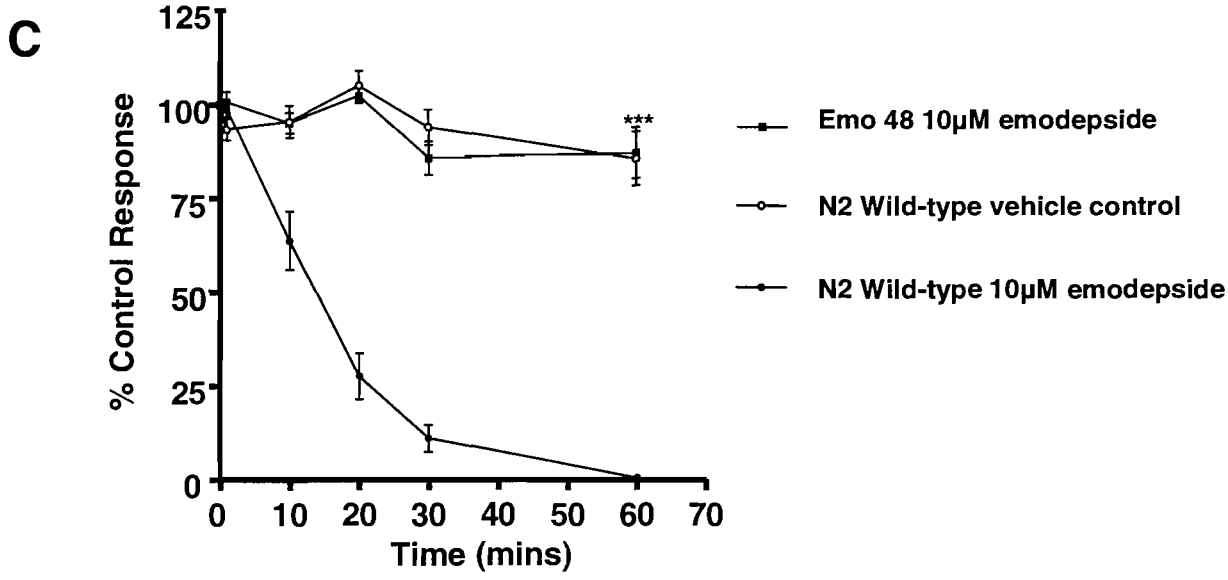

Figure 5.2 Time–dependence of the effect of emodepside (10µM) on (**A**) Emo 35 mutant *C.elegans*, (**B**) Emo 42 mutant *C.elegans* and (**C**) Emo 48 mutant *C.elegans* (thrashing assay). (○) N2 wild-type vehicle control (0.1% ethanol), (●) N2 wild-type 10µM emodepside, (■) Emodepside resistant animals. % control response is the number of body bends following emodepside application compared to the initial body bends prior to drug addition. Each point is the mean ± S.E.Mean of 27 determinations (N2 wild-type 10µM emodepside) and ± S.E.Mean of 9 determinations (emodepside resistant worms and ethanol vehicle control). *** indicates $P<0.001$ compared to N2 wild-type 10µM emodepside.

5.4 Comparison of the effect of emodepside on wild type & Emo 35 *C. elegans* pharyngeal pumping

Emodepside causes a concentration-dependent inhibition of *C. elegans* pharyngeal pumping, with an IC_{50} of 4.1nM (Willson *et al.*, 2004). To determine if these emodepside resistant mutants are also less sensitive to the anthelmintic effects on the pharynx, EPG recordings were performed. 5-HT was applied to the pharynx to activate neuronal and muscle activity, allowing a consistent level of pharyngeal pumping prior to emodepside application. In the absence of emodepside wild-type pharynxes continued to pump and re-application of 5-HT again activated the preparation (Fig 5.3A). Following 10mins application, 100nM emodepside irreversibly abolished pharyngeal pumping in N2 wild-type animals (Fig 5.3B). However, 100nM emodepside application to Emo 35 resulted in continual pharyngeal pumping throughout the time course of the experiment (n=3) (Fig 5.3C). These experiments were kindly performed by James Willson.

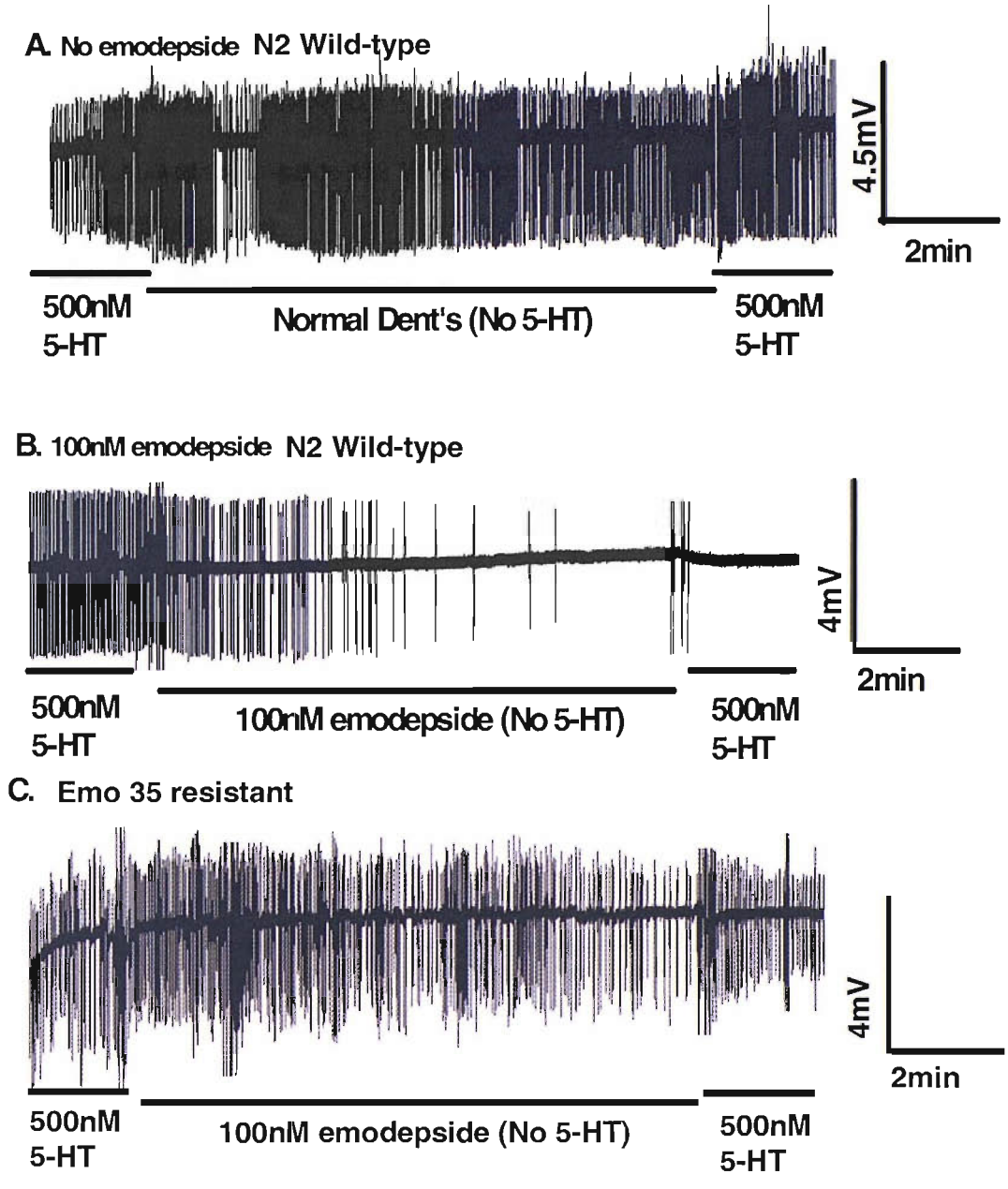

Figure 5.3 **A.** An extracellular recording of the pharyngeal muscle (EPG). Each vertical line represents the electrical activity associated with a single muscle pump; therefore this provides information of the activity of the muscle. 5-HT, 500nM, is applied to stimulate pumping. The protocol involved applying 5-HT for 2 min time periods separated by a 10min application of either vehicle control (0.1% ethanol), or emodepside. **A** typical result from a control experiment in which the pharynx continues to pump throughout the entire time-course of the experiment. **B.** The effect of 100nM emodepside on pharyngeal pumping. Note the disappearance of the pumps during the period of emodepside application and the failure of the muscle to respond to the second application of 5-HT. **C.** typical result from an Emo 35 resistant animal, in which the pharynx continues to pump throughout the entire time-course of the experiment whilst exposed to 100nM emodepside (n=3).

5.5 Effect of ivermectin on locomotion of Emo 35 and Emo 42 resistant mutants

To further investigate the nature of anthelmintic resistance in the emodepside resistant mutants, Emo 35 and Emo 48 were assayed for ivermectin sensitivity using the locomotion thrashing assay. 1μM IVM paralysed both Emo 42 and Emo 35 at a rate comparable to N2 wild-type (% inhibition of locomotion at 20mins: Emo 35 83.2 ±5.5%, Emo 42 81.3 ±5.9, and N2 wild-type 78.4 ±7.5 %), with all animals completely paralysed after 30 mins (Fig 5.4).

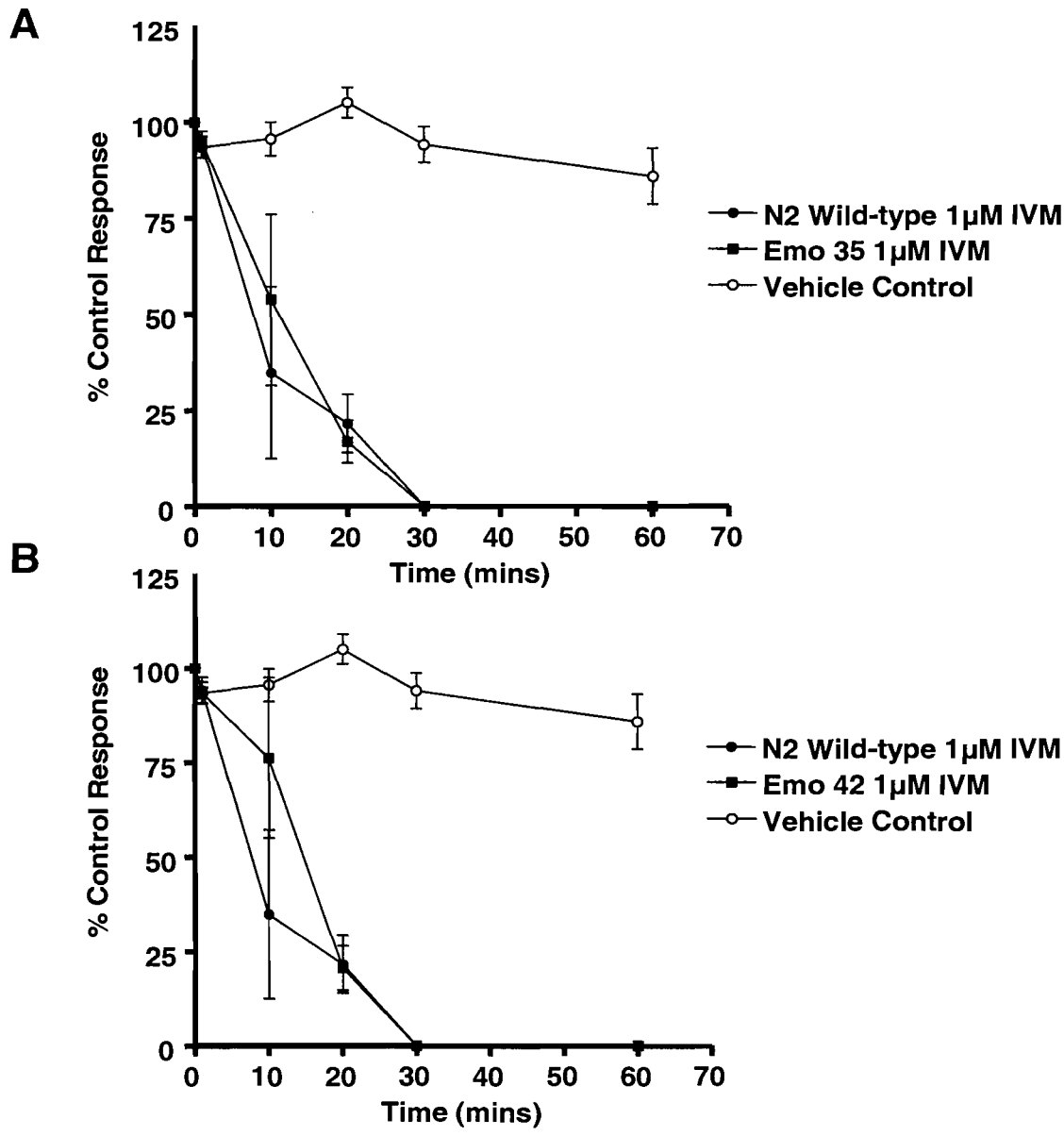

Figure 5.4 Time–dependence of the effect of ivermectin (1μM) on **A**. Emo 35 and **B**. Emo 42 (○) N2 wild-type vehicle control (0.1% ethanol), (●) N2 wild-type 1μM IVM, (■) Emo 35/42. % control response is the number of body bends following emodepside application compared to the initial body bends prior to drug addition. Each point is the mean ± S.E.Mean of 5 determinations

5.6 Snip-SNP mapping of Emo 35 and Emo 48 resistant mutants

As Emo 35 and Emo 48 showed the highest levels of resistance to 1μM emodepside in the locomotion thrashing assay, and propagated at a rate comparable to N2 wild-type with no obvious signs of lethargy, it was decided to use these two mutants for a snip-SNP mapping strategy to elucidate the mutated gene/s that convey emodepside resistance. Scoring details for the individual PCR reactions for all snip-SNP mapping in this study can be found in Appendix 3.

The first step was to assign linkage of the mutation to a chromosome; this was achieved using centrally located SNP primers for each of the six *C. elegans* chromosomes. In the case of both Emo 35 and Emo 48 linkage was assigned to chromosome V. Subsequent analysis of Emo 35 with a further 9 snip-SNPs spaced over chromosome V yielded a genetic map position of 19.34. Only 2 of 96 individual recombinations recombined at this locus and subsequent analysis of these 2 lines revealed that these were in fact false positives and not emodepside resistant. In light of this result a similar approach was adopted for Emo 48 using 3 snip-SNPs, one at map position 19.34 and two either side of this locus (15.53 and 25.95). Recombination was observed at 15.53 and 25.95 (10 out of 48 lines), however at map position 19.34 no recombination occurred (0 out of 48 lines), indicating an identical map position to Emo 35 for the mutation. To confirm that the mutations in Emo35 and Emo 48 were not only located at the same genetic map position but were in fact the same gene, a complementation assay was performed by mating Emo 35 L4 males with Emo 48 hermaphrodite adults. 5 out of 5 crosses resulted in non-complementing progeny, providing evidence that these two mutant strains are allelic.

C. elegans genetic map position 19.34 corresponds to the YAC clone Y51A2d, which has tested positive for 3 genes, *nhr-70* (a nuclear hormone receptor), *srg-34* (a serpentine receptor, G class) and *slo-1* (a Ca^{2+} activated K^+ channel) (www.wormbase.org).

5.7 Effect of emodepside on locomotion of *slo-1 (js379) C. elegans*

All 3 of the genes located at map position 19.34 (Y51A2d) were originally considered to be plausible potential mediators of emodepside action. However, *slo-1*, a calcium-activated potassium channel (BK) was considered the most interesting. Initial electrophysiological studies, using the parasitic nematode *A. suum,* to elucidate the mechanism of emodepside action suggested that emodepside may indeed act through a Ca^{2+}-activated K^+ channel (Willson *et al.*, 2003). Therefore the effect of emodepside on *slo-1 (js379)* was investigated. This mutant strain has a nonsense mutation located in the S4 transmembrane domain of the channel which results in premature termination of the protein (Wang *et al.*, 2001).

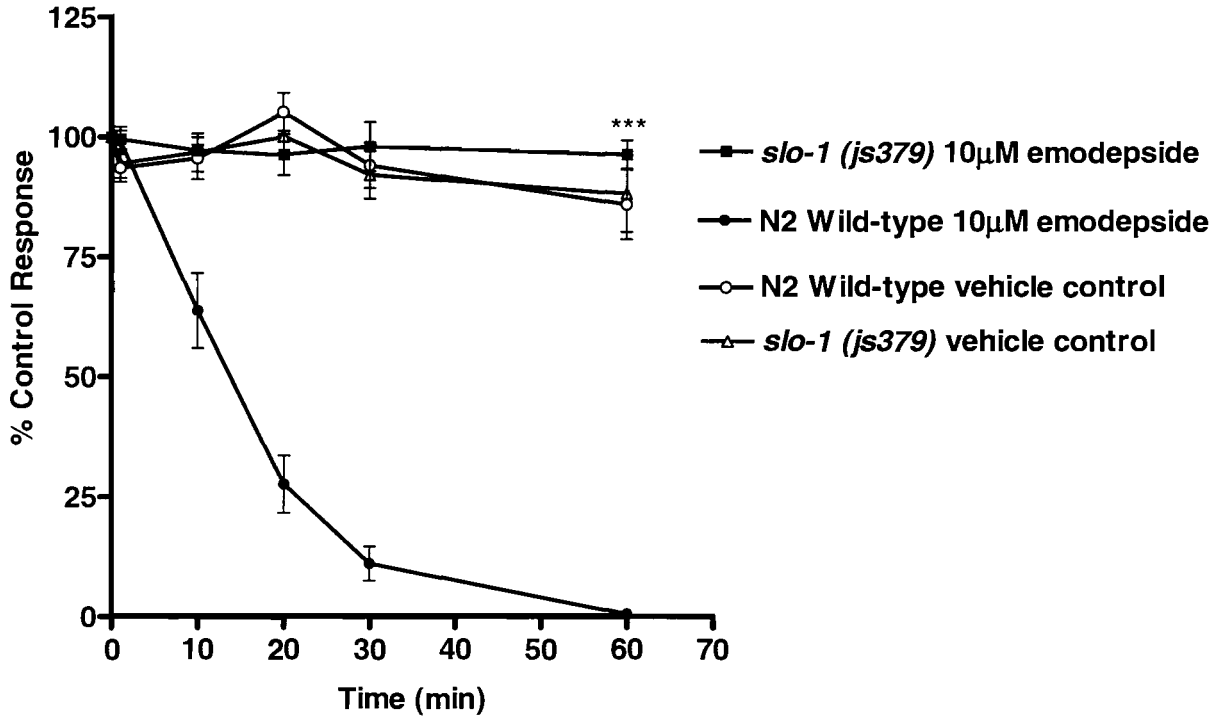

Figure 5.5 Time–dependence of the effect of emodepside (10μM) on *slo-1 (js379) C. elegans.* (○) N2 wild-type vehicle control (0.1% ethanol), (●) N2 wild-type 10μM emodepside, (■) *slo-1 (js379).* % control response is the number of body bends following emodepside application compared to the initial body bends prior to drug addition. Each point is the mean ± S.E.Mean of 27 determinations (N2 wild-type 10μM emodepside) and ± S.E.Mean of 10 determinations (*slo-1 (js379)* and ethanol vehicle control animals). *** indicates $P<0.001$ compared to N2 wild-type 10μM emodepside.

Following 60 mins incubation with 10μM emodepside there was a 25 fold reduction in the number of B.B/30sec (standardised as % inhibition compared to control response) in the emodepside treated N2 wild-type worms compared to the *slo-1 (js379)* animals (99 ± 0.2 % inhibition of body bends N2 wild-type, S.E.M n=27 10μM emodepside, compared to 4 ± 3% inhibition of body bends, S.E.M n=10 *slo-1 (js379)*) (Fig 5.5).

Two gain-of-function (gf) alleles exist for *slo-1* in *C. elegans slo-1(ky389gf)* and *slo-1(ky399gf)*. Both these alleles exhibit a degree of resistance to 0.5mM aldicarb, with *slo-1(ky399gf)* significantly more resistant over 3 hours exposure than *slo-1(389gf)* (Davies *et al.*, 2003). The CX3940 strain carrying *slo-1(ky399gf)* is balanced with *rol-6* and was therefore unsuitable for the locomotion assays used in this study. Emodepside did not elicit a hypersensitive inhibition of *slo-1 (ky389gf)* CX3933 locomotion compared to N2 wild-type (IC_{50} 4.3nM compared to 4.1nM in wild-type) (Fig 5.6).

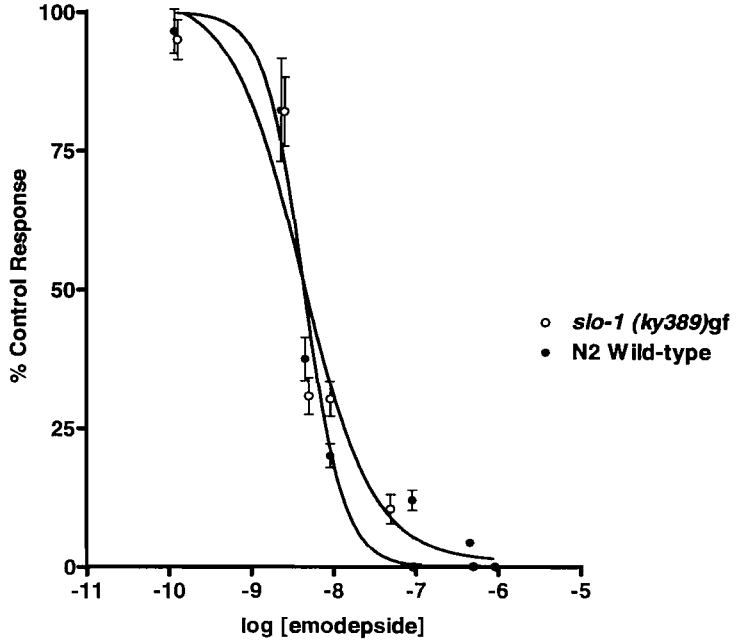

Figure 5.6 Concentration-response curves comparing the effect of varying concentrations of emodepside on locomotion of wild type N2 *C. elegans* and *slo-1(ky389)* gain-of-function. '% control response' is the number of body bends per minute following emodepside application as a % of the body bends per minute of wild type worms grown on vehicle control plates (1% ethanol). IC_{50} 4.2nM (95% confidence limits 1.1 to 15nM wild type, IC_{50} 4.3nM *slo-1(ky389)* 95% confidence limits 3.1nM to 6.1nM. Each point is the mean ± S.E.Mean of >8 determinations.

5.8 Comparison of the effect of emodepside on wild type and *slo-1 (js379) C. elegans* pharyngeal pumping

To determine if *slo-1 (js379)* mutants are also resistant to the anthelmintic effects on the pharynx EPG recordings were performed by J. Willson. 5-HT was applied to the pharynx to activate neuronal and muscle activity, allowing a consistent level of pharyngeal pumping prior to emodepside application. Following 10mins application 100nM emodepside irreversibly abolished pharyngeal pumping in N2 wild-type animals (Fig 5.7A). However, 100nM emodepside application to *slo-1 (js379)* resulted in continual pharyngeal pumping throughout the time course of the experiment, even on exposure to 1µM (n=3) (Fig 5.7B).

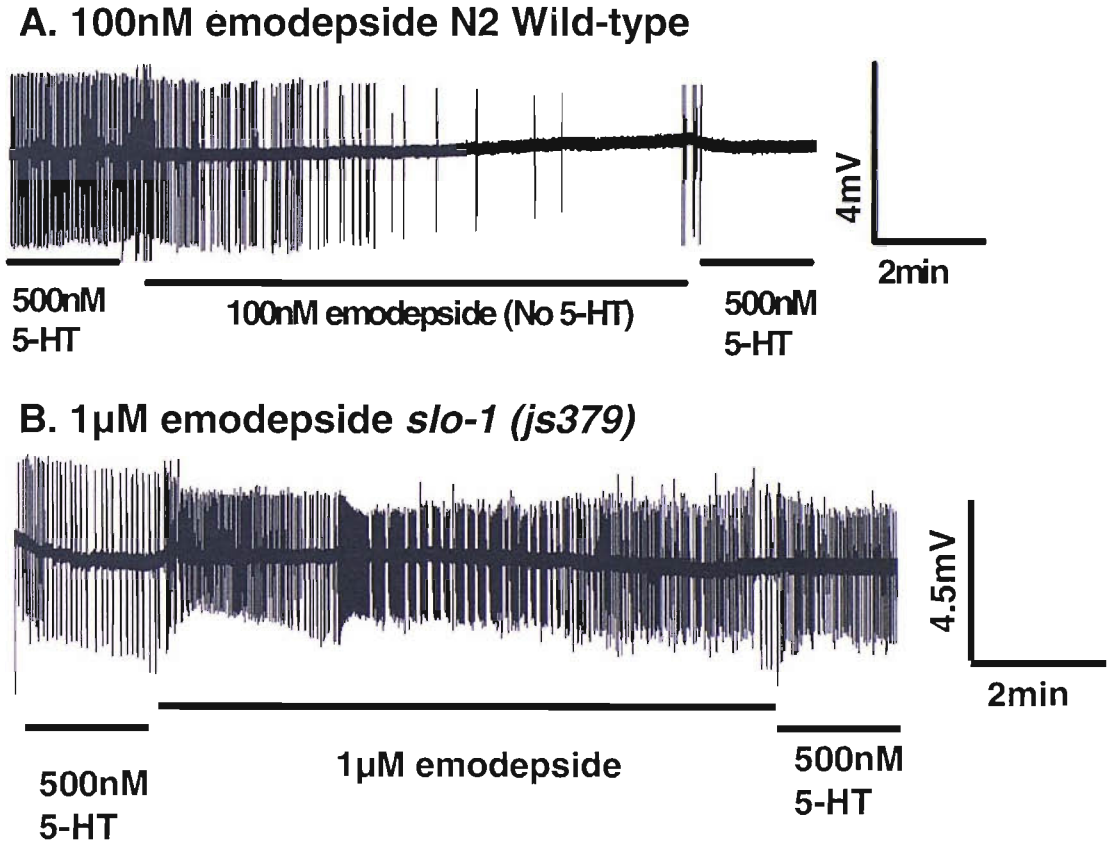

Figure 5.7 **A.** The effect of 100nM emodepside on pharyngeal pumping. Note the disappearance of the pumps during the period of emodepside application and the failure of the muscle to respond to the second application of 5-HT. **B.** typical result from a *slo-1 (js379)* animal, in which the pharynx continues to pump throughout the entire time-course of the experiment whilst exposed to 1µM emodepside (n=3).

5.9 Cloning and sequencing of *slo-1* cDNA from Emo 35 & Emo 48 *C. elegans* mutants

Combined evidence from snip-SNP mapping and the resistance to emodepside, observed in both locomotion and pharyngeal assays, provided sufficient impetus to clone and sequence the *slo-1* gene in Emo 35 and Emo 48, as the candidate gene that contains a mutation which conveys emodepside sensitivity.

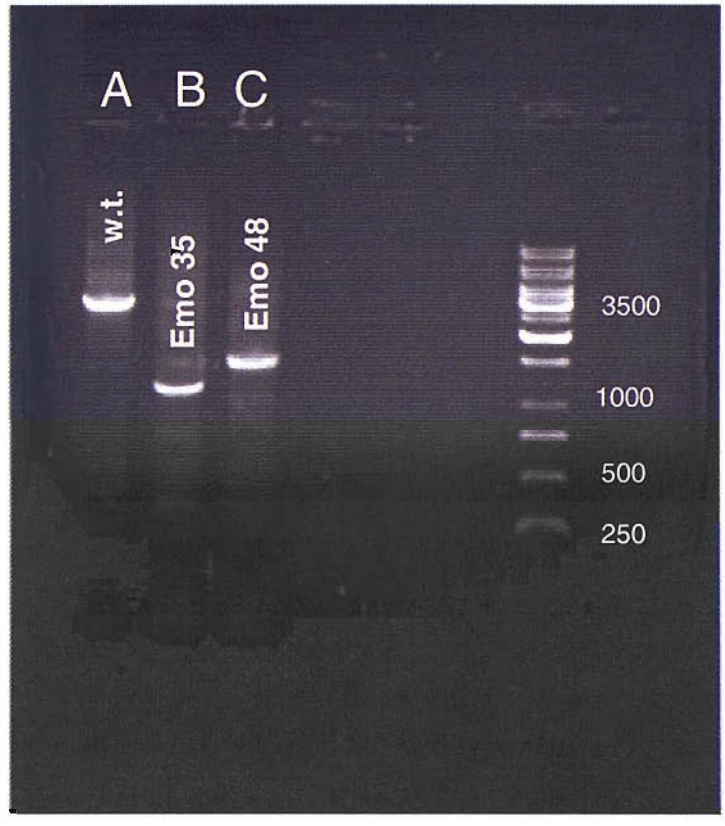

Figure 5.8 RT PCR of *slo-1* cDNA from A. N2 wild-type (~3423 bp), B. Emo 35 (~1600 bp), C. Emo 48 (~2000 bp).

Amplification of *slo-1* cDNA from N2 wild-type resulted in the expected size of 3423 bp. However, in the case of Emo 35 and Emo 48 the amplified *slo-1* cDNA ran at ~1600 bp and ~2000 bp, respectively (Fig 5.8). This indicates that in both these emodepside resistant mutant strains there is a deletion, in the order of ~1800 bp for Emo 35 and ~1400 for Emo 48.

S0

MGEIYSPSQSKGFNQPYGYPMNCNLSRVFMEMTEEDRKCLEERKYWCFLLSSITTFCASMILVVIWRVV

THLCCQRREKEFVEPIPAPEAQINMNGSKHAPSETDPFLKQQEEKHLGWMTEAKDWAGELISGQSTGRF

S1 S2

LVLLVFILSIGSLIIYFYDASFQNFQVETCIPWQDSPSQQIDLGFNIFFLVYFFIRFIAASDKVWFLLE

S3 S4 S5

MYSWIDFFTIPPSFVAIYLQRNWLGFRFLRALRLMTVPDILQYLNILKTSSSIRLTQLVTIFVAVCLTG

PORE S6

AGLVHLLENSGDFFKGFINPHRITYADSVYFVLVTMSTVGYGDIYCTTLCGRLFMIFFILFGLAMFASY

VPEIADLIGNRQKYGGEYKGEHGKKHIVVCGHITYDSVSHFLQDFLHEDRDDVDVEVVFLHRVVPDLEL

EGLFKRHFTKVEFFTGTVMDSLDLSRVKIGDADACLVLANKYSTNPDAEDAANIMRVISIKNYSSDIRV

S7

IVQLMQYHNKAYLLNIPSWDWKRGDDVICLAELKLGFIAQSCLAPGFSTMMANLFAMRSFKTSQTTPDW

S8

LNLYLCGAGMEMYTDTLSHSFVGMTFPEAVDLLFNRLGLLLLAIELKDEENKECNIAINPGPHIVIQPQ

TQGFFIAQSADEVKRAFFWCKQCHDDIKDVSLIKKCKCKNLALFRRNTKHSTAARARATDVLQQFQPQA

PAGPMGHLGQQVQLRMINQQSSTSDTHLNTKSLRFAYEIKKLMPSSGGRRNSMSIPPDGRGVDFSKDFE

S9

QQFQDMKYDSTGMFHWCPSRNLEDCVERHQAAMTVLNGHVVVCLFADQDSPLIGLRNFIMPLRSSNFHY

HELKHVVIVGDLEYLRKEWKTLYNLPKISILNGSPLSRADLRAVNINLCDMCVIISARVPNTEDTTLAD

KEAILASLNIKAMQFDDTLGFFPMRHQTGDRSPLGSPISMQKKGAKFGTNVPMITELVNDSNVQFLDQD

S10

DDDDPDTELYLTQPFACGTAFAISVLDSLMSTTYFNDSALTLIRTLVTGGATPELELILAEGAGLRGGY

STPETLSNRDRCRIAQISLQDNPYDGVVHNTTYGAMFTIALRRYGQLCIGLYRLHDQDNPDSMKRYVIT

NPPAELRIKNTDYVYVLEQFDPGLEYEPGKRHF

Figure 5.9 Amino acid sequence and conserved domains for *C. elegans* SLO-1. The motifs that are conserved between BK channels are colour coded; ion transport protein (red 177-351); calcium activated BK potassium channel alpha subunit (green 403-1139); Ca^{2+} bowl (blue). The 11 hydrophobic segments (S0–S10) and the pore are also indicated. Shaded grey area is deleted region of Emo 35.

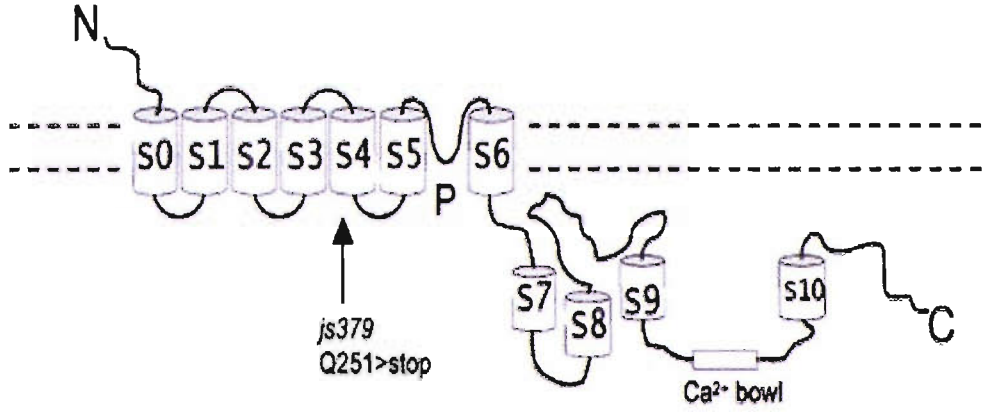

Figure 5.10 Predicted membrane topology of SLO-1. Major structural domains characteristic of BK channels, including 11 hydrophobic segments (S0–S10), the pore (P), and the Ca^{2+} bowl, are shown. Location of *slo-1 (js379)* mutation is also indicated. Adapted from (Wang *et al.*, 2001).

Following sequencing of the *slo-1* cDNA from Emo 35 and Emo 48 emodepside resistant animals, the precise nature of the deletions in these mutants was deduced. Emo 35 *slo-1* has a deletion of 1768 bp (cDNA break points at n.ts 594 and 2362), which translated as an out-of-frame deletion of amino acids 199-787 in Emo 35 SLO-1 (Fig 5.9). Therefore, Emo 35 SLO-1 has an incomplete S2 domain and totally lacks S3-S8, and the pore domain. The predicted membrane topology of SLO-1 is shown in Fig 5.10.

Emo 48 *slo-1* has a smaller deletion of 1405 bp (cDNA break points at n.ts. 1563 and 2968), which translated as an out of frame deletion of amino acids 522-988 in Emo 48 SLO-1 (Fig 5.11). Therefore, Emo 48 SLO-1 has incomplete S7 and S10 domains and totally lacks S8, S9 and the Ca^{2+} bowl domain.

Figure 5.11 Amino acid sequence and conserved domains for *C. elegans* SLO-1. The motifs that are conserved between BK channels are colour coded; ion transport protein (red 177-351); calcium activated BK potassium channel alpha subunit (green 403-1139); Ca^{2+} bowl (blue). The 11 hydrophobic segments (S0–S10) and the pore are also indicated. Shaded grey area is deleted region of Emo 48.

5.10 Chromosomal linkage of emodepside resistant mutants

Emodepside resistant line	Chromosomal linkage of mutated gene
Emo 35	**V-Mapped to *slo-1***
Emo 42	**I**
Emo 76	**V**
Emo 66	**V**
Emo 48	**V-Mapped to *slo-1***
Emo 69	**II**
Emo 13	**V**

Table 5.2 Chromosomal linkage of emodepside resistant mutants

Following successful identification of the mutated *slo-1* genes in Emo 35 and Emo 48, a similar snip-SNP mapping protocol was initiated in the remaining emodepside resistant lines. Linkage of Emo 76, 66 and 13 to chromosome V immediately suggests further alleles of a mutated *slo-1*. Indeed, in the case of Emo 66, 100% of 14 individual recombination events with CB4856 failed to recombine at map position 19.34 (*slo-1*). (Appendix 3).

More interestingly, in the case of Emo 69 and Emo 42 linkage of the mutated gene that conveys emodepside resistance was assigned to chromosome II and I, respectively (Appendix 3).

5.11 Discussion

To determine if emodepside acts solely through the latrophilin dependent signalling pathway proposed in Chapter 4, and to provide further information on important genes up/downstream of this pathway, a forward genetics approach was adopted. This involved use of the chemical mutagen EMS and a 10,000 genome screen of mutagenised worms on 1μM emodepside agar plates (a concentration which is sufficient to paralyse N2 wild-type picked to this medium within 2 hours, undocumented observation). From this screen seven resistant lines were identified as emodepside-resistant, based on their ability to continually propagate generation after generation on 1μM emodepside agar. Further resistance to emodepside was observed in Emo 35, 42 and 48 in the locomotion thrashing assay, where exposure to 10μM emodepside over 60mins resulted in little or no inhibition of locomotion. Unfortunately, due to the lethargic and highly uncoordinated nature of Emo 76, 66, 69 and 13 these lines could not be assayed to 10μM emodepside in the thrashing assay, as they do not display quantifiable body bends. Also, emodepside concentrations ≥10μM could not be tested due to solubility problems with the compound. These mutants were not resistant to paralysis induced by 1μM ivermectin.

Each of these lines displayed a slightly dumpy visible phenotype. Dumpy (dpy) mutants often result from mutations in collagen genes or collagen-modifying enzymes (Kenning *et al.*, 2004). This is interesting with regards to the postulated uptake mechanisms and the observed stage specific efficacy of emodepside in *C. elegans*, discussed in Chapter 3. If emodepside does exert an effect by absorption through the cuticle and this absorption is dependent on the differences in collagen expression both between moults and at different times during a moult, than mutations to the collagen gene/s that result in a dpy phenotype may confer altered sensitivity to emodepside. Furthermore, examination of all seven emodepside resistant strains under a high powered compound microscope (1000x magnification) showed that they had normal rectal morphology and were therefore not constipated (data not shown).

As well as a dpy phenotype all lines exhibited an uncoordinated (unc) phenotype, with the exception of Emo 42. Mutations in genes involved in the nervous system often correspond to an unc phenotype; therefore this behavioural defect correlates with previous findings that emodepside has a neuropharmacological mode of action (Willson *et al.*, 2003).

As well as paralysing numerous nematode species (Harder & Samson-Himmelstjerna, 2001) emodepside is also capable of inhibiting pharyngeal pumping in *C. elegans* (Willson *et al.*, 2004). To examine whether or not the emodepside resistant properties of these mutants are exclusively related to the effect of the anthelmintic on body wall muscle, EPGs were performed on Emo 35. This mutant continued to pump constitutively upon exposure to 100nM emodepside, a concentration which results in total cessation of pharyngeal activity in N2 wild-type (Willson *et al.*, 2004).

Using a technique of snip-SNP mapping it was found that the mutated gene in Emo 35 and 48 was located at map position 19.34. This position relates to three known genes, a hormone receptor (*nrh-70*), a serpentine receptor (*srg-34*) and lastly a Ca^{2+}-activated potassium channel (*slo-1*). Although all three of these could be reasoned as plausible targets for emodepside, it was the latter that seemed most probable. This hypothesis was based on previous electrophysiological data that demonstrated the necessity of specific ions, namely calcium (Ca^{2+}) and potassium (K^{+}), in the hyperpolarization induced by emodepside perfused over *A. suum* muscle cells (Willson *et al.*, 2003). Amalgamation of this ion dependency data led to the original hypothesis that the mechanism of emodepside action may be governed by a Ca^{2+}-activated potassium channel (see Chapter 1).

The emodepside sensitivity of *slo-1 (js379)* was determined in both the locomotion assay and pharyngeal pumping assay (the latter kindly performed by J.Willson). In both cases, a high level of resistance to supramaximal concentrations of emodepside was observed. As well as exhibiting resistance during the acute time-dependence locomotion assay, it was also observed that *slo-1 (js379)* is capable of propagating generation after generation on 1µM emodepside agar plates (data not shown). Also noteworthy is the well characterised jerky locomotion phenotype of *slo-1* mutants

(Wang *et al.*, 2001), which results in these animals having a greater frequency of backward movement. Identical locomotory behaviour is displayed in Emo 35, initially noted following the mutagenesis screen.

Slo-1 encodes SLO-1, the pore-forming α-subunit of a large conductance Ca^{2+} - activated K^+ channel (BK channel). Subsequent cloning and sequencing of *slo-1* from Emo 35 and Emo 48 confirmed the necessity of this gene in the mechanism of emodepside action, as both lines have large, out-of-frame, deletions in SLO-1.

BK channels are large conductance K^+ channels that are activated in an extremely synergistic manner by both intracellular Ca^{2+} and voltage (Pallotta *et al.*, 1981). When activated, K^+ exits the cells through the open channels, causing a more negative membrane potential, shutting down voltage-dependent Ca^{2+} and Na^+ channels. This twofold activation and resulting negative feedback on intracellular Ca^{2+} and membrane potential allows BK channels to modulate numerous physiological processes, such as smooth muscle contraction (Petkov *et al.*, 2001).

In *C. elegans*, six mutants of SLO-1 were obtained in a genetic screen for regulators of neurotransmitter release (Wang *et al.*, 2001). Mutants were isolated by their capability to suppress lethargy of an *unc-64* syntaxin mutant, which restricts neurotransmitter release. Evoked postsynaptic currents were measured at the neuromuscular junction in both wild-type and SLO-1 mutants, and it was observed that the removal of SLO-1 greatly increased quantal content, primarily by increasing duration of release. Wang *et al.* suggest that the selective isolation of *slo-1* as the only ion channel mutant derived from a whole genomic screen designed to detect regulators of neurotransmitter release indicates that SLO-1 plays an important, if not unique, role in regulating neurotransmitter release.

However, with regards to emodepside action, the evidence that SLO-1 acts in *C. elegans* to repolarise presynaptic nerve terminals, therefore terminating neurotransmitter release, does not appear to fit with the proposed mechanism outlined in Chapter 4. The current understanding is that emodepside acts presynaptically to evoke neurotransmitter release (Willson *et al.*, 2004). Therefore, one would expect that by effectively removing inhibitory regulators of this evoked release (*slo-1*) hypersensitivity to emodepside should occur. This is clearly not the

case, as demonstrated by the high degree of resistance to emodepside in *slo-1 (js379)*, Emo 35 and Emo 48. This apparent anomaly has still to be resolved.

Another functional role of SLO-1 has been identified in *C. elegans*. Ethanol has been shown to concentration-dependently slow *C. elegans* locomotion and egg-laying behaviours, with a threshold for inhibiting locomotion wave forms of 200mM (Davies *et al.*, 2003). *Davis et al.* performed a mutagenesis screen for the ability of *C. elegans* to move or lay eggs in the presence of 400mM external ethanol (22mM internal) and isolated multiple ethanol-resistant mutants. Numerous loss-of-function *slo-1* alleles emerged from these screens, indicating that *slo-1* has a central role in ethanol responses. Electrophysiological analysis showed that ethanol activates the channel *in vivo*, inhibiting neuronal activity. Furthermore, *Davis et al.* demonstrated that the behaviours of *slo-1* gain-of-function mutants resemble those of ethanol intoxicated animals. This indicates that selective activation of BK channels is responsible for the acute intoxicating effects of ethanol in *C. elegans*, which results in inhibition of locomotion.

Numerous control measures were implemented throughout this study to prevent the possibility of mistakenly identifying ethanol resistance as emodepside resistance. Firstly, all locomotion assays were performed in conjunction with an ethanol vehicle control; 1% in the agar plates and 0.1% in the thrashing assay. This equates to 170mM and 17mM ethanol concentration in these assays, respectively. *Davis et al.* observed a very small decrease in the amplitude of body bends and only a 17% inhibition in the mean rate of N2 wild-type locomotion at 200mM ethanol concentration, with 500mM causing maximal inhibition. In this study ethanol control plates were made by addition of vehicle (or drug dissolved in vehicle) once the post autoclaved media had cooled to $\leq 60°C$. Therefore it is highly likely that the actual ethanol concentration in both vehicle and emodepside plates was significantly less than 170mM, due to evaporation. Furthermore, determination of emodepside sensitivity in all assays was standardised as a % of the vehicle control response, and therefore any slight inhibitory effect of ethanol on locomotion would be eliminated from the results. However, most significant is the long-term difference between the effects of ethanol and emodepside on *C. elegans* locomotion. Prolonged exposure to 500mM exogenous ethanol for a few hours duration, results in acute tolerance with return to normal locomotion (Davies *et al.*,

2004), regardless of the fact that the internal ethanol concentration within these animals remains constant. The time-dependent effects of emodepside on locomotion are drastically different, with even threshold inhibitory concentrations causing irreversible and highly significant depression of locomotion rates. The maximal concentration of emodepside used in the agar plate assay, 1μM, is sufficient to completely paralyse *C. elegans* within 2 hours, after which time death occurs.

However, the precise involvement of SLO-1 in the mechanism of emodepside action still remains unclear. As previously mentioned, one would expect hypersensitivity to emodepside in *slo-1* mutants, if emodepside acts to evoke release of neurotransmitter at the NMJ. The fact that *slo-1* mutants are highly resistant to emodepside is intriguing, and taken together with the data that *slo-1 (gf)* mutants are not hypersensitive to emodepside, further complicates the overall picture.

One possible explanation is that the role of SLO-1 in the anthelmintic action of emodepside is not presynaptic in nature. Although SLO-1 channels and *slo-1* are predominantly found on presynaptic nerve endings and in many types of neurons (Anderson *et al.*, 1988;Wang *et al.*, 2001), gene expression can also be seen in punctuate regions throughout *C. elegans* body wall muscle (Wang *et al.*, 2001). The role of *slo-1* in regulation of neurotransmission has been shown to be dependent on neuronal gene expression, not that in muscle (Wang *et al.*, 2001). However, it is possible that, in terms of emodepside-induced paralysis, SLO-1 channels are important regulators of muscle excitability. That is, mutation of *slo-1* may disrupt the SLO-1 channels on muscle that are essential in causing the resultant paralysis which is induced by presynaptic release of a cocktail of neurotransmitters via a latrophilin, G-protein signalling pathway.

Chapter 6

Discussion

This thesis has described the actions of emodepside, a resistance breaking anthelmintic. Resistance to existing anthelmintics requires the search for such novel compounds, which are able to target unique sites. Understanding the mechanism of action of emodepside is of great importance. Elucidating this unique target site should provide information for the formulation of additional anthelmintics, which could utilise this mode of action. Determining the target site of emodepside may help confirm the desired parasite specific selective toxicity for such compounds, or enable clarification of any clinically determined therapeutic index. Furthermore, understanding the mechanism of action of emodepside will provide a novel pharmacological insight into nematode neurobiology.

Therefore, the basis of this study was to further investigate the neuropharmacologically active mode of action of emodepside, using the parasitic nematode *A. suum* and the free-living non-parasitic model genetic organism, *C. elegans*.

One of the first questions this thesis aimed to address was whether emodepside exerts anthelmintic action via a GABAergic mechanism (as discussed in Chapter 1, section 1.12). At the onset of this study it was known that the action of emodepside on the electrophysiological properties of *A. suum* muscle were not like the actions of GABA. Emodepside caused only a slight, irreversible, long-lasting hyperpolarisation of *A. suum* muscle, with no change in input conductance (Willson *et al.*, 2003). GABA had been shown to elicit a fast hyperpolarisation associated with an increased input conductance, consistent with the opening of ligand-gated chloride channels (Martin, 1982). These data highlighted an important difference between the mechanism of emodepside and that of GABA, which required further investigation. Furthermore, it was already known that application of emodepside to *A. suum* muscle caused a relaxation of basal muscle tension and a relaxation of body wall muscle pre-contracted with both ACh and the neuropeptide AF1 (Willson *et al.*, 2003).

This study provides further insight into this *A. suum* muscle relaxation effect with emodepside, by directly comparing the effect of emodepside and that of GABA on the rate of relaxation of *A. suum* muscle pre-contracted with acetylcholine. The

effect of GABA on muscle relaxation was distinctly different, being much faster than that of emodepside. Since the GABA effect on *A. suum* somatic muscle is mediated through an increase in chloride permeability (Martin, 1980), the GABA and emodepside effects on pre-contracted muscle were investigated using chloride-free saline. While the effect of emodepside was unaffected in chloride-free saline, the effect of GABA was converted to a very slow relaxation, or in some cases, a slight contraction. These data taken together provide strong evidence that the effect of emodepside is not mediated through a direct GABAergic pathway. Future experiments on *C. elegans unc-25* (glutamic acid decarboxylase necessary for GABA synthesis) (McIntire *et al.*, 1993)) and *unc-49* mutants, (which encodes the main inhibitory GABA receptor at the neuromuscular junction (Richmond *et al* 1999) will be beneficial to completely eliminate a GABA component in emodepside action.

A. suum is not well suited for the molecular and genetic techniques that were necessary to further understand the mechanism of emodepside action. A new approach was required. The use of the free-living nematode *C. elegans* has previously been shown to be highly useful for investigations into anthelmintic mechanisms, such as that of ivermectin (Dent *et al.*, 2000). However, it was firstly necessary to establish that *C. elegans* could be used as a model for emodepside screening. This study established that emodepside has an inhibitory, concentration-dependent, effect on *C. elegans* locomotion. Furthermore, this effect illustrates an interesting difference between emodepside and the parent compound PF1022A, as the latter cyclodepsipeptide has no effect on *C. elegans* locomotion (Bernt, 1998). Using a concentration range of emodepside agar plates, it was observed that emodepside exclusively paralysed locomotion of adult worms at IC_{50} 4nM. This concentration is identical to that observed for emodepside inhibition of pharyngeal pumping, as assayed by EPG (Willson *et al.*, 2004). Therefore emodepside exerts anthelmintic activity in *C. elegans* by paralysis of body wall muscle and an inhibition of feeding.

Immediately prior to initiation of this study, a latrophilin receptor was identified as a potential target site for emodepside (Saeger *et al.*, 2001) (Chapter 1, section 1.13).

Latrophilin is a seven transmembrane G-protein coupled receptor (Chapter 1, section 1.14.3). Therefore, an RNAi reverse genetics approach, using the two *C. elegans* latrophilin-like receptors (LAT-1 and LAT-2), was utilised to investigate a possible role for latrophilin in the mechanism of emodepside action.

The relative ease, low cost, and high-throughput characteristics of RNAi techniques with *C. elegans* has ensured that this strategy has been widely adopted for identifying genes putative to signalling pathways. Indeed, unlike a standard genetic screen, where positional cloning of the mutated gene can take years, the molecular nature of genes identified in an RNAi-based reverse genetics screen is known at the onset. However, over the last few years there has been much debate over the reliability of RNAi. For some time it was accepted that RNAi techniques do not always accurately phenocopy the null phenotype of all genes, such as those involved in neuronal function (Fraser *et al.*, 2000). It was therefore considered that RNAi may merely cause a knock-down of gene expression, rather than complete null, or gene knock-out. However, it has also been suggested that those RNAi screens which failed to phenocopy null phenotypes, in particular tissues, were biased towards genes for viability, and that more refined assays are required to detect subtle neuronal or muscular phenotypes (Bargmann, 2001). Such penetrance problems can often be resolved by performing RNAi in an *rrf-3* mutant background. This RNAi hypersensitive strain allows for interference in tissues that are usually refractory to RNAi in a wild-type background, such as neurons (Simmer *et al.*, 2002). Indeed, for this study all RNAi experiments were carried out using *rrf-3 (pk1426)*, as it has been demonstrated that emodepside exerts a neuropharmacological mechanism of action (Willson *et al.*, 2003).

Data presented in this study show that RNAi for *lat-1* resulted in phenotypes typical of a defect in neuronal function, longer pharyngeal pump duration (Willson *et al.*, 2004) and uncoordinated, loopy, body bends. However, RNAi of *lat-2* did not result in any detectable phenotype. This raises the question of whether the neuronal penetrance of RNAi for *lat-2* was insufficient to produce a distinct phenotype, or suggests a physiological redundancy for *lat-2*, if *lat-1* is still present. RNAi of *lat-2* did lead to a significant reduction in sensitivity to emodepside in this study; however, this degree of resistance to the anthelmintic was not as marked as that

observed with RNAi for *lat-1*. Unfortunately, simultaneous RNAi of both *lat-1* and *lat-2* appeared to be unsuccessful.

It was hoped that the availability of the *lat-1 (ok379)* RB629 would enable further investigation into the role of *lat-1* in the mechanism of emodepside action. However, as discussed in Chapter 4 (section 4.4), it was impossible to recover a homozygous *ok379* line of this strain for accurate analysis. Although the backcrossed animals of this strain were subjected to the emodepside agar plate assay, they appeared as wild-type in the emodepside-induced inhibition of locomotion. Interestingly, further analysis of RB629 confirmed that animals derived from this strain are emodepside resistant in the pharyngeal pumping assays (Willson *et al.*, 2004). However, it has also been subsequently found that animals derived from the RB629 strain can lose the *ok379* deletion but remain resistant to pharyngeal pumping inhibition by emodepside. Therefore, this resistance does not correlate with a *lat-1* deletion/chromosomal re-arrangement in the strain. This highlights an, as yet, undefined mutation/s in the RB629 strain, that specifically covey/s emodepside resistance in the *C. elegans* pharynx, but not body wall muscle. This may arise due to differences in tissue specific expression of the mutated gene/s, or suggests a point of difference in the mechanism of action of emodepside on the pharynx and body wall muscle.

During the course of this work, a *lat-2* mutant strain became available, which enabled further insight into the role of a latrophilin receptor in the mechanism of action of emodepside. Prior to assaying the strain with emodepside, *lat-2 (ok301)* VC158 were backcrossed (x1) and a PCR product corresponding to the reported homozygous deletion was successfully amplified. LAT-2 in VC158 has a deletion of the last 253 a.a of the receptor C-tail. Complimentary to the earlier *lat-2* RNAi work performed in this study, the *lat-2 (ok301)* VC158 do not exhibit any observable phenotype. Low level resistance to emodepside-induced paralysis of locomotion was observed with *lat-2 (ok301)* null mutants. However, a recent Wormbase update (Dec 2004) for *lat-2 (ok301)* has altered the predicted *lat-2* genomic sequence. The first two exons of this gene were removed based on EST (Expression-Sequence-Tags) data, a 5' exon and several internal exons were added based on mRNA data and last the 4 exons were removed, based on mRNA data.

The net result of this now places the start of the deleted region 164 bp upstream of the stop codon for *lat-2*. However, the diversity of gene products is to a major part due to alternative splicing of mRNA. Therefore, it is possible that the deletion is located at the previously determined locus, as the majority of alterations to the original predicted sequence were made based on mRNA and EST models. Recently the *lat-2 (tm463)* mutant has become available. Work on this homozygous viable deletion (exons 3-9) mutant is currently underway, and should help clarify the role for *lat-2* in the mechanism of emodepside action.

In Chapter 4, a reverse genetic approach was used to target potential components of the emodepside signalling pathway. This investigation was conducted with the rationale that emodepside inhibits *C. elegans* locomotion via a latrophilin-like receptor, and this effect may involve synaptic neurotransmission at the NMJ. Indeed, understanding this pathway is not only important for the future of anthelmintic discovery, but also provides information on the control of synaptic vesicle release. This strategy was made possible by the availability of *C. elegans* mutants deficient in proteins required for synaptic transmission. Briefly, it was found from this study that emodepside requires the G-protein $G\alpha_q$. *C. elegans* mutants with a loss-of- function of $G\alpha_q$ were resistant to emodepside, whereas a gain-of-function strain was hypersensitive to emodepside. PLCß, a key modulator of pathways that regulate vesicle release (Lackner *et al.*, 1999;Miller *et al.*, 1999), is also required in emodepside action, as PLCß mutants are resistant to emodepside. PLCß hydrolyses PIP2 to DAG. In *C. elegans*, $G_o\alpha$ negatively regulates the levels of DAG by activating DAGkinase, thus *goa-1* mutants are predicted to have increased levels of DAG. Interestingly, *goa-1* were shown to be hypersensitive to emodepside, suggesting that the second messenger DAG is important in mediating the action of emodepside.

DAG, in turn, recruits UNC-13 to the pre-synaptic membrane increasing the number of vesicles primed at the pre-synaptic membrane (Gillis *et al.*, 1996;Stevens & Sullivan, 1998). Although null mutants for UNC-13 are available, these strains exhibited a drastically abnormal locomotory behaviour that prevented the analysis of such animals in this work. However, it has been shown that UNC-13 is essential

for the mechanism of emodepside action on the pharynx (Willson *et al.*, 2004). In *C. elegans,* UNC-13-dependent vesicular release through DAG signalling is evident via a pathway involving cholinergic and serotonergic control of motorneurones (Lackner *et al.*, 1999;Miller *et al.*, 1999;Nurrish *et al.*, 1999). Taken together these data present a putative second messenger signalling cascade that results in vesicle exocytosis (Fig 6.1). This generic signalling pathway has been described in many experimental organisms to modulate vesicle release of a number of different neurotransmitters (Lackner *et al.*, 1999;Miller *et al.*, 1999;Nurrish *et al.*, 1999)

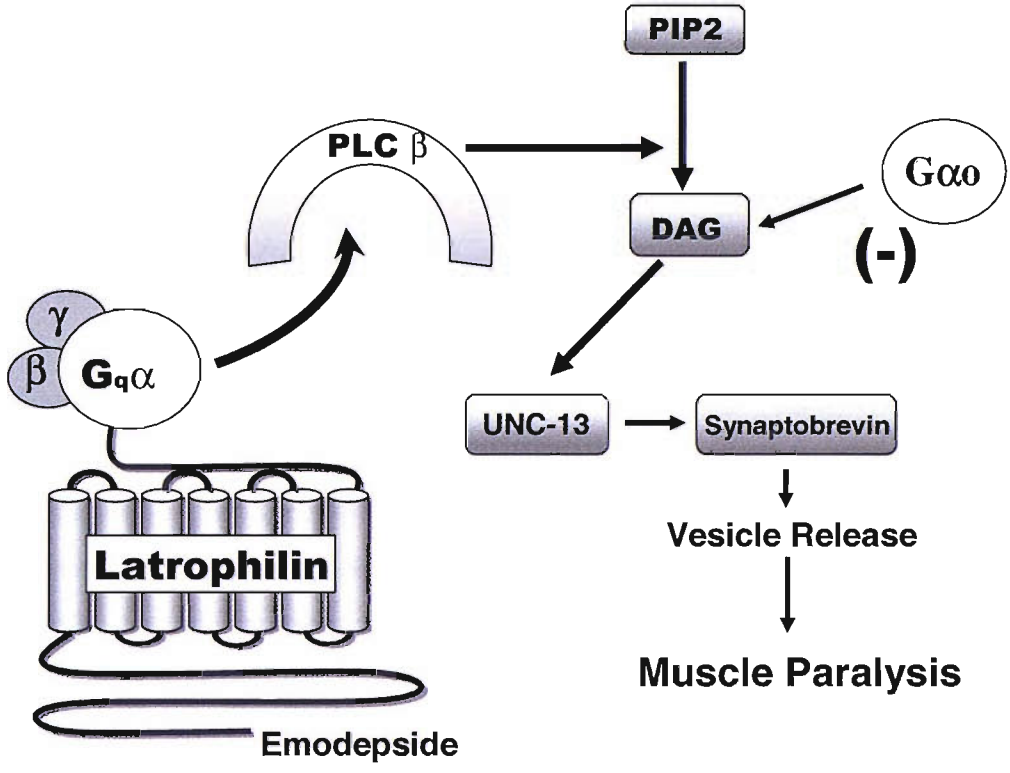

Figure 6.1. Proposed mechanism of action for the novel anthelmintic emodepside.

Chapter 4 (section 4.10) of this thesis describes the investigative approach that was used to try and identify the neurotransmitter/s that may be released as a result of this signalling cascade. A reduction in sensitivity to 2mM aldicarb in *lat-1* RNAi treated worms was observed, and indicates a decrease in the amount of ACh released at the NMJ in these knock-down worms. RNAi of the *flp-1* gene (which codes for an identical PF2 peptide in *C. elegans*) caused a resistance to emodepside,

as did RNAi for *flp-13* which encodes for neuropeptides that have an inhibitory action on body wall muscle (Reinitz *et al.*, 2000b). Mutants lacking *egl-21* CPE are defective for processing endogenously expressed FMRFamide (Jacob & Kaplan, 2003), and these animals also exhibited a reduced sensitivity to emodepside.

The FM4-64 imaging data of Willson et al. (2004) suggests that emodepside appears to stimulate release from a number of different neurones in the worm. Therefore, emodepside may stimulate release of inhibitory peptides, ACh, or a cocktail of different transmitters at the NMJ. Although this thesis provides some preliminary evidence for the latter possibility, this matter requires further investigation. Precise neuronal determination of the latrophilin expression pattern in *C. elegans*, by immunohistochemistry, could provide an insight into the neurotransmitters released through emodepside action.

The reverse genetic approach adopted in this thesis has provided considerable insight into the signalling molecules that appear to modulate the inhibitory action of emodepside on *C. elegans* muscle. However, although significant levels of resistance were observed in *C. elegans* strains with disruptions in genes putative to this signalling pathway, complete resistance to the anthelmintic was not observed. In the case of *lat-1* RNAi, this may be attributed to less than total penetrance. For this reason it would be useful to obtain a viable *lat-1* homozygous null mutant, to fully examine a role for *lat-1* in this anthelmintic action. It may be that *lat-1* is of vital physiological importance and a homozygous mutant would result in lethality. However, the *lat-2 (ok301)* null mutant, although resistant to emodepside when compared to N2 wild-type, was still susceptible to locomotion inhibition at higher emodepside concentrations. These data, combined with a lack of phenotype for this deletion mutant, would seem to indicate a physiological redundancy for *lat-2*. Future work could involve RNAi of *lat-1* on *lat-2 (tm463)* and *lat-2 (ok301)*, to determine if this results in a greater resistance to emodepside, than that observed by disruption of only a single *C. elegans* latrophilin gene. Work is still ongoing to fully understand latrophilin signalling in vertebrate systems (Ushkaryov *et al.*, 2004;Ushkaryov, 2002), and identify the endogenous ligand for these receptors. Resolving this may provide further insight as to how emodepside acts via a latrophilin receptor, to paralyse nematode muscle. Presumably selective toxicity of

emodepside is achieved by activation of latrophilin receptors that are specific to nematodes, in preference to the mammalian host. PF1022A was demonstrated not to cross the blood-brain-barrier, and in the mammalian system latrophilin-1 is primarily expressed in the brain, further adding to the selective toxicity of emodepside.

Epistasis analysis using multiple components of the proposed emodepside signalling pathway (Fig 6.1) would also be beneficial to determine if this results in a greater level of resistance. However, as the molecular components of this pathway are vital for normal nematode motility (Lackner *et al.*, 1999;Nurrish *et al.*, 1999), this may prove difficult when assaying emodepside-induced changes in locomotion.

Inositol 1, 4, 5-trisphosphate (IP_3) is an important second messenger produced from the lipid PIP2 by PLC. IP_3 acts to regulate calcium signals through a large calcium channel called the IP_3 receptor (IP_3R), located in the endoplasmic reticulum. IP_3Rs in *C. elegans* are encoded by a single gene, *itr-1*, and are widely expressed in the nervous system and pharynx, as well as other tissues (Baylis *et al.*, 1999). The up-regulation of pharyngeal pumping in response to food is dependent on intact IP_3- and IP_3R-mediated signalling (Walker *et al.*, 2002). However, it has been shown that intrinsic muscle function is not compromised by disruption of IP_3 signalling or ITR-1 function. It would therefore be interesting to conduct future work, through RNAi of *itr-1*, to determine whether emodepside-stimulated release of neurotransmitters engages an IP_3 signalling cascade that may modulate pharyngeal function.

As detailed in Chapter 5, a forward genetics approach was also used in this study. The aim of this was to determine if emodepside acts solely through the latrophilin dependent signalling pathway proposed above, and to provide further information on important genes up/downstream of this pathway. This screen identified seven emodepside-resistant lines. The level of resistance to inhibition of locomotion, exhibited by all of these lines, is far greater than that observed in any strain from the reverse genetic strategy (see Chapter 5, section 5.2 & 5.3). Emo 35 worms also

exhibited high degrees of resistance to the inhibitory effects of emodepside on *C. elegans* pharyngeal pumping.

Snip-SNP mapping techniques, and subsequent sequencing, indicated that resistance to emodepside was conveyed in both Emo 35 and Emo 48 due to large deletions in the Ca^{2+} activated K^{+} channel gene, *slo-1*. This was confirmed by assaying the emodepside sensitivity of *slo-1* deletion mutants (CGC), which also exhibited the same high levels of resistance to the inhibitory effects of emodepside, in both locomotion and pharyngeal pumping experiments.

As SLO-1 has been shown to modulate the intoxicating effects of ethanol in *C. elegans* (Davies *et al.*, 2003), it would be interesting to verify if the emodepside resistant animals from this study are also ethanol resistant. Indeed, work is currently underway to establish the concentration-response profile of Emo 35 and Emo 48 to ethanol inhibition of locomotion.

SLO-1 acts in *C. elegans* to repolarise presynaptic nerve terminals, therefore terminating neurotransmitter release (Wang *et al.*, 2001). The precise involvement of SLO-1 in the mechanism of emodepside action remains unclear, as one would expect hypersensitivity to emodepside in *slo-1* mutants, if emodepside acts to evoke release of neurotransmitter at the NMJ.

It is possible that SLO-1 channels are not presynaptically involved in the mechanism of emodepside-induced paralysis, but rather, are important postsynaptically as regulators of muscle excitability. That is, mutation of *slo-1* may disrupt the SLO-1 channels on muscle that are essential in causing the resultant paralysis which is induced by presynaptic release of a cocktail of neurotransmitters via a latrophilin, G-protein signalling pathway (Fig 6.2). Future work is currently underway to clarify this latter hypothesis. Microinjection of GFP-tagged *slo-1* constructs, with tissue specific promoters (either *myo-2* for muscle, or *snb-1* for neurons) into emodepside resistant worms aims to restore SLO-1 channel activity in either postsynaptic muscle, or presynaptic neuronal structures, respectively. The intention is to determine which construct rescues emodepside sensitivity, and thereby clarify a pre- and/or postsynaptic role for SLO-1 in emodepside action.

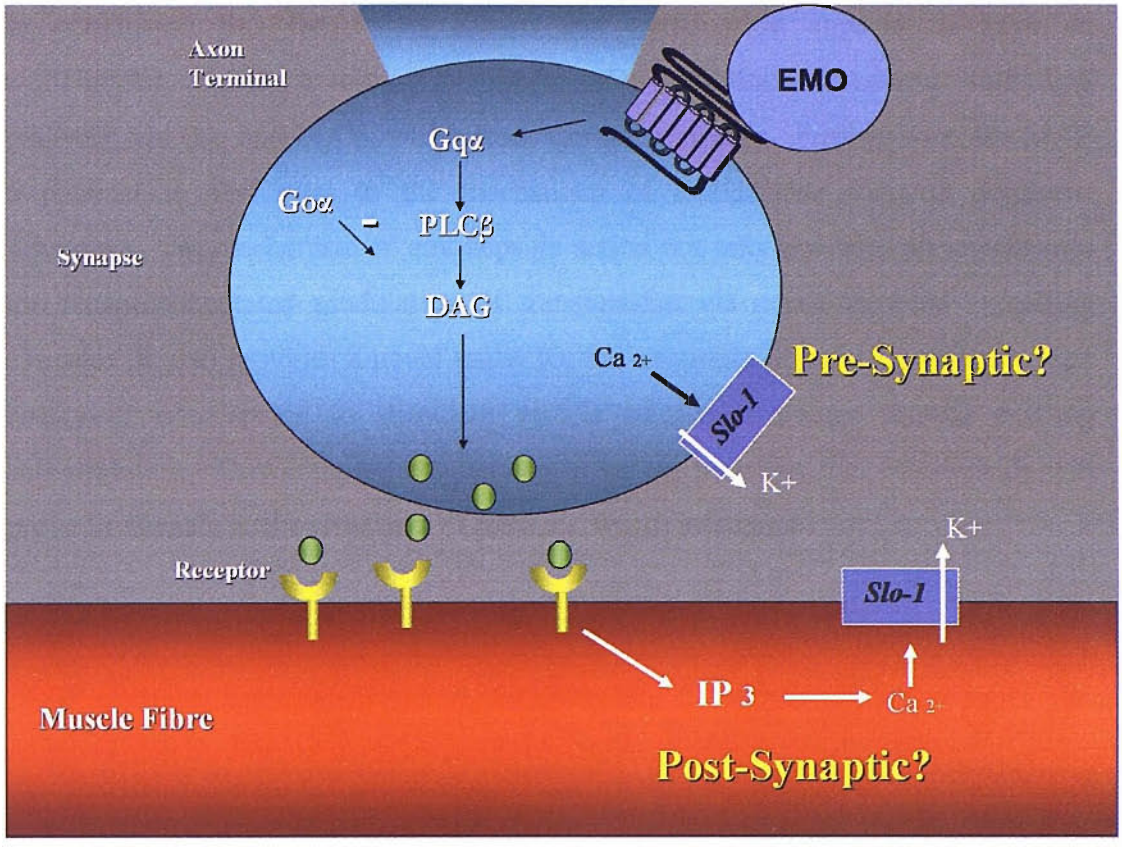

Figure 6.2 The proposed mechanism of emodepside action. Questions still remain as to the pre- or post-synaptic involvement of SLO-1 in the anthelmintic action. One possibility is that emodepside may act pre-synaptically via a latrophilin, Gqα pathway to stimulate vesicle release at the synapse. Post-synaptically, this neurotransmitter may lead to receptor mediated IP_3 production, which in turn could activate muscle SLO-1 due to increased intracellular Ca^{2+}. It is this postsynaptic modulation of muscle activity by SLO-1 which may result in emodepside induced paralysis.

Future work is also necessary on the remaining five emodepside resistant strains which have not been fully mapped. Initial linkage analysis from this study indicates that Emo 76, 66 and 13 have a mutation on chromosome V. It is highly likely that these three mutants are also alleles of *slo-1*, yet this requires confirmation. However, chromosomal allocation for Emo 42 and 69 indicates mutations on chromosomes I and II, respectively. It could be argued that of the remaining five strains, these latter two mutants are the most interesting. Indeed, determination of the genes that convey resistance in these two strains may provide further information to the latrophilin proposed pathway, and help clarify the role of SLO-1 in emodepside action. It is possible that the latrophilin pathway and SLO-1 channel represent two distinctly different modes of action for this novel anthelmintic.

In conclusion this thesis has shown that emodepside appears to have an anthelmintic action involving a presynaptic latrophilin-dependent signalling pathway, via $G_q\alpha$ and PLCβ, which leads to vesicle release. Furthermore, the SLO-1 channel is also vital to the mechanism of emodepside induced paralysis. Therefore, the mechanism of emodepside action not only provides an insight into the receptor-mediated modulation of transmission via nerve terminal signalling cascades, it also provides a novel target for the treatment of parasitic diseases. The ability of emodepside to stimulate vesicle release is unique among existing anthelmintics. This complex mechanism of action indicates that emodepside will prove invaluable in the treatment of parasitic worm infections.

Albertson, D. G. & Thomson, J. N. (1976). The pharynx of Caenorhabditis elegans. *Philos.Trans.R.Soc.Lond B Biol.Sci.* **275**, 299-325.

Altun-Gultekin, Z., Andachi, Y., Tsalik, E. L., Pilgrim, D., Kohara, Y., & Hobert, O. (2001). A regulatory cascade of three homeobox genes, ceh-10, ttx-3 and ceh-23, controls cell fate specification of a defined interneuron class in C. elegans. *Development* **128**, 1951-1969.

Anderson, A. J., Harvey, A. L., Rowan, E. G., & Strong, P. N. (1988). Effects of charybdotoxin, a blocker of Ca2+-activated K+ channels, on motor nerve terminals. *Br.J.Pharmacol.* **95**, 1329-1335.

Aravamudan, B. & Broadie, K. (2003). Synaptic Drosophila UNC-13 is regulated by antagonistic G-protein pathways via a proteasome-dependent degradation mechanism. *J Neurobiol.* **54**, 417-438.

Aravamudan, B., Fergestad, T., Davis, W. S., Rodesch, C. K., & Broadie, K. (1999). Drosophila UNC-13 is essential for synaptic transmission. *Nat.Neurosci.* **2**, 965-971.

Arena, J. P., Liu, K. K., Paress, P. S., Frazier, E. G., Cully, D. F., Mrozik, H., & Schaeffer, J. M. (1995). The mechanism of action of avermectins in Caenorhabditis elegans: correlation between activation of glutamate-sensitive chloride current, membrane binding, and biological activity. *J.Parasitol.* **81**, 286-294.

Aronin, N. & DiFiglia, M. (1992). The subcellular localization of the G-protein Gi alpha in the basal ganglia reveals its potential role in both signal transduction and vesicle trafficking. *J Neurosci.* **12**, 3435-3444.

Augustin, I., Rosenmund, C., Sudhof, T. C., & Brose, N. (1999). Munc13-1 is essential for fusion competence of glutamatergic synaptic vesicles. *Nature* **400**, 457-461.

Bargmann, C. I. (2001). High-throughput reverse genetics: RNAi screens in Caenorhabditis elegans. *Genome Biol.* **2**, REVIEWS1005.

Baylis, H. A., Furuichi, T., Yoshikawa, F., Mikoshiba, K., & Sattelle, D. B. (1999). Inositol 1,4,5-trisphosphate receptors are strongly expressed in the nervous system, pharynx, intestine, gonad and excretory cell of Caenorhabditis elegans and are encoded by a single gene (itr-1). *J.Mol.Biol.* **294**, 467-476.

Bernstein, E., Caudy, A. A., Hammond, S. M., & Hannon, G. J. (2001). Role for a bidentate ribonuclease in the initiation step of RNA interference. *Nature* **409**, 363-366.

Bernt. Effects of anthemintics with different modes of action on the behavior and development of Caenorhabditis elegans. Fundam.appl.Nematol. 21[3], 251-263. 1998.
Ref Type: Generic

Bessereau, J. L., Wright, A., Williams, D. C., Schuske, K., Davis, M. W., & Jorgensen, E. M. (2001). Mobilization of a Drosophila transposon in the Caenorhabditis elegans germ line. *Nature* **413**, 70-74.

Betz, A., Ashery, U., Rickmann, M., Augustin, I., Neher, E., Sudhof, T. C., Rettig, J., & Brose, N. (1998). Munc13-1 is a presynaptic phorbol ester receptor that enhances neurotransmitter release. *Neuron* **21**, 123-136.

Brenner, S. (1974). The genetics of Caenorhabditis elegans. *Genetics* **77**, 71-94.

Brownlee, D., Holden-Dye, L., & Walker, R. (2000). The range and biological activity of FMRFamide-related peptides and classical neurotransmitters in nematodes. *Adv.Parasitol.* **45**, 109-180.

Brownlee, D. J., Fairweather, I., Johnston, C. F., Smart, D., Shaw, C., & Halton, D. W. (1993). Immunocytochemical demonstration of neuropeptides in the central nervous system of the roundworm, Ascaris suum (Nematoda: Ascaroidea). *Parasitology* **106 (Pt 3)**, 305-316.

Brundage, L., Avery, L., Katz, A., Kim, U. J., Mendel, J. E., Sternberg, P. W., & Simon, M. I. (1996). Mutations in a C. elegans Gqalpha gene disrupt movement, egg laying, and viability. *Neuron* **16**, 999-1009.

Bundy, D. A. & de Silva, N. R. (1998). Can we deworm this wormy world? *Br.Med.Bull.* **54**, 421-432.

Burglin, T. R., Lobos, E., & Blaxter, M. L. (1998). Caenorhabditis elegans as a model for parasitic nematodes. *Int.J.Parasitol.* **28**, 395-411.

Burns, D. J. & Bell, R. M. (1991). Protein kinase C contains two phorbol ester binding domains. *J Biol.Chem.* **266**, 18330-18338.

Butz, S., Okamoto, M., & Sudhof, T. C. (1998). A tripartite protein complex with the potential to couple synaptic vesicle exocytosis to cell adhesion in brain. *Cell* **94**, 773-782.

Capogna, M., McKinney, R. A., O'Connor, V., Gahwiler, B. H., & Thompson, S. M. (1997). Ca2+ or Sr2+ partially rescues synaptic transmission in hippocampal cultures treated with botulinum toxin A and C, but not tetanus toxin. *J Neurosci.* **17**, 7190-7202.

Cappe de Baillon, P. (1911). Etude sur les fibres musculaires d'*Ascaris*. I. Fibres pariétales. *Cellule* **27**, 165-211.

Cerutti, H. (2003). RNA interference: traveling in the cell and gaining functions? *Trends Genet.* **19**, 39-46.

Chen, E. Y. & Clarke, D. M. (2002). The PEST sequence does not contribute to the stability of the cystic fibrosis transmembrane conductance regulator. *BMC.Biochem.* **3**, 29.

Chen, W., Terada, M., & Cheng, J. T. (1996). Characterization of subtypes of gamma-aminobutyric acid receptors in an Ascaris muscle preparation by binding assay and binding of PF1022A, a new anthelmintic, on the receptors. *Parasitol.Res.* **82**, 97-101.

Cioli, D. & Pica-Mattoccia, L. (2003). Praziquantel. *Parasitol.Res.* **90 Supp 1**, S3-S9.

Colquhoun, L., Holden-Dye, L., & Walker, R. J. (1991). The pharmacology of cholinoceptors on the somatic muscle cells of the parasitic nematode Ascaris suum. *J.Exp.Biol.* **158**, 509-530.

Conder, G. A., Thompson, D. P., & Johnson, S. S. (1993). Demonstration of co-resistance of Haemonchus contortus to ivermectin and moxidectin. *The Veterinary Record* **132**, 651-652.

Cox C (1992). Aldicarb. *J.Pest Reform* **12**, 31-35.

Cox, G. N., Carr, S., Kramer, J. M., & Hirsh, D. (1985). Genetic mapping of Caenorhabditis elegans collagen genes using DNA polymorphisms as phenotypic markers. *Genetics* **109**, 513-528.

Cox, G. N., Staprans, S., & Edgar, R. S. (1981). The cuticle of Caenorhabditis elegans. II. Stage-specific changes in ultrastructure and protein composition during postembryonic development. *Dev.Biol.* **86**, 456-470.

Cully, D. F., Vassilatis, D. K., Liu, K. K., Paress, P. S., Van der Ploeg, L. H., Schaeffer, J. M., & Arena, J. P. (1994). Cloning of an avermectin-sensitive glutamate-gated chloride channel from Caenorhabditis elegans. *Nature* **371**, 707-711.

Davey, K. G. (1966). Neurosecretion and molting in some parasitic nematodes. *Am.Zool.* **6**, 243-249.

Davies, A. G., Bettinger, J. C., Thiele, T. R., Judy, M. E., & McIntire, S. L. (2004). Natural variation in the npr-1 gene modifies ethanol responses of wild strains of C. elegans. *Neuron* **42**, 731-743.

Davies, A. G., Pierce-Shimomura, J. T., Kim, H., VanHoven, M. K., Thiele, T. R., Bonci, A., Bargmann, C. I., & McIntire, S. L. (2003). A central role of the BK potassium channel in behavioral responses to ethanol in C. elegans. *Cell* **115**, 655-666.

Davis, R. E. & Stretton, A. O. (1989). Signaling properties of Ascaris motorneurons: graded active responses, graded synaptic transmission, and tonic transmitter release. *J.Neurosci.* **9**, 415-425.

Davletov, B. A., Krasnoperov, V., Hata, Y., Petrenko, A. G., & Sudhof, T. C. (1995). High affinity binding of alpha-latrotoxin to recombinant neurexin I alpha. *J Biol.Chem.* **270**, 23903-23905.

Davletov, B. A., Shamotienko, O. G., Lelianova, V. G., Grishin, E. V., & Ushkaryov, Y. A. (1996). Isolation and biochemical characterization of a Ca2+-independent alpha- latrotoxin-binding protein. *J.Biol.Chem.* **271**, 23239-23245.

Dent, J. A., Davis, M. W., & Avery, L. (1997). avr-15 encodes a chloride channel subunit that mediates inhibitory glutamatergic neurotransmission and ivermectin sensitivity in Caenorhabditis elegans. *EMBO J.* **16**, 5867-5879.

Dent, J. A., Smith, M. M., Vassilatis, D. K., & Avery, L. (2000). The genetics of ivermectin resistance in Caenorhabditis elegans. *Proc.Natl.Acad.Sci.U.S.A* **97**, 2674-2679.

Doi, M. & Iwasaki, K. (2002). Regulation of retrograde signaling at neuromuscular junctions by the novel C2 domain protein AEX-1. *Neuron* **33**, 249-259.

Doi, N., Zenno, S., Ueda, R., Ohki-Hamazaki, H., Ui-Tei, K., & Saigo, K. (2003). Short-interfering-RNA-mediated gene silencing in mammalian cells requires Dicer and eIF2C translation initiation factors. *Curr.Biol.* **13**, 41-46.

Filipov, A. K., Kobrinsky, E. M., Tsurupa, G. P., Pashkov, V. N., & Grishin, E. (1990). Expression of Receptor for α-latrotoxin in Xenopus oocytes after injection of mRNA from rat brain. *Neuroscience* **39**, 809-814.

Finklestein, A., Rubin, L. L., & Tzeng, M. C. (1976). Black widow Spider venom: Effect of Purified toxin lipid bilyaer membranes. *Science* **193**, 1009-1011.

Fire, A. (1999). RNA-triggered gene silencing. *Trends Genet.* **15**, 358-363.

Fraser, A. G., Kamath, R. S., Zipperlen, P., Martinez-Campos, M., Sohrmann, M., & Ahringer, J. (2000). Functional genomic analysis of C. elegans chromosome I by systematic RNA interference. *Nature* **408**, 325-330.

Frontali, N., Ceccarelli, B., Gorio, A., Mauro, A., Siekevitz, P., Tzeng, M. C., & Hurlbut, W. P. (1976). Purification from black widow spider venom of a protein factor causing the depletion of synaptic vesicles at neuromuscular junctions. *J Cell Biol.* **68**, 462-479.

Geary, T. G., Klein, R. D., Vanover, L., Bowman, J. W., & Thompson, D. P. (1992). The nervous systems of helminths as targets for drugs. *J Parasitol* **78**, 215-230.

Gebner, G., Meder, S., Rink, T., & Harder, A. (1996). Ionophore and anthelmintic activity of PF 1022A, a cyclooctadepsipeptide, are not related. *Pestic.Sci* **48**, 399-407.

Geerts and Gryseels. Anthelmintic resistance in human helminths: a review. Tropical Medicine and International Health 6[11], 915-921. 2001. Blackwell Science.
Ref Type: Generic

Geppert, M., Khvotchev, M., Krasnoperov, V., Goda, Y., Missler, M., Hammer, R. E., Ichtchenko, K., Petrenko, A. G., & Sudhof, T. C. (1998). Neurexin I alpha is a major alpha-latrotoxin receptor that cooperates in alpha-latrotoxin action. *J.Biol.Chem.* **273**, 1705-1710.

Geßner, G., Meder, S., Rink, T., Boheim, G., Harder, A., Jeschke, P., Scherkenbeck, J., & Londershausen, M. (1996). Ionophore and Anthelmintic Activity of PF1022A, a Cyclooctadepsipeptide, are not related. *Pesticide Science* **48**, 399-407.

Gillis, K. D., Mossner, R., & Neher, E. (1996). Protein kinase C enhances exocytosis from chromaffin cells by increasing the size of the readily releasable pool of secretory granules. *Neuron* **16**, 1209-1220.

Grant, S. R. (1999). Dissecting the mechanisms of posttranscriptional gene silencing: divide and conquer. *Cell* **96**, 303-306.

Grishin, E. V. (1998). Black widow spider toxins: the present and the future. *Toxicon* **36**, 1693-1701.

Harder, A. & Samson-Himmelstjerna, G. (2001). Activity of the cyclic depsipeptide emodepside (BAY 44-4400) against larval and adult stages of nematodes in rodents and the influence on worm survival. *Parasitol Res.* **87**, 924-928.

Harder, A. & Samson-Himmelstjerna, G. (2002a). Cyclooctadepsipeptides--a new class of anthelmintically active compounds. *Parasitol Res.* **88**, 481-488.

Harder, A. & Samson-Himmelstjerna, G. (2002b). Cyclooctadepsipeptides--a new class of anthelmintically active compounds. *Parasitol.Res.* **88**, 481-488.

Harris, J. E. & Crofton, H. D. (1957). Structure and function in the nematodes. Internal pressure and cuticular structure in *Ascaris*. *Journal of Experimental Biology* **34**, 116-130.

Harrow, I. D. & Gration, K. A. F. (1985). Mode of Action of the anthelmintis morantel, pyrantel and levamisole on the muscle cell membrane of the nematode *Ascaris suum*. *Pesticide Science* **16**, 672.

Hart, A. C., Sims, S., & Kaplan, J. M. (1995). Synaptic code for sensory modalities revealed by C. elegans GLR-1 glutamate receptor. *Nature* **378**, 82-85.

Hodgkin, J. (2001). What does a worm want with 20,000 genes? *Genome Biol.* **2**, COMMENT2008.

Holden-Dye, L., Franks, C. J., Williams, R. G., & Walker, R. J. (1995). The effect of the nematode peptides SDPNFLRFamide (PF1) and SADPNFLRFamide (PF2) on synaptic transmission in the parasitic nematode Ascaris suum. *Parasitology* **110** (**Pt 4**), 449-455.

Holden-Dye, L., Krogsgaard-Larsen, P., Nielsen, L., & Walker, R. J. (1989). GABA receptors on the somatic muscle cells of the parasitic nematode, Ascaris suum: stereoselectivity indicates similarity to a GABAA-type agonist recognition site. *Br.J.Pharmacol.* **98**, 841-850.

Horvitz, H. R., Chalfie, M., Trent, C., Sulston, J. E., & Evans, P. D. (1982). Serotonin and octopamine in the nematode Caenorhabditis elegans. *Science* **216**, 1012-1014.

Hurlbut, W. P., Chieregatti, E., Valtorta, F., & Haimann, C. (1994). Alpha-latrotoxin channels in neuroblastoma cells. *J.Membr.Biol.* **138**, 91-102.

Ichtchenko, K., Bittner, M. A., Krasnoperov, V., Little, A. R., Chepurny, O., Holz, R. W., & Petrenko, A. G. (1999). A novel ubiquitously expressed alpha-latrotoxin receptor is a member of the CIRL family of G-protein-coupled receptors. *J.Biol.Chem.* **274**, 5491-5498.

Ichtchenko, K., Khvotchev, M., Kiyatkin, N., Simpson, L., Sugita, S., & Sudhof, T. C. (1998). alpha-latrotoxin action probed with recombinant toxin: receptors recruit alpha-latrotoxin but do not transduce an exocytotic signal. *EMBO J.* **17**, 6188-6199.

Jacob, T. C. & Kaplan, J. M. (2003). The EGL-21 carboxypeptidase E facilitates acetylcholine release at Caenorhabditis elegans neuromuscular junctions. *J.Neurosci.* **23**, 2122-2130.

Jahn, R. & Sudhof, T. C. (1999). Membrane fusion and exocytosis. *Annu.Rev.Biochem.* **68**, 863-911.

Johnson, C. D. & Stretton, A. O. (1985). Localization of choline acetyltransferase within identified motoneurons of the nematode Ascaris. *J.Neurosci.* **5**, 1984-1992.

Johnstone, I. L. (1994). The cuticle of the nematode Caenorhabditis elegans: a complex collagen structure. *Bioessays* **16**, 171-178.

Kachi, S. & Terada, M. (1994). Effects of PF 1022A on Angiostrongylus cantonensis staying in the CNS of rats and mice. *Jpn.J.Parasitol* **43**, 483-488.

Kachi, S., Terada, M., & Hashimoto, H. (1998). Effects of amorphous and polymorphs of PF1022A, a new antinematode drug, on Angiostrongylus costaricensis in mice. *Jpn.J.Pharmacol.* **77**, 235-245.

Kaibuchi, K., Fukumoto, Y., Oku, N., Takai, Y., Arai, K., & Muramatsu, M. (1989). Molecular genetic analysis of the regulatory and catalytic domains of protein kinase C. *J Biol.Chem.* **264**, 13489-13496.

Kamath, R. S., Fraser, A. G., Dong, Y., Poulin, G., Durbin, R., Gotta, M., Kanapin, A., Le Bot, N., Moreno, S., Sohrmann, M., Welchman, D. P., Zipperlen, P., &

Ahringer, J. (2003). Systematic functional analysis of the Caenorhabditis elegans genome using RNAi. *Nature* **421**, 231-237.

Kenning, C., Kipping, I., & Sommer, R. J. (2004). Isolation of mutations with dumpy-like phenotypes and of collagen genes in the nematode Pristionchus pacificus. *Genesis.* **40**, 176-183.

Ketting, R. F., Fischer, S. E., Bernstein, E., Sijen, T., Hannon, G. J., & Plasterk, R. H. (2001). Dicer functions in RNA interference and in synthesis of small RNA involved in developmental timing in C. elegans. *Genes Dev.* **15**, 2654-2659.

Khvotchev, M. & Sudhof, T. C. (2000). alpha-latrotoxin triggers transmitter release via direct insertion into the presynaptic plasma membrane. *EMBO J* **19**, 3250-3262.

Kim, K. & Li, C. (2004). Expression and regulation of an FMRFamide-related neuropeptide gene family in Caenorhabditis elegans. *J.Comp Neurol.* **475**, 540-550.

Knight, S. W. & Bass, B. L. (2001). A role for the RNase III enzyme DCR-1 in RNA interference and germ line development in Caenorhabditis elegans. *Science* **293**, 2269-2271.

Koch, R., van Luenen, H. G., van der, H. M., Thijssen, K. L., & Plasterk, R. H. (2000). Single nucleotide polymorphisms in wild isolates of Caenorhabditis elegans. *Genome Res.* **10**, 1690-1696.

Kohn, R. E., Duerr, J. S., McManus, J. R., Duke, A., Rakow, T. L., Maruyama, H., Moulder, G., Maruyama, I. N., Barstead, R. J., & Rand, J. B. (2000). Expression of multiple UNC-13 proteins in the Caenorhabditis elegans nervous system. *Mol.Biol.Cell* **11**, 3441-3452.

Krasnoperov, V., Lu, Y., Buryanovsky, L., Neubert, T. A., Ichtchenko, K., & Petrenko, A. G. (2002). Post-translational proteolytic processing of the calcium-independent receptor of alpha-latrotoxin (CIRL), a natural chimera of the cell adhesion protein and the G protein-coupled receptor. Role of the G protein-coupled receptor proteolysis site (GPS) motif. *J Biol.Chem.* **277**, 46518-46526.

Krasnoperov, V. G., Beavis, R., Chepurny, O. G., Little, A. R., Plotnikov, A. N., & Petrenko, A. G. (1996). The calcium-independent receptor of alpha-latrotoxin is not a neurexin. *Biochem.Biophys.Res.Commun.* **227**, 868-875.

Krasnoperov, V. G., Bittner, M. A., Beavis, R., Kuang, Y., Salnikow, K. V., Chepurny, O. G., Little, A. R., Plotnikov, A. N., Wu, D., Holz, R. W., & Petrenko, A. G. (1997). alpha-Latrotoxin stimulates exocytosis by the interaction with a neuronal G-protein-coupled receptor. *Neuron* **18**, 925-937.

Lackner, M. R., Nurrish, S. J., & Kaplan, J. M. (1999). Facilitation of synaptic transmission by EGL-30 Gqalpha and EGL-8 PLCbeta: DAG binding to UNC-13 is required to stimulate acetylcholine release. *Neuron* **24**, 335-346.

Lee, C. H., Park, D., Wu, D., Rhee, S. G., & Simon, M. I. (1992). Members of the Gq alpha subunit gene family activate phospholipase C beta isozymes. *J Biol.Chem.* **267**, 16044-16047.

Lee, R. Y., Sawin, E. R., Chalfie, M., Horvitz, H. R., & Avery, L. (1999). EAT-4, a homolog of a mammalian sodium-dependent inorganic phosphate cotransporter, is necessary for glutamatergic neurotransmission in caenorhabditis elegans. *J.Neurosci.* **19**, 159-167.

Lelianova, V. G., Davletov, B. A., Sterling, A., Rahman, M. A., Grishin, E. V., Totty, N. F., & Ushkaryov, Y. A. (1997). Alpha-latrotoxin receptor, latrophilin, is a novel member of the secretin family of G protein-coupled receptors. *J.Biol.Chem.* **272**, 21504-21508.

Lewis, J. A., Wu, C. H., Berg, H., & Levine, J. H. (1980a). The genetics of levamisole resistance in the nematode Caenorhabditis elegans. *Genetics* **95**, 905-928.

Lewis, J. A., Wu, C. H., Levine, J. H., & Berg, H. (1980b). Levamisole-resistant mutants of the nematode Caenorhabditis elegans appear to lack pharmacological acetylcholine receptors. *Neuroscience* **5**, 967-989.

Li, C. & Chalfie, M. FMRFamide-like immunoreactivity in *C.elegans*. Society for Neuroscience Abstracts 12, 246. 1986.
Ref Type: Generic

Li, C., Kim, K., & Nelson, L. S. (1999a). FMRFamide-related neuropeptide gene family in Caenorhabditis elegans. *Brain Res.* **848**, 26-34.

Li, C., Nelson, L. S., Kim, K., Nathoo, A., & Hart, A. C. (1999b). Neuropeptide gene families in the nematode Caenorhabditis elegans. *Ann.N.Y.Acad.Sci.* **897**, 239-252.

Li, L. & Chin, L. S. (2003). The molecular machinery of synaptic vesicle exocytosis. *Cell Mol.Life Sci.* **60**, 942-960.

Liu, J. & Misler, S. (1998). alpha-Latrotoxin alters spontaneous and depolarization-evoked quantal release from rat adrenal chromaffin cells: evidence for multiple modes of action. *J Neurosci.* **18**, 6113-6125.

Loer, C. M. & Kenyon, C. J. (1993). Serotonin-deficient mutants and male mating behavior in the nematode Caenorhabditis elegans. *J.Neurosci.* **13**, 5407-5417.

Mackenstedt, U., Schmidt, S., Mehlhorn, H., Stoye, M., & Traeder, W. (1993). Effects of pyrantel pamoate on adult and preadult Toxocara canis worms: an electron microscope and autoradiography study. *Parasitol.Res.* **79**, 567-578.

Martin, R. J. (1980). The effect of gamma-aminobutyric acid on the input conductance and membrane potential of Ascaris muscle. *Br.J.Pharmacol.* **71**, 99-106.

Martin, R. J. (1982). Electrophysiological effects of piperazine and diethylcarbamazine on Ascaris suum somatic muscle. *Br.J Pharmacol.* **77**, 255-265.

Martin, R. J. (1997). Modes of action of anthelmintic drugs. *Vet.J.* **154**, 11-34.

Martin, R. J. & Harder, A. (1996). Anthelmintic actions of the Cyclic Depsipeptide PF 1022A and its electrophysiological effects on muscle cells of *Ascais suum. Pestic.Sci* **48**, 343-349.

Martin, R. J., Harder, A., Londershausen, M., & Jeschke, P. (1996). Anthelmintic Actions of the Cyclic Depsipeptide Pf1022A and its Electrophysiological Effects on Muscle Cells of *Ascaris suum. Pesticide Science* **48**, 343-349.

Martin, R. J., Pennington, A. J., Duittoz, A. H., Robertson, S., & Kusel, J. R. (1991). The physiology and pharmacology of neuromuscular transmission in the nematode parasite, Ascaris suum. *Parasitology* **102 Suppl**, S41-S58.

Martin, R. J. & Valkanov, M. A. (1996). Effects of acetylcholine on a slow voltage-activated non-selective cation current mediated by non-nicotinic receptors on isolated Ascaris muscle bags. *Exp.Physiol* **81**, 909-925.

Maruyama, I. N. & Brenner, S. (1991). A phorbol ester/diacylglycerol-binding protein encoded by the unc-13 gene of Caenorhabditis elegans. *Proc.Natl.Acad.Sci.U.S.A* **88**, 5729-5733.

Mastwal. The function and evolution of Latrophilins and Celsr, G-protein coupled receptors of the secretin family that are conserved in *C.elegans*, *Drosophila* and vertebrates. East Coast Worm Meeting abstract 149-Personal Communication . Ref Type: Generic

Matsushita, H., Lelianova, V. G., & Ushkaryov, Y. A. (1999). The latrophilin family: multiply spliced G protein-coupled receptors with differential tissue distribution. *FEBS Lett.* **443**, 348-352.

Maule, A. G., Bowman, J. W., Thompson, D. P., Marks, N. J., Friedman, A. R., & Geary, T. G. (1996). FMRFamide-related peptides (FaRPs) in nematodes: occurrence and neuromuscular physiology. *Parasitology* **113 Suppl**, S119-S135.

Maule, A. G., Geary, T. G., Bowman, J. W., Marks, N. J., Blair, K. L., Halton, D. W., Shaw, C., & Thompson, D. P. (1995). Inhibitory effects of nematode FMRFamide-related peptides (FaRPs) on muscle strips from Ascaris suum. *Invert.Neurosci.* **1**, 255-265.

McIntire, S. L., Jorgensen, E., & Horvitz, H. R. (1993). Genes required for GABA function in Caenorhabditis elegans. *Nature* **364**, 334-337.

Mendel, J. E., Korswagen, H. C., Liu, K. S., Hajdu-Cronin, Y. M., Simon, M. I., Plasterk, R. H., & Sternberg, P. W. (1995). Participation of the protein Go in multiple aspects of behavior in C. elegans. *Science* **267**, 1652-1655.

Miller, K. G., Alfonso, A., Nguyen, M., Crowell, J. A., Johnson, C. D., & Rand, J. B. (1996). A genetic selection for Caenorhabditis elegans synaptic transmission mutants. *Proc.Natl.Acad.Sci.U.S.A* **93**, 12593-12598.

Miller, K. G., Emerson, M. D., & Rand, J. B. (1999). Goalpha and diacylglycerol kinase negatively regulate the Gqalpha pathway in C. elegans. *Neuron* **24**, 323-333.

Missler, M. & Sudhof, T. C. (1998). Neurexins: three genes and 1001 products. *Trends Genet.* **14**, 20-26.

Missler, M., Zhang, W., Rohlmann, A., Kattenstroth, G., Hammer, R. E., Gottmann, K., & Sudhof, T. C. (2003). Alpha-neurexins couple Ca2+ channels to synaptic vesicle exocytosis. *Nature* **424**, 939-948.

Napoli, A., van der, O. J., Sensen, C. W., Charlebois, R. L., Rossi, M., & Ciaramella, M. (1999). An Lrp-like protein of the hyperthermophilic archaeon Sulfolobus solfataricus which binds to its own promoter. *J.Bacteriol.* **181**, 1474-1480.

Nelson, L. S., Kim, K., Memmott, J. E., & Li, C. (1998a). FMRFamide-related gene family in the nematode, Caenorhabditis elegans. *Brain Res.Mol.Brain Res.* **58**, 103-111.

Nelson, L. S., Rosoff, M. L., & Li, C. (1998b). Disruption of a neuropeptide gene, flp-1, causes multiple behavioral defects in Caenorhabditis elegans. *Science* **281**, 1686-1690.

Nguyen, M., Alfonso, A., Johnson, C. D., & Rand, J. B. (1995). Caenorhabditis elegans mutants resistant to inhibitors of acetylcholinesterase. *Genetics* **140**, 527-535.

Nicolay, F., Harder, A., Samson-Himmelstjerna, G., & Mehlhorn, H. (2000). Synergistic action of a cyclic depsipeptide and piperazine on nematodes. *Parasitol.Res.* **86**, 982-992.

Nonet, M. L., Grundahl, K., Meyer, B. J., & Rand, J. B. (1993). Synaptic function is impaired but not eliminated in C. elegans mutants lacking synaptotagmin. *Cell* **73**, 1291-1305.

Nurrish, S., Segalat, L., & Kaplan, J. M. (1999). Serotonin inhibition of synaptic transmission: Galpha(0) decreases the abundance of UNC-13 at release sites. *Neuron* **24**, 231-242.

Orlova, E. V., Rahman, M. A., Gowen, B., Volynski, K. E., Ashton, A. C., Manser, C., van Heel, M., & Ushkaryov, Y. A. (2000). Structure of alpha-latrotoxin oligomers reveals that divalent cation-dependent tetramers form membrane pores. *Nat.Struct.Biol.* **7**, 48-53.

Pallotta, B. S., Magleby, K. L., & Barrett, J. N. (1981). Single channel recordings of Ca2+-activated K+ currents in rat muscle cell culture. *Nature* **293**, 471-474.

Parri, H. R., Holden-Dye, L., & Walker, R. J. (1991). Studies on the ionic selectivity of the GABA-operated chloride channel on the somatic muscle bag cells of the parasitic nematode Ascaris suum. *Exp.Physiol* **76**, 597-606.

Pashkov, V., Grico, N., Tsurupa, G., Storchak, L., Shatursky, O., Himmerlreich, N., & Grishin, E. (1993). Monoclonal antibodies can uncouple the main alpha-latrotoxin effects: toxin-induced Ca2+ influx and stimulated neurotransmitter release. *Neuroscience* **56**, 695-701.

Petkov, G. V., Bonev, A. D., Heppner, T. J., Brenner, R., Aldrich, R. W., & Nelson, M. T. (2001). Beta1-subunit of the Ca2+-activated K+ channel regulates contractile activity of mouse urinary bladder smooth muscle. *J.Physiol* **537**, 443-452.

Petrenko, A. G., Kovalenko, V. A., Shamotienko, O. G., Surkova, I. N., Tarasyuk, T. A., Ushkaryov, Y., & Grishin, E. V. (1990). Isolation and properties of the alpha-latrotoxin receptor. *EMBO J.* **9**, 2023-2027.

Rahman, M. A., Ashton, A. C., Meunier, F. A., Davletov, B. A., Dolly, J. O., & Ushkaryov, Y. A. (1999). Norepinephrine exocytosis stimulated by alpha-latrotoxin requires both external and stored Ca2+ and is mediated by latrophilin, G proteins and phospholipase C. *Philos.Trans.R.Soc.Lond B Biol.Sci.* **354**, 379-386.

Reinitz, C. A., Herfel, H. G., Messinger, L. A., & Stretton, A. O. (2000a). Changes in locomotory behavior and cAMP produced in Ascaris suum by neuropeptides from Ascaris suum or Caenorhabditis elegans. *Mol.Biochem.Parasitol.* **111**, 185-197.

Reinitz, C. A., Herfel, H. G., Messinger, L. A., & Stretton, A. O. (2000b). Changes in locomotory behavior and cAMP produced in Ascaris suum by neuropeptides from Ascaris suum or Caenorhabditis elegans. *Mol.Biochem.Parasitol.* **111**, 185-197.

Rew, R. S., Urban, J. F., Jr., & Douvres, F. W. (1986). Screen for anthelmintics, using larvae of Ascaris suum. *Am.J.Vet.Res.* **47**, 869-873.

Rhee, J. S., Betz, A., Pyott, S., Reim, K., Varoqueaux, F., Augustin, I., Hesse, D., Sudhof, T. C., Takahashi, M., Rosenmund, C., & Brose, N. (2002). Beta phorbol ester- and diacylglycerol-induced augmentation of transmitter release is mediated by Munc13s and not by PKCs. *Cell* **108**, 121-133.

Richmond, J. E. & Broadie, K. S. (2002). The synaptic vesicle cycle: exocytosis and endocytosis in Drosophila and C. elegans. *Curr.Opin.Neurobiol.* **12**, 499-507.

Richmond, J. E., Davis, W. S., & Jorgensen, E. M. (1999). UNC-13 is required for synaptic vesicle fusion in C. elegans. *Nat.Neurosci.* **2**, 959-964.

Richmond, J. E., Weimer, R. M., & Jorgensen, E. M. (2001). An open form of syntaxin bypasses the requirement for UNC-13 in vesicle priming. *Nature* **412**, 338-341.

Riddle, D. L. (1997). *C. elegans II* Cold Spring Harbor Laboratory Press, Plainview, N.Y.

Rogers, W. P. (1968). Neurosecretory granules in the infective stage of Haemonchus contortus. *Parasitology* **58**, 657-662.

Rosoff, M. L., Burglin, T. R., & Li, C. (1992). Alternatively spliced transcripts of the flp-1 gene encode distinct FMRFamide-like peptides in Caenorhabditis elegans. *J.Neurosci.* **12**, 2356-2361.

Saeger, B., Schmitt-Wrede, H. P., Dehnhardt, M., Benten, W. P., Krucken, J., Harder, A., Samson-Himmelstjerna, G., Wiegand, H., & Wunderlich, F. (2001). Latrophilin-like receptor from the parasitic nematode Haemonchus contortus as target for the anthelmintic depsipeptide PF1022A. *FASEB J.* **15**, 1332-1334.

Saibil, H. R. (2000). The black widow's versatile venom. *Nat.Struct.Biol.* **7**, 3-4.

Samson-Himmelstjerna, G., Harder, A., Schnieder, T., Kalbe, J., & Mencke, N. (2000). In vivo activities of the new anthelmintic depsipeptide PF 1022A. *Parasitol.Res.* **86**, 194-199.

Sangster, N. C. (2001). Managing parasiticide resistance. *Vet.Parasitol.* **98**, 89-109.

Sangster, N. C., Davis, C. W., & Collins, G. H. (1991). Effects of cholinergic drugs on longitudinal contraction in levamisole-susceptible and -resistant Haemonchus contortus. *Int.J.Parasitol.* **21**, 689-695.

Sangster, N. C. & Gill, J. (1999). Pharmacology of Anthelmintic Resistance. *Parasitology Today* **15**, 141-146.

Sangster, N. C., Riley, F. L., & Wiley, L. J. (1998). Binding of [3H]m-aminolevamisole to receptors in levamisole-susceptible and -resistant Haemonchus contortus. *Int.J.Parasitol.* **28**, 707-717.

Schafer, W. R. (2002). Genetic analysis of nicotinic signaling in worms and flies. *J.Neurobiol.* **53**, 535-541.

Scheller, R. H. (1995). Membrane trafficking in the presynaptic nerve terminal. *Neuron* **14**, 893-897.

Sedgwick, S. G. & Smerdon, S. J. (1999). The ankyrin repeat: a diversity of interactions on a common structural framework. *Trends Biochem.Sci.* **24**, 311-316.

Shoop, W. L., Haines, H. W., Michael, B. F., & Eary, C. H. (1993). Mutual resistance to avermectins and milbemycins: oral activity of ivermectin and moxidectin against ivermectin-resistant and susceptible nematodes. *The Veterinary Record* **133**, 445-447.

Sijen, T., Fleenor, J., Simmer, F., Thijssen, K. L., Parrish, S., Timmons, L., Plasterk, R. H., & Fire, A. (2001). On the role of RNA amplification in dsRNA-triggered gene silencing. *Cell* **107**, 465-476.

Simmer, F., Tijsterman, M., Parrish, S., Koushika, S. P., Nonet, M. L., Fire, A., Ahringer, J., & Plasterk, R. H. (2002). Loss of the putative RNA-directed RNA polymerase RRF-3 makes C. elegans hypersensitive to RNAi. *Curr.Biol.* **12**, 1317-1319.

Stepek, G., Behnke, J. M., Buttle, D. J., & Duce, I. R. (2004). Natural plant cysteine proteinases as anthelmintics? *Trends Parasitol.* **20**, 322-327.

Stevens, C. F. & Sullivan, J. M. (1998). Regulation of the readily releasable vesicle pool by protein kinase C. *Neuron* **21**, 885-893.

Stretton, A. O., Cowden, C., Sithigorngul, P., & Davis, R. E. (1991). Neuropeptides in the nematode Ascaris suum. *Parasitology* **102 Suppl**, S107-S116.

Stretton, A. O., Fishpool, R. M., Southgate, E., Donmoyer, J. E., Walrond, J. P., Moses, J. E., & Kass, I. S. (1978). Structure and physiological activity of the motoneurons of the nematode Ascaris. *Proc.Natl.Acad.Sci.U.S.A* **75**, 3493-3497.

Sudhof, T. C. (1995). The synaptic vesicle cycle: a cascade of protein-protein interactions. *Nature* **375**, 645-653.

Sudhof, T. C. (2001). alpha-Latrotoxin and its receptors: neurexins and CIRL/latrophilins. *Annu.Rev.Neurosci.* **24**, 933-962.

Sugita, S., Ichtchenko, K., Khvotchev, M., & Sudhof, T. C. (1998). alpha-Latrotoxin receptor CIRL/latrophilin 1 (CL1) defines an unusual family of ubiquitous G-protein-linked receptors. G-protein coupling not required for triggering exocytosis. *J.Biol.Chem.* **273**, 32715-32724.

Sugita, S., Khvochtev, M., & Sudhof, T. C. (1999). Neurexins are functional alpha-latrotoxin receptors. *Neuron* **22**, 489-496.

Tabara, H., Sarkissian, M., Kelly, W. G., Fleenor, J., Grishok, A., Timmons, L., Fire, A., & Mello, C. C. (1999). The rde-1 gene, RNA interference, and transposon silencing in C. elegans. *Cell* **99**, 123-132.

Tabara, H., Yigit, E., Siomi, H., & Mello, C. C. (2002). The dsRNA binding protein RDE-4 interacts with RDE-1, DCR-1, and a DExH-box helicase to direct RNAi in C. elegans. *Cell* **109**, 861-871.

Taylor, S. J. & Exton, J. H. (1991). Two alpha subunits of the Gq class of G proteins stimulate phosphoinositide phospholipase C-beta 1 activity. *FEBS Lett.* **286**, 214-216.

Terada, M. (1992). Neuropharmacological mechanism of action of PF1022A, an antinematode anthelmintic with a new structure of cyclodepsipeptide, on *Angiostrongylus cantonensis* and isolated frog rectus. *Jpn J Parasitol* **32**, 633-642.

The C.elegans Sequencing Consortium (1998). Genome sequence of the nematode C. elegans: a platform for investigating biology. *Science* **282**, 2012-2018.

Timmons, L. & Fire, A. (1998). Specific interference by ingested dsRNA. *Nature* **395**, 854.

Timmons, L., Tabara, H., Mello, C. C., & Fire, A. Z. (2003). Inducible systemic RNA silencing in Caenorhabditis elegans. *Mol.Biol.Cell* **14**, 2972-2983.

Trent, C., Tsuing, N., & Horvitz, H. R. (1983). Egg-laying defective mutants of the nematode Caenorhabditis elegans. *Genetics* **104**, 619-647.

Umbach, J. A., Grasso, A., & Gundersen, C. B. (1990). Alpha-latrotoxin triggers an increase of ionized calcium in Xenopus oocytes injected with rat brain mRNA. *Brain Res.Mol.Brain Res.* **8**, 31-36.

Ushkaryov, Y. (2002). Alpha-latrotoxin: from structure to some functions. *Toxicon* **40**, 1-5.

Ushkaryov, Y. A., Petrenko, A. G., Geppert, M., & Sudhof, T. C. (1992). Neurexins: synaptic cell surface proteins related to the alpha- latrotoxin receptor and laminin. *Science* **257**, 50-56.

Ushkaryov, Y. A., Volynski, K. E., & Ashton, A. C. (2004). The multiple actions of black widow spider toxins and their selective use in neurosecretion studies. *Toxicon* **43**, 527-542.

Vassilatis, D. K., Arena, J. P., Plasterk, R. H., Wilkinson, H. A., Schaeffer, J. M., Cully, D. F., & Van der Ploeg, L. H. (1997). Genetic and biochemical evidence for a novel avermectin-sensitive chloride channel in Caenorhabditis elegans. Isolation and characterization. *J.Biol.Chem.* **272**, 33167-33174.

Waggoner, L. E., Hardaker, L. A., Golik, S., & Schafer, W. R. (2000). Effect of a neuropeptide gene on behavioral states in Caenorhabditis elegans egg-laying. *Genetics* **154**, 1181-1192.

Walker, D. S., Gower, N. J., Ly, S., Bradley, G. L., & Baylis, H. A. (2002). Regulated disruption of inositol 1,4,5-trisphosphate signaling in Caenorhabditis

elegans reveals new functions in feeding and embryogenesis. *Mol.Biol.Cell* **13**, 1329-1337.

Walker, R. J., Colquhoun, L., & Holden-Dye, L. (1992). Pharmacological profiles of the GABA and acetylcholine receptors from the nematode, Ascaris suum. *Acta Biol.Hung.* **43**, 59-68.

Walker, R. J., Franks, C. J., Pemberton, D., Rogers, C., & Holden-Dye, L. (2000). Physiological and pharmacological studies on nematodes. *Acta Biol.Hung.* **51**, 379-394.

Wang, Z. W., Saifee, O., Nonet, M. L., & Salkoff, L. (2001). SLO-1 potassium channels control quantal content of neurotransmitter release at the C. elegans neuromuscular junction. *Neuron* **32**, 867-881.

Wanke, E., Ferroni, A., Gattanini, P., & Meldolesi, J. (1986). alpha Latrotoxin of the black widow spider venom opens a small, non-closing cation channel. *Biochem.Biophys.Res.Commun.* **134**, 320-325.

Weber, T., Zemelman, B. V., McNew, J. A., Westermann, B., Gmachl, M., Parlati, F., Sollner, T. H., & Rothman, J. E. (1998). SNAREpins: minimal machinery for membrane fusion. *Cell* **92**, 759-772.

White, J. G., Southgate, E., Thomas, E. M., & Brenner, S. (1986). The structure of the nervous system of the nematode *C.elegans. Philosophical Transactions of the Royal Society of London.Series B, Biological Sciences,* **314**, 1-340.

White, J. G., Southgate, E., Thomson, J. N., & Brenner, S. (1983). Factors that determine connectivity in the nervous system of Caenorhabditis elegans. *Cold Spring Harb.Symp.Quant.Biol.* **48 Pt 2**, 633-640.

Willson, J., Amliwala, K., Davis, A., Cook, A., Cuttle, M. F., Kriek, N., Hopper, N. A., O'Connor, V., Harder, A., Walker, R. J., & Holden-Dye, L. (2004). Latrotoxin Receptor Signaling Engages the UNC-13-Dependent Vesicle-Priming Pathway in C. elegans. *Curr.Biol.* **14**, 1374-1379.

Willson, J., Amliwala, K., Harder, A., Holden-Dye, L., & Walker, R. J. (2003). The effect of the anthelmintic emodepside at the neuromuscular junction of the parasitic nematode Ascaris suum. *Parasitology* **126**, 79-86.

Winston, W. M., Molodowitch, C., & Hunter, C. P. (2002). Systemic RNAi in C. elegans requires the putative transmembrane protein SID-1. *Science* **295**, 2456-2459.

Zahner, H., Taubert, A., Harder, A., & Samson-Himmelstjerna, G. (2001). Effects of Bay 44-4400, a new cyclodepsipeptide, on developing stages of filariae (Acanthocheilonema viteae, Brugia malayi, Litomosoides sigmodontis) in the rodent Mastomys coucha. *Acta Trop.* **80**, 19-28.

Appendix 1

C. elegans Strain	Gene/Allele	Obtained From	Description
DA1051	*avr-15/ad501*	Joe Dent	*avr-15* encodes, via alternative splicing, two glutamate-gated chloride channel α-2 subunit homologs.
PS211	*dpy-20 /e1282*	N. Hopper	*dpy-20* encodes a zinc finger protein, with no known homologs outside of nematodes, that is required for normal body morphology.
RM2221	*egl-8/ md1971*	CGC	Encodes a phospholipase C beta homolog.
MT1083	*egl-8/ n488*	CGC	Encodes a phospholipase C beta homolog.
MT1071	*egl-21/ n476*	CGC	Encodes zinc carboxypeptidase.
DA1096	*egl-30/ ad810*	CGC	Encodes an ortholog of the heterotrimeric G protein alpha subunit Gq (Gq/G11 class).
MT1434	*egl-30/ n686*	CGC	Encodes an ortholog of the heterotrimeric G protein alpha subunit Gq (Gq/G11 class).
KY26	*egl-30 (gf)/ tg26*	Dr K Iwasaki	Encodes an ortholog of the heterotrimeric G protein alpha subunit Gq (Gq/G11 class).
MT2426	*goa-1/ n1134*	Lauren Segalat	Encodes an alpha subunit of G protein (G alpha o).

RB629	*lat-1/ ok379*	Oklahoma Med. Res. Found	*lat-1* encodes a predicted latrophilin that affects embryonic elongation, pharyngeal development, and reproductive organ formation; apically localized in developing epithelia and localized to presynaptic surfaces in neurons.
VC158	*lat-2 /ok301*	CGC	*lat-2* encodes a predicted transmembrane protein that is homologous to vertebrate latrophilins. LAT-2 is predicted to function as a peptide hormone receptor that couples ligand binding to heterotrimeric G protein-mediated stimulation of secretion; lat-2 is expressed in the g1 gland cells and in the arcade cells in the head, and its expression has been reported to cycle with larval molts.
NL2099	*rrf-3 /pk1426*	CGC	Encodes an RNA-directed RNA polymerase. Increased sensitivity to RNAi when compared to Wild type animals.

NM1968	*slo-1/ js379*	CGC	Encodes Ca^{2+}-activated K^+ channel Slowpoke, alpha subunit. *slo-1* mutants have wild-type levels of motor activity, but have less smooth movement and tend to stop and reverse direction.
CX3933	*slo-1 (gf)/ ky389*	CGC	Encodes Ca^{2+}-activated K^+ channel Slowpoke, alpha subunit.
ZZ20	*unc-38/ x20*	CGC	*unc-38* encodes an alpha subunit of the nicotinic acetylcholine receptor (nAChR) superfamily; UNC-38 is required for normal locomotion and egg-laying, and functions as a subunit of a ligand-gated ion channel that likely mediates fast actions of acetylcholine at neuromuscular junctions and in the nervous system.
Wild Type (Hawaiian CB4856)	-	CGC	Isolated in Hawaii.
Wild Type Bristol N2)	-	CGC	Isolated from mushroom compost near Bristol, England.

CGC Caenorhabditis Genetics Centre.

Appendix 2

RNAi Oligonucleotide Primer Description	Sequence 5'---3'
B0457.1 (*lat-1*) Forward	CGTTCCATCCAACATCAACTG
B0457.1 (*lat-1*) Reverse	CCATTCCATAAAGCGGCTGAC
B0286.2 (*lat-2*) Forward	ATTCCAGGCATGGACAGAAC
B0286.2 (*lat-2*) Reverse	CTCGATTTCGTTGTTGCTCA
FLP-13 Forward	CTCTGCTCTACCAAGTAGGGT
FLP-13 Reverse	AAATGAAGTACAGATATCACG

SNP Oligonucleotide Primer Description	Sequence 5'---3'
AC3 Forward	CTCTTAGATACCCTTTCTGCGC
AC3 Reverse	TTCAGCGTTTGGTCTGACGTAG
B0379 Forward	AGTCTTCTGCTTCTGCTCAACACC
B0379 Reverse	CAAAACTACACGAGCCACATAGTGC
C13D9 Forward	TTCGCAGTTCACTCTTGTGCTC
C13D9 Reverse	GGCCAAATTCTCCGTTTCAC
F57G8 Forward	AGCTGCAACCAACACTGCTC
F57G8 Reverse	GGCGGAAAGCAATTTCTATC
F21D9 Forward	GTGTCGATTTTCTTGTATGGC
F21D9 Reverse	GTACTACAGCCATATCCCCTTC
F48F5 Forward	ATGCTCTTCACATTTTCCTGG
F48F5 Reverse	GCTTTGGAGACATTGAGCCGTG
F38A6 Forward	TTTATCCGCAGGGACTTGAC
F38A6 Reverse	TCTCCTCTCCCTCATGGTTAAC
F15D4 Forward	TTCCCATTTTCCTCCCAG

F15D4 Reverse	TCAAAAACCCAGACACTGG
F42A6 Forward	ACTTTCAGCTGCTCGTACTCTC
F42A6 Reverse	TCTGCCTTTTCACTTGCC
H04J21 Forward	GAGAAGAATGAGCAGAGCG
H04J21 Reverse	AAAGTTCGGCCACCTATC
K08F4b Forward	AGTATAGAGTTGAGTTGTTG
K08F4b Reverse	TTGTCGCAACAACTGGAATAC
M162 Forward	GACTTTTCGGATTGTCCATCAG
M162 Reverse	GACTTTTCGGATTGTCCATCAG
T09F5 Forward	GCACACAAATGATACCACGC
T09F5 Reverse	CTTAAAGCGCTGCAGAAAGC
T27C5 Forward	TTCGGTGACGTCCTTTTC
T27C5 Reverse	TCAGTTACAAACCACCCGAC
T13C2 Forward	TCCACACTATTTCCCTCGTG
T13C2 Reverse	GAGCAATCAAGAACCGGATC
T28D6 Forward	TTTCGTGTACGAACGTCTCC
T28D6 Reverse	CATTTCTCCCACTCTTGCTG
W03D8 Forward	CGAACTTTTATCCGTCACCG
W03D8 Reverse	CACCCCAATTAATCTGTGCG
Y51A2d Forward	CAGGCATATTACATGGGATAGG
Y51A2d Forward	CAATCTCACCTCCATTCTGTG
Y41E3 Forward	GCGTTACCCTACTTATGTCCAC
Y41E3 Reverse	AAGTAGCTTCGTAACTGCGC
ZK470 Forward	CCAAAACGGCCAAGTATCAG
ZK470 Reverse	TTGCACTCTTTCTCCTTCCG

lat-1 (ok379) **nested oligonuleotides for deletion detection (R. Barstead)**	**Sequence 5'---3'**
OUTER FORWARD	CTCCTAGCAAACTCGCCAA
OUTER REVERSE	CTTTTCTATCTTGCCGCCTG
INNER FORWARD	AACATCGTGACGACATGGA
INNER REVERSE	GAAGTGGACATCTCGGGAA

Nested oligonuleotides for *slo-1* cDNA amplification by RT-PCR	**Sequence 5'---3'**
OUTER FORWARD	GGTGGACCCTTCGTCGACACG
OUTER REVERSE	AAAATCGGATAAAATTAGGCC
INNER FORWARD	ATGGGCGAGATTTACTCGCCT
INNER REVERSE	CTAAAAGTGTCGTTTGCCCGG

Sequencing Oligonucleotide Primer Description	**Sequence 5'---3'**
lat-1 (ok379) Forward	GATGACGCGTGTCCAATGATG
lat-1 (ok379) Reverse	CTCGTGGATGAATACTCTGAA
slo-1 cDNA 0	ATGGGCGAGATTTACTCGCCT
slo-1 cDNA 1	GGACTGGGCTGGCGAGCTGAT
slo-1 cDNA 2	ACATTCTACAGTACCTCAACA
slo-1 cDNA 3	AAGCACATAGTGGTCTGTGGC
slo-1 cDNA 4	GGCCTACCTTCTAAATATCCC
slo-1 cDNA 5	TCATCCAGCCTCAAACTCAAG
slo-1 cDNA 6	AATTCGATGAGTATTCCGCCA

slo-1 cDNA 7	GCTATCTCGAGCAGATTTACG
slo-1 cDNA 8	TCGCCATTTCAGTGTTGGATT
slo-1 cDNA 9	AGGATTAAAAATACTGATTAC

Appendix 3

SNIP-SNP linkage of Emo 35 resistant *C. elegans* to chromosome V.

	Chrom I		Chrom II		Chrom III		Chrom IV		Chrom V		X
	W03D8		T13C2		T28D6		K08F4b		AC3		ZK470
SAMPLE 1	N		N		N		N		N		N
2	C		C		C		C		C		C
3	H		H		C		C		N		H
4			H						N		
5	N		H		H		H		C		H
6	H		N		C		H		N		N
7	H		N		H				N		H
8	N		H		H		H		N		H
9	N		H		H		C		N		N
10	N		H		H		N		N		H
11	N		H		H		C		N		H
12	N										
13	H		H		H		H		N		N
14											

				Chrom V									
	C13D9			AC3		T09F5	F57G8	T27C5	Y51A2d	F21D9	M162	F48F5	F38A6
POSITION	-6.16			2.53		7.45	11.54	15.35	19.34	21.82	23.62	25.95	27.08
1	C			N									
2				C		H	N	N	N	N	N	N	
3	C			N		N	N	N	N	N	N	N	
4	H			N						N		N	
5				C		N	N	N	N	H	H	H	H
6	N			N									
7				N		N	N		N		N	N	N
8	N			N		N	N	N	N	N	N		
9	N			N		N	N	N	N	N	N	N	
10	N			N		N	N	N	N	H	N	H	
11	N			N		N	N	N	N	N	N	N	
12	C					N	N	N	N	N	N	N	
13	N			N		N	N	N	N	N	N	N	
14	N									N		N	
15													
16				N			N			N	N	N	
17				N		N	N	N	N	N	N	N	N
18							N	N	N	N	N		
19				N		N	N	N	N	H	H	H	H
20				N		N	N	N	N	N	N	N/H	N
21						N	N	N	N	H	H	H	H
22						N							
23				N		N	N						
24						N	N	N	N		N	N	
25				N		N	N	N	N	N	N	N	
26				N		N	N	N	N		N	N	N
27				N			N		N	N	N	N	
28				N		N							
29							N			N			
30						N	N	N	N	N	N	N	
31						N	N	N	N		N	N	N
32				N		N	N	N	N	N	N	N	N
33													
34						N	N	N	N	N	N	N	
35				N		N							
36				N			N						
37													
38				H		N							
39						N	N						
40						N	N	N	N	N	N	N	
41						N	N	N	N	N	N	N	N
42						N	N	N	N	N	N	N	N
43													
44				C		N					N		
45				N		N							
46				N		N	N	N		N	N	N	
47													
48				H		N	N	N		N	N	N	
49				N						N	N		
50						N	N	N	N	N	N	N	
51						N	N						
52						N	N	N	N	N	N	N	N
53						N	N	N	N	N	N	N	N
54						H	N	N	N		N	N	N
55				N			N						
56				H		H	N		N	N	N	N	
57						N	N	N	N	N	N	N	
58				N		N	N	N	N		N	N	
59						N	N		N	N	N	N	
60				N		N	N	N	N		N	H	
61						H	H	N	N		H	H	
62						N	N	N	N	N	N	N	
63													
64						N	N	N	N	N	N	N	N
65							N						
66						N	N	N	N	N	N	N	
67						N	H	H	H	H	H	H	
68						H	N	H	N		N	N	
69							C						
70						N	N	N	N	N	N	N	N
71							N			N	N	N	
72						H	H	H	N	N	N	N	
73						N	N		N	N	N	N	
74							H						
75						C	H	H	C		H	H	H/C
76						N	N	N	N	N	N	N	N
77						N	H						
78						N	N	N	N	N	N	N	N
79						N	N	N	N		N	N	
80							N				N		
81										N	N	N	
82						N	H/N	N	N	N	N	N	H/N
83						N	N	N	N	N	N	N	
84						N	N	N	N	N	N	N	
85							N			N		N	
86						N	N	N		N	N	N	N
87						N	H	N	N	N	N	N	
88						N	N	N	N	H	N	H	H
89						N		H	N	N	N	N	
90							N						
91						N	N	N		N	N	N	
92						N	N	N	N	N	N	N	
93						N	N	N	N	N		N	N
94						N	N	N	N	N	N	N	
95							N	H	N		H		
96						H		C	N	N	N		

SNIP-SNP analysis of Emo 35 chromosome V.

SNIP-SNP linkage of Emo 48 resistant *C. elegans* to chromosome V.

	Chrom I		Chrom II		Chrom III		Chrom IV		Chrom V		X
	W03D8		T13C2		T28D6		F42A6		AC3		ZK470
SAMPLE 1	H		H		N		C		N		N
2	N		N		N		H		N		N
3	N		C		H		H		N		H
4	H		C		C		C		N		H
5	H		H		H		C		N		H
6	H				C		H		H		C
7	H		H		N		H		N		N
8	H		N		H		H		N		N
9	H		H		H		C		N		N
10	H		H		C		N		N		N
11	H		H		N		C		N		H
12	H		N		H		H		N		H
13	H		H		H				H		H
14	H		H		N				C		H

SNIP-SNP analysis of Emo 48 chromosome V.

					Chrom V					
					AC3	TC27C5		Y52A2d		F48F5
POSITION					2.53	15.53		19.34		25.95
SAMPLE 1					N	N		N		N
2					N	N		N		N
3					N	N		N		N
4					N	H		N		H
5					N	N		N		N
6					H	N		N		N
7					N	N		N		N
8					N	N		N		N
9					N	N		N		
10					N	N		N		N
11					N	N		N		N
12					N	N		N		N
13					H	N		N		N
14					C	N		N		N
15						H		N		H
16						N		N		N
17						N		N		N
18						H		N		H
19								N		N
20						H		N		H
21						N		N		N
22						N		N		N
23						N		N		N
24						H		N		H
25						H		N		H
26						N		N		N
27						N		N		N
28						H		N		H
29						H		N		H
30						H		N		H
31						N		N		N
32						N		N		N
33						H		N		H
34						N		N		N
35						N		N		N
36						N		N		N
37						N		N		N
38						N		N		N
39						N		N		N
40						N		N		N
41						N		N		N
42						N		N		N
43						N		N		N
44						N		N		N
45						N		N		N
46						N		N		N
47						N		N		N
48						N		N		N

SNIP-SNP linkage of Emo 42 resistant *C. elegans* to chromosome I.

	Chrom I	Chrom I	Chrom II	Chrom II	Chrom III	Chrom III	Chrom IV	Chrom IV	Chrom V	Chrom V	X
	W03D8	B0379	T13C2	F15D4	H04J21	T28D6	K08F4b	Y41E3	AC3	Y51A2D	ZK470
POSITION	-6.15	4.23	0.08	13.65	-15.5	8.54	4.52	17.6	2.53	19.34	-8.69
SAMPLE 1	N		C		N	H			N	H	N
2	N	N	H	N	C	H		H	N	H	C
3	N	N	N			H			N	H	
4	H	C	H		N	C	C	H	H	H	H
5	H	C	H		H	H	C	H	H		H
6	N	N	C	C	C	N	C	H	N	N	C
7	N	N	H	H	C	H	C	N	H	H	C
8	N		H						H	H	
9	N	N	H	N	C	H		C	N	H	N
10											
11	H	H	C	C	C	H		H	C	H	N
12	N		H	H	N	N	C	H	H	H	
13											
14	N				C	C		C	N	H	H

SNIP-SNP linkage of Emo 66 resistant *C. elegans* to chromosome V.

	Chrom I	Chrom I	Chrom II	Chrom III	Chrom IV	Chrom V	Chrom V	X
	W03D8	B0379	T13C2	T28D6	F42A6	AC3	Y51A2d	ZK470
POSITION	-6.15	4.23	0.08	8.54	-4.27	2.53	19.34	-8.69
SAMPLE 1	C	C	C	H	H	N	N	H
2	N	C	N	H	N	N	N	
3	N		H	N	N	N	N	C
4	H	C	N	H	C	N	N	
5	N		C	N	H	H	N	C
6	H	C	N	H	C	N	N	H
7	H		H	C	H	C	N	H
8	N	H	H	H	H	H	N	H
9	N		C	C	C	N	N	C
10	H	C	C	H	H	N	N	N
11	N	N	H	H	H	N	N	N
12	C	C	H	N	C	C	N	N
13	N		N	C		H	N	C
14	H	H	H	H	C	H	N	H

SNIP-SNP linkage of Emo 69 resistant *C. elegans* to chromosome II.

	Chrom I	Chrom II	Chrom III	Chrom IV	Chrom V	X
	W03D8	T13C2	T28D6	F42A6	AC3	ZK470
POSITION	-6.15	0.08	8.54	-4.27	2.53	-8.69
SAMPLE 1	H	N	H	H	C	H
2			N	N	C	
3	H	H	H	N	N	C
4	H	N	H	H	C	C
5	N	N	C	C	C	C
6	N	N	C	C	C	C
7	H	N				H
8	H	N	C		N	
9	C	N	N	C	C	H

SNIP-SNP linkage of Emo 76 resistant *C. elegans* to chromosome V.

	Chrom I	Chrom II	Chrom III	Chrom IV	Chrom V	X
	W03D8	T13C2	T28D6	F42A6	AC3	ZK470
POSITION	-6.15	0.08	8.54	-4.27	2.53	-8.69
SAMPLE 1	N	H			C	H
2	H	H		C	N	
3	N		H	C		C
4	N	N			N	
5	H	H		C		H
6	H	C			N	H
7				C		
8			H			
9	H	H	C	H	N	C
10		C	N		N	
11		H				C
12	N	H			N	H
13	N	H	N		C	
14	N	H	H	C		H
15						
16	H	H			N	H
17	N	C	H		N	
18	C	H			N	H
19						
20	H					H
21	H	H		C	N	N
22	H	N	H	C	N	N
23	H	N	C	C	N	
24	H		N		N	
25			H			
26	H	H	H	C		N
27		H	H	C		
28	H				N	

SNIP-SNP linkage of Emo 13 resistant *C. elegans* to chromosome V.

	Chrom I	Chrom I	Chrom II	Chrom III	Chrom IV	Chrom V	Chrom V	X
	W03D8	B0379	T13C2	T28D6	F42A6	AC3	Y51A2d	ZK470
POSITION	-6.15	4.23	0.08	8.54	-4.27	2.53	19.34	-8.69
SAMPLE 1	C	C	C	H	H	N	N	H
2		H	N	C	C	N		
3	N	H		C	N	N	N	C
4	H	H		H	C	N	N	N
5			C	N	C	H		C
6	C	C	N	H	C	N	N	C
7			H	C	C	C	N	C
8	N	H	H	C	H	H	N	H

Table to show SNIP-SNPs used

SNIP-SNP Name	Map Position	Chromosome	Enzyme	N2 product size (bp)	CB4586 product size (bp)
W03D8	-6.15	I	Dra I	355,150	508
B0379	4.23	I	Dra I	481,375,83,11	564,375,11
T13C2	0.08	II	Dra I	299, 125, 70	369, 125
F15D4	13.65	II	Dra I	516	396, 120
T28D6	8.40	III	Dra I	500	283, 217
H04J21	-15.5	III	Dra I	670, 75	745
K08F4b	4.52	IV	Dra I	489	248,207,34
Y41E3	17.6	IV	Dra I	391, 217	609
F42A6	-4.27	IV	Dra I	234, 163	397
AC3	2.53	V	Dra I	387, 105	492
C13D9	-6.16	V	Dra I	344, 171	515
T09F5	7.45	V	EcoRI	627, 60	360, 240,
F57G8	11.54	V	Dra I	528	272,256
T27C5	15.35	V	Dra I	288,282	570
Y51A2d	19.34	V	Dra I	393	119,274
F21D9	21.82	V	SspI/Tsp509I	225,65	290
M162	23.62	V	Tsp509I	164, 162, 60	326,60
F48F5	25.95	V	TaqI/Hyp188III	375, 64/439	194,181,/258,181
F38A6	27.08	V	Dra I	676, 182, 125	858, 125
ZK470	-8.69	X	Dra I	422, 71, 41	328, 94, 71,

Appendix 4

Deleted region of *lat-1 (ok379)* (genomic DNA)

ATGCGACGTAACAAAACGACTTATTCGTTGCTCCAAACGATTCTGGTAGCTTGTCTACTGACTGTTACTCCAACTTTCGC
CAGCAACAAGCCGACAACGGATGAAAGTGGTGAGTATTTTGATTTTAAAATTTTCAAAATGACCGGATCTTTGTTCTTAA
ATGAATTAGAAAAAAATTCAAAAAATTACTAAGCTATCATAGTTCTTATAAAAGTGAAAACGCCATAGGAACACTTCTTC
TTCTATTCTAATGCTGCAGTTTTCCCCCTCAATTCCACACTTGAGATCATTGCCGATTAGTTAACGATGCGCCTAGTTAA
CGATGCTTATTCTCTTGTTTCCGACTTGAAAGATCATGTCATTTTCTTAATTATGCATCGCCGACACGTCTCCCGGGGGA
CGGAAACATCCTGGTCCTTGGTCCAAAATCGAGCCGACTTCCTGTATGTGTCCCAGTTCGCCAACACCACTACCTCCATC
CCACAAAAGTGTTAATCGTGCAGTTGTCGGTTGGGGGTCTGGTGAGCGGTGAGCATAGCCTTTGTTGCGTAATGTTATCT
TACCGGTCCGGAAGTGCACATTTCTGTGTGGACCTCCTGGTGAGCACCGCCATATTAATAGTTGTCCTAGAACACCACTC
GTCATTGATCGAACTTATCAGTCTAGGAAATGGAAACTGCAAAATATTTATTTGTTTGGATGAGCGTGCCTCCTCCTTCT
CGAGATGTATATATTTCCAGCCTAGATGGGATTAAGAAAAGGTGTCGAGAGGGAAAGAGGGTGGCAGGCATCATTCCTAC
GTTTTTGAGAGTTTCCCTCAAATTCTCTTCCGAAATGGAAGTTTCTTTCCGCTTGACGGTTTTTGGGGTTTGTTTGCATT
TGGGACGAACCTAGAATTGAATAAATGTAAAGCGCTTGCAACTCCTACTTTTTCACTTGAATTGTTGTTTATATGAAAGT
CATTGTCCTCATCAACTGCTAGGTACGGGTCGGATTAAGGTGTTATTTGGGTGGAAAAGGCACCTGTGGATGATTTCCAC
TACCACCTGCCCTTGTTATCGTTCGCCAAATGATCGTTAGCCCCCCGCTTCTGCTTGCTTATCCAGGAATACGGACATTT
TTGGAGGGTATATATGACATTGTTGCAGCCATAATTTTGTGAGGATGCACAACAAATTAGACGTACACAATACCCCGCAT
TGTTCCAAATCTCGCGCATTTGGTTTCGATGGCATGGTGGTTGTGTCCTCGAATTAATTTGTTCTGCTAACGAACTCATC
AATTAGAAACTAATATATTGGAAAATCATTCACATTTCTATGACAACTGTCTCAAAGTTTTTTTTCTCGAGTGCATCCAC
TTCAAACTGTTTTGTCGGCGTTGTCACAACATGGAAACTCGAATAATAGTAGTGGTAGTAATATAACTGATTGATATGCT
TACTAATCTCATTGGTACATAAAAAACTTTTTCGAGTTTTGATCTTGCCGACAGACTACTCATCTGCCCAGCAGTTTCCG
AGTGGTGATCACCGATACTTTTAGTAAACATACTGAAGATGGCTCCTTCCTGCTGATGCTTCTTGCTAGTCACCCAAATT
GAGTCAATTAGAGGGGCAAGTAAAGGAAAGATAGTGGAGGGCAAGAAAGACAGCTTGCACGAAAACAGACGTATCTACAA
TTAGATGCTGCCGCCGATTTTGGTGATGCACTTTTTAGCAGAAGTAAAACAACACATGGTAGTCATTTTCACAGTAGGAG
GTGTCGAAAGTAGGCATATGTCGGTTTCGCGGATTAGCACTCTGATGGATGCGGTGGCGACAGAAACATTGAGTTGCACA
ATCGTCAGGCGGTCAGGGCTGTGTTTATCTATATATGAAAAAGGTCCGAGATTCTTATCTGTCATCTCTTCCCTTTTTGG
CGGGTGTGTGTGCATCCATTCGCATCCGAGATTGAATTGATAGACAAGTAAGTAATATGCTGTGAACAGGCAGGCGTCAA
TTGTCATATTCGAAACAATAAGAGCATAAAACGAGCGGCTCACTTGCCTTCTTTCTTTTAGGTTTTTTGTGTCTGGCGGC
ATTATATCTTTAGAGCTATAATCTATCATTCATTTATTTTTTGAATGTGAACGGTCATAAAAGGTGACCCATAGCTCAAT
TATTCATTTGTTCATGATCCTCTCCCGACGGCACATGTAATCTGAATCCGGCGTTTTAGGGCCAAAGAAACTCAATCCGC
GGCTCTCGTTGTTTGCTTTTACTGGTTTCTCGCGCACATGCGACGAATTCCCACAAGTTTCGATGTGTCGTTTTCGTTGA
TGGCTCCTAGTAGAACACAATTTATTGAATAAAGAGGCGCCCGGTGATGATGGAAAAGTTGTTGAAGAGCCACTTATGAC
TGGTAAAGAGGGGAGCACATCTCTGAATAAGACACACACACACACACACGTAATTCGTAATTGGTATGCCAGTGTC
ATCGTCAGCTTCTAAACGAATTAGTTGAGACTAAGAGCCTAACAATCGTTTACTGCCGGATATTTTCCACAAAACAGTTA
TCCTAACGGGCCTAACATTTTCTCTTCCGTTAACCAGGTGAATCGGTGTACGATTACGGTTTTGATGGCGTAATGTTGCC
CTGATCGGACAGAGGCTACTCGTCGCAATGGAGAGCCTGTTGTTATACTGTTCACATAGATAGTATGAGAAATTAGGAGA
CGCTGACTGAAACGTGAGCACGCGCTGCGCAACAGCAGACGGGGGAGACGAAAATGAAGAAGAACGGTATGCATATGAAT
GAATGAATGAAACAAACATAAGAAAATTATTATTATGCAAGTCATGTCGAGAAGGAAGCTCCTCGCGGAAATTGAAAAAA
AATTTTGAGGGCAATTTGAATATAAATATTAAATTTCAGGAACCATCTCACACACAATATGTGATGGTGAAGCTGCTGAA
CTGAGTTGTCCTGCTGGAAAAGTAATCTCGATTGTCCTAGGAAACTATGGAAGATTCTCTGTCGCTGTTTGCCTTCCTGA
CAATGACATCGTTCCATCCAACATCAACTGCCAAAACCACAAGACAAAGTCAATTCTGGAGAAGAAGTAAGTTTTAAAAT
TTCAAAGGCTACTTTACTATTACTATTCTGGGGACTTGTGGGGGGCACCCTATGCTTTGACCTAACTAACATATTCAACG
AGTTATGAATAGGTGCAAGCCGCATTTGTAATAGCTTACTCACACACCTTTTCGCGACTATCAATTGTTGTATTTGTCGG
ACTTTGGAATACGTTGAACATGTTTGAAGAGCTGACCGACACATAAATACACGTATAGTTTTATGTCCCAGTGCCATTGT
TCAGTCTTATCAGTTGAAGCGAACTGTACAGAAAGACCTTGGCATGGGATTTATCCGTGGCAGGTGAAAGATTAATAATT
CATTGTGAATACACTAATTGAACATCCGGCCATGTATGTACAGCAATCGGTCGAATAATTCAAATTGGCACATCCTGGCC
GAGCAGTCACAGACAATACCGCTATAAAAATGATGATGATATTGCCTTCGTGTGCGCGATCAGCCTCCCGTTGTCTACAC
AAGGTCGTTTGTCATTTGTGCCCGTTTTTTTGTAACGAAGTGCTGTCGAAAAGAGAACATTCATTAGCCGACCTCCATGT
CTGCCAGTTATTCTACCATTTTTCTACCGGAGGGGGAAATCATGCCCCGGACGCCGCTCACGGCGTGCTGCCTTCTTGTC
GAAACGCATCATTTCACACTATCAAATGACTGCCTTTCCTCTCATTTTTTGAATGAATTGAGGCCGCGATCGTGCTGCTT
TCCAACTGCAGCTGTCTCGAAAATCTGTCTTCGTTCGTTGGAAAAAAGAATGAAAAAGATGAAGAATAGTAAGAAGTGAA
GAAAGAGAGTACCGAGGAAACGGAAATGACTCTAGCGCCTTTCTTCGAATTGTGCTCTTCTCCAGTTTGAGTTTAAATTT
TTGGAATTTGAGACTATAGCACGGGAAGGAGCACTATTAGATTGATGACCGAAATTGTGAAGAAGACCCTTTTGGAGAAA
CCACCATATGTTGTTGTAGTTCCGAACCTCTTATGCTCCAAGAGCAAAACAAGGAGACCGAATAAAGATGGCGACGAATA
GAAGACATTTGTTTGCAGCGGATTCTCATGGATCATCATCATTTACCAATTAGAAATGGAACACATTCCGCAATCTAACT
GTTTGTCTCTTTTCGCCAAGCAATAAGGGACCTAGCAGTTGCTTTCGAAATGGTTTGTAGATGAGAGATGAGGCGACAGT
TGTGCAAATAAAGCAGCAGTCAATTAGCTGCGCAAACTACTTTGAAACTGCCAGTCAAGGAGCTCATACCAACTCTCACC
AAGAAAATAGTTTTGTCCATATTACTAGGGATTTATTAGTTTGAAAAAACTAATTTGTTCTTGTTTCAATGATCTAGTGT
TGCGGAATACGAATGACAGATGTTGTTCATTTCATGTTTGGGAAGTGCAAACGAATTGCGGGAAACGGTGCCCAGTGTAC
CGTATGTTGAACACATGTTGTTACCATGTTTCCATTTTGTCGATTTTCTGCTGCTACTGCTACATCAGTTAGTACTCAAT
AAATTTCCACCATTAATTGCTGCTGTTCTGTACAATTAGGTCTCTTTTGGAGCATGAAATAGAAAAACAGTGGTCCATCG
AGGTGTCAAATTGATGGCTTCTGCCCATTTTTGACCAATCTTGGTTATCCTACCAACCCATCGCTCTTTCCATCAATCTG

AACTCGCGTCACTATGGGACTGGCTCCAGTGGACGACGGCCGCCGAGCTCAAAGATGAGTGATGACTCTGCATATTCGGA
TGGGTCATCATCGATGTTGACAACTGAAGTGACACCACAAGGACAGACGGTGCTTCGAATTGATTTGAACAAGCCGAGCA
TGTATTGTCAAGATTTATAG

Green = Deleted region (6420-8474).

Emo 35 deleted region within *slo-1* (cDNA)

ATGGGCGAGATTTACTCGCCTTCGCAGTCGAAGGGCTTCAATCAACCATATGGATACCCGATGAATTGTAACCTTAGTCGAGTA
TTCATGGAGATGACTGAAGAAGATCGAAAGTGCCTGGAGGAGCGCAAATATTGGTGTTTTTTACTGAGCAGCATCACCACATTC
TGCGCCTCAATGATATTGGTCGTAATATGGCGAGTGGTGACACACCTGTGCTGTCAACGCCGAGAAAAAGAGTTTGTGGAGCCC
ATACCTGCTCCGGAAGCCGTCCAAATAAATATGAACGGGTCGAAGCACGCGCCAAGTGAAACCGACCCGTTTTTGAAGCAACAA
GAGGAAAAACACTTGGGATGGATGACAGAAGCCAAGGACTGGGCTGGCGAGCTGATATCCGGACAAAGTCTGACGGGACGGTTT
CTGGTACTTTTGGTGTTCATTTTATCGATTGGATCGTTGATTATTTATTTTTACGACGCTAGTTTCCAAAACTTCCAAGTAGAA
ACGTGCATCCCGTGGCAGGACAGTCCCTCGCAACAAATCGACCTGGGCTTCAACATATTTTTTCTCGTCTATTTTTTCATTAGA
TTCATCGCCGCGTCCGACAAAGTTTGGTTTCTGCTTGAAATGTACAGCTGGATTGATTTTTTCACGATTCCGCCAAGCTTCGTG
GCAATTTACTTGCAGAGGAATTGGCTCGGATTCCGTTTCCTCCGTGCTCTTCGCCTCATGACCGTACCCGACATTCTACAGTAC
CTCAACATCCTGAAAACATCTTCATCAATCCGATTGACACAGTTGGTCACAATTTTCGTGGCGGTTTGTCTGACTGGAGCCGGC
TTGGTGCACTTACTGGAAAATTCTGGGGACTTCTTCAAAGGATTTATAAATCCGCACAGAATCACTTATGCGGACTCTGTGTAC
TTTGTACTGGTCACAATGTCTACTGTCGGATATGGAGATATCTATTGTACGACGCTTTGCGGCCGACTTTTCATGATTTTCTTC
ATTCTGTTCGGTTTGGCCATGTTTGCAAGTTACGTACCAGAAATTGCCGATTTGATTGGAAACCGGCAAAAATACGGTGGGGAG
TACAAAGGAGAGCACGGGAAGAAGCACATAGTGGTCTGTGGCCATATCACCTACGATTCGGTGTCCCATTTTCTTCAAGATTTC
CTACACGAGGACCGTGATGACGTGGATGTCGAAGTGGTGTTTTTGCATCGTGTCGTGCCGGATTTGGAGCTGGAAGGCTTGTTT
AAGCGGCATTTCACAAAAGTCGAATTTTTCACGGGGACTGTCATGGATTCTCTGGATCTTAGCAGAGTCAAGATCGGGGACGCC
GACGCCTGCCTGGTCCTTGCCAACAAGTACAGTACCAATCCGGACGCCGAGGACGCCGCAAACATTATGCGTGTAATTTCGATC
AAAAACTACTCATCGGACATCAGAGTTATTGTGCAACTAATGCAATATCACAATAAGGCCTACCTTCTAAATATCCCCTCCTGG
GACTGGAAACGAGGTGATGACGTCATCTGTCTCGCGGAGCTTAAGCTCGGATTCATTGCTCAAAGCTGTCTGGCACCCGGATTC
TCTACGATGATGGCTAATTTATTTGCAATGAGAAGTTTCAAAACGTCACAAACCACACCGGACTGGCTGAACCTGTACCTTTGC
GGTGCCGGAATGGAAATGTACACCGACACGCTATCCCACTCGTTCGTCGGAATGACTTTTCCTGAAGCTGTCGACCTATTATTC
AACCGCCTGGGGCTTCTTCTTCTGGCGATTGAGCTTAAAGATGAGGAAAATAAAGAATGCAATATTGCAATCAATCCAGGCCCA
CATATTGTCATCCAGCCTCAAACTCAAGGATTTTTCATTGCTCAGAGCGCTGACGAGGTGAAGCGGGCGTTTTTCTGGTGTAAG
CAGTGTCATGACGATATTAAGGACGTTTCCTTGATCAAAAAATGTAAATGCAAAAATTTGGCCCTCTTCCGTCGCAACACCAAA
CACTCGACAGCGGCCCGTGCAAGAGCCACCGATGTGCTCCAGCAGTTCCAGCCACAAGCGCCAGCAGGTCCGATGGGCCATTTG
GGCCAACAAGTTCAGCTAAGGATGATTAATCAACAGAGTTCGACGAGTGATACTCATCTCAACACGAAATCCCTTCGATTTGCC
TATGAAATCAAAAAACTCATGCCATCTTCCGGAGGACGCCGAAATTCGATGAGTATTCCGCCAGACGGCAGGGGTGTCGATTTT
AGCAAGGATTTTGAGCAGCAATTCCAAGACATGAAATATGACAGTACTGGAATGTTCCACTGGTGTCCATCCCGTAACCTAGAG
GACTGTGTTCTGGAGCGCCACCAGGCCGCTATGACCGTACTCAACGGCCACGTGGTGGTTTGTTTGTTCGCTGATCAGGATTCT
CCGCTAATTGGGCTCCGGAACTTCATAATGCCACTAAGAAGCTCAAACTTCCATTATCATGAGCTCAAACACGTGGTTATTGTG
GGAGACCTGGAATATTTGAGGAAAGAGTGGAAGACGCTGTACAACTTGCCGAAAATCTCGATTTTGAATGGCTCCCCGCTATCT
CGAGCAGATTTACGCGCCGTCAACATTAACCTCTGCGACATGTGTGTCATAATCTCTGCCCGGGTCCCAAATACCGAAGATACC
ACTTTGGCAGATAAGGAAGCGATTCTGGCATCATTGAACATTAAAGCTATGCAATTTGATGATACCCTTGGCTTTTTCCCGATG
AGGCATCAAACTGGCGATCGGAGCCCGCTGGGCTCCCCGATTTCCATGCAGAAGAAGGGCGCCAAGTTTGGGACCAATGTGCCG
ATGATTACGGAGCTTGTTAACGACTCAAATGTGCAATTCCTCGACCAGGACGACGACGACGATCCGGACACCGAGCTCTACCTC
ACGCAGCCCTTCGCCTGCGGAACTGCCTTCGCCATTTCAGTGTTGGATTCTTTGATGAGTACTACCTACTTCAACGACTCGGCC
CTGACCCTCATCCGAACTCTGGTCACTGGTGGAGCCACACCGGAGCTTGAACTTATTCTGGCAGAAGGCGCCGGGCTCCGAGGT
GGCTACAGTACCCCGGAGACCCTCTCAAACAGAGATCGGTGCCGAATTGCTCAGATTTCGCTGCAGGATAACCCGTACGATGGA
GTTGTGCACAACACTACCTATGGTGCAATGTTCACGATAGCTCTGAGGAGGTACGGCCAACTTTGTATCGGGCTGTATAGGCTT
CACGACCAGGATAATCCGGACTCTATGAAGCGATATGTTATCACTAATCCTCCAGCAGAATTGAGGATTAAAAATACTGATTAC
GTCTACGTACTTGAACAATTCGATCCGGGACTGGAGTACGAGCCGGGCAAACGACACTTTTAG

Green = Deleted region (594-2362) .

Emo 48 deleted region within *slo-1* (cDNA)

ATGGGCGAGATTTACTCGCCTTCGCAGTCGAAGGGCTTCAATCAACCATATGGATACCCGATGAATTGTAACCTTAGTCGAGTA
TTCATGGAGATGACTGAAGAAGATCGAAAGTGCCTGGAGGAGCGCAAATATTGGTGTTTTTTACTGAGCAGCATCACCACATTC
TGCGCCTCAATGATATTGGTCGTAATATGGCGAGTGGTGACACACCTGTGCTGTCAACGCCGAGAAAAAGAGTTTGTGGAGCCC
ATACCTGCTCCGGAAGCCGTCCAAATAAATATGAACGGGTCGAAGCACGCGCCAAGTGAAACCGACCCGTTTTTGAAGCAACAA
GAGGAAAAACACTTGGGATGGATGACAGAAGCCAAGGACTGGGCTGGCGAGCTGATATCCGGACAAAGTCTGACGGGACGGTTT
CTGGTACTTTTGGTGTTCATTTTATCGATTGGATCGTTGATTATTTATTTTTACGACGCTAGTTTCCAAAACTTCCAAGTAGAA
ACGTGCATCCCGTGGCAGGACAGTCCCTCGCAACAAATCGACCTGGGCTTCAACATATTTTTTCTCGTCTATTTTTTCATTAGA
TTCATCGCCGCGTCCGACAAAGTTTGGTTTCTGCTTGAAATGTACAGCTGGATTGATTTTTTCACGATTCCGCCAAGCTTCGTG
GCAATTTACTTGCAGAGGAATTGGCTCGGATTCCGTTTCCTCCGTGCTCTTCGCCTCATGACCGTACCCGACATTCTACAGTAC
CTCAACATCCTGAAAACATCTTCATCAATCCGATTGACACAGTTGGTCACAATTTTCGTGGCGGTTTGTCTGACTGGAGCCGGC
TTGGTGCACTTACTGGAAAATTCTGGGGACTTCTTCAAAGGATTTATAAATCCGCACAGAATCACTTATGCGGACTCTGTGTAC
TTTGTACTGGTCACAATGTCTACTGTCGGATATGGAGATATCTATTGTACGACGCTTTGCGGCCGACTTTTCATGATTTTCTTC
ATTCTGTTCGGTTTGGCCATGTTTGCAAGTTACGTACCAGAAATTGCCGATTTGATTGGAAACCGGCAAAAATACGGTGGGGAG
TACAAAGGAGAGCACGGGAAGAAGCACATAGTGGTCTGTGGCCATATCACCTACGATTCGGTGTCCCATTTTCTTCAAGATTTC
CTACACGAGGACCGTGATGACGTGGATGTCGAAGTGGTGTTTTTGCATCGTGTCGTGCCGGATTTGGAGCTGGAAGGCTTGTTT
AAGCGGCATTTCACAAAAGTCGAATTTTTCACGGGGACTGTCATGGATTCTCTGGATCTTAGCAGAGTCAAGATCGGGGACGCC
GACGCCTGCCTGGTCCTTGCCAACAAGTACAGTACCAATCCGGACGCCGAGGACGCCGCAAACATTATGCGTGTAATTTCGATC
AAAAACTACTCATCGGACATCAGAGTTATTGTGCAACTAATGCAATATCACAATAAGGCCTACCTTCTAAATATCCCCTCCTGG
GACTGGAAACGAGGTGATGACGTCATCTGTCTCGCGGAGCTTAAGCTCGGATTCATTGCTCAAAGCTGTCTGGCACCCGGATTC
TCTACGATGATGGCTAATTTATTTGCAATGAGAAGTTTCAAAACGTCACAAACCACACCGGACTGGCTGAACCTGTACCTTTGC
GGTGCCGGAATGGAAATGTACACCGACACGCTATCCCACTCGTTCGTCGGAATGACTTTTCCTGAAGCTGTCGACCTATTATTC
AACCGCCTGGGGCTTCTTCTTCTGGCGATTGAGCTTAAAGATGAGGAAAATAAAGAATGCAATATTGCAATCAATCCAGGCCCA
CATATTGTCATCCAGCCTCAAACTCAAGGATTTTTCATTGCTCAGAGCGCTGACGAGGTGAAGCGGGCGTTTTTCTGGTGTAAG
CAGTGTCATGACGATATTAAGGACGTTTCCTTGATCAAAAAATGTAAATGCAAAAATTTGGCCCTCTTCCGTCGCAACACCAAA
CACTCGACAGCGGCCCGTGCAAGAGCCACCGATGTGCTCCAGCAGTTCCAGCCACAAGCGCCAGCAGGTCCGATGGGCCATTTG
GGCCAACAAGTTCAGCTAAGGATGATTAATCAACAGAGTTCGACGAGTGATACTCATCTCAACACGAAATCCCTTCGATTTGCC
TATGAAATCAAAAAACTCATGCCATCTTCCGGAGGACGCCGAAATTCGATGAGTATTCCGCCAGACGGCAGGGGTGTCGATTTT
AGCAAGGATTTTGAGCAGCAATTCCAAGACATGAAATATGACAGTACTGGAATGTTCCACTGGTGTCCATCCCGTAACCTAGAG
GACTGTGTTCTGGAGCGCCACCAGGCCGCTATGACCGTACTCAACGGCCACGTGGTGGTTTGTTTGTTCGCTGATCAGGATTCT
CCGCTAATTGGGCTCCGGAACTTCATAATGCCACTAAGAAGCTCAAACTTCCATTATCATGAGCTCAAACACGTGGTTATTGTG
GGAGACCTGGAATATTTGAGGAAAGAGTGGAAGACGCTGTACAACTTGCCGAAAATCTCGATTTTGAATGGCTCCCCGCTATCT
CGAGCAGATTTACGCGCCGTCAACATTAACCTCTGCGACATGTGTGTCATAATCTCTGCCCGGGTCCCAAATACCGAAGATACC
ACTTTGGCAGATAAGGAAGCGATTCTGGCATCATTGAACATTAAAGCTATGCAATTTGATGATACCCTTGGCTTTTTCCCGATG
AGGCATCAAACTGGCGATCGGAGCCCGCTGGGCTCCCCGATTTCCATGCAGAAGAAGGGCGCCAAGTTTGGGACCAATGTGCCG
ATGATTACGGAGCTTGTTAACGACTCAAATGTGCAATTCCTCGACCAGGACGACGACGACGATCCGGACACCGAGCTCTACCTC
ACGCAGCCCTTCGCCTGCGGAACTGCCTTCGCCATTTCAGTGTTGGATTCTTTGATGAGTACTACCTACTTCAACGACTCGGCC
CTGACCCTCATCCGAACTCTGGTCACTGGTGGAGCCACACCGGAGCTTGAACTTATTCTGGCAGAAGGCGCCGGGCTCCGAGGT
GGCTACAGTACCCCGGAGACCCTCTCAAACAGAGATCGGTGCCGAATTGCTCAGATTTCGCTGCAGGATAACCCGTACGATGGA
GTTGTGCACAACACTACCTATGGTGCAATGTTCACGATAGCTCTGAGGAGGTACGGCCAACTTTGTATCGGGCTGTATAGGCTT
CACGACCAGGATAATCCGGACTCTATGAAGCGATATGTTATCACTAATCCTCCAGCAGAATTGAGGATTAAAAATACTGATTAC
GTCTACGTACTTGAACAATTCGATCCGGGACTGGAGTACGAGCCGGGCAAACGACACTTTTAG

Green = Deleted region (1563-2968).

Chromatogram sequence information for Emo 35

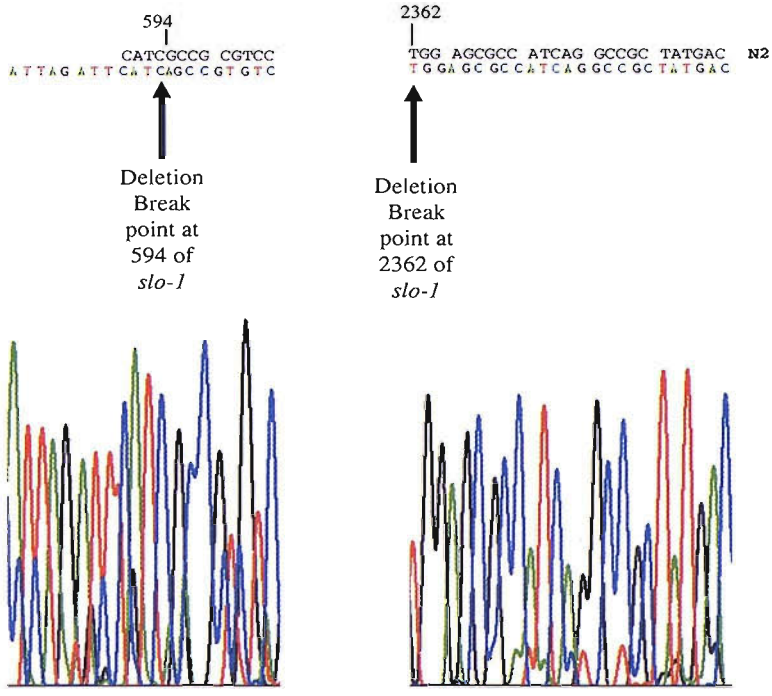

Chromatogram sequence information for Emo 48